Université de Montréal

Effets de l'estradiol et du chargement mécanique sur la régulation de la POC5 et du récepteur ADGRG7 dans la scoliose idiopathique

par
Amani Hassan

Département de Sciences Biomedicales
Faculté de médecine

Thèse présentée à la Faculté des études supérieures
en vue de l'obtention du grade de Ph.D.
en Sciences Biomedicales

Avril 2018

Université de Montréal

Faculté des études supérieures et postdoctorales

Cette thèse intitulée:

Effets de l'estradiol et du chargement mécanique sur la régulation de la POC5 et du récepteur ADGRG7 dans la scoliose idiopathique

Présentée par:

Amani Hassan

A été évaluée par un jury composé des personnes suivantes:

Dr. Valérie Marcil, président-rapporteur
Dr. Florina Moldovan, directeur de recherche
Dr. Isabelle Villemure, co-director de recherche
Dr. Stéphane Roy, membre du jury
Dr. Monzur Murshed, examinateur externe
Dr. Arlette Kolta, représentante du doyen de la FES

Résumé

La scoliose est une déformation complexe en 3D de la colonne vertébrale ayant une prévalence de 1.5-3% dans la population générale. La forme la plus commune est la scoliose idiopathique (SI) qui inclue la scoliose idiopathique de l'adolescent (SIA) affectant principalement les filles au cours de la puberté. L'étiologie est largement inconnue, mais les observations cliniques révèlent un rôle de l'hérédité ainsi que d'une croissance rapide dans le développement de la SIA. Il existe une forte évidence qu'une composante génétique entre en jeu dans cette pathologie. Récemment, de nombreux gènes ont été suspectés d'être responsables ou de contribuer à la SI. Notre équipe a identifié des variantes du gène *POC5*, codant pour une protéine centriolaire, dans une large famille française dont plusieurs membres sont atteints de SI. Dans cette même famille, nous avons suspecté l'implication d'une mutation du gène *ADGRG7* (récepteur orphelin appartenant aux récepteurs d'adhésion couplés aux protéines G) dans la pathogénicité de la SI. Au travers de nos travaux, nous nous sommes concentrés sur l'élucidation du rôle des protéines POC5 sauvages et mutantes (*in vitro* et *in vivo*) ainsi que sur la régulation de l'expression de POC5 et ADGRG7 par l'estradiol (E2), dans le but de tester si ces gènes pourraient être fonctionnellement liés à la scoliose.

Afin d'investiguer le rôle du gène *POC5* dans la SI, nous avons surexprimé la protéine POC5 mutante dans des lignées cellulaires par transfection transitoire (*in vitro*) et nous avons induit une perte de fonction du gène *POC5* dans un modèle animal, le poisson zèbre (*in vivo*). Le rôle de POC5 a été étudié par : 1) Analyses de spectroscopie de masse et co-immunoprécipitation afin d'identifier les différents partenaires de liaisons entre la protéine sauvage (wt POC5) et mutante (mut POC5); 2) immunolocalisation de la protéine sauvage et mutante au niveau cellulaire; 3) histologie et immunohistochimie réalisés sur des tissus issus de poissons zèbres contrôles (wt POC5) et scoliotiques (mut POC5). Notre travail a permis d'identifier plusieurs protéines partenaires de la POC5, et nous avons trouvé des interactions fonctionnelles entre ces protéines et la POC5 reliées aux cils et centrosome. Un certain nombre de protéines ciliaires ont été identifiées comme interagissant avec wt POC5 et non avec mut POC5 comme CEP290, RAB11, CKAP5, Annexine 2 et Septine 9. Au niveau cellulaire, la localisation et la colocalisation des protéines wt POC5 et POC5 mutée avec la

tubuline alpha acétylée (marqueur ciliaire), confirme la conséquence de la mutation sur la localisation subcellulaire en relation avec la longueur et l'intensité de la coloration du cil. *In vivo*, nous avons identifié de nombreux défauts de la rétine et de l'oreille interne chez le poisson zèbre *POC5* mutant par rapport au contrôle. Enfin, en utilisant différents marqueurs des couches rétiniennes et la tubuline acétylée, nous avons localisé ces défauts dans le segment externe et les cônes de la rétine.

Afin d'étudier le rôle possible de *POC5* et *ADGRG7* dans la SI, nous avons examiné comment *POC5* et *ADGRG7* est régulé au niveau transcriptionnel. Nous avons utilisé des modèles cellulaires, des ostéoblastes humains dérivées de contrôles et de SIA patient, et nous avons étudié l'expression de la protéine POC5 et ADGRG7 en réponse à une stimulation par l'E2. La région promotrice du gène *ADGRG7* a été clonée et analysée pour les éléments cis médiant les effets de l'E2. Les analyses de délétion du promoteur indiquent que le site SP1 dans le fragment 474bp est requis pour une activité basale ainsi que pour une activation hormone-dépendante, et des mutations dans les sites de liaison au sein de cette région résultent en la perte de transactivation. Les résultats d'immunoprécipitation de la chromatine (ChIP) ont montré que le site SP1 ESRα lie le promoteur d'ADGRG7. Nos résultats suggèrent que la régulation de l'expression d'ADGRG7 par l'E2 est due à l'association des protéines ESRα et SP1 au promoteur d'*ADGRG7*.

La même stratégie expérimentale a été appliquée pour l'étude de la régulation de *POC5* par E2. L'analyse de délétion et ChIP ont confirmé la régulation de *POC5* à travers ESRα. Basé sur des études de promoteur, qPCR, Western blot et ChIP, cette étude clarifie comment *POC5* et *ADGRG7* sont régulées par l'E2.

Un autre aspect de ce projet était d'étudier les différents effets du chargement mécanique sur des cellules, incluant des ostéoblastes humains, exprimant POC5 sauvage ou mutée. Les cellules ont été soumises à un stress mécanique à différents temps, et différentes voies de signalisations (incluant ERK, p38, NFκB) ont été testées. Nos résultats montrent une différence dans la réponse des cellules surexprimant POC5 mutée par rapport aux cellules contrôles. Les effets du chargement comprenant les différentes voies de signalisations ont été

montrés comme étant initiés via TRPV4, un canal calcique perméable activé par l'étirement localisé dans le cil primaire et la membrane plasmique.

L'importance de ce travail réside dans le fait qu'il couvre plusieurs facteurs contribuant à la pathogenèse de l'SIA. Basé sur nos résultats, la SIA est une maladie multifactorielle complexe où POC5, le cil primaire, l'E2 et le chargement mécanique interagissent dans la physiopathogenèse. L'intérêt de ce travail est qu'il pose les bases permettant la compréhension des mécanismes moléculaires impliqués dans la SIA.

Mots-clés: Scoliose idiopathique de l'adolescent, gène *POC5*, Protein d'adhesion –Couplé au Receptor-G7 (ADGRG7), Estradiol (E2), stress mécanique, sigle anglais pour transient receptor potential vanilloide 4 récépteur (TRPV4), et cils.

Abstract

Scoliosis is a complex three-dimensional deformity of the spine, with 1.5–3% prevalence in the general population. The most commonly known type of scoliosis is idiopathic scoliosis (IS), including adolescent idiopathic scoliosis (AIS) affecting principally girls during puberty. The etiology is largely unknown, but clinical observations revealed the role of hereditary and rapid growth in the development of this condition. There exists strong evidence that there is a genetic component to the disease. More recently, several genes were suspected to cause or contribute to IS. Our group identified gene variants of *POC5* centriolar protein in a large French family with multiple members affected with IS. In the same family, we suspected the involvement of *ADGRG7* (an orphan receptor that belongs to the Adhesion G protein-coupled receptors) gene mutation in the pathogenicity of IS. In the present work, we focused on elucidating the role of wild type (wt) and mutant (mut) POC5 proteins (*in vitro* and *in vivo*) as well as the regulation of POC5 and ADGRG7 by estradiol (E2), with the goal to test whether these genes could be functionally connected with scoliosis.

To investigate the role of *POC5* gene in IS, we overexpressed mutant *POC5* in cell lines by transient transfection (*in vitro* study) and created a loss-of-function model in zebrafish (*in vivo* study). The role of POC5 was investigated by: 1) mass spectroscopy analysis and co-immunoprecipitation to identify differences in binding partners between the wt POC5 and mut POC5 proteins; 2) immunolocalization of wt and mut POC5 proteins at the cellular level; 3) histology and immunohistochemistry performed on tissues from wt (control) and scoliotic (poc5 mut) zebrafish. Our work identified several interacting partners with POC5, and documented functional connections with respect to cilia and centrosome dysfunction. A number of ciliary proteins were identified to be interacting with wt POC5 but not mut POC5 like CEP290, RAB11, CKAP5, Annexin 2 and Septin 9. At the cellular level, localization and co-localisation of wt POC5 and mut POC5 protein with alpha acetylated tubulin (cilia marker), confirmed the consequence of the mutation on subcellular location with respect to cilium length and staining intensity. *In vivo*, several defects in the retina of zebrafish and inner ear were identified in mutpoc5 zebrafish compared to wt zebrafish. Finally, using different

markers for retinal layers and alpha acetylated tubulin, the defects were localized in the outer segment layer and cones of the retina.

To further investigate the possible roles of *POC5* and *ADGRG7* in IS, we examined how *POC5* and *ADGRG7* are regulated at the transcriptional level. Human osteoblasts derived from control and AIS patients were used as a cell model, and the expression of POC5 and ADGRG7 protein was monitored upon E2 stimulation. The promoter region of the human *POC5* and *ADGRG7* gene was then cloned and analyzed for functional cis-elements mediating effects of E2. Deletion analysis of the *ADGRG7* promoter indicates that the SP1 site in the 474bp fragment is required for both basal activity and hormone-induced activation, and mutations of the binding sites within this region result in the loss of transactivation. Further results from chromatin immunoprecipitation (ChIP) assay showed that SP1 and ESRα bind to *ADGRG7* promoter. Our results suggest that the regulation of *ADGRG7* expression by E2 is due to the association of ESRα and SP1 proteins to *ADGRG7* promoter. The same experimental strategy was applied for studying the *POC5* regulation by E2. Deletion analysis and ChIP confirmed the regulation of *POC5* through ESRα. Through promoter studies, qPCR, and western blot and (ChIP) assay, this study clarifies how *POC5* and *ADGRG7* are regulated by E2.

Another aspect of this project was to study the differential effects of mechanical stress on wt and mut *POC5* expressing cells, including human osteoblasts. Cells were exposed to mechanical stress for different time points and then different signalling pathways (including ERK, p38, NFκB) were tested. Our results show that there is difference in the response of control normal cells and cells overexpressing the mut *POC5*. The effects of loading including the signalling pathways were found to be initiated through TRPV4 which is a stretch-activated Ca^{2+}- permeable channel and localizes to the primary cilium and plasma membrane.

The importance of this work is that it covers several factors that contribute to the pathogenesis of AIS. Based on our findings, AIS is a complex multifactorial disease where POC5, cilia, E2 and mechanical load intreplay in the pathogenesis of the disease. The significance of this work is that it puts the basics for understanding the molecular mechanisms that are implicated in AIS.

Keywords: Adolescent Idiopatic Scoliosis, POC5, ADGRG7, E2, Estrogen receptor, mechanical stress, TRPV4, cilia

Table of contents

List of table

List of figures

List of abbreviations

4α-PDD	4α-Phorbol 12,13-didecanoate
AD	Autosomal-Dominant
ADGRG6	Adhesion G protein coupled Receptor 6
ADGRG7	Adhesion G protein coupled Receptor 7
AIS	Adolescent Idiopathic Scoliosis
AJAP1	adherens junctions associated protein
AKAP2	A-kinase anchoring protein
ATP	Adenosine Triphosphate
BBS	Bardet-Biedl syndrome
BCL-2	B-cell CLL/lymphoma
bHLH	basic helix-loop-helix family
BMD	Bone Mineral Density
BMI	Body MassIndex
BNC2	Basonuclin
CaM	Calmodulin
cAMP	cyclic adenosine monophosphate
Cas9	CRISPR-associated protein-9 nuclease
CENPJ	Centromere protein J
Cen	Centrins
CEP290	Centrosomal protein 290
CFC	Cardiofaciocutaneous
ChIP	Chromatin Immunoprecipitation
CHL1	neural cell adhesion molecule L1-like protein
JNK	c-Jun N-terminal kinase
CKAP5	Cytoskeleton associated protein
CLASP1	Cytoplasmic linker associated protein
COL11A2	Collagen type XI alpha 2 chain
CSF	Cerebrospinal fluid
CSL-type	CBF1, Suppressor of Hairless, and LAG-1

CTD	Curly-tail-down
dpf	days post fertilization
DHEA	Dehydroepiandrosterone
DHEAS	Dehydroepiandrosterone sulfate
DHT	5α-dihydrotestosterone
DC	Double cones
E2	Estrogens; 17-β-estradiol, Estrogen
EDC	Extensor digitorum communis muscle
EGFR	Epidermal growth factor receptor
EHD4	E-domain containing
ER	Endoplasmic reticulum
ERK	Extracellular regulated Kinase
ESR1	Estrogen Receptor
ESR2	Estrogen Receptor
ESRα	Estrogen Receptor alpha
ERE	Estrogen response elements
ERK	Extracellular signal-regulated kinase
FBN1	Fibrillin-1
FBN2	Fibrillin-2
FGF	Fibroblast growth factor
FGFR	Fibroblast growth factor receptor
FoxD3	Forkhead box D3
FoxJ1	Forkhead box J1
GPCRs	G protein-coupled Receptors
GWAS	Genome wide association studies
GH	Growth hormone
GAG	Glycosaminoglycans
GPER	G protein-coupled Estrogen Receptor
GPR126	G protein coupled Receptor 126
GPS	GPCR proteolysis site

HE6	Human Epididymis-Specific Protein 6
HEF1-AuroraA-HDAC6	human enhancer of filamentation1-AuroraA-histone deacetylase-6
HES	Histone deacetylase 6
HNRNPD	Hairy enhancer of split
hpf	heterogeneous nuclear ribonucleoprotein D
IEMG	hours post fertilization
IGF	Higher maximal integrated electromyography
IL-6	Insulin like growth factor
IS	Interleukine 6
JBS	Idiopathic Scoliosis
JNK	Joubert syndrome
KCNJ2	c-Jun N-terminal kinase
kif6	potassium voltage-gated channel subfamily J member
Kif9	Kinesin family member
KIFs	kinesin-family member 9
KV	kinesin ins
LBX1	Kupffer's vesicle
LEPR	Ladybird homeobox 1
LR	Leptin receptor
LRRC6	Left-Right
MAF	leucine rich repeat containing
MAGI1	Minor allele frequency
MRI	Membrane associated guanylate kinase, WW and PDZ domain containing
MAPK7	Magnetic resonance imaging
MATN1	mitogen-activated protein kinase 7
MIM	Matrillin1
MAPK	Missing in metastasis
	Mitogen-initiated protein kinase

MKS	Meckel-Gruber syndrome
MMP	Matrix metalloproteinsase
MT	Melatonin receptor
MTNR1B	Melatonin receptor 1B
Mut	Mutant
NEDD1	Neural precursor cell expressed developmentally down-regulated protein 1
NFκB	Nuclear factor kappa B subunit
NICD	Notch intracellular domain
ODA	Outer dynein arms
PAX3	Paired box 3
PAX6	Paired box protein
PBMC	Peripheral blood mononuclear cells
PCD	Primary ciliary dyskinesia
PCM	Pericentriolar material
PE	Pectum excavatun
PELP1	Proline-, glutamic acid-, and leucine-rich protein 1
PKA	Protein kinase A
PKC	Protein kinase C
POC5	Protein of centriole 5
PARP1	Poly (ADP-ribose) polymerase family, member 1
PGE2	prostaglandin E2
ptk7	Tyrosine-protein kinase-like 7
PTPN11	Protein-tyrosine phosphatases non-receptor type 11, Protein-tyrosine phosphatases non-receptor type 11
qPCR	Quantitative Polymerase Chain Reaction
RAB11	Ras related protein RAB11
RAS-MAPK	Ras-mitogen-activated protein kinase Mitogen activated protein kinase
RhoA	Ras homolog family member A

RLX	Raloxifene
RP	Retinitis pigmentosa
RTTN	Rotatin
SERM	Selective Estrogen Receptor Modulator
SCs	Single cones
SNP	single nucleotide polymorphism
SNV	Single Nucleotide Variant
sOB-R	Soluble leptin receptor
SOX9	SRY (sex determining region Y)-box9
SP1	Specificity protein 1
TACE	Tumor necrosis factor alpha converting enzyme
tBMD	trabecular bone mineral density
TGFB1	Transforming growth factor beta-1
TIMP-2	TIMP metallopeptidase inhibitor 2
TMX	Tamoxifen
TNIK	TRAF2 and NCK interacting k
TPH1	Tryptophan hydroxylase 1
TRPV4	Transient receptor potential cation channel subfamily V member 4
UV	Ultraviolet
VMR	Visual motor response
Wnt/PCP	wingless-type MMTV integration site family, member/Planar cell polarity
Wnt5b	wingless-type MMTV integration site family, member 5A
wt	wild type
ZMYND10	zinc finger, MYND-domain-containing

I dedicate this thesis to my parents

Acknowledgement

First of all, I am very gratefull for my supervisor Dr. Florina Moldovan for her guidance throughout my PhD studies. She was very supportive, encouraging and always positive and available for discussing and sharing ideas that was always very helpful for my experiments. She was a mother when needed, a supervisor and a friend.

Secondly, I would like to thank Dr. Isabelle Villemure for her coodirection. I also would like to thank Dr. Stefan Parent, Mrs Soraya Barchi, and Mr. Francois Cereel for their contribution and for providing human tissues.

I would to thank Dr. Patten for providing the zebrafish. I would like to thank my work progress committee members Dr. Andree Tremblay and Dr. Philippe Campeau for being part of supervision. Thank you Dr. Campeau for giving me the opportunity for working in new field that was very essential in my PhD training. Thank you Dr. Tremblay for giving me the opportunity to do some experiments in your lab and for your students Dr. Samira, Lydia and Stephanie.

I would like to thank Dr. Perrine Gaub from Dr. Joyal Laboratory, for giving all the guidance for using the Zeiss microscope that I have used extensively for my immunofluorescence experiments.

I am thankfull for MEDITIS Biomedical Technology Training Program, for proving me with the fund for three years and also University of Montreal, faculty of dentistry, Reseau de recherche en santé buccodentaire et osseuse (RSBO) for supporting conference expenses.

I would like to thank Dr. Edward Baggu who was always available for providing advice and ideas for my research and helping in manuscript writing. I would like to thank my friends at CHU Sainte Justine for their help during my PhD: Mrs. Charlotte Zaouter, Dr. Mathieu Levesque, Dr. Julie Couillard, Dr. Irene Londono, Dr. Justine Rousseau, Dr. Severine Leclerc, Mrs. Anita Franco, Dr. Anne-Laure Mernard and Dr. Rosa Kaviani.

I am thankfull for madam Sirinat Moldiperee (Doy), madam Stephanie Vanier, Mrs. Hélène Mathieu and madam Aurélia Sapataru for their help and support during my PhD.

Throughout my PhD, I supervised several students from CGEP and from Europe to which I'm thankfull for having learned good supervisory experience.

Finally, I would like to thank a person who was supporting my PhD and me personally. She was always there sacrificing, giving in all ways, being there in hard time, it's you MAMA thank you. I would like to thank my father who always believed in me since I decided to cross the Atlantic and do my education in Canada. You always said follow your dream and here is the dream coming true. Ghenwa my little sister, I wanted to thank you for everything, you're a true sister and a loyal friend.

I dedicate this work for the patients especially children who are suffering from scoliosis and have to go through the painfull bracing and surgery. I hope to be one of the millions who are trying to find less painful strategies for curing patients with scoliosis.

CHAPTER I. GENERAL INTRODUCTION

I. Pathogenesis of AIS

Scoliosis is a complex three-dimensional deformity of the spine, with 1.5–3% prevalence in the general population (Altaf, Gibson et al. 2013). The most commonly known type of scoliosis is idiopathic scoliosis (IS), including adolescent idiopathic scoliosis (AIS) affecting principally girls during puberty (de Seze and Cugy 2012). In fact, classification of scoliosis includes idiopathic (unknown cause or scoliosis without co-existing diagnoses), congenital (vertebral anomalies present at birth), or neuromuscular scoliosis. IS, which comprises about 80 percent of all cases, is subclassified as infantile (age 0-3), juvenile (age 3-10), adolescent (age 10-18), or adult (age >18), according to the onset of scoliosis. There is no preventive treatment for AIS. The curve progression in patients is predicted by several factors including maturity (age at diagnosis, menarchal status, and the amount of skeletal growth remaining), curve size, and position of the curve apex. The manifestations of AIS are highly heterogenous; while some patients develop rapidly progressive and severe curves, other patients have a loosely nonsevere curve. The treatment of AIS includes bracing, which is sometimes associated with significant morbidity. Surgery is recommended in adolescents with a curve of a Cobb angle more than 45-50° (Altaf, Gibson et al. 2013).

Researchers tried over decades to understand the pathophysiology of idiopathic scoliosis and several hypotheses have been proposed. Most experts agree that the causes of AIS are multifactorial but there is no generally accepted theory of pathogenesis. The hypothetical etiological factors can be grouped into biomechanical, genetic, metabolic, and neurosensorial abnormalities, but AIS is most probably a complex multifactorial cascade of events that occurs during growth and development. Development, growth and puberty, which are all under hormonal control, could play a critical role in AIS. Particularly the sex steroids hormones (i.e estrogens (E2)), that are responsible for the onset of puberty in female, could contribute to the pathogenesis of AIS.

Physiopathological hypothesis for factors driving both AIS development and progression can be divided into extrinsic and intrinsic factors (Fig.1). Factors were classified based on whether the abnormality has a direct or indirect impact on the spinal growth mechanisms. There is increasing evidence that intrinsic spinal biomechanics of the upright human spine as well as genetics play a central role in the pathology and progression of AIS (Schlosser, van der Heijden et al. 2014, Newton Ede and Jones 2016). Briefly, (1) extrinsic factors are grouped into body asymmetry, hormonal factors, nervous system abnormalities and vestibular abnormalities (de Seze and Cugy 2012) while intrinsic factors are grouped into intervertebral disc and growth plate, spinal growth abnormalities and biomechanical factors, spinal bone, paraspinal muscles, role of erect posture and genetic.

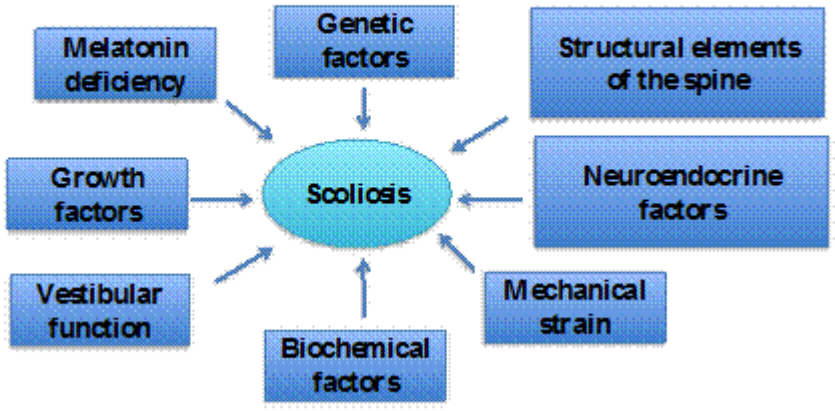

Figure 1: Different factors contributing to scoliosis pathogenesis.

The etiology and molecular mechanisms of AIS are not clear, however, several factors have been suggested to be involved in AIS pathogenesis including genetic, neuroendocrine, vestibular, biochemical and structural. Also, the mechanical loading, which is one of the proposed factors, is applied on the spine during puberty and could aggravate the progression of the scoliotic curve. Adapted from Leboeuf et al. (Leboeuf, Letellier et al. 2009).

II. Extrinsic factors:

II.1. Body asymmetry

AIS is characterized by having several types of curve patterns such as proximal thoracic, main thoracic, and thoracolumbar/lumbar are designated as either the major curve (largest Cobb measurement) or minor curves with the minor curves separated into structural and nonstructural types (Lenke 2005), trunk asymmetry, and thoracic vertebral right rotation. However, it was reported that even in the normal spine, trunk asymmetry (Burwell, James et al. 1983) and thoracic vertebral right rotation (Grivas, Vasiliadis et al. 2006, Janssen, Kouwenhoven et al. 2011) exist. Interestingly, after adolescence, asymmetry in normal spine trunk may become prominent. In normal people, with higher age, the body tends to bending on the right of the dorsal spine. It is possible that in normal individuals the development and progression of the deformities could explain the defects in AIS progression. It was found that in normal people there is a right thoracic curvature in the normal spine, the cause of this curvature is yet to be determined such as heart location and when this curvature worsens (Doi, Harimaya et al. 2011), it develops to scoliosis.

II.2. Connective tissue abnormalities

Scoliosis is observed in patients with connective tissue disease, such as osteogenesis imperfecta, Marfan's disease or the Ehler-Danlos syndrome (Hadley-Miller, Mims et al. 1994, Miller, Mims et al. 1996, Sponseller, Thompson et al. 2009). Patients with scoliosis have defects in elastic fiber in the yellow ligaments (Hadley-Miller, Mims et al. 1994). Elastic fibers are composed of the amorphous core of elastin and microfibrils that constitutes mostly of fibrillin. To study the role of elastic fiber system in scoliosis, the elastic fiber system of the ligamentum flavum was examined in patients who had scoliosis and in age-matched individuals who did not. Histological specimens of ligamentum flavum that are isolated from patients were stained for elastic fibers and fibrillin. Also, fibroblasts were isolated and cultured to study the biosynthesis and secretion of fibrillin and its incorporation into the extracellular matrix *in vitro*. Elastic fibers had reduction in fiber density (the number of fibers

per unit area) and a non-uniform distribution of fibers throughout the ligament. Specimens showed defect in fiber arrangement and lowered staining as compared to normal specimens without scoliosis. Fibroblasts from patients could produce fibrillin normally and secrete it. However, there was defect in the incorporation of fibrillin to the extracellular matrix. Thus based on this study, the defects in elastic fiber system could play a role in the pathogenesis of AIS (Hadley-Miller, Mims et al. 1994).

II.3. The role of the nervous system and postural control

Current studies also suggest that the etiopathogenesis of AIS involves intrinsic factors and extrinsic factors, such as defects in the central nervous system. Abnormalities in the organization of the cortical network on the brain were observed in AIS patients. It was reported that the network is preserved in AIS patient brains but there is hemispheric asymmetry of AIS brain. Also, there was decreased structural connectivity between hemispheres and increased connectivity observed in several cortical regions. These results shed light on the defects of the structural network alteration in AIS brain, and would help in understanding the mechanism and etiopathogenesis of AIS (Wang, Shi et al. 2013). Dysfunction and abnormalities in the morphology of the cerebellum could be linked to pathogenesis. The cerebellar volume in AIS patients was found larger compared with normal controls in the cerebellum regions. These affected regions have several functions that involve motor control, somatosensory, working memory, language, and response to visual stimulation (Shi, Wang et al. 2013). AIS patients have been found to have higher incidence of tonsillar ectopia thus the position of the cerebellar tonsil could be associated with AIS pathogenesis (Sun, Qiu et al. 2007). AIS patients were found in several studies to have abnormalities of posture, proprioception, and equilibrium control. The functions that are mentioned are controlled by the brain stem. With magnetic resonance imaging (MRI), the anatomy of the brain stem in patients with AIS was studied. Imaging was conducted from the hypothalamus to the spinal cord at C3. Asymmetry in the ventral pons or medulla in the area of the corticospinal tracts was noted in some patients with one patient had an enlarged cisterna magna and one an inconclusive (incomplete) study (Geissele, Kransdorf et al. 1991).

Using MRI, several studies have shown that several cases of "idiopathic" scoliosis show neurologic abnormalities including syringomyelia and Chiari 1 malformation. Some cases of "idiopathic" scoliosis include a craniovertebral malformation (Inoue, Nakata et al. 2003). Abnormalities in the cerebral structure, the brain stem and spinal cord was reported in patients with idiopathic scoliosis (Wang, Shi et al. 2012). Changes in the nervous system in patients with AIS in the left thoracic versus right thoracic AIS were studied by volume based morphometry. This study found that there is downregulation of the genu of the corpus callosum and left internal capsule in the white matter of patients with left thoracic AIS but not in right thoracic AIS and in control. The corpus callosum and left internal capsule in the white matter function as inner hemispheric communication and conduit of the corticothalamic projectional fibers, respectively (Shi, Wang et al. 2009).

II.4. Vestibular system abnormalities

There is extensive research on the role of vestibular system in scoliosis. The vestibular system influences several pathways including vestibulospinal pathway, the hypothalamus, and the cerebellum. It is suggested that the vestibular system is a possible cause of later morphological, hormonal and neurosensory anomalies observed in AIS. There are five inertial sensors in the vestibular system, which are the three semicircular canals and two otolith organs. The function of the semicircular canals involves sensing rotations of the head. Each canal acts as a tube filled with fluid, which opens at both ends into the vestibule. The three canals are oriented orthogonally to each other so that a rotation in any direction can be represented as the summed response from all three canals (Hawasli, Hullar et al. 2015).

Semicircular canal abnormalities of the left inner ear might be one reason behind scoliosis development. The reason for the dysfunction might consist in a morphological and genetic anomaly of the semicircular canals of the left inner ear. Vestibular morphological anomalies were postulated to be already existing at birth and could possibly have caused other abnormalities. In an attempt to address the above-mentioned hypothesis, MRI was used to study the vestibular organ in adolescents with AIS and in controls. Precisely, the orientation of the lateral semicircular canal and the three semicircular canal positions were studied

relative to the midline. The function of the lateral semicircular canal was also investigated. Indeed, abnormalities in the orientation of the left lateral semicircular canal were present. It was more vertical and further from the midline in AIS. The significance of the anomaly in the semicircular canal could be used as early detection of AIS (Hitier, Hamon et al. 2015).

One of the proposed hypothesis is that there are abnormalities in the anatomy of the vestibular system in AIS patients. In AIS patients, the distance between centers of lateral and superior canals and the angle with vertex at the center of posterior canal were significantly smaller than control subjects, but not in the right-side counterparts. The significance of this finding could explain the defects in subclinical postural, vestibular and proprioceptive observed frequently in AIS patients (Shi, Wang et al. 2011). Problems in the development of the semicircular canals could be a result of genetic defects. The body posture could be affected and this might be a driving factor in the initiation of the curvature of the spine. The possible impact of semicircular canal abnormalities is that it leads to defects in the transmission of sensory signal of the rotational movement of the body to the central nervous system, leading to an alteration in the neuronal circuit of balance (Patten and Moldovan 2011).

III. Intrinsic factors:

III.1. Intervertebral disc and growth plate

Growth plate and intervertebral disc abnormalities are one of the primary defects that occur in AIS. Several studies tried to explain the causes behind this abnormality, such as disorganisation of columns of chondrocytes in the convex zone of the growth plate (Day, Frawley et al. 2008). Also, patients with AIS have degeneration of the intervertebral disc matrix. The morphology and composition of the intervertebral disc and also of the cartilage end-plate in patients with idiopathic or congenital scoliosis show a reduction in the proteoglycan and water in both structures in specimens from scoliotic patients, particularly toward the concavity of the curve, compared with autopsy material. Also, some collagen types were not similarly distributed in tissue from scoliotic patients and autopsy tissue. In the patients studied and except for three, there was calcification of the end plate and sometimes of

the adjacent disc, while the autopsy specimen had minimal calcification. The observed findings could be a result of variable loading in scoliotic patients and this might be a contributing factor for scoliosis (Roberts, Menage et al. 1993). Patients with idiopathic scoliosis were found to have increased concentrations of keratan sulfates and unmodified keratan sulfates in the vertebral body growth plate. There was also a reduction in the sulfation and acetylation of total glycosaminoglycans (GAG) by 50 and 30%, respectively. These modifications are due to the decrease in the biological activity of molecules that modulate function of the growth plate (Rusova, Rykova et al. 2005). One of the possible factors contributing to the progression of scoliosis could be due to defects in the maturation process of nucleus pulposus. Analysis of the intervertebral discs in scoliotic patients show reduced stainability of cartilaginous plate, reduction in the cleft and vacuolation of the matrix of annulus fibrosus as well as cellular composition as compared to control biopsies. Patients with scoliosis and with a curvature of the spine by more than 60 degrees and patients with very high rotation had in common matrix degeneration of cartilaginous plate and irregular fiber running of annulus fibrosus. However, chordal cells in nucleus pulposus were not common in higher rotation cases. Chordal cell fragments were prominent in nucleus pulposus in scoliotic patients (Nakamura 1980).

III.2. Spinal growth abnormalities and biomechanical factors

The hypothesis on spinal growth abnormalities and biomechanics was mainly elaborated by Dr. Ian Stokes. He introduced the concept of mechanical modulation of the vertebral body growth in the pathogenesis of progressive adolescent idiopathic scoliosis. He believes that the Hueter-Volkman or Deplech (Veldhuizen, Wever et al. 2000) can be explained by the fact that constant pathologic strong pressure decelerates endochondral longitudinal growth while reduced compression accelerates growth, where the direction of gowth is changed by the exterted pressure. The clinical significance of this law is that brace treatment is based on this effect although the efficacy of bracing continues to be debated and questioned and research is now targeted and focused on compression-based fusionless tethers that can replace the brace treatments (Braun, Ogilvie et al. 2004, Aubin, Clin et al. 2018).

In more details, the Hueter-Volkman concept of 'growth modulation' explains, in a phenomenological way, how the development of vertebrae and the vertebral wedging could be generated by the asymmetrical loading on vertebral epiphyseal growth plate. This generated deformity is part of a vicious cycle in which the vertebral asymmetry is generating a spinal curvature, then accentuating the load asymmetrical distribution in the global spine, leading to further asymmetrical growth and so on (Stokes, McBride et al. 2013). *'Vicious cycle'* is clarified by Stokes, and it is referred to the impact of mechanical weight on the vertebral development in the spine with scoliosis. Stoke is not the first researcher to address the vicious cycle. Roaf had already utilized the term 'vicious cycle' to depict the impacts of gravity on thoracic vertebral endplate physes in Scheuermann's illness. Despite the fact that this theory is appealing, the legitimacy of this mechanical stress development relationship speculation stays to be demonstrated. This thusly requires quantitative data about the loading condition of the spine with scoliosis, considerable development changes and geometrical changes (Stokes, Burwell et al. 2006) .

Biomechanical stress reduces axial growth by inducing different effects on bone. The effect of compression is the reduction in the axial growth, with reduced numbers of proliferating chondrocytes and reduced chondrocytic enlargement in the hypertrophic zone. The wedging of discs that is seen in scoliosis may involve an asymmetrical tissue remodeling or selective concave side degeneration. It was reported that the growth rates at axially loaded growth plates (tail vertebrae and proximal tibiae) were found to be modulated relatively uniformly (independent of anatomical location) and proportional to stress magnitude. The growth data were therefore expressed in a linear formulation of growth G as a function of compressive stress (Stokes, McBride et al. 2011). Mechanical modulation of growth (Hueter-Volkmann standard) is thought to be included in the pathomechanism of the dynamic deformation of the vertebrae. Changes in the mechanical environment may incorporate modifications and asymmetry of stacking and movement (Stokes 2007). In an attempt to understand the mechanism of progression of scoliosis during growth, it was reported that there is proportional alteration in growth rate of vertebral and proximal tibial growth plates of three different species (rat, rabbit, and calf), in response to differing magnitudes of stress. The relationship was apparently linear and a value of growth sensitivity (percent change per unit stress) was

reported for both vertebrae and tibiae. The results of this work support the vicious cycle theory of scoliosis progression (Lafortune, Aubin et al. 2007).

Mechanical loading affects the endochondral bone development. In particular, increased weight on the physis decreases development while reduced weight quickens development. Studies show that chondrocytic hypertrophy plays a key role in the development plate mechanobiology, as it is likewise in typical regulation of development. The zone of hypertrophy is the slightest inflexible development plate part and would encounter the highest deformity under development loading, and this makes it as a consequence the basic mechano-transductive zone. It was found by Villemure et al. that the development plate pressure decreases hypertrophic zone thickness, diminishes hypertrophic chondrocyte volume and additionally creates a loss of hypertrophic columnar game plan and decreased outflow of the chief collagenous extracellular network proteins (sort II and X collagens). The reason for collagenous corruption (mechanical versus enzymatic) is not known. The arrangement of changes (network creation, tissue and cell morphometry) is not decided either, yet unmistakably these variables are closely related.

III.3. Vertebral bone tissue

It is increasingly believed that one of the primary intrinsic factors in AIS pathogenesis is abnormal vertebral bone tissue. There are several examples of studies that show a corrolation between changes in bone quality/quantity and scoliosis. Lumbar spine bone mineral density and altered vertebral growth cause rotational lordosis, suggesting that low bone mineral status could be correlated with AIS. Using energy X-ray absorptiometry and peripheral quantitative computer tomography respectively, it was found that AIS patients have low bone mineral density (BMD) (Cheng, Qin et al. 2000). The tibial BMD showed the most significant difference. The most significant effect was seen in the trabecular bone mineral density (tBMD) of the distal tibiae (Cheng, Qin et al. 2000, Cheng, Tang et al. 2001, Lam, Hung et al. 2011). In another study, and in correlation to the low BMD, bone histology of patients with AIS was found to have significantly less osteocytes (Sun, Qiu et al. 2009). Bone histology showed significant less osteocytes count in the trabecular bone with smooth and

continuous borders. This suggests that AIS patients have alteration in the bone turnover. Possible causes of the low BMD are the abnormal metabolism associated with several factors like Runx2 expression (Sun, Qiu et al. 2009, Wang, Sun et al. 2014) that could play an important role in the etiology and pathogenesis of AIS. Curve progression prognosis was corrolated with osteopenia that could be considered as one of the risk factors of progression of the curve in AIS patients during brace treatment. It is possible that the status of the BMD will help predict the outcome of brace treatment (Sun, Wu et al. 2013).

III.4. Paraspinal muscles

One of the factors that could be involved in the progression of the scoliotic curve is dysfunction in the paraspinal muscles. It was found that patients with AIS have asymmetries in these muscles as detected by electromyography. Subjects with AIS had higher maximal integrated electromyography (IEMG) activities in the left lumbar muscle, recorded at the onset and during the early (submaximal) phases of muscle contraction, (Avikainen, Rezasoltani et al. 1999) and also abnormalities in neuromuscular transmission that could be of pathogenetic significance. The paraspinal and intercostal muscles at the apex of the scoliotic curvature examined in some of the patients showed similar abnormalities. The paraspinal and intercostal muscles at the apex of the scoliotic curvature examined in some of the patients showed similar abnormalities. Study on the extensor digitorum communis muscle (EDC) found moderate but significant increase in fiber density, mild but significant abnormality in neuromuscular transmission, and moderate prolongation of the mean interspike interval was observed (Trontelj and Fernandez 1988). In addition, defects in paraspinal and intercostal muscles at the apex of the scoliotic curvature were observed (Trontelj and Fernandez 1988).

Assymmetries between the convex and concave sites of the muscle were observed from reduced protein synthesis in the bottom of thoracic curve of children with idiopathic scoliosis. Muscle protein synthesis was measured bilaterally at the top, apex and bottom. Analysis showed that there was increased synthesis on the convexity more than on the concavity at the apex of the spinal curve. The RNA activity at the muscle was lower at the curve apices on the concave vs the convex side, also with differences in muscle histology and a lower type I fiber

diameter, and a lesser proportion of type I fibers on the concavity. Muscle protein turnover differences are secondary to an increased muscle contractile activity on the curve convexity and functional immobilization of the muscle on the curve concavity and greater fibrosis and fatty acid involution in the concave site compared to the convex site (Gibson, McMaster et al. 1988, Wajchenberg, Martins et al. 2015). Myopathy, muscular atrophy due to necrosis, presence of hyaline fibers, and mitochondrial proliferation were observed at both sides (Gibson, McMaster et al. 1988, Wajchenberg, Martins et al. 2015).

III.5. Role of erect posture

The human is the only naturally occurring bipedal being who is affected by scoliosis disease. This strengthens the significance of the bipedal posture, where the orangutan spine was used as a model for human spine. Analysis of this model shows that it has characteristics of human AIS such as the predominant right side curve, vertebral rotation to convexity, displacement of the spinal cord to the concavity, and an unequal number of ribs on either side. Congenital anomaly was not seen. The difference and unusual features of this animal model to human AIS include male gender, a short curve, and kyphosis at the apex. The observations in orangutan model suggest that erect posture is important in the morphology of human idiopathic scoliosis (Taylor 1983, Machida, Murai et al. 1999, Naique, Porter et al. 2003). To study if the bipedal position is essential for development of scoliosis, chickens were pinealectomized shortly after hatching and this resulted in scoliosis closely resembling human idiopathic scoliosis. No scoliosis developed in quadripedal rats. The bipedal condition, such as that in chickens or humans, plays an important role in the development of scoliosis. The findings suggest a critical influence of a postural mechanism for the development of scoliosis. This upright stature causes weakening of the spinal column with backward shear stress. This will lead to rotator instability, which could be the origin of scoliosis (Machida, Murai et al. 1999, Machida, Saito et al. 2005).

III.6. Genetic factors

Several genes and chromosomal loci have been associated with scoliosis. This part is discussed in details in the next sections.

IV. Genetics of AIS:

The genetic causes of IS are not well understood, although there is clear evidence that there is a genetic component to the disease. Several genetic factors affect the etiology of this disorder; however, the mode of inheritance is unclear. Twin studies have resulted in a wide range of concordance estimates for IS, with rates ranging from 0.73 and 0.92, 0.36 and 0.63 for monozygotic and dizygotic twins, respectively. Monozygous twins have a statistically significant higher rate of concordance than dizygous twins, and the curves in monozygous twins develop and progress together. These data support the hypothesis of a genetic etiology for AIS (Kesling and Reinker 1997, van Rhijn, Jansen et al. 2001, Andersen, Thomsen et al. 2007). The study of concordance rates in mono and dizygotic twins should support the fact that AIS should have genetic basis. Also, familial clusters put the ground for the importance of heredity in IS. It was found that there is 55, 12 and 7 times higher presence of AIS among relatives than in a given population. In one of the studies on the genetics of AIS, it was found that the inheritance was 88% in first degree relatives, 70% in relatives of male index patients and 10% in the female relatives. Several reports in literature suggest that AIS could have an autosomal dominant, X-linked dominant and autosomal recessive mode of inheritance. The first examples of dominant mendelian inheritance of AIS was given by Hugh G. Garland in 1934 (Garland 1934), who described that in a family with scoliosis transmitted through five generations and the deformity appears to be primary-disease and not secondary to another disease. Segregation analysis using a model with age and gender effects was applied to 101 pedigrees ascertained through a proband with IS. The transmission probability model was used to detect major gene effect. When the pedigrees were analyzed, affected status was assigned to persons with a Cobb's angle of more than 5 degrees, no significant major gene effect was observed. However, when the affected status was assigned to persons with pronounced forms of disease only (a curve of at least 11 degrees), a significant contribution of a major causal

gene could be established and inheritance could be described according to a dominant major gene diallele model, assuming incomplete sex and age dependent penetrance of genotypes. According to this model, the pronounced forms of idiopathic scoliosis should never occur in the absence of the mutant allele. This indicates that only the carriers of the mutant allele develop pronounced forms of the disease. At the same time, only a fraction of the carriers of the mutant gene should manifest the disease (30% of males and 50% of females) (Garland 1934, Wynne-Davies 1968, Cowell, Hall et al. 1972, Riseborough and Wynne-Davies 1973, Czeizel, Bellyei et al. 1978, Carr 1990, Axenovich, Zaidman et al. 1999, Justice, Miller et al. 2003).

Although a strong inherited component has been reported in familial studies in AIS, the predisposition genes are still to be established. Genome wide association studies (GWAS) allowed the investigation and identification of genes associated with AIS. Table 1 represents a summary of gene variants identified through Sanger sequencing and GWAS studies.

Table 1**:** List of genes and identified mutations variants.

Gene name	Function	Position SNP
BNC2	Zinc finger transcription factor	rs10738445 (Ikegawa 2016, Xu, Xia et al. 2017) rs3904778 (Ogura, Takeda et al. 2018)
MIR4300HG	The host gene of a microRNA, MIR4300. Enhancer activity	rs3533356 (Ogura, Kou et al. 2017)
MAPK7	Regulates gene expression	c.886G> A, c.1943C> T c.1760C> T (Gao, Chen et al. 2017)
MEIS1 *MAGI1* *TNIK*	Normal development Scafolding protein at cell-cell junction Activator of Wnt signalling pathways	rs7593846 rs7633294 rs9810566 (Zhu, Xu et al. 2017)
POC5	Centriolar protein	[c.304_305delGA (p. D102*)] (Weisz Hubshman, Broekman et al. 2017) rs6892146 (Xu, Sheng et al. 2017) c.G1336A (p.A446T), c.G1363C (p.A455P), and c.C1286T (p.A429V) (Patten, Margaritte-Jeannin et al. 2015)
SOX9 and KCNJ2	Master transcription factor of cartilage Potassium channel, a component of the inward rectifier current IK1	rs12946942 (Ikegawa 2016) rs12946942 (Bae, Cho et al. 2012, (Miyake, Kou et al. 2013)

Gene name	Function	Position SNP
ESR2	Estrogen response Skeletal growth and maturation	rs1256120 SNP (Zhao, Roffey et al. 2016)
VANGL1	Regulators of WNT/planar cell polarity (PCP) signaling	p.I136N and p.F44 (Andersen, Farooq et al. 2016)
LBX1	Control the expression of genes that guide migrating muscle precursors and maintain their migratory potential	rs11190870 (Jiang, Qiu et al. 2013, Grauers, Wang et al. 2015, Guo, Yamashita et al. 2016, Ikegawa 2016, Ogura, Kou et al. 2016, Li, Gao et al. 2018, Nada, Julien et al. 2018) rs678741 29(Zhu, Tang et al. 2015, Nada, Julien et al. 2018)
ADGRG6	Spinal development	rs6570507 (Kou, Takahashi et al. 2013, Ikegawa 2016) rs7755109 (Xu, Yang et al. 2015) Rs9403380 (Qin, Xu et al. 2017)
AKAP2	Skeletal development	c.2645A>C (p.E882A) (Li, Li et al. 2016)
COL11A2	Extracellar matrix gene	Novel coding variants (Haller, Alvarado et al. 2016)
AJAP1	Cell–cell and cell-extracellular matrix interactions that could be involved incell adhesion, migration and invasion	rs241215 (Zhu, Tang et al. 2015)

Gene name	Function	Position SNP
PAX3 and *EPHA4*	Mediate developmental events, particularly in the nervous System regulates both myogenesis and neurogenesis in the neural tube	rs13398147 (Zhu, Tang et al. 2015)
BCL-2	Key role in apoptosis	rs4940576 (Zhu, Tang et al. 2015)
LEPR	Modulating the serum leptin level, Metabolism, body energy, glucose	rs2767485 (Liu, Wang et al. 2015)
FBN1 and *FBN2*	Extracellular matrix genes	Rare variants (Buchan, Alvarado et al. 2014)
TGFB1	Cellular proliferation, growth, differentiation, adhesion, inter-cell signaling, as well as on the formation and degradation of extracellular matrix proteins	rs1800469 rs1800471 (Ryzhkov, Borzilov et al. 2013)
MATN1	Organization of chondrocyte into distinct zones of growth plate	rs1149048 (Chen, Tang et al. 2009, Zhang, Zhao et al. 2014) rs1065755 (Bae, Cho et al. 2012)

Gene name	Function	Position SNP
IL-17RC	Promoting the production of several pro-inflammatory cytokines	rs708567 (Zhou, Qiu et al. 2012)
GPER	Take part in the estrogen-related regulation of skeletal development	rs3808351, rs10269151 and rs426655s3 (Peng, Liang et al. 2012)
TIMP-2	Natural inhibitors of the MMPs, major TIMP expressed during endochondral ossification,	rs8179090 (Jiang, Qian et al. 2012)
CHL1 and *LOC642891*	Axonal guidance and neuronal migration	rs10510181 rs1400180 (Sharma, Gao et al. 2011)
ERβ	Modulate estrogen effects on bone	458T>C (Zhang, Lu et al. 2009)
TPH1	Rate-limiting enzyme TPH of serotonin biosynthesis in pinealocyte	rs10488682 (Wang, Wu et al. 2008)
IL-6 and *MMPs*	Acute-phase proteins	MMP-3 5A/5A gene polymorphism and - G/G genotype IL-6 (Aulisa, Papaleo et al. 2007)
MTNR1B	Mediates Melatonin biologic effects	rs4753426 (Qiu, Tang et al. 2007)
IGF-I	Pivotal role in bone growth	rs5742612 and rs2288377 (Yeung, Tang et al. 2006)
ESR1	Mediates estrogen effects on bone	PvuII T/C polymorphism, dbSNP#: rs2234693and XbaI (A/Gpolymorphism,dbSNP#: rs9340799)(Tang, Yeung et al. 2006)

IV.1. Selected candidate genes involved in AIS and their biological roles

IV.1.1.Different gene groups involved in AIS

Table 1 shows some of the genes associated with AIS. Based on the function, these genes can be classified into extracellular genes (*COL11A2*, *AJAP1*, *FBN1* and *FBN2*, *TGFB1*, *MATN1*), genes important for development (*AKAP2*, *PAX3* and *EPHA4*, *CHL1* and *LOC642891*, *ADGRG6*, *MATN1*, *MEIS1*, *MAPK7*, *SOX9*, *VANGL1*, *LBX1*), gene regulation (*BNC2*, *MAPK7*), inflammation (*IL-17RC*, *IL-6* and *MMPs*), estrogen response (*ESR2*, *GPER*, *ERβ*, *ESR1*) and cell cycle (*POC5*). In the upcoming paragraphs, I will be discussing the genes that have been widely associated with AIS based on data from literature.

The phenotype of AIS patients share several characteristics with cartilage extracellular matrix (ECM) disorders, this fact was the basis for studying the genes associated with the assembly of the ECM. Several ECM genes, such as *COL1*, *FBN1* and *FBN2*, are major components in the supporting structures of the spinal column (Bae, Cho et al. 2012). The *MATN1* is highly expressed in the cartilage and is essential for the organization of the ECM (Deak, Wagener et al. 1999). *AJAP1* plays a role in cell–cell and cell-extracellular matrix interactions and hence it could be implicated in cell adhesion, migration and invasion. The latter is an important factor in regulating bone growth and osteoblast differentiation, both are significant factors in AIS pathogenesis (Zhu, Tang et al. 2015). Thus GWAS and exome sequencing studies were targeted on identifying gene variants in different populations especially in Asian (Chen, Tang et al. 2009, Bae, Cho et al. 2012, Zhang, Zhao et al. 2014, Zhu, Tang et al. 2015) European (Buchan, Alvarado et al. 2014, Haller, Alvarado et al. 2016) and Russian (Ryzhkov, Borzilov et al. 2013) populations.

Developmental genes have been widely studied in AIS. *AKAP2* is involved in skeletal development. Through exome sequencing, *AKAP2* co segregated with AIS in all of the family members in Chinese Han population (Li, Li et al. 2016). Through GWAS study in Chinese girls, variants in *EPH* receptors and *PAX3* were found to be associated with AIS (Zhu, Tang et al. 2015). *EPH* receptor is involved in the development of the nervous system (Frisen and

Barbacid 1997). The *PAX3* is also a developmental gene that regulates both myogenesis and neurogenesis in the neural tube (Schubert, Tremblay et al. 2001, Buckingham and Relaix 2007). Both are important for the development of vertebral muscle. Paravertebral muscle abnormalities have been suggested as the cause of AIS (Kouwenhoven and Castelein 2008) and *PAX3* mutations cause muscular, neural tube and vertebral column defects (Farin, Mansouri et al. 2008, Xiao, Zhang et al. 2011). Through GWAS studies in Texas families, both overlapping genes, *CHL1* and *LOC642891*, were associated with AIS (Sharma, Gao et al. 2011). *CHL1* is closely related to *Robo3*, mutations in the latter causes horizontal gaze palsy characterized by severe scoliosis (Jen, Chan et al. 2004). *CHLI* have functions in axonal guidance and neuronal migration, when mutated this possibly might end up with aberrant axonal growth and directionality. As described above, the nervous system is an important factor in AIS pathogenesis. Several studies focused on the association of the *LBX1* gene with AIS in several populations including French Canadian (Nada, Julien et al. 2018), Chinese Han (Gao, Peng et al. 2013, Jiang, Qiu et al. 2013, Liu, Wu et al. 2017), Scandinavian (Grauers, Wang et al. 2015), East Asian (Chen, Zhao et al. 2014, Liang, Xing et al. 2014), Asian and non-Hispanic white groups (Londono, Kou et al. 2014), Southern Chinese (Fan, Song et al. 2012) and Japanese (Takahashi, Kou et al. 2011). *LBX1* belongs to the group of homeobox genes and is expressed in the dorsal part of the spinal cord and hindbrain. *LBX1* plays a role in development of the sensory pathway in the spinal cord by controlling the fate of dorsal spinal and hindbrain somatosensory neurons (Gross, Dottori et al. 2002, Sieber, Storm et al. 2007). Mutations in *LBX1* cause somatosensory defect and thus contribute to AIS (Takahashi, Kou et al. 2011). Another widely studied gene in AIS is *ADGRG6*. GWAS and sequencing analysis were performed in Chinese (Xu, Yang et al. 2015, Qin, Xu et al. 2017) and Japanese (Kou, Takahashi et al. 2013) populations. The *ADGRG6* gene belongs to the family of adhesion G protein coupled receptors, and *ADGRG6* might play important roles in development and disease (Patra, Monk et al. 2014). The *ADGRG6* was found to have high expression in the cartilage (Kou, Takahashi et al. 2013) and vertebral bodies (Patra, van Amerongen et al. 2013).

Transcriptional factors are also implicated in AIS pathogenesis. *BNS2* mutations have been found in Chinese (Ogura, Kou et al. 2015, Xu, Xia et al. 2017) and Japanese populations to be

associated with AIS (Ogura, Kou et al. 2015, Ogura, Takeda et al. 2018). *BNC2* is a zinc finger transcriptional factor highly expressed in musculoskeletal tissues such as spinal cord, bone and cartilage (Ogura, Kou et al. 2015). The suggested function of *BNC2* is the nuclear processing of mRNA (Lamond and Spector 2003). Mutations in *BNS2* are suggested to regulate the transcriptional activity of *BNC2* (Ogura, Kou et al. 2015). Another gene that is involved in transcriptional regulation is the *MAPK7*. Little is known about the association of *MAPK7* and AIS. Recently, sequencing in Chinese family identified disease associated variants (Gao, Chen et al. 2017). The *MAPK* gene belongs to the family of MAP kinases that are activated by growth factors and cellular stress and has a function in transducing intracellular signals.

Inflammatory factors also play a role in AIS pathogenesis. There exists a correlation between matrix metalloproteinases (MMPs) and disc degeneration. *MMP* is differentially expressed between the concave and the convex sides of the scoliotic curves and thus, this strengthens the role of these enzymes in the pathogenesis and progression of scoliosis (Crean, Roberts et al. 1997). Hence, polymorphisms in *MMP*s have been studied in Italian (Aulisa, Papaleo et al. 2007), and Hungarian (Morocz, Czibula et al. 2011) and the studies found that gene variants in MMPs might be involved in the susceptibility to scoliosis. Not only MMP but other inflammatory factors like IL-6 has been also investigated for possible roles in AIS. IL-6 is a proinflammatory cytokine, whose concentration is increased in the nucleus pulposus of scoliotic discs in response to exogenous pro-inflammatory stimulus. As a consequence, the inflammatory reaction is amplified and this results in more degeneration of the intervertebral disc (Burke, RW et al. 2003). Polymorphisms of *IL-6* has been described in Italians (Aulisa, Papaleo et al. 2007) Hungarians (Morocz, Czibula et al. 2011) populations and have been associated with AIS. The mutation in *IL-6* affects function and activity of the protein.

The ciliary genes, Estrogen receptor polymorphisms and *POC5* will be described in section III.2. (Ciliary genes: Cilia and its connection with AIS), chapter II (Hormonal factors associated with AIS) and chapter III (POC5 AND AIS) respectively.

IV.2. Ciliary genes: Cilia and its connection with AIS

The role of cilia in AIS is emerging. Several studies (Kamiya, Shen et al. 2015, Grimes, Boswell et al. 2016, Kobayashi, Asano-Hoshino et al. 2017, Oliazadeh, Gorman et al. 2017) indicate a significant involvement of cilia in the pathogenesis of AIS. Cilia plays important roles in motility, mechanotransduction and sensory perception and they are expressed in most-mitotic epithelial cells and differentiated cells, which have exited the cell cycle. Given the critical role the cilia plays, I will focus on the upcoming paragraphs on the studies that found correlation between ciliary anomalies and AIS occurance.

IV.2.1. *KIF 6*

KIF6 belongs to the family of kinesins (KIFs). Kinesin-9 superfamily has only been identified in vertebrates and protozoa and that's why they have been suggested to have a role in cilia and flagella. *Kif6* is downregulated in *Forkhead box J1* (FoxJ1)-null mice, which suggests a role of *Kif6* in cilia (Jacquet, Salinas-Mondragon et al. 2009). *FoxJ1* has significant roles in the differentiation of ependymal cells (Li, Handsaker et al. 2009) which have cilia and line ventricles in the brain and the central canal in the spinal cord. The function of ependymal cells also includes the circulation of cerebral spinal fluid. *KIF6* expression is limited to the ependymal layer of the ventricle (Li, Handsaker et al. 2009) and central canal of the spinal cord. In a recent work in identifying new genes in AIS, *kif6* mutant zebrafish were found to have scoliotic phenotype. These proteins were identified as transport proteins for organelles, protein complexes, and mRNAs to specific destinations in a microtubule and ATP-dependent manner. During mitosis and meiosis, kif proteins have a cooperative role in the movement of chromosomes and spindles. These proteins contain a highly conserved amino acid sequence among all eukaryotic phyla studied thus far. The motor domain includes a conserved sequence that is proximal to a Walker ATP binding motif and a microtubule binding domain. Kifs have different sequences postside the motor domain. Kifs interact with cargo molecules and it occurs outside the motor domain. It has been shown recently that by the interaction with adaptor proteins, this helps kifs in attachment to cargos (Miki, Setou et al. 2001). Although KIF6 was originally distinguished as an orphan kinesin (Miki, Setou et al. 2003, Miki, Okada

et al. 2005) it was considered a member of the kinesin-family member 9 (kif9) in the Kinesin-9 superfamily. KIF9 and KIF6 have a conserved sequence near the kinesin motor domain which is specific to the Kinesin-9 superfamily (Miki, Okada et al. 2005), knowing that however, the two proteins are phylogenetically distant (Miki, Setou et al. 2001). Zebrafish mutant of *kif6* was reported to show spinal deformity and they were named skolios. The phenotype that was seen is primary and not secondary to other phenotypes. In skolios, there was noted sexual dimophism like in human IS. Unlike in humans, in skolios both genders were affected, but over time, adult male mutants developed a more severe spinal deformity compared with adult females. This observation doesn't apply to humans and it can be explained that the gender factor could be involved in progression but not susceptibility (Buchan, Gray et al. 2014). The significance of this study is that the presented skolios could represent a model for human IS and could help understand pathogenesis of AIS. The skolios were viable and not lethal which could also help in understanding molecular events in the progression of AIS. The mentioned study presents a new role of *KIF6* in spinal development and stability, and hence expanding the functions of kinesins.

IV.2.2. *PTK7*

In mammals the somites give rise to vertebral bodies. This is an organized pathway that is regulated by the network of Notch, canonical Wnt/β-catenin and FGF signalling pathways which will regulate the expression of multiple genes along the posterior body axis that drive rhythmic somite production from the presomitic mesoderm (Pourquie 2007). *PTK7* is one of the key organizers of canonical Wnt/β-catenin and non-canonical Wnt/PCP signalling activity and is essential for vertebrate embryonic patterning and morphogenesis. Experiments in *ptk7* mutant zebrafish reveal an important role of this gene in developmental pattering and morphogenesis (Hayes, Naito et al. 2013).

The *PTK7* is a typical tyrosine kinase that is conserved through evolution and has been found to have a role in Wnt, Semaphorin/Plexin and VEGF signal transduction. PTK7 could be part of the Wnt receptor complex since it interacts with Wnt ligands, Frizzled 7 and LRP6 co-receptors (Takeuchi 1966, Shnitsar and Borchers 2008, Peradziryi, Kaplan et al. 2011). It was

found that both canonical Wnt/b-catenin and non-canonical Wnt/PCP signalling activity were disrupted by the *PTK7P545A* allele, which confirms the effect of dysregulated Wnt signalling in IS (Hayes, Gao et al. 2014). The activation of the receptor complex endocytosis is an essential step in Wnt/PCP and Wnt/b-catenin signal activation, *PTK7P545A* was found to be more localized at the plasma membrane which possibly could result in defective Wnt signalling altering complex trafficking (Hayes, Gao et al. 2014).

Animal models of scoliosis are limited unless bipedal posture is acquired which necessitates the upright posture that is found in humans. Knowing that, in Teleosts there is biomechanical forces along the spine that can make fish more susceptible to late-onset spinal curvatures (Gorman and Breden 2007, Gorman and Breden 2009, Janssen, de Wilde et al. 2011, Ouellet and Odent 2013). This fact makes fish a good model of human scoliosis. Depending on the timing of the loss of function of *ptk7*, mutant zebrafish develops spinal deformities that model congenital and idiopathic scoliosis. Interestingly female mutant zebrafish had more severe curves than males and hence this makes the model a good representation of human AIS (Hayes, Gao et al. 2014).

As discussed above, *ptk7* mutant zebrafish develop scoliosis (Hayes, Gao et al. 2014). To understand the etiopathogenesis of IS, in another work, dysfunction of motile cilia was investigated. Motile cilia function in the flow of extracellular fluid. Wnt/PCP and Wnt/Catenin play a role in cilia function (Park, Mitchell et al. 2008, Caron, Xu et al. 2012). The proof of possible defects of cilia in AIS is suggested by the fact that there is abnormal L-R asymmetries and defective flow in IS patients (Wang, Yeung et al. 2011), and an elevated incidence of scoliosis among primary ciliary dyskinesia patients (Engesaeth, Warner et al. 1993). Analysis of *ptk7* mutants shows that they have abnormal CSF flow within the ventricular system that goes along with a role for EC motile cilia defects in the etiology of IS (Grimes, Boswell et al. 2016).

IV.2.3. *ZMYND10*

The *ZMYND10* gene (zinc finger, MYND-domain-containing 10, NM_015896.2) is located on chromosome 3p21 and it encodes a tumor suppressor protein. ZMYND10 downregulates cell proliferation either through apoptosis or by cell cycle regulation. It was found that it inhibits the growth of nasopharyngeal carcinoma cells, arrests the cell cycle at the G1 phase, downregulates JNK (c-Jun N-terminal kinase) and cyclin D1 promoter activities, and inhibits phosphorylation of c-Jun (Zhang, Liu et al. 2012). Recently, mutations in *ZMYND10* were identified as primary ciliary dyskinesia (PCD) disease causing gene (Moore, Onoufriadis et al. 2013). PCD is caused by defects in motile cilia that result in recurrent respiratory functions and male infertility. ZMYND10 interacts with LRRC6 (Zariwala, Gee et al. 2013). *LRRC6* is a gene that is essential for proper axonemal assembly of inner and outer dynein arms. Mutations in *LRRC6* cause primary ciliary dyskinesia (Kott, Duquesnoy et al. 2012).

Recently, in medaka zebrafish, reduced expression of *zmynd10* lead to the loss of the outer dynein arms (ODA), loss in Kupffer's vesicle (KV) cilia, and resulted in a motility defect. Morphants had curly-tail-down (CTD) and LR asymmetry, which are characteristic motile ciliary mutant phenotypes in fish. The LR asymmetry phenotype was variable. Embryos were characterized by having reversed ambiguous heart looping and/or reversed liver position. The knockout medaka zebrafish were analyzed at later stages of development and they were characterized with complete loss of motility of sperm, scoliosis and progressive polycystic kidney (Kobayashi, Asano-Hoshino et al. 2017). Not only in *zmynd10* fish, there was scoliosis but also another medaka mutant, joi/mii, which suggests that scoliosis is the phenotype resulting from defects in the motility of cilium (Kobayashi, Iijima et al. 2010). In humans, it is quite rare to have PCD with scoliosis, however, scoliosis association with PCD was presented in some studies (Engesaeth, Warner et al. 1993, Tanaka, Sutani et al. 2007, Yazicioglu, Alici et al. 2016). It seems that fish PCD mutants are more sensitive to developing scoliosis than humans. Probably, fish as aquatic species do not need to maintain posture; and hence there is no requirement for strong connections between vertebrae. However, in humans, the rigidity of the vertebra is a must due to the terrestrial environment and bipedalism.

IV.3. Adhesion GPCRs

The adhesion *ADGRG6* has been widely associated with AIS. Through GWAS studies and sequencing analysis studies, it was found that mutations in *ADGRG6* (Table 1) are causative of AIS in Chinese populations (Kou, Takahashi et al. 2013, Xu, Yang et al. 2015, Qin, Xu et al. 2017). Edery et al (Edery, Margaritte-Jeannin et al. 2011), identified the AIS disease causing gene to be located on chromosomes 3 and 5. Further studies by Patten et al (Patten, Margaritte-Jeannin et al. 2015), found variants of *ADGRG7* in AIS patients. In the next paragraphs, I will discuss structural and functional characteristics of ADGRGs specifically *ADGRG7*.

IV.3.1. ADGRG6 and *ADGRG7*

Adhesion GPCRs belong to the large group of G protein-coupled receptors (GPCRs). Thirty-three members were found in human and thirty in mice. A large extracellular N-terminus is present in all members of this group. This part of the receptor include various adhesion domains such as epidermal growth factor-like repeats, thromospondin-like repeats and cadherin like repeats (Paavola and Hall 2012). A characteristic feature of this group of membrane proteins is GPCR proteolysis site (GPS), its function is to help in the catalytic processing of the extracellular N-terminus or the 7 transmembrane C-terminal fragment (Monk, Hamann et al. 2015). It was reported that mutations in this domain can lead to the misfolding of the receptor and human disease. Most members of the adhesion GPCRs are orphan with no assigned ligand (Tang, Wang et al. 2012) (Fig. 2).

An interesting feature of these proteins is that a N-terminal truncation can result in the activation of the adhesion GPCR constitutively. Several data from different work on GPR56, BQAI2 and CD97 suggest that it could be a general feature for activation of adhesion GPCRs. To elucidate more, it is suggested that when there is cleavage of the N terminus by autoproteolysis, with the maintenance of the association to the 7TM of the receptor, this exerts an inhibitory effect on receptor signaling.

Common variants near *GPR126/ADGRG6* (encoding the adhesion G protein-coupled receptor) were found in several studies to be associated with AIS in humans through GWAS studies (Qin, Xu et al. 2017, Liu, Liu et al. 2018). The knockdown of adgrg6 in zebrafish resulted in delayed ossification of the developing spine (Kou, Takahashi et al. 2013). In mice, the loss of Gpr126 result in scoliosis without affecting the structure of the vertebra (Karner, Long et al. 2015). Not only scoliosis, but also the loss of *Gpr126* caused pectum excavatun (PE) by upregulating *Gal3st4*, a gene implicated in human PE, encoding Galactose-3-O-sulfotransferase 4 (Karner, Long et al. 2015).

ADGRG7 belongs to the adhesion family of GPCRs that was identified in the celera database. *ADGRG7* relates phylogenetically to the cluster that was previously known for a few years including *HE6, GPR56, GPR97, GPR112,* and *GPR114*. ADGRG7 have common motifs with ADGRG6 that include FTWMG(A)E(S)A in TMIII and the Trp in TMIV with the other receptors in this phylogenetic cluster such as GPR97 and HE6. So far, there is no other domain apart from GPS that have been identified in ADGRG7. This fact is also applied to the phylogenetically related (ADGRG2, ADGRG1, ADGRE5, and ADGRG5) (Fredriksson, Gloriam et al. 2003). However, the physiological function of ADGRG7 is not well described. In one of recent work on ADGRG7, it was found that ADGRG7 has an important role in body weight (Ni, Chen et al. 2014). In another study, two variants were identified one in *ADGRG7* and one in *POC5* (Edery, Margaritte-Jeannin et al. 2011). It is possible that *ADGRG7* is acting as modifier, contributer gene rather than a causative gene in AIS.

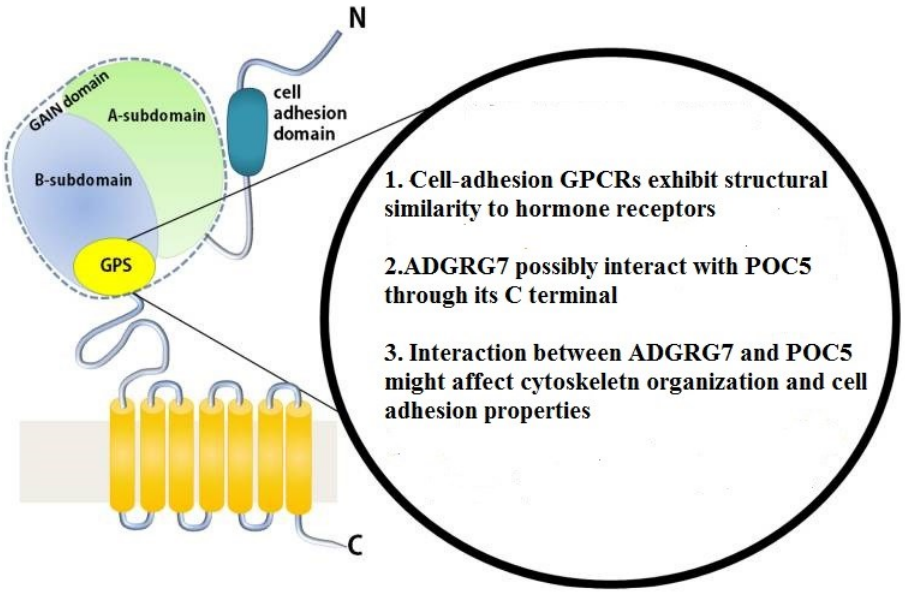

Figure 2: Schematic diagram of an adhesion-GPCR. The typical adhesion GPCR consists of a gain domain, a 7 transmembrane domain associated with GPS domain and a cell adhesion domain. The GAIN and 7 transmembrane domains are located at the C-terminus of the receptor. The cell adhesion GPCRs share structural homology to the hormone receptors. The hypothesis that there is interaction between ADGRG7 and POC5, which will eventually affect cytoskeleton organization and cell adhesion properties, is to be investigated. Adapted from Hamann et al. (Hamann, Aust et al. 2015).

V. Hormonal factors associated with AIS

Based on several observations, hormonal factors, specifically estrogens, were found to play significant roles in bone mass acquisition and/or formation and, consequently, in the pathogenesis of AIS, however the mechanisms involved are not clear. Estrogens crosstalk with melatonin and other biochemical factors like calmodulin (Letellier, Azeddine et al. 2008, Leboeuf, Letellier et al. 2009). Other hormones like leptin (Qiu, Sun et al. 2007, Tam, Liu et al. 2016) were also found to be associated with AIS. The role of each hormone in AIS will be discussed.

V.1. Role of estrogen

Several studies suggest that AIS is an endocrinal disease (Barrios, Cortes et al. 2011). It's possible that growth hormone play a role in AIS pathophysiology (Allen 1996). The fact that young females with scoliosis have osteopenia is an indication of estrogen (E2) deregulation in these patients. There is progressive reactivation of estrogen system subsequent to menupause in scoliosis (Cheng and Guo 1997, Cheng, Tang et al. 2001) and the latter support the estrogen receptor (*ESR*) polymorphisms in AIS patients (Wu, Qiu et al. 2006). Until now it is not clear how E2 could have effects on the initiation or progression AIS, however it's possible that estrogens interact with many physiopathological factors that are believed to influence the development of scoliosis (Fig.3).

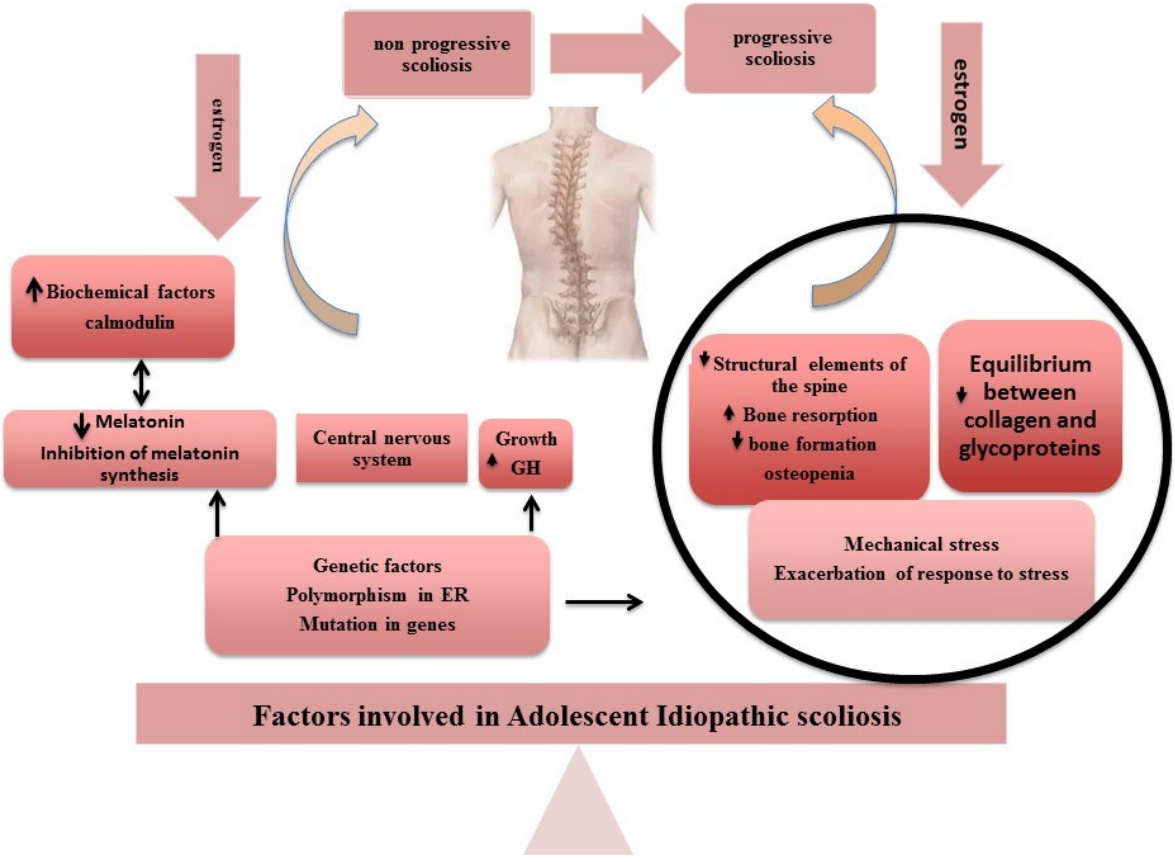

Figure 3: E2 interaction with etiopathogenic factors of AIS. The presence of progression or absence of progression of AIS could be controlled by E2 that crosstalks with several factors like genetic (gene mutations and ER polymorphism). E2 is responsible for maintaining bone

through its effects on osteoblast differentiation, the ratio of Gi to Gs proteins, and keeping balance between collagen and glycoproteins in bone tissues. When these factors are distrupted, this leads to osteopenia. When the initial deformity develops, scoliosis will progress concominatly to the spinal growth by exerting its effects on bone structural and compositional characteristics and biomechanics. Adapted from Leboeuf et al. (Leboeuf, Letellier et al. 2009).

These factors could be melatonin, biomechanical stress and growth. AIS with significant clinical deformities has increased occurance in girls during puberty (Weinstein, Dolan et al. 2008). Scoliosis progresses during puberty, a period of life where estrogens contribute both to the puberty and growth (Eastell 2005). During menarche period, a stage characterized with rise in E2 levels in girls (Eastell 2005), there is large reduction in bone turnover markers. This reduction leads to the closure of the epiphyseal growth plates, the reduction in periosteal apposition and endosteal resorption within cortical bone, and in bone remodelling within cortical and cancellous bone. These effects of E2 on bone are induced through promoting apoptosis of chondrocytes in the growth plate (Grivas, Vasiliadis et al. 2006). Low levels of E2, that occurs during late menarche, will result in reduction in osteoblast proliferation and activity reduction in osteoblast differentiation. This in turn will result in a defect in the rigidity, elasticity and strength properties of bone, including mineralization. Given all these facts, however, the molecular mechanisms and targets of E2 are not known. Recent studies support the hypothesis that it is not the presence or absence of E2 that induces scoliosis but rather the response of bone cells to E2. Effects of combined melatonin and E2 on human osteoblasts from AIS patients and signalling pathways were analyzed, where AIS cells were treated with E2. The level of 3', 5'-cyclic adenosine monophosphate (cAMP) was significantly decreased when compared with the level observed in the presence of increasing concentrations of melatonin alone (Letellier, Azeddine et al. 2008). This finding indicates a cross talk between E2 and melatonin signalling in human AIS osteoblasts. Combined treatments control the coupling of G (S) alpha protein and melatonin receptor (MT2) on human osteoblasts. Based on the mentioned results, treatment with E2 or ESR agonists become important compounds to consider in AIS osteoblast cell functioning (Letellier, Azeddine et al. 2008).

Research is focused on identifying link between ESR polymorphisms and scoliosis however results are contradictory. The cause could be attributed to ethnic group differences, environmental factors that might cause the difference in the result of the studies. Estrogen affects growth hormone secretion (Ylikoski 2003, Perry, McDougall et al. 2008). The fact that children with scoliosis are taller than their peers of the same age can be due to the effect of estrogen on increasing growth hormone secretion (Ylikoski 2003, Perry, McDougall et al. 2008).

V.2. ER AND AIS

AIS occurs mostly in girls during puberty and this has put the ground for extensive research on the role of E2 and *ESR* gene polymorphisms. There is no clear conclusion about the correlation between hormone content, E2, and the development or progression of AIS. Recent research found that the level of intracellular levels of E2 is associated with skeletal muscle strength and power in female (Sipila, Finni et al. 2015). These findings support the fact about the role of muscle E2 in IS.

E2 assumes basically a significant part in cell proliferation and is viewed as chiefly an ovarian sex hormones in charge of cell duplication and development of tissues. E2 has a wide variety of effects that range from regulation of skeletal homeostasis, lipid and digestive system, electrolyte balance, skin physiology (Liang and Shang 2013, Bilal, Chowdhury et al. 2014), the cardiovascular (Baker, Meldrum et al. 2003, Nevzati, Shafighi et al. 2015) system and the focal sensory system (Maggi, Ciana et al. 2004). A very well described activity of E2 is the intense impact on veins to strengthen vasodilation and protect against vascular harm (Cheskis, Greger et al. 2007). E2 likewise assume an imperative part in male physiology. The generation of E2 is not exclusively in the ovaries, there are other extragonadal tissues that deliver E2. The production of E2 in extragonadal tissues is subject to the accessibility of C19 steroids, to be specific testosterone, androstenedione, dehydroepiandrosterone (DHEA) and dehydroepiandrosterone sulfate (DHEAS). In target tissues, testosterone can be changed over to either 5α-dihydrotestosterone (DHT), the vital ligand for androgen receptors, or to E2, the

most powerful of the estrogens. Interestingly, girls with AIS were found to have increased testosterone levels (Raczkowski 2007).

How E2 applies its impact on target tissues? E2 binds to particular receptors assigned as ESR. Despite the significance of E2 signalling, there are just three known receptors that take over the greater part of the E2 actions that are the ERα, ERβ and the G protein coupled estrogen receptor 1.

ERα was the first receptor to be found and is the most fully examined. The other receptor, which is the homologues ERβ was recognized four decades after ERα (Baker 2002). After one decade, G protein-coupled estrogen receptor 1 (GPER1) association with estrogen signaling was recognized.

There are three types of estrogen dependent signallings: 1) Direct genomic signalling pathway, 2) Indirect genomic signalling, and 3) Non-genomic signalling.

Estrogen dependent signaling is grouped into genomic and non-genomic, and this depends on the outcome of activated signalling pathways. Besides, binding of the estrogen-ER complex to DNA can be either direct or indirect.

Direct genomic signaling pathway is considered as the traditional E2 signalling. E2 binds either to ERα or ERβ in the cytoplasm of target cells which prompts conformational changes that result in receptor dimerization, translocation to the nucleus and binding to the estrogen response elements (EREs) placed in or close to the promoters of target genes. The coupling of the ligand to the receptor additionally brings together a mixture of coregulators in a complex that adjusts chromatin structure and enhances the recruitment of the RNA polymerase II transcriptional machinary. Thusly, estrogen-ER complex functions as a transcriptional activator (Keay and Thornton 2009).

Indirect genomic signalling of 17β-estradiol (E2) can also play a role in the expression of genes that do not have EREs in their promoter. Indeed, around 33% of the estrogen responsive

genes don't acquire ERE-like elements. In the ERE-free genomic pathway, there is no immediate binding of the ligand-bound ERs to DNA directly, binding occurs through protein-protein interaction with different classes of transcriptional factors at binding sites. This results in either initiation or inhibition of signalling.

Non-genomic estrogen signalling is regularly connected with a subset of membrane bound ER, e.g. GPR30 and certain variations of ERα and ERβ. E2 can bind to receptors at the cell surface (GPR30) and this results in the activation of intracellular calcium, recruitment of adenylate cyclase and cAMP production, activation of the MAPK signalling pathway, initiation of the phosphoinositol 3-kinase pathway and recruitment of membrane tyrosine kinase receptors (Nilsson, Makela et al. 2001, Eick and Thornton 2011). It is worth to say that the ER could be initiated without E2. The receptors could be phosphorylated on specific sites and this can cause ligand-autonomous ER activation. The two frequently phosphorylated amino acids are serine and tyrosine. Controllers of general cell phosphorylation state, for example, protein kinase A (PKA) or protein kinase C (PKC), extracellular membranes, cytokines or neurotransmitters and cell cycle controllers are part of this pathway.

ESR-1 is a high predisposition factor in AIS because it plays a significant function in the bone turnover during puberty. Sex hormone plays a key role in skeletal growth and maturation. Estrogen receptor, encoded by the gene *ESR1*, is present in both osteoblast and osteoclast (Juul 2001).

Proline, glutamic acid, and leucine-rich protein 1 (PELP1) was recently identified as an important coactivator of the estrogen signaling pathway. PELP1 indirectly activates ESR1 through its interaction with coactivator-associated arginine methyl-transferase. In this study, interestingly PELP1 expression was identified in skeletal muscles (Vadlamudi, Wang et al. 2001) but not in deep paravertebral muscles. There was significantly higher expression level of PELP1 in the deep intrinsic spine muscle (longissimus) comparing to the superficial back muscle (trapezius), the latter belonging to the upper limb girdle muscles. These findings go along with the role of different muscles in scoliosis, where it's the deep muscles and not the superficial, which are involved in scoliosis pathogenesis (Ford, Bagnall et al. 1984). Also, the

work found a correlation between PELP1 expression on the concave side with Cobb angle of the primary thoracic scoliosis. There was also a correlation between the PELP1 and the ESR1 expression but not ESR2. PELP1 was found to be localized in the nucleus within muscular tissue which suggests a function in the chromatin remodeling at target gene promoter (Skibinska, Tomaszewski et al. 2016).

Both melatonin and calmodulin could play a role in the progression of AIS. The administration of TMX, which is a Selective Estrogen Receptor Modulator (SERM) and Calmodulin (CaM) antagonist, help in reducing the rate of progression of the scoliotic curve but doesn't inhibit its development in either pinealectomized chicken or melatonin deficient mice models (Akel, Demirkiran et al. 2009, Akel, Kocak et al. 2009). Also treatment with TMX may revert the curves in treated animals as compared to controls. It's not clear how TMX is inducing its effects in AIS, whether it's through calmodulin or through E2. Raloxifene (RLX) is another SERM - which is similar to TMX - both having estrogenic agonist effects on bone but has less side effects than TMX on humans. RLX exerts its effect on bone by increasing bone density in both animals and humans. The effect of TMX and RLX in pinealictemozied bipedal mice was investigated (Demirkiran, Dede et al. 2014). Bipedal pinealectomized mice were receiving orally TMX or RLX. The effects in treated animals, similar to what was observed before, is the reduction of curve magnitudes but not the incidence of scoliosis curve magnitudes. Higher bone density in RLX receiving groups was correlated with lesser curve. The significance of this work is that both TMX and RLX are possible treatments for the osteopenia observed in AIS patients, and in parallel the scoliotic deformity. It could be also that both RLX and TMX treatments lead to early maturation of vertebral growth plates and decelerating or inhibiting growth process, thus preventing progression of the curves by this mechanism. The significance of this study, is that the usage of E2 modulators could be a promising medical treatment in AIS (Demirkiran, Dede et al. 2014).

Since *ESR1* gene is a highly candidate predisposition gene in AIS, a genetic association study was performed by Inoue et al (Inoue, Minami et al. 2002). In their work, they wanted to identify an association between XbaI polymorphism in *ESR1* and curve severity in AIS. The

results show that XbaI polymorphism can be considered as a disease modifier and could be a strong disease predisposition allele. This work goes along with previous research which showed that XbaI polymorphism could be used to predict curve progression (Wu, Qiu et al. 2006).

In girls with AIS, there is abnormal growth and osteopenia (Cheung, Lee et al. 2006, Villemure and Stokes 2009). In various Asian populations, it was found that there is a link between BMD and *ERS1* genotypes (Boot, van der Sluis et al. 2004, Nam, Shin et al. 2005). Also, the PvuII (T/C polymorphism, dbSNP#: rs2234693) and XbaI (A/G polymorphism, dbSNP#: rs9340799) sites in the first intron of *ESR1*, were associated with risk of osteoporosis and bone mineral density (BMD) at several femoral sites in post menaupause korean population, in Caucasian children, adolescents, and young adults (Boot, van der Sluis et al. 2004, Nam, Shin et al. 2005).

Based on the mentioned evidence, this makes *ERS1* a strong candidate gene for AIS. However, in several studies, they failed to detect any association between the two *ESR1* SNPs and the occurrence of AIS. The results indicated that these two SNPs were not the primarly causative or predisposition allele leading to AIS (Tang, Yeung et al. 2006, Yang, Li et al. 2014).

Finally, to study the possible association between XbaI polymorphism in *ERα* and the effectiveness of brace treatment, it was shown that patients with G allele at the rs9340799 site of the *ESR1* were found to be resistant to brace treatment. Thus, the G allele could be considered a risk factor leading to failure of brace treatment in AIS patients. The significance of this work is that by identifying factors that affect the outcome of brace treatment could help identify whether patient has to undergo brace treatment or continue to receive brace treatment (Xu, Qiu et al. 2011).

V.3. Melatonin

Pinealectomized chicken develop scoliosis (Thillard 1959). In 1959, Marie-Jeanne Thillard found unexpectedly that pinealectomy in young chickens results in spinal deformities. Only on bipedal condition, pinealectomy will lead to reduced levels of melatonin which could result in scoliosis. Bipedalism could be obtained by taking off the forelimbs from baby. In human, progressive scoliosis is correlated with low plasmatic melatonin (Machida, Dubousset et al. 2009). Levels of platelet calmodulin that is usually regulated by melatonin was found to be upregulated in scoliosis (Lowe, Lawellin et al. 2002). The mentioned findings support the hypothesis that AIS could be due to an inherited disorder of neuro-transmitters from neuro-hormonal origin, associated with bipedal condition, where localized neuro-muscular imbalance starts and produces the scoliotic deformity of the fibro-elastic and bony structures (Dubousset and Machida 2001).

Since melatonin is the pineal gland hormone, this puts the ground-supporting hypothesis that defects in posture is due to melatonin deficiency (Thillard 1959, Dubousset and Machida 2001, Machida, Dubousset et al. 2001). In humans, low melatonin levels have been observed in AIS patients (Machida, Dubousset et al. 2009). Some questions need to be answered: is there a correlation between melatonin levels and the curve progression in AIS? Does administration of melatonin into scoliotic patients reduce curve progression? Patients were followed up for a period of 3 to 6 years for serum melatonin. Patients with scoliosis and with low levels of melatonin were receiving melatonin therapy but not normal controls. A big number of patients with scoliosis receiving melatonin had stable curve without progression, however, the untreated patients had progressive scoliosis. Based on the study, low melatonin plays a role in the prognosis of idiopathic scoliosis. The significance of this finding is that severe scoliotic cases could be improved with melatonin supplementation.

Although evidence on the role of melatonin in AIS is documented, there are some contradictory results which show no significant change in circulating levels of melatonin in patients with AIS (Bagnall, Raso et al. 1996, Brodner, Krepler et al. 2000, Sadat-Ali, al-Habdan et al. 2000). Moreau et al. (Moreau, Wang et al. 2004) reported that the melatonin

signalling is indeed defective in patients as demonstrated by cAMP assay. Also, conducted by Moreau et al (Akoume, Azeddine et al. 2010), blood test was designed to serve as a screening test in order to identify asymptomatic children at risk of developing IS and may be used to improve curve progression in patients, hence allowing clinicians to improve therapy outcome. The advantage of this test happens to be that it could be done regardless if patients have IS susceptibility genes. The basis of this test is collection of peripheral blood mononuclear cells (PBMC) and analysis of melatonin signal transduction by cellular dielectric isotropy. This test will allow the assessment of melatonin signalling defects in IS patients compared to normal patients as well as the determination of risk of developing scoliosis in asymptomatic children (Moreau, Wang et al. 2004, Akoume, Azeddine et al. 2010).

V.4. Leptin

Patients with AIS are characterized by having lower body weight, taller stature, lower body mass index (BMI), and abnormal bone quality (Tam, Liu et al. 2016). Leptin is an important factor in regulating energy and bone metabolism and has been reported as one of the etiologic factors of AIS. To confirm the role of leptin in AIS, research was conducted in patients with AIS and in animal models of AIS. In AIS patients, it was reported that they have altered leptin bioavailability. The latter might be the reason why these girls have lower body weight, lower BMI, and abnormal body composition (Tam, Liu et al. 2016).

The association between circulating central leptin and AIS suggests that increased risk of developing scoliosis is enhanced by increased central leptin. In a mouse model, mice were divided into two groups: one receiving injections of leptin in the hypothalamus and one group with no leptin overexpression. Mice receiving leptin had lowered body weight, with higher incidence of developing scoliosis and progression as well (Wu, Sun et al. 2015).

AIS patients could have defects in leptin signalling pathway and bone metabolism (Qiu, Sun et al. 2007, Tam, Yu et al. 2014). AIS girls have low bone mineral density (BMD) that causes development of osteopenia. As discussed earlier, leptin has been suggested as one of the etiologic factors of AIS because of its profound effects on bone metabolism and pubertal

growth. Soluble leptin receptor (sOB-R), is the modulator of leptin, and it plays a role in leptin bioavailability and signalling (Schaab and Kratzsch 2015). The possible correlation between the serum leptin and sOB-R levels and bone quality has been investigated. Compared with normal controls, AIS girls had numerically higher sOB-R lower average vBMD, lower cortical vBMD, higher cortical bone perimeter and higher trabecular area. Only in AIS patients there was correlation between serum leptin level and trabecular bone parameters (Liang, Gao et al. 2012) .

By looking at anthropometric data from scoliotic and normal girls, unexpected findings for skeletal maturation, asymmetries and overgrowth couldn't be explained by currently existing theories of AIS pathogenesis. A new theory in AIS girls has been postulated based on several findings. These findings include (1) thoracospinal concept for right thoracic AIS in girls; (2) the corrolation between sympathetic nervous system to bone formation/resorption and bone growth; (3) the storage of triglycerides in the white adipose tissue; and finally (4) the resistance to leptin by central nervous system in obesity and possibly in healthy females. The suggested theory that explains the high incidence of AIS in girls is that there is disharmony in spine and trunk between autonomic (Burwell, Dangerfield et al. 2008) and somatic (Burwell, Dangerfield et al. 2008) nervous systems. Double neuro-osseous theory for AIS pathogenesis in girls explains that there is selectively increased sensitivity of the hypothalamus to circulating leptin, which results in asymmetry. The origins of the asymmetry are located in the sympathetic nervous system and extend to the growing axial skeleton. This concept is stated as leptin-hypothalamic-sympathetic nervous system concept: LHS concept. In some younger preoperative AIS girls, there is upregulation of leptin by the hypothalamus which also involves the somatotropic (growth hormone/IGF) axis that will result in exaggerated asymmetric skeletal effects and contributes to curve progression. In the somatic nervous system, the central nervous system is responsible for the dysfunction of the spinal deformity in AIS in girls (escalator concept) (Burwell, Aujla et al. 2009). The developmental disharmony in spine and trunk, which is a consequence of increased sensitivity of the hypothalamus to leptin, is translated by osteopenia, biomechanical spinal growth modulation, disc degeneration and platelet calmodulin (Burwell, Aujla et al. 2009).

V. 5. Calmodulin

Patients with AIS have muscle tone disorder (Yarom and Robin 1979). Calmodulin with its ability to bind calcium ions and its role in muscle contraction could be strongly associated with AIS. There are not a lot of studies that target the association between calmodulin and AIS (Kindsfater, Lowe et al. 1994, Lowe, Lawellin et al. 2002, Zhao, Qiu et al. 2009). It was found that calmodulin levels were increased in all the patients with progressive curves, remained stable in 73% of the patients with non progressive curves and were higher generally in curves greater than 30 degrees and double structural curves (Lowe, Burwell et al. 2004). Calmodulin levels usually decreased in patients undergoing brace treatment or spine fusion. Based on the mentioned results, measurement of the calmodulin levels in the platelets could be closely associated with curve progression and stabilization by bracing or spine fusion. Based on this, calmodulin may serve as a biochemical marker of curve progression and to help identify stable and progressive curves (Lowe, Lawellin et al. 2002).

Melatonin and calmodulin have been reported as key factors in scoliosis etiology. Calmodulin is melatonin second messenger and has been shown to have effects on muscle contractility. A possible role of calmodulin in AIS could be regulating spinal alignment. To confirm the role of calmodulin in AIS, platelets from AIS patients undergoing surgery were collected and paravertebral muscle tissue samples from both sides were obtained at T12-L1 level intraoperatively (Acaroglu, Akel et al. 2009). Levels of melatonin and calmodulin were analyzed in the platelets and in the muscle. The calmodlulin concentration in the platelets and in both convex and concave sides muscle was not different between groups. However, the convex side muscle calmodulin to total muscle calmodulin was increased and the concave side muscle calmodulin to total muscle calmodulin was decreased (Acaroglu, Akel et al. 2009). In AIS patients, there is change in paraspinal muscle activity and this could be explained by platelet calmodulin level changes (Lowe, Lawellin et al. 2002). Another hypothesis linking platelet skeletal defects in AIS was suggested and includes: 1) a small scoliosis curve; 2) mechanical loading that is transmitted directly from the intervertebral discs to vertebral body growth plates; 3) a stress that will result in dilatation of juxta-physeal vessels and, in deformation of vertebrae, vascular damage with exposure of subendothelial collagen and other

agonist protein. When the vessels get dilated in the deformed vertebra, platelets will be activated and then calmodulin protein levels will change. Due to platelet activation, vessels will release growth factors that, after extravasation, will result in hormone driven vertebral endplate physes, which ends by overgrowth anterior spine and curve progression of AIS. To summarize this hypothesis, the defect in calmodulin could induce microangiopathy at the level of the compressed vertebral bodies and thereby amplify asymmetric vertebral dystrophy (Burwell and Dangerfield 2006).

VI. POC5 AND AIS

Recent work was targeted on understanding the association between the *POC5* gene and AIS. *POC5* variants were found to be associated with AIS in Chinese (Xu, Sheng et al. 2017) and in French Canadian populations (Patten, Margaritte-Jeannin et al. 2015). Hence, this emphasizes the role that *POC5* plays in the pathogenesis of AIS and makes it an interesting factor to study.

The *POC5* gene was recently distinguished as a causative gene in scoliosis (Patten, Margaritte-Jeannin et al. 2015). Centrioles are essential for the assembly of the centrosomes, which will switch with basal bodies in the formation of cilia. At the same time, they also give rise to the poles of the mitotic spindle. The centrosome is an organelle which is located in the center of eukaryotic cells, and acts as an organizing center (Rieder, Faruki et al. 2001). The centrosome is known as the cytoskeleton's microtubule organizing center of the eukaryotic cell animal that radiates in a star way or ASTER during mitosis. Research shows that when the centrosomes are absent, this will result in the inhibition of the cytogenesis process; that cell division will be stopped at the G1 (Nigg and Holland 2018). The centrosomes consist of a displosome that is perpendicularly, located near the nucleus. The centrioles of the centrosome are divided into two groups the mother centriole (mature) and the daughter one that are associated with different complexes that have different functions. The mother centriole is associated with proteins forming distal (related to cilia and flagella; a centriole at the base of each cilium or flagellum) and subdistal, involved in microtubule nucleation of the pericentriolar material, the dense part of the cytosol (amorphous-looking material) and the

aster fibers (microtubules organized in rays). The main function of the centrosome is to assemble the microtubules (Veland, Awan et al. 2009).

Centrins (Cent) are found to be located within the centriole and basal body in most eukaryotes. Members of the centrin family hCent2 and hCent3 are ubiquitous proteins that are located at assembly sites of procentrioles and are found within the distal lumen of full-length centrioles. Through a two-hybrid approach, it was found to be associated with Centrin2 and in mass spectroscopy analysis, POC5 has been found in centriole fractions. The amino acid sequence of hPOC5 predicted three putative Sfi1p-like CBRs. All of the potential hPOC5 homologues contain the tandem repeat of centrin-binding sequences and the short coiled-coil regions.

The centrin binding motifs in POC5 are essential since they direct the binding between human POC5 and hCen2 and hCen3 in a Ca^{2+} independent manner and this interaction is specific as hPOC5 was not able to bind CaM, a closely related protein to centrin.

POC5 is a centrosomal protein that is localized at the mother and daughter centrioles throughout the cell cycle. The recruitment of POC5 into the centrioles occurs late in the duplication phase of the cell cycle, G2/M phase. Through knockdown studies, hPOC5 was found to be essential for the assembly of full-length centrioles and for cellular proliferation. The soluble hPOC5 was found to be phosphorylated during mitosis, however, the centriole associated hPOC5 fraction is hyperphosphorylated, which suggests that the recruitment of hPOC5 to the centriole could be dependent on phosphorylation (Fig. 4). POC5 could be essential for centriole maturation since it is progressively recruited in centrioles (Azimzadeh, Hergert et al. 2009).

In another work, the dependency of centrosomal localization of POC5 on centrin was studied (Dantas, Daly et al. 2013). When the chicken poc5 was overexpressed, this induces the assembly of linear non centriolar structure that includes centrins and components of the PCM. These structures failed to form in cells that are expressing the mutant form of centrin. The linear structures contain a small fraction of γ-tubulin and NEDD1 but has no stabilised α-tubulin (acetylated/polyglutamylated tubulin) or any microtubule marker in them. Centrin

deficiency results in hypersensitivity to UV. Cells with mutant centrin and overexpressing POC5, were not able to form the observed linear structure but could rescue the UV hypersensitivity phenotype caused by centrin deficiency. Hence nucleotide excision repair (NER) could include different pool of centrin and the multimeric assembly of centrins is not a requirement for NER. The assembly of centrin-POC5 structures does require the calcium-binding capacity of centrin 2 (Dantas, Daly et al. 2013).

Very recently, a gene mutated in microcephaly, Rotatin (RTTN) was found to be essential for the proper loading of centriolar proteins (e.g. POC5 and POC1B) to the distal-half centrioles at a later stage. When RTTN was lost or depleted, this didn't affect the localization of centriolar proteins to the newborn centrioles, but the recruitment of POC5 and POC1B to the distal-half centrioles was affected (Fig. 4) (Chen, Wu et al. 2017).

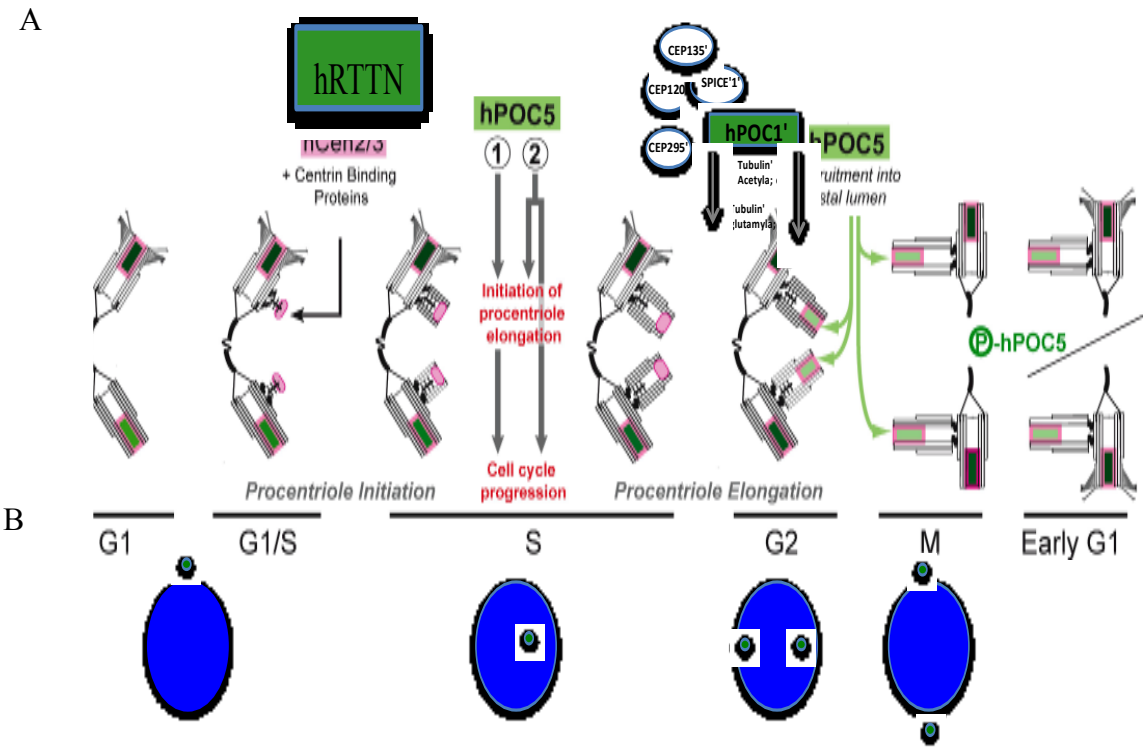

Figure 4: Scheme representing the role of POC5 in centriole assembly

A) In control cells, the late G1 or early S phase are the primary phases where duplication of centrioles takes place. This process is initiated by the assembly of a precursor structure containing a cartwheel that contains centrin proteins (shaded in pink). The POC5 is not yet assembled. Centrin proteins are likely to interact at this step with another unidentified centrin-binding protein. The microtubule singlets and then doublets are assembled around the cartwheel during early S phase. During early S phase, RTTN is recruited to the inner luminal wall of newborn centrioles. The proper loading of later-born centriolar proteins (e.g., POC5 and POC1B) depends on the RTTN-stabilized primitive procentrioles to the distal-half centrioles at a later stage. During mid or late S phase, there are two possibilities for the role of POC5 in centriole elongation, the first possibility is that (1) hPOC5 could be required for the initiation of procentriole elongation and this, in turn, will allow the progression of the cell cycle; secondly (2) hPOC5 triggers procentriole elongation and then it will perform an additional function that is essential for the cell cycle progression through S phase in an

independent manner. During G2 phase, hPOC5 (shaded in green) is accumulated in the distal lumen of procentrioles, at the same time it's phosphorylated, it continues to accumulate together with centrin for the rest of the cell cycle. **B)** Schematic representation of hPOC5 localization at different phases of cell cycle. POC5 is differentially localized within the cell at different phases of the cell cycle. The POC5 protein expression is represented by green circles; nucleus is represented by blue circles. Adapted from Dantas et al (Dantas, Daly et al. 2013)

In a further study, whole-exome sequencing was performed on 3 affected individuals with AIS (Patten, Margaritte-Jeannin et al. 2015). The study focused on variants that are novel or rare which lead to 172 variants. Minor allele frequency [MAF] was less than <5%, and this resulted in 2 candidate SNVs, one in *ADGRG7* and the other in *POC5*. The SNV, c. G1336A, is located in the *POC5* gene (and the effect of mutation is a change in a single amino acid p. A446T). Sanger sequencing confirmed the presence of this mutation in all affected members of family 2. Two other SNVs in *POC5*, c. G1363C (p. A455P) and c. C1286T (p. A429V), were detected in IS patients in the family. An additional *POC5* SNV was detected in affected members of IS family. Both the c. G1336A (p. A446T) and c. C1286T (p. A429V) *POC5* SNVs were found more frequently in 191 IS probands than in the controls. The *POC5* gene is highly conserved among species. The amino acid sequence is homologous between human and zebrafish poc5 where there is around 50% homology. Zebrafish was used to study the effects of mutations on the spine in zebrafish. Knockdown of *poc5* in zebrafish results in curly tailed phenotype. However, the fish doesn't survive after 72 hour post fertilization (hpf). Rescue experiments with the wtpoc5 corrected the observed phenotype. When the embryos were injected with mutant *poc5* mRNA but not wt*poc5* RNA, they developed an axial phenotype after 72 hpf, ranging from mild to severe curvature of the body axis in approximately 50% of injected embryos. The fish with mutant *poc5* was left to reach juvenile stages (50–60 days post-fertilization [dpf]), the vertebral column was fully mineralized however it showed a very strong curvature with vertebral rotation that is similar of the situation in AIS human patients. In this work, the hypothesis that there is another gene that pays a role as a modifier allele and amplifies disease expression arises. This modifier allele could be located on 3q12.2 possibly *ADGRG7*. This modifier allele segregated in all 11 affected patients but not the non affected c. G1336A (p. A446T) *POC5* SNV carrier (Patten, Margaritte-Jeannin et al. 2015).

AIS is a multifactorial pathology where several factors including genetic, hormonal (Estrogens), ciliary and biomechanical are involved in AIS pathogenesis. Recent work from our lab identified functional variants of centrosomal protein-encoding gene *POC5* and the adhesion GPCR *ADGRG7* in patients with idiopathic scoliosis (Patten et al 2015 JCI).

In the present thesis, we are addressing several aspects of the molecular mechanisms involved in AIS and we propose several hypotheses and objectives that will be discussed in manuscripts presented in this thesis (CHAPTER II).

CHAPTER II: HYPOTHESIS AND OBJECTIVES

II.1. General Hypothesis

Candidate genes of AIS were maped to the loci 3q12.2 and 5q13.3 (Edery, Margaritte-Jeannin et al. 2011) and the two variants were identified in *POC5* and *ADGRG7* genes (Patten, Margaritte-Jeannin et al. 2015). Our main hypothesis is that both *POC5* and *ADGRG7* contribute to the AIS pathogenesis. *POC5* gene mutations were reported as a cause of AIS in both patients and zebrafish animal models. To further prove the pathogenicity and validate the role of *POC5* mutations, and the regulation of *POC5* and *ADGRG7* by E2, both *in vitro* and *in vivo* work in human osteoblasts from normal and AIS patients was carried out.

II.1.1. Specific hypotheses:

In this thesis, the following working hypotheses were investigated

(1) The POC5 is a ciliary protein and the wt and mutPOC5 proteins have different cellular localizations
(2) The *POC5* mutation (c. C1286T; p. A429V) affects interaction with other proteins
(3) The mut*poc5* zebrafish have anomalies other than the spinal deformity
(4) Estrogen regulates *POC5* and *ADGRG7*
(5) Mechanical stress modulates gene expression and signaling pathways in AIS osteoblasts

II.2. General Objectives

This research project aims to investigate mechanistically how the defective genes or more specifically, the gene mutations could be responsible for AIS. We recently identified, in a large multiplex French family, using whole-exome sequencing, 2 genes mapped on two new AIS loci (3q12.3 and 5q13.3, identified by Edery et al. 2011). As a logical extension of our previous work during this research project we will investigate:

II.2.1. Specific Objectives:

II.2.1.1. The pathogenicity of identified gene mutations.

To prove the pathogenicity and validate the role of these gene mutations, both in vitro site-directed mutagenesis through overexpression of wt and mutant genes in human osteoblasts and study the effect on cellular localization, cell cycle, cilia and differentially interacting protein partners and in vivo, gene knockdown and dominant-negative approaches in zebrafish studies will be performed. This project will enable us to demonstrate the pathogenicity of gene mutations we recently identified, using molecular and genetic tools including: location analysis of the mutation, prevalence of gene mutations in additional AIS familial and sporadic cases, expression studies in patient-derived cells. Validation of the role of the mutated gene in vivo (using zebrafish and knockdown morpholino approach) and in vitro (using directed mutagenesis) will be performed.

II.2. 1.2. The regulation of two selected AIS candidate genes

Studies of the cloning and the characterization of the promoter regions involved in the response of the estrogen will be conducted. Promoter regions will be isolated from genomic DNA, screened and transcriptional activities tested in vitro after transfection into Huh-7 cells. Probably co-activators of the estrogens receptors will be also identified. The mechanism of regulation by estrogen will be determined and potential sites responsible for regulation will be determined. ChIP will be performed to confirm the regulation and to confirm binding sites in the *ADGRG7* and *POC5* gene sites. The impact of estrogens and biomechanical loading on the gene expression and biological activities of osteoblasts (mineralization) will be conducted in human osteoblast cells, in vitro (wild type or mutant constructs will be transiently transfected into proliferating osteoblasts). Modulation of gene expression profile by E2 and biomechanical loading will be investigated by both qPCR analysis of RNA isolated from normal and scoliotic osteoblast cells after exposure to E2 and/or monitored mechanical load. Also, the regulation by E2 at the protein level will be assessed in both normal and AIS osteoblasts by western blot.

The cellular localization of both genes and its response to E2 will be analyzed using immunofluorescence. Controllable mechanical and physiological environment for simulation in vivo condition in vitro (bone) will be performed. The purpose of this objective is to characterize the genetic-hormonal-biomechanical environment interaction in vitro. This PhD work will focus on two genes. This project could help to provide new insights into potential genes and molecular pathways that contribute to the understanding the pathophysiology of idiopathic Scoliosis.

CHAPTER III: RESEARCH MANUSCRIPTS

This thesis includes 4 manuscripts, 3 submitted and 1 in preparation:

Manuscript 1 entitled: POC5 and cilia anomalies in Adolescent Idiopathic Scoliosis (Submitted to the PLOS ONE journal). In this manuscript, we are studying the connection between POC5, cilia and AIS. Immunofluorescence was used to study the cellular localization of both wt and mutPOC5 proteins and mass spectroscopy was applied to investigate interacting partners. Histology combined with immunofluorescence using specific markers for zebrafish retinal layers were performed to check if there are other than spinal anomalies in mut*poc5* zebrafish. We localized the wtPOC5 at the cilium and confirmed that by mass spectroscopy. The mutPOC5 had different cellular localization with respect to cilia. Ciliary anomalies were studied both in *in vitro* (human osteoblast cells) and *in vivo* (zebrafish retina).

Major Contributions: I have performed most of the experiments of this manuscript from cell culture, transfections, immunofluorescence in vitro and in vivo, western blot and immunoprecipitation. Dr. Shunmoogum A Patten generated the zebrafish with the help of Ms. Charlotte Zaouter. Histology (Hematoxylin and eosin staining) was performed by Mrs. Sirinart Molidperee and Ms. Charlotte Zaouter. I have written the first manuscript draft and Dr. Florina Moldovan, Ms. Helene Mathieu, Dr. Shunmoogum A Patten, Dr. Stefan Parent and Mrs. Soraya Barchi edited it.

Manuscript 2 and 3 investigated the effect of E2 on *ADGRG7* and *POC5* genes. Promoter studies (molecular cloning and the characterization of the promoter regions involved in the response of the E2) were conducted. Promoter regions were isolated from genomic DNA, screened and transcriptional activities tested *in vitro*. The mechanism of regulation by estrogen and potential sites responsible for regulation was determined. ChIP experiment was performed to confirm the regulation and to confirm binding sites in the *ADGRG7* and *POC5* gene sites. The impact of estrogens on the gene and protein expression was investigated by qPCR, western blot and immunofluorescence respectively.

Manuscript 2 entitled: The 17β-Estradiol induced upregulation of the Adhesion G-protein coupled receptor (ADGRG7) is modulated by the estrogen receptor (ESRα) and specific protein 1 (SP1) complex (Submitted to the Journal of Biology Open). In this manuscript, we are investigating the regulation of ADGRG7 gene and protein by E2. We found that ADGRG7 expression is upregulated by E2. We also found differences in the response of normal control osteoblasts (NOB) and scoliotic osteoblasts (AIS) cells to E2. We established the mechanism of *ADGRG7* regulation through indirect genomic signaling by SP1 and ESR1.

Manuscript 3 entitled: POC5 is regulated by E2 through direct genomic signaling by ESRα (In preparation). In this manuscript, we are studying the regulation of POC5 by E2 in different cell lines. We found that the POC5 is upregulated by E2 through direct genomic signalling by ESR1.

Major Contributions: I have generated all the constructs that were used in promoter analysis. I performed the ChIP experiments with the help of two students Dr. Samira Benhadjeba and Dr. Lydia Edjekoyane. I have also performed the transfections and luciferase assay experiments. I have written the first draft of the two manuscripts. Dr. Edward T. Bagu, Dr. Florina, Dr. Shunmoogum A Patten, Dr. Andre Tremblay, Mrs. Soraya Barchi and Dr. Isabelle Villemure helped in writing and editing the fist draft versions of the manuscripts.

Manuscript 4 entitled: The role of TRPV4 in normal and scoliotic osteoblasts during mechanical stress (In preparation). In this work, we are studying implication of the TRPV4 channel in the response of wt and mut*POC5* cells to mechanical stress as well as the gene expression and signalling pathways. Using specific agonists and antagonists for TRPV4 as well antagonists of PKA pathways, expression pattern of ciliary and bone markers were studied by qPCR and western blot. Effects of mechanical stress on mineralization, apoptosis and cilia length and number were assessed. This work also included *in vivo* work on zebrafish retina, where we investigated the trpv4 expression, apoptosis and annexin 5 in wt*poc5* and mut*poc5* zebrafish retina. We found that TRPV4 channel plays a role in the stress response of mut*POC5* human osteoblasts

Major Contributions: I have designed and performed all the experiments for this manuscript. Dr. Irene Londono helped with the alizarin red staining. Dr. Shunmoogum A. Patten generated the zebrafish that were used in this study, with the help of Ms. Charlotte Zaouter. I have written the first draft of the manuscript and Dr. Florina Moldovan and Dr. Isabele Villemure corrected the manscript.

III. 1. MANUSCRIPT 1

Full title: POC5 and cilia anomalies in Adolescent Idiopathic Scoliosis

Short title: Role of POC5 in Adolescent Idiopathic Scoliosis

Amani Hassan [1,2], Stefan Parent [2], Helene Mathieu[2], Charlotte Zaouter [2], Sirinart Molidperee [2], Soraya Barchi [2], Isabelle Villemure [3], Shunmoogum A. Patten [4] and Florina Moldovan[1,2]

[1]Faculty of Dentistry, Université de Montréal, Montréal, Quebec, Canada,

[2] Research Center of CHU Sainte-Justine, Montréal, Quebec, Canada

[3] École Polytechnique de Montréal, Montréal, Quebec, Canada

[4] INRS–Institut Armand-Frappier, Université du Québec, Laval, Montréal, Quebec, Canada

Corresponding author: email address: florina.moldovan@umontreal.ca (FM)

Author Contribution:

A.H and F.M designed experiments and wrote the first version of the manuscript. AH performed the experiments. S.P.A generated the zebrafish line used in the study. C.Z and S.M. prepared histology samples. S.P, S.B provided normal and scoliotic bone cells. A.H., S.P., H.M., C.Z., S.M., S.P.A., S.B., I.V. and F.M contributed to the revision, writing and editing of the manuscript. All authors approved the final version of this manuscript.

Abstract

Adolescent Idiopathic Scoliosis (AIS) is a spinal deformity that affects approximately 4 percent of human adolescents. The etiologic and molecular basis of AIS is not yet fully understood, but several genes are suspected of causing this condition. To study the role of *POC5* in AIS, we investigated the subcellular localization of POC5 in the cilia of cells overexpressing wild type (wt) or a *POC5* variant (c. C1286T; p. A429V) and in human osteoblasts carrying this mutant (mut*POC5)* variant and in normal control cells. The POC5 protein was strongly associated with acetylated-α-tubulin in wt but not in mut*POC5* expressing cells. We observed that loss of POC5 connection with acetylated-α-tubulin impaired cell-cycle progression (S phase arrest), and induced ciliary retraction in osteoblasts carrying mut*POC5* variant. Using immunoprecipitation coupled to mass spectrometry, we identified specific protein-protein interaction partners of POC5, most of which were components of cilia, microtubules, cytoskeleton and centrosomes. We also immunolocalized POC5 with the acetylated-α-tubulin in the retina of zebrafish expressing wt*poc*5 or mut*poc5*, and we observed colocalization of both proteins in wt but not in mut*poc5*. These results demonstrate the role of mutated *POC5* in a ciliopathy underlying AIS pathogenesis.

Introduction

The etiology and biological mechanisms of adolescent idiopathic scoliosis (AIS) are still poorly understood. Several etiological hypotheses and pathways are suggested, including bone growth and metabolism [1], biomechanics [2-7], connective tissue abnormalities [8-10], asymmetries in the central nervous system [11-16], vestibular [17-20], postural, hormonal [21-25], and recently, cilia abnormalities affecting spinal fluid flow [26-28]. In addition to the phenotype complexity and clinical unpredictability of AIS, there is also strong evidence of a genetic predisposition and high genetic heterogeneity. Over the last decades, several genes and genetic variants were reported to be associated with or to contributing to susceptibility to AIS [29] . Indeed, our recent work identified the centrosomal protein-encoding gene *POC5* to be connected to the familial form of AIS [30]. Very recently, *POC5* involvement in AIS was validated in a case-control study [31]. This study reported that common variants (rs6892146) of *POC5* were associated with susceptibility to AIS [31] and found mRNA overexpression of *POC5* in the muscles of AIS patients when compared to the controls.

The *POC5* gene is located on chromosome 5q13 and encodes one of the most abundant centriolar proteins essential for the assembly of the distal half of centrioles and required for centriole elongation. POC5 is a ubiquitously expressed protein that interacts with centrin and inversin and is involved in specific cell functions such as cell polarity, division, motility, primary cilia [32, 33]. The POC5 protein is part of the cytoskeleton complex network that is important for cell dynamics [34]. POC5 is also important for retinal function as it was recently

reported that in autosomal recessive retinitis pigmentosa (RP), POC5 has a distinct localization and function at the photoreceptor connecting cilium **[35]**.

A cilium connection with scoliosis was also reported in a zebrafish model with a mutation in the *protein-tyrosine kinase-7 (ptk7)* gene **[27]**. In this model, defects *were observed in the* formation and function of motile cilia in the central nervous system. These abnormalities were suspected as the cause of abnormal spine curvature and linked to the disturbed flow of cerebrospinal fluid (CSF). *Cilia* are organelles that extend from the surface of almost all mammalian cells. The role of cilia is connected to cell cycle progression and proliferation; thus, cilia undertake a vital part in human and animal embryonic development. The recognized role of cilia is mechanosensation where they work as a sensory protuberance (antenna) by receiving cell-to-cell signals or from the extracellular fluids as well as projecting out of the cell various receptors to monitor the environment [36].

POC5 is a ciliary protein but the mechanisms associated with ciliary defects in AIS are unknown, thus to investigate the mechanisms by which POC5 could be connected with AIS and how it functionally affects the cells and tissues, we examined: 1) the subcellular localization of POC5 in cell lines overexpressing wild type (wt) or mutated (mut) *POC5* gene (c. C1286T; p. A429V) and in human osteoblasts with *POC5* mutation (c. C1286T, p. A429V) with respect to cilia; 2) the protein binding partners of POC5; and, 3) the tissue analysis of poc5 and acetylated-α-tubulin as well as different retinal markers in wt and scoliosis (mut *poc5*) zebrafish retina.

Materials and Methods

Ethical considerations

All human tissue samples were obtained in accordance with the policies concerning the use of human tissues for research. The protocol was approved by the Ethics Committee of the Research Center of CHU Sainte-Justine (# 3704). For the Zebrafish (in-vivo animal study), the experimental protocol and all animal procedures were carried out in accordance with the guidelines of the Canadian Council on Animal Care (CCAC), and the protocol was approved by the University of Montreal's Animal Care Committee (ZF-09-60/Category B).

Cellular localization of POC5

In order to investigate the role of POC5 in the centriole, centrosome and cilia, we examined the co-localization of POC5 with acetylated-α-tubulin (cilia protein marker) by double immunofluorescence staining. All the cells were cultured in an eight-well-chamber glass slide (Fisher scientific cat#354108), DMEM (Wisent cat# 319-015-CL). HeLa cells were transfected with either myc tagged wt *POC5* (Origene cat# RC211731) or mutP*OC5*, (generated by site directed mutagenesis [30]), using lipofectamine (Invitrogen, cat #11668-019). Immunofluorescence was performed 24 hrs (hr) post-transfection after fixation with (70 % ethanol/0.2 %triton/on ice) and permeabilization with 0.1 % triton in PBS (PBT) then incubated with anti POC5 antibodies (rabbit polyclonal antibody abcam cat # ab188330 1/250) and anti-acetylated-α-tubulin (mouse monoclonal antibody, Sigma Aldrich cat# T7451 1/2000) diluted in 2 % BSA/PBT. They were incubated for one hr at room temperature (RT). Cells were then washed three times with PBT and incubated with secondary antibodies Alexa

fluor 488 anti-rabbit (life technologies cat# A11008 1/500) and Alexa fluor 555 anti-mouse (Life technologies cat A21422 1/500) for one hr at RT. Mounting was done using prolong gold anti-fade reagent with diamidino-2-phenylindole dye for fixed cells (DAPI) (Life technologies cat #P36931). Images were taken using Zeiss microscopy. We also performed Z-stack digital imaging (a technique which combines multiple images taken at different focal distances to give a subsequent image with a greater depth of field) to reveal more details of the position of POC5 with respect to cilia. Acetylated-α- tubulin (ciliary marker) was visualised in red, POC5 protein in green, and DAPI nuclear counterstain in blue.

To analyse expression and cellular localization of POC5 at different phases of the cell cycle, HeLa cells were cultured in DMEM Medium (Wisent cat# 319-015-CL) with 10 % FBS (Wisent cat# 080-110) and 1 % penicillin streptomycin Glutamine (Wisent cat #50-202-EL) (PSG) then synchronized to be within the same cell cycle phase by serum starvation for 24 hrs. Serum starvation was performed by culturing confluent cells in DMEM medium without FBS, supplied with 1 % PSG to block in G1 phase. To block cells in S phase, cells were then supplied with DMEM medium with FBS (10 %) and 1 % PSG for 24 hrs. Cells were then examined by double immunofluorescence as described above. Immunofluorescence studies were also performed on normal human osteoblasts (carrying *POC5* variant mutation C1286T (p. A429V). For mutation analysis of the osteoblasts collected during surgery from patients with scoliosis, DNA was extracted from cells using pure link genomic DNA mini kit (cat # k 1820-01). Polymerase chain reaction was performed for exon 10 using primers: Forward: 5'CTTTTCATAAGGTGGGACCT3' Reverse: 5'TCCGATGCCCTTACCAG3'. Bands corresponding to the correct molecular weight of *POC5* were excised from gel and then purified using GenElute Gel extraction kit (Cat # NA1111-1KT). Samples were sent for Sanger sequencing.

Nuclear and Cytoplasmic Extract Preparation

Cells were washed with 4ml of PBS (1x) and then harvested in PBS by scraping. The lysate was collected in eppendorf tube and spinned for 5 min in a microcentrifuge at low speed (4000 rpm). Pellet was washed twice with 500 ul of buffer A (Hepes 10mM, KCl 10mM, DTT 0.5mM)(w/o NP-40) and then cell pellet was resuspended in 20 ul of buffer A (w/ NP-40 (1%)) and incubated at 4 °C for 10 min with rocking. The cell pellet was then spinned down in microcentrifuge for 2 min at max speed. The supernatant is the cytoplasmic extract (C extract) by adding 55 ul of buffer C and stored at –80 °C. The nuclear extract was resuspended in 55 ul of buffer C (Hepes 20mM, glycerol 20%, KCl 500mM, EDTA 0.2mM, PMSF 0.5mM, DTT 0.5mM and MgCl2 1.5mM); and incubated at 4 °C for 15 min with rocking. The nuclei were then spinned in microcentrifuge for 5-10 min at max speed. At this stage, the supernatant is the nuclear extract (N extract).

Immunoprecipitation coupled to mass spectrometr(IP-MS), co-Immunoprecipitation and Western Blot

To identify specific protein-protein interaction partners of POC5, immunoprecipitation coupled to mass spectrometry, co-immunoprecipitation, and Western Blot analyses was performed on Hek293 cells transfected with wt or mutPOC5 expressing vectors. Hek293 cells were cultured in DMEM medium (Wisent cat #319-015-CL) with 10 % FBS and 1 % PSG. When confluent, cells were transfected using lipofectamine 2000 (Invitrogen cat #11668027) with control (mock empty vector), wt or mut*POC5* expressing vectors. For transfection, cells were maintained in antibiotic free medium overnight. On the second day, cells were transfected based on the lipofectamine protocol provided by the manufacturer (Invitrogen). For protein extraction, cells were lysed in IP lysis buffer (Pierce Thermoscientific, cat# 87787) supplied with 1 x protease inhibitor cocktail (Roche cat# 04693116001). Lysate was then centrifuged for 15 min at 8000 rpm. Supernatant was collected for protein quantification by Bradford (Bradford Biorad cat# 500-0006). For immunoprecipitation, 3000 µg of proteins were immunoprecipitated with 2.5 µg/ml of anti-myc antibody (Origene, cat# TA15021)

overnight (ON) at 4 °C. Magnetic beads (Biorad cat #161-4023) were washed with PBS and blocked using 2 % BSA/PBS (BSA from Sigma-Aldrich cat #A7906) ON at 4 °C. On the second day, beads were washed 3 x with PBS and then incubated with protein lysate and antibody complex at 4 °C ON. On the third day, the flow through was collected and the beads were heated for 10 min in laemeli 2 x (biorad cat# 161-0737) at 55 °C. Protein samples and dual plus molecular weight ladders (Bio-rad cat #161–0374) were separated by SDS-PAGE approximately 90 min at 100 V in running buffer (25 mM Tris base, 192 mM glycine, 1% SDS, pH 8.3). The gel was stained with Coommasie blue (Biorad cat G-250 #1610406) for 3 hrs. After staining the gel with Coomassie blue, the bands corresponding to the molecular size of POC5 (63 kDa) were excised and analysed by mass spectroscopy. The gels were subjected to trypsin digestion then an aliquot of the tryptic digest (prepared in 5 % acetonitrile/0.1 % trifluoroaceticacid in water) was analyzed by LC-MS on an LTQ-Orbitrap mass spectrometer system (ThermoElectron) coupled to a Dionex 3000 nano-LC system (Camberley). Mass spectroscopy analysis was evaluated using scaffold software [37].

In parallel, an aliquot of protein samples was transferred to nitrocellulose membranes (Bio-Rad cat # 9004700) and ran 90 min at 90 V and 250 mA. The total proteins on membranes were detected with Ponceau S staining (Sigma cat #P3504). Membranes were blocked with 20 % non-fat milk (Santa-Cruz cat #Sc2324) in PBST (10 mM phosphate, 137 mM NaCl, 2.7 mM KCl, containing 0.05 % Tween-20, pH 7.4) for 1 hr and then incubated with anti-POC5 antibody in PBST with 5% BSA in PBT at 4 °C ON. The secondary antibody was (anti-rabbit IgG secondary antibody (Thermoscientific cat# 31460) diluted at 1: 10000 for one hr at RT. For the validation of mass spectroscopy data, and to confirm the interaction of several ciliary proteins with POC5, Western blot was performed by stripping the same membrane by Restore stripping buffer (Thermofisher cat #21059) and then probing with different antibodies: Annexin2 (sc-374394), Galectin 3 and 7 (sc-32790 and sc-137085), CKAP5 (sc-374394), Desmocollin1 (sc-398590), CEP290 (ab84870), Septin9 (sc-293291), Acetylated-α-tubulin (Sigma Aldrich cat# T7451 1/2000), RAB11 (ab3612), EHD4 (sc-376373), Annexin5 (sc-

32321), and CystatinA (sc-376759). All antibodies from Santa Cruz (Sc) are mouse monoclonal used at a 1/500 dilution. For CEP290 and Rab11, both rabbit antibodies were used at 1/250. The secondary antibody (anti-rabbit IgG secondary antibody (Thermoscientific cat# 31460) was diluted 1:10000, and anti-mouse IgG secondary antibody (Thermoscientific Catalog #:31430) was diluted 1:10000 for one hr at RT. Membranes were exposed to ECL prime Western blotting detection reagent (GE healthcare cat# RPN2232) for 5 min at RT room.

Immunoprecipitation phosphatase assay

Hek293 cells were transfected with wtPOC5 myc tagged or mutPOC5 myc tagged vectors (as described above) and then were synchronized at G1 or S phases. To block cells at G1 phase, cells were serum starved for 24 hr. To block cells at S phase, cells were first starved for 24hr and then complete medium with serum (10% FBS) was added for 24 hr. For immunoprecipitation-phosphatase assays, total lysates were incubated with 2.5 µg anti-myc antibody as described above. Beads were blocked with 1% BSA and then washed three times and resuspended in 100 ul PBS. Then, protein antibody complex were incubated with beads. Alkaline phosphatase (NEB cat# M0290S) was added to the mixture and incubated at 37 °C for 1 hr. Western blot was performed using POC5 antibody (abcam cat# 188330) as described above.

Histology and immunohistochemistry of wt and mut*POC5* injected zebrafish

Wild-type and mut versions of human *POC5* were obtained using a myc-tagged ORF clone of human *POC5* (Origene) and were injected in zebrafish embryos as previously described [30]. Wt and mut-*poc5* injected embryos were grown in a facility and raised over the course of 60

days (corresponding to juvenile age) at 28 °C ± 1 °C, with water and air temperature readings collected daily [38]. The zebrafish were collected, fixed in 4 % paraformaldehyde (PFA) overnight at 4 °C, and screened for spinal deformity by micro CT scan to confirm the scoliosis phenotype. The wt and mut*poc5* specimen tissues were then decalcified and embedded in paraffin. Staining with hematoxylin and eosin was performed according to standard protocol. Briefly, sections were deparaffinized by xylene and then rehydrated with different concentrations of ethanol followed by water wash, Nuclei were stained with alum haematoxylin. The slides were rinsed in running tap water followed by differentiation with 0.3 % acid alcohol. The slides were rinsed in running tap water and stained with eosin for two mins. Finally, slides were dehydrated, cleared, and mounted.

Immunofluorescence

Immunolocalization of POC5 and colocalization with cilia or centrin was performed by double immunofluorescence carried out through a mixture of anti-POC5 antibody (abcam cat # ab188330) and anti-acetylated-α-tubulin (Sigma Aldrich cat # T7451) or centrin antibody (Santa Cruz cat# sc-365697). Eye tissue sections (1.5 μm) were deparaffinized in xylene, rehydrated in a graded series of ethanol, washed several times in PBS, and permeabilized for 30 min in 4 % Triton-X 100 containing 2 % bovine serum albumin (BSA) and 10 % goat serum. Following permeabilization, retinal sections were incubated with the primary antibody POC5 (1/250) and acetylated-α-tubulin (1/2000) simultaneously during 24 hr at 4 °C. Tissue sections were washed several times in PBS and then incubated with the secondary antibody conjugated with Alexa Fluor 488 (life technologies cat# A11008 1/500) and Alexa Flour 555 (Life technologies cat # A21422 1/500) for 1 hr at RT. Images were acquired using confocal microscope under a 20x objective. For the retinal marker immunostaining, the same protocol

was followed as described above but instead using zpr1 and zpr3 antibodies obtained from the Zebrafish International Resource Center (ZIRC) and the 3A10 obtained from Hybridomas Bank (cat# AB_531874). The retina sections were incubated with these antibodies for 24 hr with rotation at 4 °C.

Quantification and Statistical analysis:

The length of the cilia was quantified using ImageJ by measuring the acetylated α-tubulin signals. For ciliation experiments with NOB and AIS cells (Fig. 2), approximatly 300 cilia were counted per experiment. For cell cycle analysis, the number of cells in S phase and G1 phase were counted (Fig. 4). The percentage of cells in each phase over the number of total cells was determined. Approximatly 100 cells were counted per phase. Mean values of individual experiments were plotted in bar graphs with ±SD between the individual sets. P-values were calculated by one-way ANOVA. $P<0.05$ considered statistically significant.

Results

Differential subcellular localization of POC5 with respect to acetylated-α-tubulin in wt *POC5* and mut*POC5* expressing cells

We first examined the subcellular distribution of POC5 in HeLa cells. Positive staining for POC5 was observed in both wt*POC5* and mut*POC5* cells. In wt *POC5* cells, POC5 protein was immunolocalized at the acetylated-α-tubulin ring (Fig 1 a). In the mut*POC5* cells, positive staining was observed in the nucleus (Fig. 1 b). In the cells expressing mut*POC5 (*c. C1286T; p. A429V*)*, the lack of colocalization of POC5 with acetylated-α-tubulin was further demonstrated with Z-stack imaging at different focal planes. The Z-stack for the wt*POC5*

showed a combination of both red (acetylated-α-tubulin) and green staining (POC5); however, for the mut*POC5*, only POC5 was visualized (green color). Based on these observations, we confirmed that *POC5* mutation affects the co-localization of POC5 protein with the acetylated-α-tubulin.

Ciliary colocalization of wtPOC5 and ciliary retraction in mutPOC5 osteoblasts with mutation (c. C1286T; p. A429V)

To confirm our observation in HeLa cells, we next sought to investigate the effect of mutation in *POC5* on the subcellular localization in normal (nonscoliotic) (Fig 2 a-d) and human osteoblasts carrying variant (c. C1286T; p. A429V) (Fig 2 e-h), as this would be a more clinically-relevant model for the disease. The variant was first confirmed by Sanger sequencing (Fig 2 I). The results of immunofluorescence showed a differential cellular localization of POC5 between normal and scoliotic osteoblasts even though the cells were synchronized at the same cell cycle stage by serum starvation. Interestingly, wtPOC5 (Fig 2 d) was mostly located at the cilium. In mutPOC5 cells (c. C1286T; p. A429V), POC5 was located within the nucleus (Fig 2 h). Also, low level of immunostaining for the acetylated-α-tubulin (marker for cilia) and retraction of cilium was observed (Fig 2 h). Comparison of cilia length shows that most AIS cells have significantly shorter cilia than NOB cells (Fig. 2 I). A high number of AIS cells had cilium shorter than 3μm. These results confirm the consequence of the mutation on the subcellular localization of POC5 with respect to the absence of cilium.

POC5 interacting protein partners are mostly ciliary and cytoskeletal proteins

To further analyse the potential protein-protein interaction partners, mass spectrometry studies were conducted in transiently transfected cells with myc-tagged wt or mut*POC5*. Using mass spectroscopy, we identified 85 proteins that potentially interact with wtPOC5 and that were not found in the mutPOC5 (Table 1). Using immunoprecipitation coupled to mass spectrometry (IP–MS), we identified 12 ciliary and cytoskeletal proteins that potentially interact with the wtPOC5 or with mutPOC5. Immunoprecipitation of POC5 (using myc antibody) showed similar levels of POC5 expression in wt and mut transfected samples and slightly lower levels in control (mock vector) transfected cells (S1 A, B, C). There was high expression of acetylated-α-tubulin in wtPOC5 when compared to the mutPOC5 and to the control (S1 D). The Western blot (WB) for Annexin2, Cytoskeleton-associated protein5 (CKAP5), Desmocollin1, Centrosomal protein 290kDa (CEP290), and Septin9 showed that only wtPOC5, but not mutPOC5 protein, interacts with these proteins (Fig 3). Weak interaction existed among Galectin 3 and 7, Ras-related protein (RAB11), Acetylated-α-tubulin**,** EH domain-containing protein 4 **(**EHD4), Annexin5, Cystatin A, and mutPOC5 when compared to wtPOC5.

In the mut*POC5* overexpressing cells, only five proteins were identified that were selective for mutPOC5 and not wtPOC5: Protein disulfide-isomerase A4 (9), duronate 2-sulfatase (5), golgi resident protein GCP60 (3), aminopeptidase B (2) cDNA FLJ53442 - highly similar to poly (ADP-ribose) polymerase 1 (2) (Table 2).

Defects in cell-cycle progression in cells overexpressing the mutPOC5

Because POC5 is localized to the distal portion of centrioles and is recruited to procentrioles for full centriolar maturation and normal cell-cycle progression, it was considered necessary to determine how mutPOC5 protein is localized during cell cycle progression. HeLa cells (transfected with either myc tagged wt or mut*POC5* were synchronized in the growth phase (G1) cell cycle phase and then stained for POC5 using specific antibodies. In cells transfected with wt*POC5*, specific staining for POC5 protein was observed outside the nucleus (cytoplasm) during the G1 phase (Fig 4 a). During the Synthesis (S)-phase, in the wt*POC5* cells, specific staining for POC5 protein was observed in the nucleus (Fig 4 b). In mut*POC5* expressing cells, staining for POC5 was observed to be permanently localized in the nucleus through the S and G1 phases (Fig 4 c and d). A significant increase in the proportion of S-phase cells was detected by the nuclear localization of mutPOC5 (4%). The pattern of phosphorylation of wt and mutPOC5 during the cell cycle progression was also tested. We found that the mutPOC5 was hyper phosphorylated independently of the phase of the cell cycle. In all cell cycle phases, we observed that mutPOC5 protein had lower migration than wtPOC5 protein and that treatment with alkaline phosphatase shifted back mutPOC5 to an apparent molecular weight similar to wtPOC5 levels (S3 Fig.).

WtPOC5 but not mutPOC5 colocalizes with centrin

The wtPOC5 and mutPOC5 had different localization with respect to cilia (Fig 2) and different cellular localizations within the cell at different phases of the cell cycle (Fig 4). To precisely localize POC5 and to study the consequence of mutation on POC5 recruitment to cilia, we performed double immunostaining for POC5 and centrin in cells overexpressing wtPOC5 or mutPOC5. In immunofluorescence microscopy, anti-hPOC5 antibody staining

labeled two dots for wtPOC5 and one dot for mutPOC5. These dots represent centrioles, as confirmed by colocalization with human centrin (Fig 5 A). Quantification of centrin, centrin percentage per cell shows that there is significantly higher centrin staining intensity in wtPOC5 expressing cells than mutPOC5 cells. Interestingly, mutPOC5 expressing cells had mainly one dot of centrin while wtPOC5 had predominantly 2 or more dots (Fig 5 B).

Different subcellular localization of wtPOC5 and mutPOC5 in the cytoplasm and nucleus

We observed a permanent localization of mutPOC5 in the nucleus while wtPOC5 was localized in the nucleus and cytoplasm at different phases of the cell cycle (Fig 4). To confirm this observation, we performed cellular fractionation of cytoplasmic and nuclear extracts of cells overexpressing wt or mutPOC5. As expected, wtPOC5 was concentrated in both nuclear and cytoplasmic fractions with higher level of expression in the cytoplasm. Interestingly, the mutPOC5 was exclusively found in the nucleus (Fig 6).

POC5 and acetylated-α–tubulin colocalize in the retina of wt but not mutpoc5 zebrafish

An impairment in cell-cycle progression (S phase arrest) due to mutations in POC5 will likely have severe consequences on cell fate. The POC5 variants were recently associated with the retinal anomalies in humans [35] and with scoliosis (30, 31). Studying the retina has led several insights on cell cycle and cell fate determination. Therefore, we next sought to investigate any defects in the retina in vivo in zebrafish model of scoliosis expressing mutpoc5. The distribution of poc5 and cilia (stained by the acetylated-α-tubulin) showed co-localization in the retina of wtpoc5 (Fig 7 c) in the retinal pigmented epithelium (RPE) and

inner nuclear layers (INL) but in the mutpoc5, we observed absence of overlap in localization between POC5 and acetylated-α-tubulin. Immunostaining of acetylated-α-tubulin was reduced in the RPE and INL in the retina of the mutpoc5 compared to the wt (Fig 7 e). POC5 specific immunostaining was detected at the RPE and INL of both wt and mutpoc5 retina (Fig 7 a and d). However, wtpoc5 retina had stronger staining in the RPE layer. Several spaces in the pattern of poc5 staining was observed in INL of the mutpoc5 retina suggesting retinal degeneration.

Defects in cones and photoreceptor layers in mutpoc5 retina

In recent work by Wieze et al [35], the loss of function of *poc5* was responsible for retinal degeneration in zebrafish. The zebrafish *poc5* morphants had shorter photoreceptor outer segments. We sought to further explore the retinal phenotype of the poc5 scoliosis model used in this study. To exactly localize the various layers (rods and cones of the retina), zinc finger protein (zpr) zpr3, zpr1 and 3A10 were employed [39, 40]. Zpr-3 positive immunostaining (high signal) was observed in the rod (ROS) and double-cone outer segment layer (DCOS) (Fig 9 a). Zpr3 immunostaining of wt*poc5* was found in the rods and double cone outer segment layers but only low intensity of the staining was found in the mut*poc5* retina (Fig 9 b). The thickness of the rod layer in the mut*poc5* zebrafish was less than the wt. Also, zpr1 immunostaining (which is a marker for double cones) showed the presence of severe loss of cone pigment proteins and outer plexiform layer (OPL) in mut*poc5* zebrafish (Fig 9 d). Strong staining of double cone of outer segment (DCOS), long single cone outer segment (LSCOS) and short single cone outer segment (SSCOS) cones in wt retina (Fig 9 c) was found, but this staining was totally absent from the retina of mut*poc5* (Fig 9 d). Using the neurofilament-

associated antigen (3A10) antibody, anomalies in the cone cell layer (CC) and in the mutpoc5 zebrafish were found (Fig 9 f) which consisted of reduced staining intensity and disrupted cellular organization.

Discussion

In this study, we demonstrate the involvement of POC5 and cilia in scoliosis. This involvement of POC5 occurs through its loss of interaction of POC5 with acetylated-α-tubulin and involves primary cilia retraction. This study demonstrated that the mutation in *POC5* (c. C1286T; p. A 429V), previously described in patients with AIS, resulted in distinct localization with respect to cilia. The interacting protein partners of POC5 were identified and immunolocalized, and interestingly, it was found that most of these were components of the cilia, microtubules, cytoskeleton, and centrosomes. In human osteoblasts carrying the *POC5* variant (c. C1286T; p. A429V), the loss of POC5 connection with acetylated-α-tubulin and impaired cell cycle progression (arrest in S phase) was shown and, as a consequence, ciliary retraction (Fig 10).

.

In French families with AIS, various functional variants (c. G1336A (p. A446T), c. G1363C (p. A455P), and c. C1286T (p. A429V)) are contributing to the occurrence of AIS [30]. In French Canadians with AIS, only one of those variants (c. C1286T; p. A429V) was found (data not published), and recently in the Chinese population, a common variant of POC5 was associated with the susceptibility to AIS (single-nucleotide polymorphism (SNP) rs6892146)). This common SNP has a significantly different distribution of minor allele frequency in patients with the GG and with CC genotype. Interestingly, in patients with the GG genotype, POC5 mRNA expression was found to be significantly increased when compared to the

controls [31]; however, little is known about the function of POC5 and its role in AIS pathologies. The POC5 variant, c. C1286T (p. A429V), is a rare variant that was identified in 5/300 chromosomes (~1.65%) from IS patients but not in familial IS. The c. C1286T (p. A429V) POC5 SNVs was found more frequently in 191 IS probands than in the controls (P = 0.0445 and P = 0.0273, respectively [30]. All patients with scoliosis and carrying mutation were from normal parents which suggests that the inheritance is recessive. The wild-type allele not compensating for the c. C1286T variant suggests that there is other mutations contributing to the observed phenotype and yet to be determined.

In addition to the association of POC5 with AIS [30], recently, new mutations in POC5 gene were associated with Retinitis pigmentosa (RP) [35]. Retinitis pigmentosa is a photoreceptor degenerative disease, characterized by the degeneration of rod and cone photoreceptors and is classified as ciliopathy disease. An interesting feature of all forms of RP is that the genetic mutation occurs in the rods exclusively; the cones die, but the cause of this death in RP is not understood [35, 41]. Our work pointed out some similar retina alterations, including a missing outer segment layer (a zebrafish model of scoliosis induced by *poc5* overexpression).

Weisz et al [35] reported POC5 to be localized at the connection cilia in the photoreceptors, and when mutated, the length of photoreceptor outer segments is reduced. In our in vitro work, in cells overexpressing mut*POC5*, POC5 was disconnected from the acetylated-α-tubulin ring (Fig. 1 b), dispatched from centrin (Fig 5) and solemnly localized in the nucleus (Fig 6). POC5 was found to be interacting with ciliary proteins suggesting that POC5 is a ciliary protein (Table 1).

Also, *in vivo*, we observed that there is disruption of acetylated-α-tubulin colocalization in the photoreceptor and inner nuclear layers (INLs) in the mut*poc5* retina (Fig 7 f). Moreover, mut*poc5* zebrafish had a missing outer segment layer as determined by hematoxylin and eosin staining (Fig 8 b). Indeed, POC5 appear to be a ciliary protein that is located at the base of the cilium. Surprisingly, the study by Weisz et al failed to prove the colocalization of centrin with POC5 in the connecting cilium and found that localization of centrin in the connecting cilium is not dependent on POC5. However, in our work, we found that poc5 colocalizes with centrin in the outer segment layer (OS) and connecting cilium (CC) (S4 Fig.). Interestingly, in mutpoc5 retina, defects in the pattern of centrin staining was observed in the CC layer, several spaces exits suggesting degeneration in this layer. In our work, we used different markers not only for the outer segment layer, but also for the cones and rod layers by zpr1, zpr3 and 3A10 staining (Fig 9). These results showed that not only the defect exists at the level of the rods but also at the level of the cones.

The homozygous nonsense mutation (c.304_305delGA [p. D102*] in *POC5* that causes RP does not cause a scoliosis phenotype, suggesting that the phenotypic outcome of each mutation can be very different. Of course, more data is needed regarding the role of *POC5* in vivo in humans, but some observations support the likelihood of a neurologic deficit in idiopathic scoliosis (IS), probably visual deficiency with space perception difficulties. Subsequently, the association between AIS and postural control, in which vision is involved, was observed in patients [42]. Several studies suggested the postural problem in the etiology of scoliosis where it was found that the occurrence of scoliosis was higher in the blind population [42]. These patients had difficulty in stabilizing themselves in the standing position. For maintaining a stable position in humans, three types of sensory information are involved: visual (controlled

by retinal sensors), somatosensory (muscle and joint sensors, also feet and some organs are involved), and vestibular (from inner ear sensors).

Other studies suggested the involvement of neurological deficits in AIS and pointed out the motor behavior of patient in maintaining postural sway [43]. The balance instabilities in AIS patients could also be associated with the alteration in sensory signal processing [44-46]. It appears that in all tests, scoliotic patients have significantly poorer postural control compared with healthy patients; this raises the possibility that postural disequilibrium is a causative factor of this disorder [47]. Based on the observations reported in the present study, we can also infer that sensory information (retinal sensors) play a part in AIS.

Our immunofluorescence results showed a differential localization of wt and mutPOC5 with respect to the acetylated-α-tubulin signal that is a marker for cilia. WtPOC5 was found to be attached to acetylated-α-tubulin (Fig 1 a), while mutPOC5 was found to be disconnected (Fig 1 b). This result was confirmed by co-IP experiments. Interestingly, we found more expression of acetylated-α-tubulin in wt but not in mut and control expressing cells, although we had similar expression levels of precipitated POC5 (S1 Fig.). This supports the finding of differential localization of wt and mutPOC5 with respect to cilia, and this is also supported by our mass spectroscopy and co-IP data (Fig 3) that showed several ciliary proteins to be interacting exclusively with wtPOC5 but not mutPOC5. Centrin staining confirmed the differential localization of wt and mutPOC5 (Fig 5). Among these proteins are RAB11 and CEP290. Multiple GTPases include RAB6, RAB11, and RAB8A which are involved in the trafficking to the cilium. In cilia pathologies (some of them include scoliosis as a secondary manifestation), several studies have shown that the potential handover mechanisms may exist between RAB11 and RAB8 at the base of the cilium [48]. Rab8 and Rab11 were found to be

associated with the Bardet-Beidl syndrome (BBS) pathway [49]. CEP290 is also known to be an important component of the primary cilium, localizing to the Y-links of the ciliary transition zone and having a role in the regulation of transport in and out of the ciliary compartment [50]. Furthermore, CEP290 mutations lead to a range of ciliopathy syndromes with variable clinical manifestations in humans: BBS, Joubert syndrome and Meckel-Gruber syndrome [51]. Given that both proteins (POC5 and CEP290) are located at the base of the cilium, and that CEP290 interacts solely with wtPOC5, this supports the role of POC5 as a ciliary protein operating at the base of the cilium.

Interestingly, some of the proteins, such as Annexin A2 and Calmodulin interacting with wtPOC5 were previously associated with scoliosis. Annexin A2, has a high expression in osteoblasts, osteoarthritic chondrocytes, hypertrophic, and terminally differentiated growth plate chondrocytes. Annexin A2 plays an essential role in bone mineralization which appears to be critical in AIS patients. It was found that the osteogenic differentiation of mesenchymal stem cells from AIS patients was altered; this points to a role of Annexin A2 in scoliosis and makes it an interesting candidate for future studies [52]. Calmodulin-like protein 3 (immunoprecipitated with wtPOC5 but not mutPOC5) is another interesting candidate that may be linked with POC5 and AIS. Calmodulin-like protein is a calcium sensor protein that is closely related to the ubiquitous calmodulin, which is considered potential key molecule in the etiology of scoliosis because of its effects on muscle contractility. However unlike calmodulin, calmodulin-like protein 3 is tissue specific and is expressed specifically in differentiated epithelia [53]. Patients with AIS experience some muscle tone disorder. Calmodulin, with its ability to bind calcium ions and its role in muscle contraction, could be strongly associated with AIS [54] (Table 1). Only five proteins were found to be associated with mutPOC5

protein 5. Interestingly, among those proteins is iduronate 2-sulfatase. Iduronate 2-sulfatase is associated with Hunter syndrome clinical disorder (mucopolysaccharidosis type II, MPS-II) in which patients may present, among other skeletal diseases, scoliosis [55, 56]. Also, the cellular stress gene protein disulfide isomerase (PDIA4) was found to be associated with mutPOC5. PDIA4 is up-regulated in mouse models of brain neurodegenerative diseases involving protein misfolding. Although not much is known about the physiological role of PDIA4, studies indicate that this gene is upregulated following endoplasmic reticulum ER stress [57, 58]. A very interesting observation is that the mutPOC5 was found to be hyper-phosphorylated (S3 Fig.), which could be one of the factors that lead to the loss of POC5 connection with several ciliary and cytoskeletal proteins. It is known that posttranslational modifications are one of the ways to regulate protein activity, subcellular localization, and stability. The phosphorylation can control the strength of interactions. Further studies are needed to determine where the phosphate group is added and the exact consequences on the physico-chemical properties, stability, kinetics, and dynamics [59].

One of the most intriguing results of our study was the immunofluorescence on human cells carrying the *POC5* variant (c. C1286T; p. A429V mutation) showing the mislocalization of POC5 with respect to cilia. We observed ciliary retraction in scoliotic osteoblasts (Fig 2 h) with the POC5 mutation when compared to normal osteoblasts (Fig 2 d). The primary cilium is an antenna-like projection of the cell that plays a critical role in the perception and integration of environmental signals like mechanotransduction. Cilia are also essential for left-right (L-R) symmetry during embryonic development [60, 61] and for cerebrospinal fluid (CSF) flow [62]. Recently, it was found that IS patients have an abnormal left–right (L-R) asymmetries and defective CSF flow, and therefore, it was suggested that motile cilia

dysfunction may contribute to the etiopathogenesis of IS [27]. Interestingly, restoration of motile cilia activity blocked spinal curve progression. This supports our results that show a defect in cilia organization as well as perturbed localization of POC5 with respect to the cilia in cells expressing a *POC5* mutation (Fig 2 g). Another interesting observation is the defect in the cell cycle in mut*POC5* overexpressing cells. The cells were synchronized to be at the same cell cycle stage, and a different subcellular localization of wt and mutPOC5 at different stages of the cell cycle was observed. MutPOC5 was permanently located within the nucleus in G1 and S phases (Fig 4 c and d). By cellular fractionation, we confirmed the different subcellular localization of wt and mutPOC5 (Fig. 6). Previous work [32] also showed that a depletion of POC5 in Hela cells affects the progression through S phase. Human h-POC5-depleted cells had a significant increase in the proportion of S-phase cells; thus, hPOC5 depletion induced an accumulation of cells in S phase where procentriole assembly was probably initiated; however, these procentrioles failed to elongate.

The cilia and neurological component of this pathology merits further investigation through various functional tests in patients with AIS in order to evaluate the possible functional defect connected with the altered structures identified in this work. Further study, focused on the primary cilia-mediated function, will provide more insights into the molecular mechanisms and etiology of AIS. As well, this can demystify the development of this disease.

Conclusion:

In conclusion, our findings confirm the involvement of *POC5* in scoliosis. A role for *POC5* with respect to the primary cilia was found. These findings open new avenues for the understanding the primary causes of AIS at the molecular and physiological levels.

Acknowledgment:

Proteomics analyses were performed by the Proteomics Platform of the Institute of Research in immunology and Cancer (IRIC) in Montreal, Canada**.**

References:

1. Allen, D.B., *Safety of human growth hormone therapy: current topics.* J Pediatr, 1996. **128**(5 Pt 2): p. S8-13.
2. Veldhuizen, A.G., D.J. Wever, and P.J. Webb, *The aetiology of idiopathic scoliosis: biomechanical and neuromuscular factors.* Eur Spine J, 2000. **9**(3): p. 178-84.
3. Stokes, I.A., et al., *Metabolic Effects of Angulation, Compression and Reduced Mobility on Annulus Fibrosis in a Model of Altered Mechanical Environment in Scoliosis.* Spine Deform, 2013. **1**(3): p. 161-170.
4. Stokes, I.A., et al., *Biomechanical spinal growth modulation and progressive adolescent scoliosis--a test of the 'vicious cycle' pathogenetic hypothesis: summary of an electronic focus group debate of the IBSE.* Scoliosis, 2006. **1**: p. 16.
5. Stokes, I.A., et al., *Intervertebral disc changes with angulation, compression and reduced mobility simulating altered mechanical environment in scoliosis.* Eur Spine J, 2011. **20**(10): p. 1735-44.
6. Stokes, I.A., *Analysis and simulation of progressive adolescent scoliosis by biomechanical growth modulation.* Eur Spine J, 2007. **16**(10): p. 1621-8.
7. Lafortune, P., et al., *Biomechanical simulations of the scoliotic deformation process in the pinealectomized chicken: a preliminary study.* Scoliosis, 2007. **2**: p. 16.
8. Hadley-Miller, N., B. Mims, and D.M. Milewicz, *The potential role of the elastic fiber system in adolescent idiopathic scoliosis.* J Bone Joint Surg Am, 1994. **76**(8): p. 1193-206.
9. Miller, N.H., et al., *Genetic analysis of structural elastic fiber and collagen genes in familial adolescent idiopathic scoliosis.* J Orthop Res, 1996. **14**(6): p. 994-9.
10. Sponseller, P.D., et al., *Growing rods for infantile scoliosis in Marfan syndrome.* Spine (Phila Pa 1976), 2009. **34**(16): p. 1711-5.
11. Wang, D., et al., *Altered topological organization of cortical network in adolescent girls with idiopathic scoliosis.* PLoS One, 2013. **8**(12): p. e83767.
12. Shi, L., et al., *Volumetric changes in cerebellar regions in adolescent idiopathic scoliosis compared with healthy controls.* Spine J, 2013. **13**(12): p. 1904-11.
13. Sun, X., et al., *Variations of the position of the cerebellar tonsil in idiopathic scoliotic adolescents with a cobb angle >40 degrees: a magnetic resonance imaging study.* Spine (Phila Pa 1976), 2007. **32**(15): p. 1680-6.
14. Geissele, A.E., et al., *Magnetic resonance imaging of the brain stem in adolescent idiopathic scoliosis.* Spine (Phila Pa 1976), 1991. **16**(7): p. 761-3.

15. Wang, D., et al., *Abnormal cerebral cortical thinning pattern in adolescent girls with idiopathic scoliosis.* Neuroimage, 2012. **59**(2): p. 935-42.
16. Maiocco, B., et al., *Adolescent idiopathic scoliosis and the presence of spinal cord abnormalities. Preoperative magnetic resonance imaging analysis.* Spine (Phila Pa 1976), 1997. **22**(21): p. 2537-41.
17. Hawasli, A.H., T.E. Hullar, and I.G. Dorward, *Idiopathic scoliosis and the vestibular system.* Eur Spine J, 2015. **24**(2): p. 227-33.
18. Hitier, M., et al., *Lateral Semicircular Canal Asymmetry in Idiopathic Scoliosis: An Early Link between Biomechanical, Hormonal and Neurosensory Theories?* PLoS One, 2015. **10**(7): p. e0131120.
19. Shi, L., et al., *Automatic MRI segmentation and morphoanatomy analysis of the vestibular system in adolescent idiopathic scoliosis.* Neuroimage, 2011. **54 Suppl 1**: p. S180-8.
20. Patten, S.A. and F. Moldovan, *Could genetic determinants of inner ear anomalies be a factor for the development of idiopathic scoliosis?* Med Hypotheses, 2011. **76**(3): p. 438-40.
21. Barrios, C., et al., *Anthropometry and body composition profile of girls with nonsurgically treated adolescent idiopathic scoliosis.* Spine (Phila Pa 1976), 2011. **36**(18): p. 1470-7.
22. Zhang, H.Q., et al., *Association of estrogen receptor beta gene polymorphisms with susceptibility to adolescent idiopathic scoliosis.* Spine (Phila Pa 1976), 2009. **34**(8): p. 760-4.
23. Sanders, J.O., et al., *Maturity assessment and curve progression in girls with idiopathic scoliosis.* J Bone Joint Surg Am, 2007. **89**(1): p. 64-73.
24. Raczkowski, J.W., *The concentrations of testosterone and estradiol in girls with adolescent idiopathic scoliosis.* Neuro Endocrinol Lett, 2007. **28**(3): p. 302-4.
25. Grivas, T.B., et al., *Association between adolescent idiopathic scoliosis prevalence and age at menarche in different geographic latitudes.* Scoliosis, 2006. **1**: p. 9.
26. Hayes, M., et al., *ptk7 mutant zebrafish models of congenital and idiopathic scoliosis implicate dysregulated Wnt signalling in disease.* Nat Commun, 2014. **5**: p. 4777.
27. Grimes, D.T., et al., *Zebrafish models of idiopathic scoliosis link cerebrospinal fluid flow defects to spine curvature.* Science, 2016. **352**(6291): p. 1341-4.
28. Engesaeth, V.G., J.O. Warner, and A. Bush, *New associations of primary ciliary dyskinesia syndrome.* Pediatr Pulmonol, 1993. **16**(1): p. 9-12.
29. Yee, A., et al., *Understanding the Basis of Genetic Studies: Adolescent Idiopathic Scoliosis as an Example.* Spine Deform, 2014. **2**(1): p. 1-9.
30. Patten, S.A., et al., *Functional variants of POC5 identified in patients with idiopathic scoliosis.* J Clin Invest, 2015. **125**(3): p. 1124-8.
31. Xu, L., et al., *Common variant of POC5 is associated with the susceptibility of adolescent idiopathic scoliosis.* Spine (Phila Pa 1976), 2017.
32. Azimzadeh, J., et al., *hPOC5 is a centrin-binding protein required for assembly of full-length centrioles.* J Cell Biol, 2009. **185**(1): p. 101-14.
33. Dantas, T.J., et al., *Calcium-binding capacity of centrin2 is required for linear POC5 assembly but not for nucleotide excision repair.* PLoS One, 2013. **8**(7): p. e68487.

34. Chang, C.W., et al., *CEP295 interacts with microtubules and is required for centriole elongation.* J Cell Sci, 2016. **129**(13): p. 2501-13.
35. Weisz Hubshman, M., et al., *Whole-exome sequencing reveals POC5 as a novel gene associated with autosomal recessive retinitis pigmentosa.* Hum Mol Genet, 2017.
36. Pazour, G.J. and G.B. Witman, *The vertebrate primary cilium is a sensory organelle.* Curr Opin Cell Biol, 2003. **15**(1): p. 105-10.
37. Searle, B.C., *Scaffold: a bioinformatic tool for validating MS/MS-based proteomic studies.* Proteomics, 2010. **10**(6): p. 1265-9.
38. Singleman, C. and N.G. Holtzman, *Growth and maturation in the zebrafish, Danio rerio: a staging tool for teaching and research.* Zebrafish, 2014. **11**(4): p. 396-406.
39. Huang, T., et al., *The role of microglia in the neurogenesis of zebrafish retina.* Biochem Biophys Res Commun, 2012. **421**(2): p. 214-20.
40. Wang, Y.J., et al., *Effect of titanium dioxide nanoparticles on zebrafish embryos and developing retina.* Int J Ophthalmol, 2014. **7**(6): p. 917-23.
41. Narayan, D.S., et al., *A review of the mechanisms of cone degeneration in retinitis pigmentosa.* Acta Ophthalmol, 2016. **94**(8): p. 748-754.
42. Grivas, T.B., et al., *Prevalence of scoliosis in women with visual deficiency.* Stud Health Technol Inform, 2006. **123**: p. 52-6.
43. Nault, M.L., et al., *Relations between standing stability and body posture parameters in adolescent idiopathic scoliosis.* Spine (Phila Pa 1976), 2002. **27**(17): p. 1911-7.
44. Lao, M.L., et al., *Impaired dynamic balance control in adolescents with idiopathic scoliosis and abnormal somatosensory evoked potentials.* J Pediatr Orthop, 2008. **28**(8): p. 846-9.
45. Guo, X., et al., *Balance control in adolescents with idiopathic scoliosis and disturbed somatosensory function.* Spine (Phila Pa 1976), 2006. **31**(14): p. E437-40.
46. Machida, M., et al., *Pathogenesis of idiopathic scoliosis: SEPs in chicken with experimentally induced scoliosis and in patients with idiopathic scoliosis.* J Pediatr Orthop, 1994. **14**(3): p. 329-35.
47. Sahlstrand, T., R. Ortengren, and A. Nachemson, *Postural equilibrium in adolescent idiopathic scoliosis.* Acta Orthop Scand, 1978. **49**(4): p. 354-65.
48. Knodler, A., et al., *Coordination of Rab8 and Rab11 in primary ciliogenesis.* Proc Natl Acad Sci U S A, 2010. **107**(14): p. 6346-51.
49. Westlake, C.J., et al., *Primary cilia membrane assembly is initiated by Rab11 and transport protein particle II (TRAPPII) complex-dependent trafficking of Rabin8 to the centrosome.* Proc Natl Acad Sci U S A, 2011. **108**(7): p. 2759-64.
50. Drivas, T.G. and J. Bennett, *CEP290 and the primary cilium.* Adv Exp Med Biol, 2014. **801**: p. 519-25.
51. Rachel, R.A., T. Li, and A. Swaroop, *Photoreceptor sensory cilia and ciliopathies: focus on CEP290, RPGR and their interacting proteins.* Cilia, 2012. **1**(1): p. 22.
52. Zhuang, Q., et al., *Differential proteome analysis of bone marrow mesenchymal stem cells from adolescent idiopathic scoliosis patients.* PLoS One, 2011. **6**(4): p. e18834.
53. Brooks, M.D., et al., *Human Calmodulin-Like Protein CALML3: A Novel Marker for Normal Oral Squamous Mucosa That Is Downregulated in Malignant Transformation.* Int J Dent, 2013. **2013**: p. 592843.

54. Acaroglu, E., et al., *Comparison of the melatonin and calmodulin in paravertebral muscle and platelets of patients with or without adolescent idiopathic scoliosis.* Spine (Phila Pa 1976), 2009. **34**(18): p. E659-63.
55. Roberts, S.B. and A.I. Tsirikos, *Thoracolumbar kyphoscoliosis with unilateral subluxation of the spine and postoperative lumbar spondylolisthesis in Hunter syndrome.* J Neurosurg Spine, 2016. **24**(3): p. 402-6.
56. Wilson, P.J., et al., *Hunter syndrome: isolation of an iduronate-2-sulfatase cDNA clone and analysis of patient DNA.* Proc Natl Acad Sci U S A, 1990. **87**(21): p. 8531-5.
57. Galligan, J.J. and D.R. Petersen, *The human protein disulfide isomerase gene family.* Hum Genomics, 2012. **6**: p. 6.
58. Kaplan, A., et al., *Small molecule-induced oxidation of protein disulfide isomerase is neuroprotective.* Proc Natl Acad Sci U S A, 2015. **112**(17): p. E2245-52.
59. Nishi, H., K. Hashimoto, and A.R. Panchenko, *Phosphorylation in protein-protein binding: effect on stability and function.* Structure, 2011. **19**(12): p. 1807-15.
60. Yoshiba, S. and H. Hamada, *Roles of cilia, fluid flow, and Ca2+ signaling in breaking of left-right symmetry.* Trends Genet, 2014. **30**(1): p. 10-7.
61. Shinohara, K. and H. Hamada, *Cilia in Left-Right Symmetry Breaking.* Cold Spring Harb Perspect Biol, 2017. **9**(10).
62. Huang, B.K. and M.A. Choma, *Microscale imaging of cilia-driven fluid flow.* Cell Mol Life Sci, 2015. **72**(6): p. 1095-113.

Fig 1: Differential localization of POC5 with acetylated-α-tubulin in wtPOC5 and mutPOC5 expressing cells. Confocal imaging of HeLa cells transiently transfected with wt*POC5* (a) or mut*POC5* (b). POC5 and acetylated-α-tubulin were determined using specific antibodies and positive signal revealed by green and red coloration respectively. Localization of POC5 with respect to acetylated-α-tubulin (marker for cilia) is shown: in cells transfected with wtPOC5 (a) where positive immunostaining was enriched at the perinuclear acetylated-α-tubulin ring, while in cells expressing mutPOC5 (b), POC5 was visualized inside the nucleus (disconnected from the perinuclear acetylated-α-tubulin ring). The Z-stack imaging (recording images at different focal planes) allows the visualization of the three-dimensional structure containing both POC5 and acetylated-α-tubulin (green and red) for the wtPOC5, while only POC5 (green) was visualized for the mutPOC5. Images were taken using the Zeiss microscopy

Mag x40. Scale bar 1.6 µm. POC5 in green, acetylated-α-tubulin in red and DNA was stained with DAPI (blue).

Fig 2: Human osteoblasts carrying POC5 variant mutation (c). C1286T; p. A429V) show short cilia. Representative immunodetection of POC5 and acetylated-α-tubulin by immunofluorescence in osteoblasts from normal (non scoliotic) (a, b, c, d) and cells with the variant c. C1286T (p. A429V) (e, f, g, h). Merged images (d and h) show differential colocalization of POC5 with respect to cilia. Zoomed image shows that POC5 is located at the nuclear membrane at the cilium level marked by acetylated-α-tubulin. Human osteoblasts carrying the variant POC5 (c. C1286T; p. A429V) (e, f, g, h), show decreased staining intensity and absence or retraction of cilium (h). MutPOC5 protein was seen to be localized within the nucleus (zoomed image). POC5 (green coloration), acetylated-α-tubulin (red coloration) and the nucleus was stained with DAPI (blue). Images were taken using the Zeiss microscopy Mag x 40. Scale bar 1.6 µm. (I) The graphs represent the percentage of cilia for each length category in NOB and AIS cells. Each bar represents the mean of three independent experiments (±SD). $P< 0.05$ considered statistically signifcant. (G) Sequence alignment with Sanger sequencing confirm AIS cells to have the c. C1286T mutation.

Fig 3: Validation of mass spectrometric results. Proteins identified by mass spectroscopy interacting with the wtPOC5 were analysed by CO-IP. Coimmunoprecipitation of myc-POC5 using anti-Myc antibodies in Hek293 cells. Proteins in the immune complexes were revealed by Western blotting with different antibodies as described in materials and methods. Controls (Non transfected (NT) or cells transfected with Mock pCMV-entry vector) were used along cells transfected with myc tagged wt or mut POC5 expressing cells. CO-IP shows the binding of CKAP5, Desmocollin1, CEP290, RAB11, and Septin9 exclusively with wtPOC5. There is

no interaction of mutPOC5 with CKAP5, Desmocollin1, CEP290, RAB11 and Septin9. Very weak interaction was observed between mutPOC5 with Acetylated-α-tubulin, Galectin3 and 7, EHD4, CystatinA and Annexin2 and 5 as compared to wtPOC5.

Fig 4: MutPOC5 expressing cells are arrested in S phase. Confocal imaging of HeLa cells overexpressing wtPOC5 or mutPOC5. Specific staining for POC5 was performed using POC5 antibody. The subcellular localization pattern of POC5 was used as a specific marker for the cell cycle phase. During G1 phase, obtained by serum starvation (a), wtPOC5 is located within the cytoplasm, while in the S phase (b) (serum replacement after deprivation), POC5 is located within the nucleus. WtPOC5 expressing cells have normal progression through G1 and S phase, as detected by position of POC5 (a, b). In the cells overexpressing mutPOC5, POC5 is located within the nucleus in both G1 and S phases (c, d). Cells are blocked in S phase and unable to progress through the cell cycle as determined by the permanent localization of POC5 within the nucleus of HeLa cells. Images were taken using the Zeiss microscopy. POC5 (visualized in red), DNA was stained with DAPI (blue). Mag x 40. Scale bar 1.6 μm. E) Bar diagram representing the percentage of G1 and S phase cells after serum starvation for 24 h. The percentage of Sphase cells is significantly higher ($p<0.01$) in mutPOC5 than wtPOC5 expressing cells. The wtPOC5 cells are mostly in G1 phase ($p<0.001$).

Fig 5: Differential colocalization of wtPOC5 and mutPOC5 with respect to centrin

A) Immunoflourescence staining was performed in HeLa cells non-transfected (NT) overexpressing pCMV-entry empty vector (mock), wtPOC5 or mutPOC5. Staining of POC5 (red), centrin 2 (green) shows colocalization of wtPOC5 and centrin 2 (merge orange colour), and absence of colocalization with mutpoc5 and centrin 2. B) Statistical analysis of centrin 2 expression, intensity and number of centrin dots per cell in mock, wtPOC5 and mutPOC5

expressing HeLa cells. Percentage of centrin 2 number and intensity are reduced in mutPOC5 expressing cells. Unlike wtPOC5 cells, most mutPOC5 cells have one dot of centrin but majority of wtPOC5 expressing cells have two dots of centrin 2. Centrin count and intensity was performed using ZEN software. Images (n=6) were used for quantification. Error bars are the mean ± SD. POC5 (red), centrin (green) and DAPI (blue). NT: non transfected. NS: non significant.

Fig 6: Differential subcellular localization of wtPOC5 and mutPOC5 in Hek293

Nuclear and cytoplasmic cell extracts were obtained using protocol as described in materials and methods. Equal nuclear and cytoplasmic protein samples loaded were determined using β-actin as loading control and subjected to immunoblotting using anti-POC5 antibody. Controls were cells non transected or transfected with pCMV-entry vector. The wtPOC5 is mainly expressed in the cytoplasm and the mutPOC5 is mostly nuclear.

Fig 7: Distribution of poc5 and cilia in 2mpf zebrafish. Double staining for poc5 and acetylated-α-tubulin with specific antibodies was performed on the retinas of wt and mut zebrafish. Merged co-staining of poc5 (green) and acetylated-α-tubulin as marker for cilia (red) shows colocalization in the eyes of wt (c) but not mut (f). Poc5 staining (green) was seen at the retinal pigmented epithelium (RPE) and inner nuclear layers (INL) in both wt (a) and mut (d) retina. However, the intensity of staining of poc5 in the wt retina is stronger than in mut. Acetylated-α-tubulin immunoreactivity was seen throughout the RPE and INL of wtpoc5 retina but not in mut zebrafish. Immunostaining of acetylated-α-tubulin was reduced in the pigmented epithelial layer of the retina of the mutpoc5 (e) when compared to the wt (b) and was totally absent in the INL of mutpoc5 retina. Mag x 20. Scale bar: 2.1 μm.

The morphology of the mut*poc5* retina was then investigated. The mut*poc5* zebrafish were characterized with the loss of outer segment layer (*OSL) (Fig 8 b) as the thickness of this layer was highly reduced in the mut*poc5* retina. Also, the structural organization of the cone cell layer (CC) and outer nuclear layer (ONL) was disrupted in the mut*poc5*. No difference was observed in the RPE, inner nuclear layer (INL), inner plexiform layer (IPL), and ganglion cell layers (GCL) (Fig 8 a and b).

Fig 8: Photoreceptor outer segments are not developed in mutpoc5 zebrafish. OSL: outer segment layer; CC: cone cell layer; RPE: retinal pigment epithelium; ONL: outer nuclear layer; INL: inner nuclear layer; IPL: inner plexiform layer. Histology of wt and mutpoc5 zebrafish retina was performed using hematoxylin and eosin staining. Photoreceptor OSL (*) is absent in the retina of mutpoc5 zebrafish as shown by haematoxylin & eosin staining (b). The OSL, the portion of the photoreceptor cell cilium linking the photoreceptor inner and outer segments is missing in the mutpoc5 retina. All the other different layers of the retina (RPE, ONL, INL, OPL) are present in the mut expressing zebrafish. Wtpoc5 retina has highly organized cells of the CC and ONL as compared to mutPOC5, which is fully disorganized. Analysis of wt and mutpoc5 retina was performed using light microscopy. Mag x 40; scale bar 1.6 μm.

Fig 9: Mutpoc5 expressing zebrafish have abnormities in the cones.

Staining for different layers (Rods and cones) was performed using the specific antibodies zpr3, zpr1, and 3A10 respectively. ROS: rod outer segment; DCOS: double cone outer segment; LSCOS: long single cone outer segment, SSCOS: short single cone outer segment, ONL: outer nuclear layer, OS: outer segment; CC: connecting cilium; IS: inner segment; CB: cell body, IF: inner fiber; P: perdicle. Representative image of the retina of the wt and

mutpoc5 zebrafish stained for zpr3 in (a, b), zpr1 (c, d) and 3A10 (e, f). Nuclei were stained with DAPI (blue). (a-d) Zpr-3 signal is seen in rod and double-cone outer segment layer included in the surrounded area. Zpr3 immunostaining of wtpoc5 (a) retina labeled rod photoreceptors in the ONL. Lower staining was observed in mutpoc5 retina (b). Not only the intensity, but also the thickness of the ROS in the mut zebrafish is much lower than the wt. Zrp3 staining is also seen in the DCOS of wtpoc5 retina but with lower intensity of staining in the mut retina. Zpr1 is a marker for double cones. There is severe loss of rod and cone pigment proteins in mut zebrafish (d). There is strong staining of double cones in wt retina (c) but this staining is totally absent from mut retina (d). The perdicle is also absent in the retina of mutpoc5 (d). (e-f) 3A10 staining of retina from both wt and mutpoc5. The 3A10 antibody also stains the OS and CC which showed reduced thickness, and intensity in the retina of mutpoc5 zebrafish (f) as compared to retina of wtpoc5 zebrafish (e). Images were taken using the Zeiss microscopy Mag x20. Scale bar 20 μm.

Fig 10: Proposed model for the mechanisms of ciliary retraction in mutPOC5 expressing cells. Under normal conditions, POC5 is an essential protein for normal cell cycle progression, and this process is a tightly regulated mechanism. In cycling cells, with wtPOC5, POC5 protein is found interacting with several ciliary proteins that assemble before entering to G1 phase. This complex is essential for the formation of a normal cilium. Weak or no interaction of mutPOC5 with ciliary proteins (revealed in this study by immunofluorescence, mass spectroscopy, and CO-IP) results in incorrect assembly and cilium retraction

Supporting Information:

S1 Fig: Acetylated-α-tubulin is highly enriched in precipitated wtPOC5 lysate but not mutPOC5. Hek293 cells were transfected with empty pCMV entry vector, wtPOC5 or mutPOC5 myc tagged vectors. Immunoprecipitation of POC5 was performed using myc antibody (origene). A) Western blot on total cell lysate using POC5 antibody. Wt and mutPOC5 tranfected cells have same expression levels of POC5. Mock transfected sample have very low expression of POC5. POC5 is observed at the expected size 63kDa. A band at higher level than the wtPOC5 is observed in the mutPOC5 (p: phosphorylated). B) Coommasie blue staining shows similar levels of POC5 expression in wt and mut transfected samples. POC5 is observed at the expected size 63kDa. Also the heavy and light chains of antibody are observed. C) Western blot using anti-POC5 antibody shows absence of expression in control sample (Mock) and similar protein expression levels of wt and mutPOC5. Two bands are observed in mutPOC5 overexpressing cells. One band at same level of wtPOC5 and one at higher levels (p: phosphorylated). D) Western blot of acetylated-α-tubulin after immunoprecipitation of POC5, shows high expression of acetylated-α-tubulin in the wtPOC5 expressing sample and lower levels in mutPOC5. Very low levels are observed in mock transfected sample.

S2 Fig: Zebrafish screening for the spinal deformity by micro CT scan confirmed the scoliosis phenotype. Representative micro-CT scans (MicroCT, 9 microns): images of wt (a) and mutpoc5 (b) juvenile zebrafish. MicroCT images of wtpoc5 fish showed a fully mineralized with non-curved spine, while mutpoc5 fish present mineralized spine, with rotational deformity (curvature) the spine.

S3 Fig: Phosphorylation state of wtPOC5 and mutPOC5 at G1 and S phases of cell cycle. The immunoprecipitated samples were either non treated or treated with alkaline phosphatase

and then western blot was performed using POC5 antibody (abcam). The presence or absence of phosphorylation with wtPOC5 and mutPOC5 is shown at G1 and S phase. POC5 wt is not phosphorylated, but the mutPOC5 is phosphorylated, and treatment with phosphatase dephosphorylates mutPOC5 that returns back to the same levels of wtPOC5. Phosphorylation of mutPOC5 is seen at both G1 and S phases.

S4 Fig: Poc5 colocalizes with centrin2 in zebrafish retina of wtpoc5 but not mutpoc5. Poc5 and centrin are co-expressed in the OS and CC in wtpoc5 zebrafish retina. No staining of poc5 is observed in mutpoc5 retina and no colocalization of poc5 and centrin is observed. In addition, the organization of centrin in the cone layer is disrupted with several spacing in the CC layer. OS: outer segment layer, CC: cone cell layer. Poc5 labelled in green, centrin labeled in red and DAPI in blue. Scale bar: 20 μm, Mag x40.

S5 Fig: Colocalization of poc5 and acetylated-α–tubulin the ear of wt*poc5* zebrafish: A) Acetylated-α-tubulin staining of the hair cell kinocilia of the inner ear of wt and mutpoc5 zebrafish. Acetylated-α– tubulin (red) and DAPI (blue). B) In blue is the cell nuclei, green the poc5 and in red fluorescence labels cilia of the cell membranes. Immunostaining for poc5 and acetylated-α-tubulin was performed on the wtpoc5 and mutpoc5 zebrafish head. Poc5 and acetylated-α-tubulin are strongly expressed in the ear of wtpoc5 zebrafish and they colocalize, but not in mutpoc5 zebrafish ear. Scale bar 20μm and Magx40.

Protein ID	Description	Score	Peptide Number
P15924	Desmoplakin	3984	119
Q08554	**Desmocollin-1**	581	12
P68363	**Tubulin alpha-1B chain**	368	10
P07355	**Annexin A2**	221	9
Q9NSK0-3	Isoform 3 of Kinesin light chain 4	155	9
F8VW92	Tubulin beta chain	251	7
P47929	**Galectin-7**	338	6
Q9H223	**EH domain-containing protein 41**	62	4
Q6IB90	**Cystatin**	84	3
Q9NZT1	Calmodulin-like protein 5	243	3
Q14574-2	Isoform 3B of Desmocollin-3	63	3
Q14008	**Cytoskeleton-associated protein 5**	57	3
Q9Y5P4-2	Isoform 2 of Collagen type IV alpha-3-binding protein	45	2
P27482	Calmodulin-like protein 3	144	2
P08758	**Annexin A5**	164	2
Q08380	Galectin-3-binding protein	76	2
B4DF70	cDNA FLJ60461; highly similar to Peroxiredoxin-2 (EC 1.11.1.15)	88	2
Q59FR8	**Galectin 3**		2
Q9UHD8-5	**Isoform 5 of Septin-9**	46	2
J3KNF5	**Centrosomal protein of 290 kDa**	20	1
Q8N6N5	Tubulin; beta 2C	85	1
B4E0R6	Importin-5	69	1
Q86YS3-2	**Isoform 2 of Rab11 family-interacting protein 4**	27	1

Protein ID	Description	Score	Peptide Number
A8MUB1	**Tubulin alpha-4A chain**	183	1
A9X9K9	Desmocollin 2	46	1
r-Q5T802	RUNX2	15	1
Q02413	Desmoglein-1	1584	21
Q13835	Plakophilin-1 2	536	17
F5GWP8	Junction plakoglobin	3102	16
O76021	Ribosomal L1 domain-containing protein 1	294	11
P36952	Serpin B5	385	7
P25311	Zinc-alpha-2-glycoprotein	141	3
Q9GZZ8	Extracellular glycoprotein lacritin	98	3
E9PBV3	Suprabasin	190	3
Q9Y5P4-2	Isoform 2 of Collagen type IV alpha-3-binding protein	45	2
B4DT31	Far upstream element-binding protein 1	151	9
E9PIN3	Nuclear RNA export factor 1 (Fragment)	149	5
O43776	Asparagine--tRNA ligase; cytoplasmic	94	4
Q9Y2X3	Nucleolar protein 58	113	4
B8ZZD1	U4/U6.U5 tri-snRNP-associated protein 2	43	2
P35579	Myosin-9	555	18
P58107	Epiplakin	200	10
Q8WVV4	Protein POF1B	242	6
Q15149-9	Isoform 9 of Plectin	84	2

Table 1: Mass spectroscopy results of proteins interacting exclusively with wtPOC5.

Scaffold software was used for the analysis of the identified proteins interacting with wtPOC5. Protein identification in wtPOC5 expressing cells, detected 85 candidates interacting with wtPOC5. Clustering proteins by biological function indicated: ciliary proteins (17 proteins); cell adhesion (7 proteins); cytoskeleton-associated protein (4 proteins); RNA processing (9 proteins); extracellular matrix (3 proteins); response to estrogen (1 protein); cell cycle and cytokinesis (1 protein). Most of the identified proteins interacting with POC5 are ciliary proteins (As shown in the table) and those marked in bold were considered for further analysis. Other protein groups belong to cell cycle and cytokinesis, extracellular proteins, RNA processing, cell adhesion, and response to estrogen.

Protein ID	Description	Score	Peptide Number
P13667	Protein disulfide-isomerase A4	226	9
P22304	Iduronate 2-sulfatase	138	5
Q9H3P7	Golgi resident protein GCP60	193	3
Q7RU04	Aminopeptidase B	95	2
B4E0E1	cDNA FLJ53442; highly similar to Poly (ADP-ribose) polymerase 1	61	2

Table 2: Mass spectroscopy results of proteins interacting exclusively with mutPOC5 Five proteins were found to be interacting exclusively with mutPOC5. Protein disulfide-isomerase A4, Iduronate 2-sulfatase, Golgi resident protein GCP60, Aminopeptidase B and cDNA FLJ53442; highly similar to Poly (ADP-ribose) polymerase

Fig 1

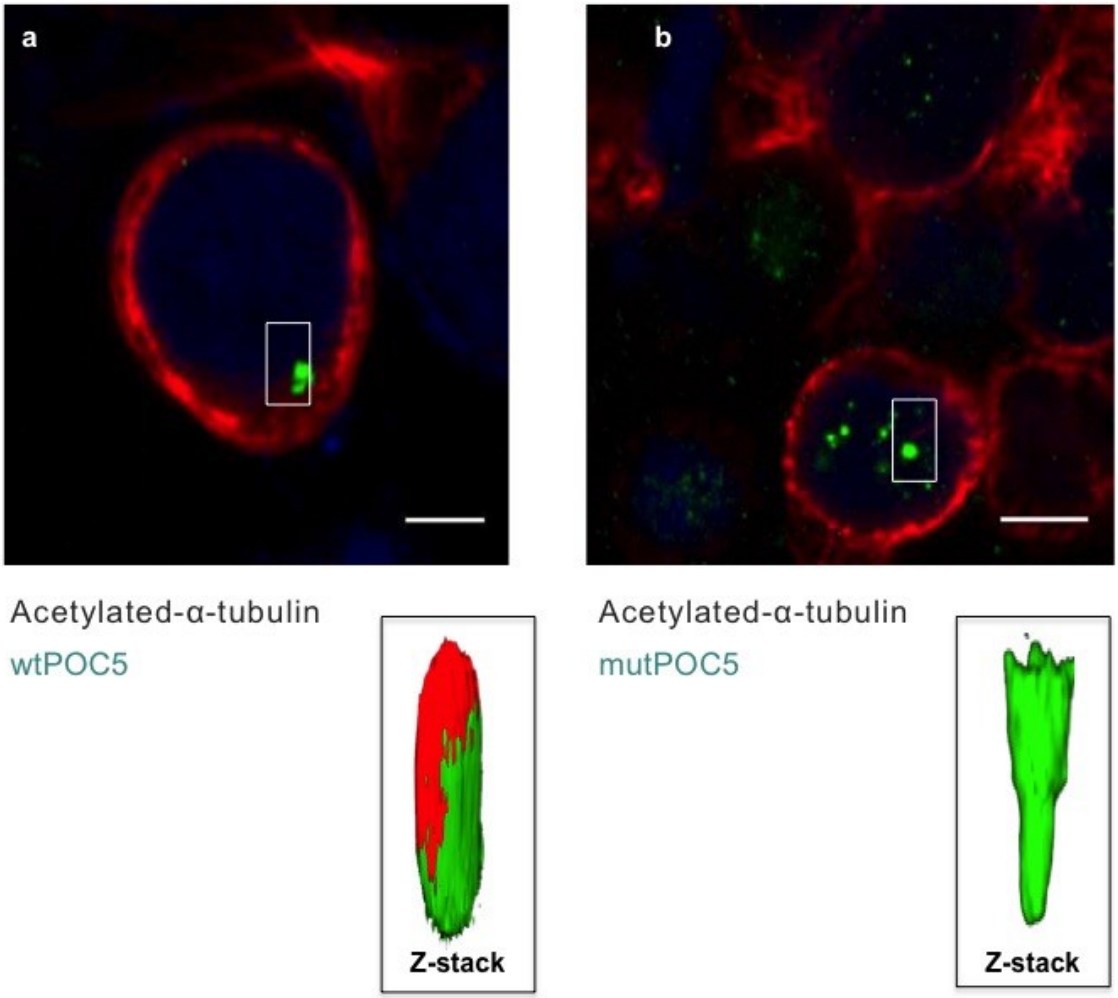
a
b
Acetylated-α-tubulin
wtPOC5
Z-stack
Acetylated-α-tubulin
mutPOC5
Z-stack

Fig. 2

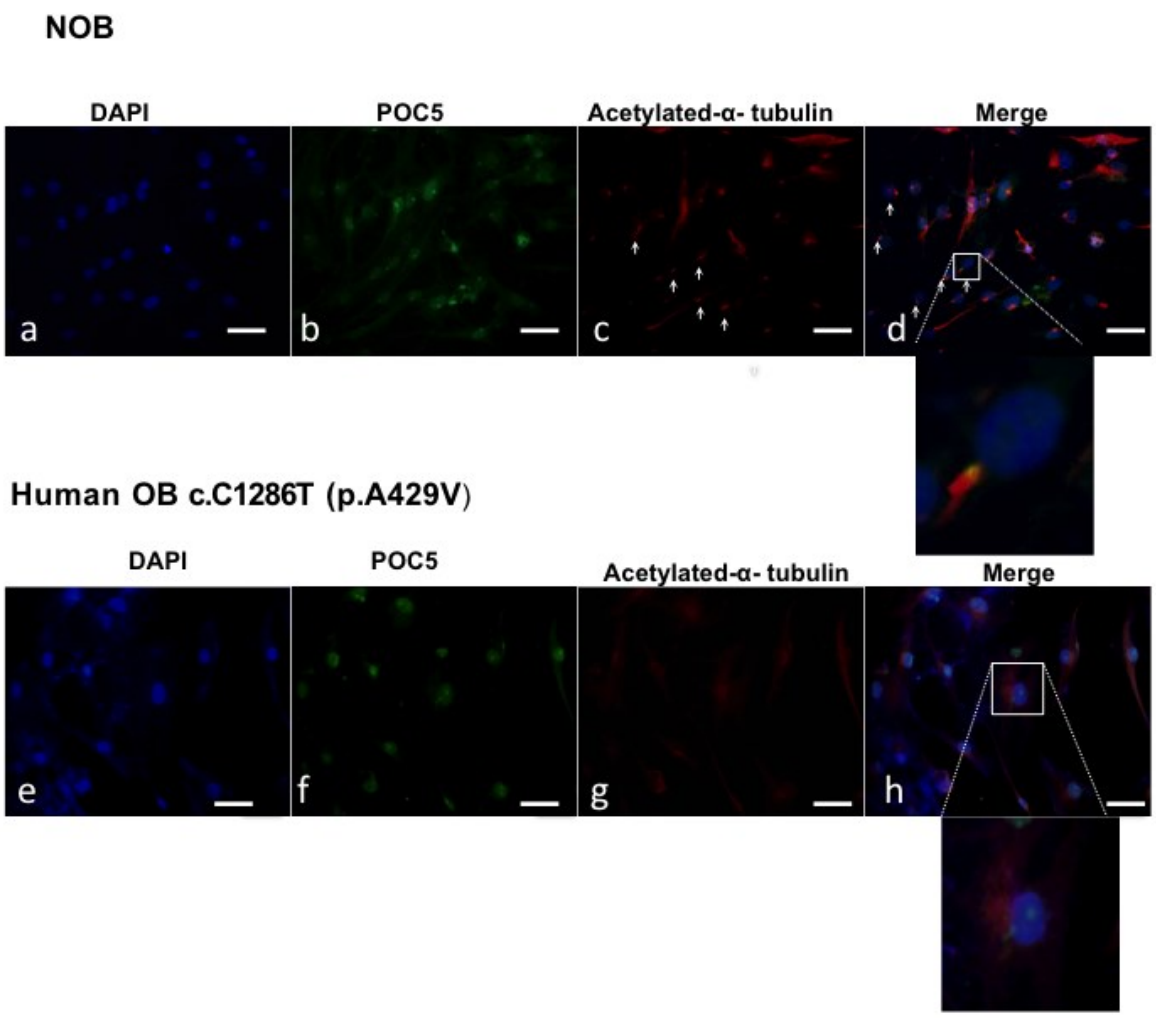
NOB
DAPI
POC5
Acetylated-α- tubulin
Merge
a
b
c
d
Human OB c.C1286T (p.A429V)
DAPI
POC5
Acetylated-α- tubulin
Merge
e
f
g
h

Fig. 2 I

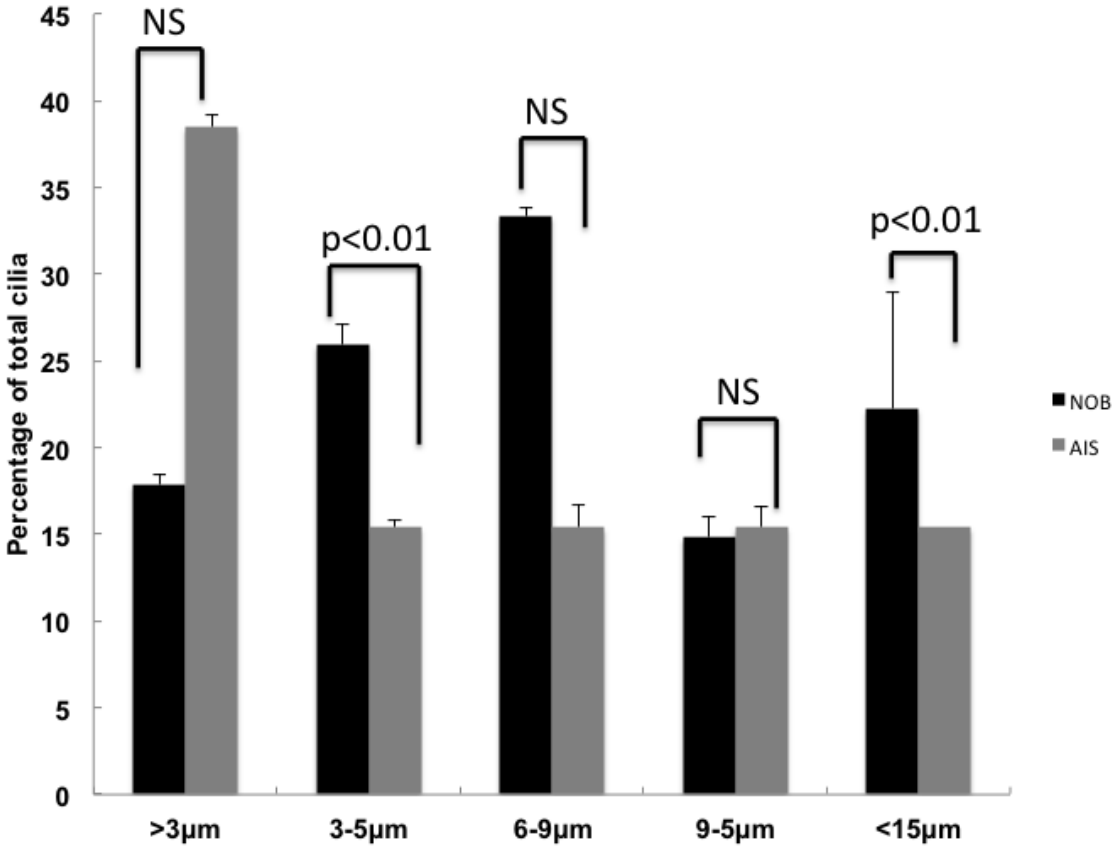
45
40
35
30
25
20
15
10
5
0
Percentage of total cilia
NS
p<0.01
NS
NS
p<0.01
>3µm
3-5µm
6-9µm
9-5µm
<15µm
NOB
AIS

Fig 2 - G

Human OB c.C1286T
(p.A429V)

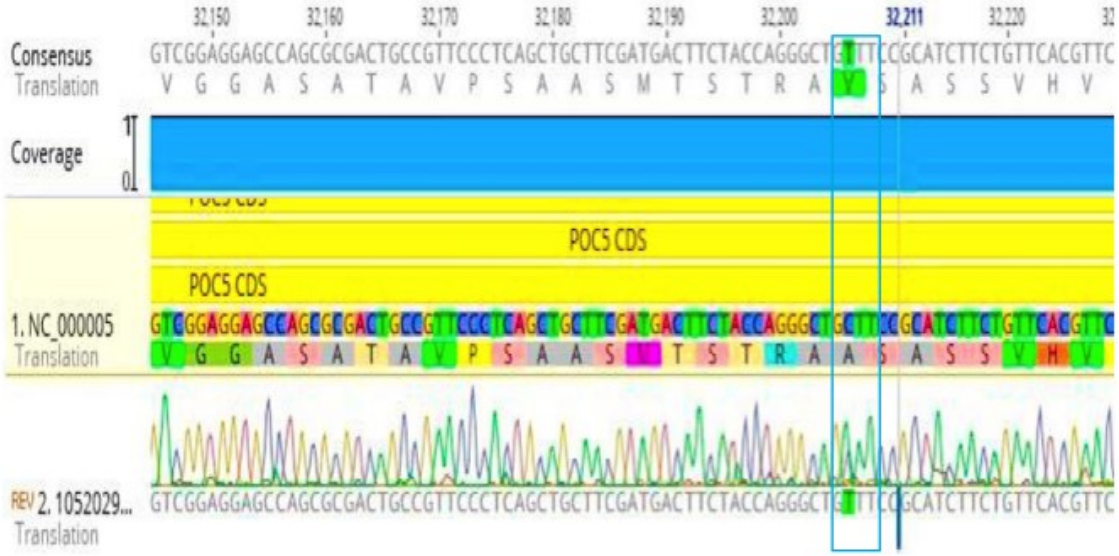

Fig 3

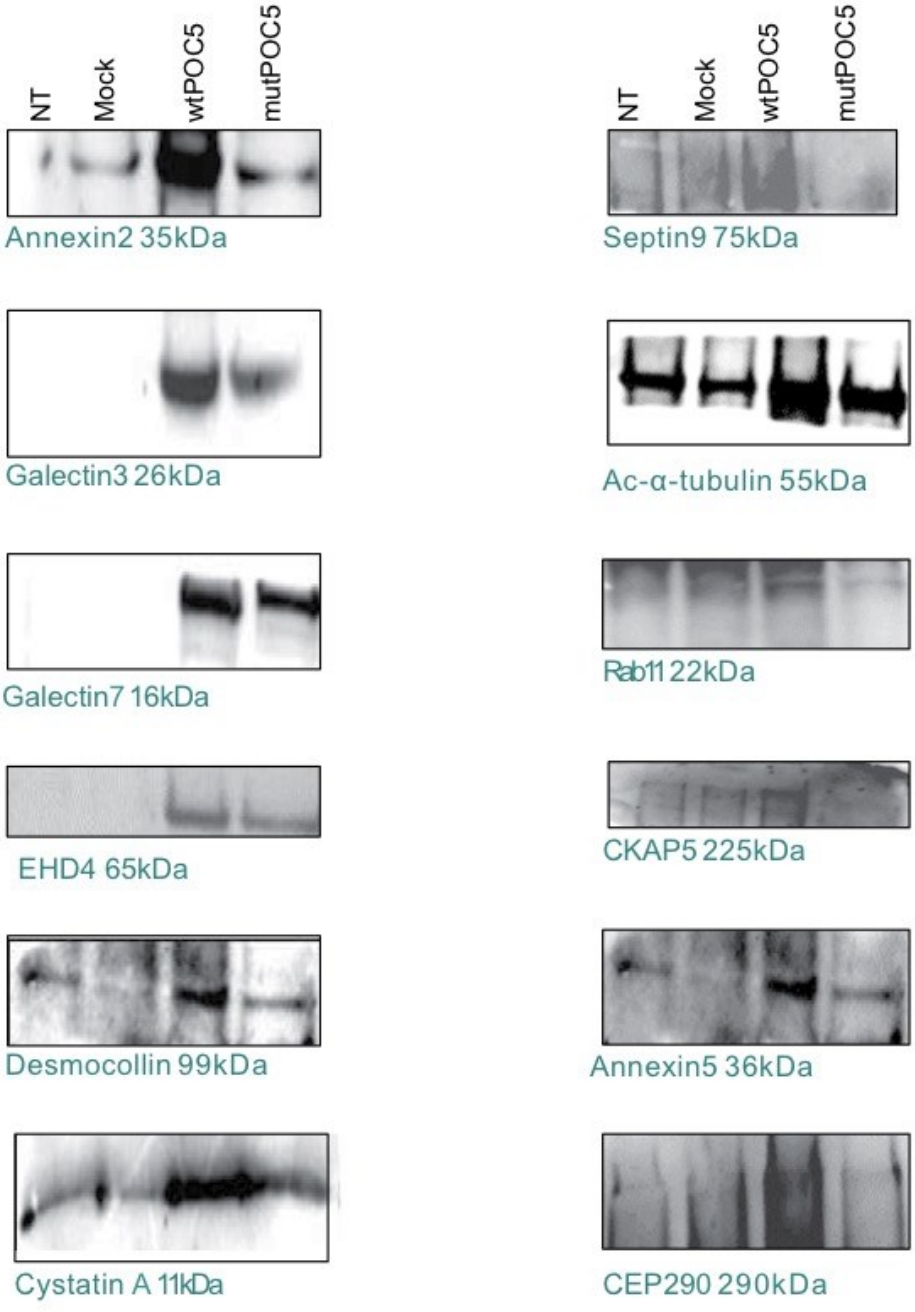
NT
Mock
wtPOC5
mutPOC5
Annexin2 35kDa
Septin9 75kDa
Galectin3 26kDa
Ac-α-tubulin 55kDa
Galectin7 16kDa
Rab11 22kDa
EHD4 65kDa
CKAP5 225kDa
Desmocollin 99kDa
Annexin5 36kDa
Cystatin A 11kDa
CEP290 290kDa

Fig 4

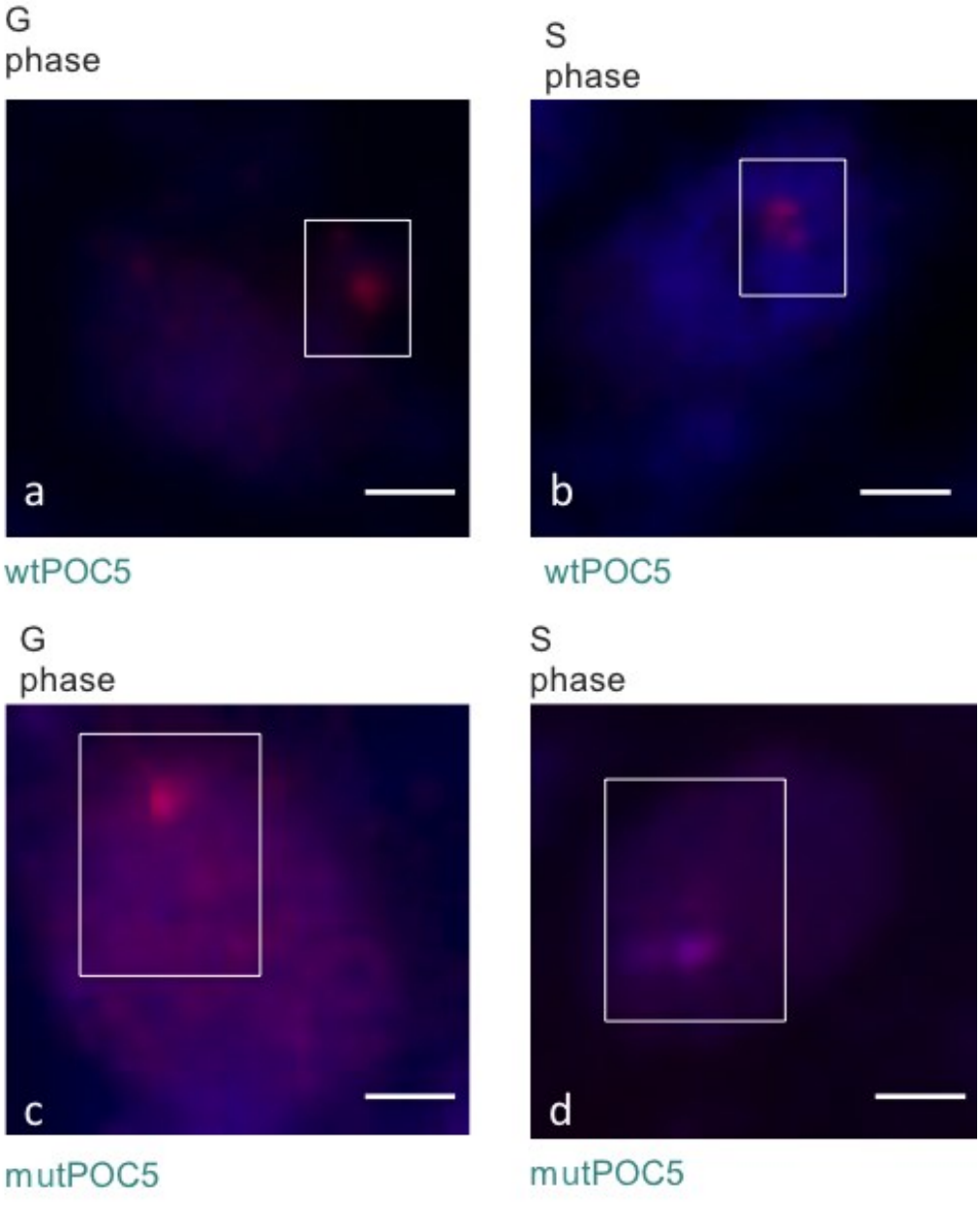
G
phase
S
phase
a
b
wtPOC5
wtPOC5
G
phase
S
phase
c
d
mutPOC5
mutPOC5

Fig. 4 E

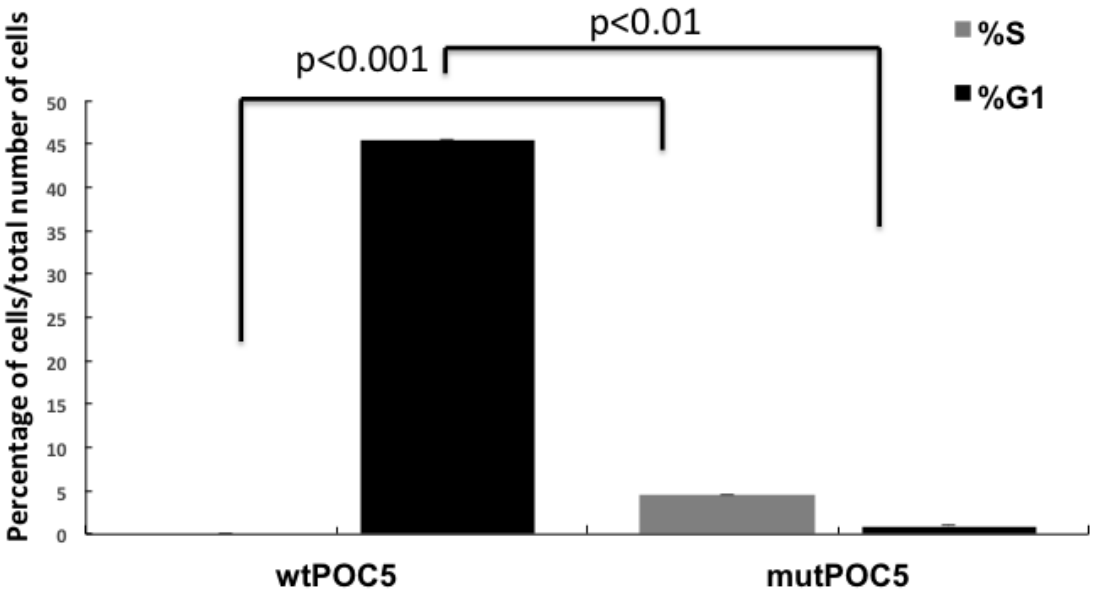
p<0.01
p<0.001
%S
%G1
Percentage of cells/total number of cells
50
45
40
35
30
25
20
15
10
5
0
wtPOC5
mutPOC5

Fig 5-a

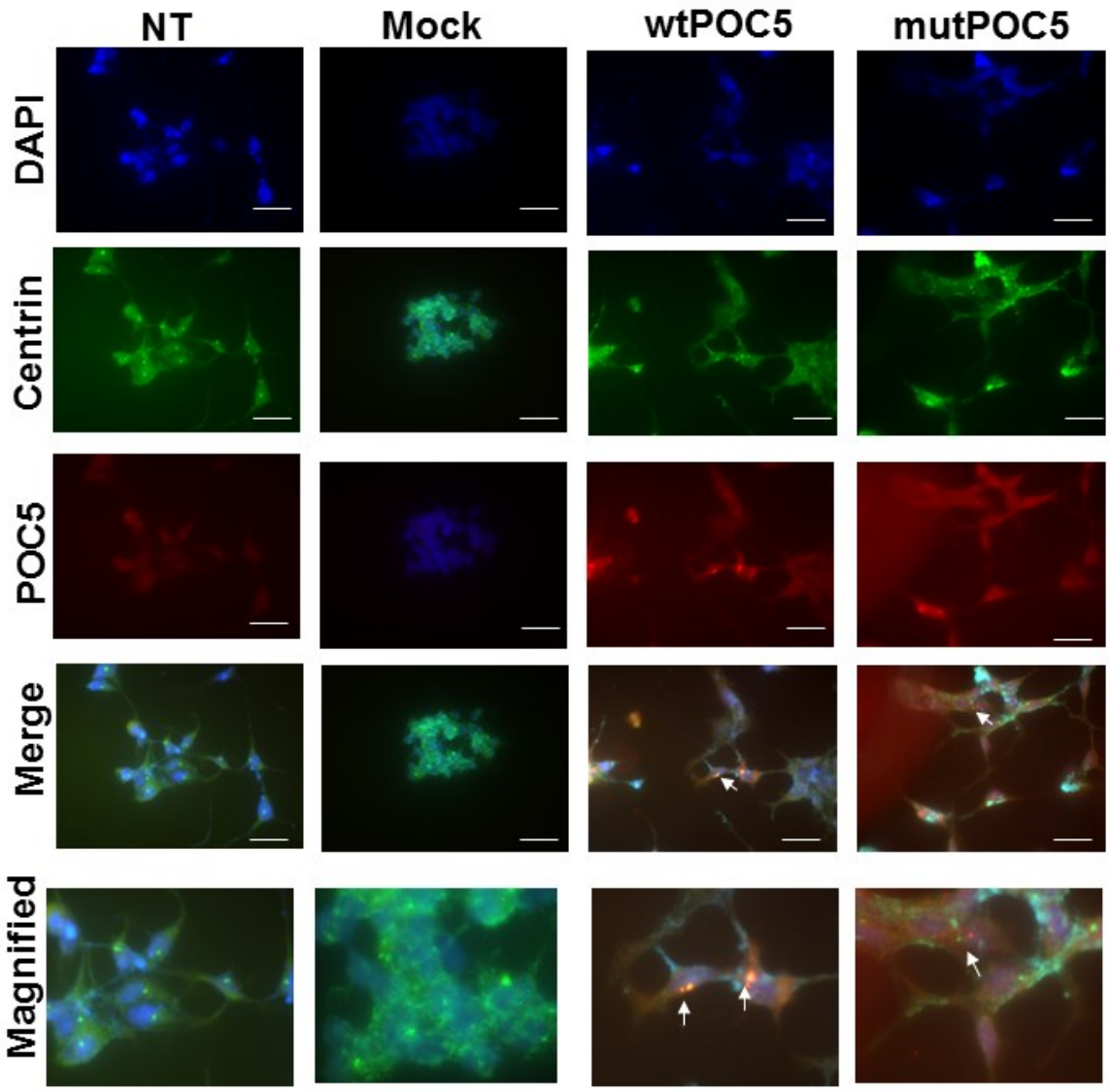

Fig 5 -b

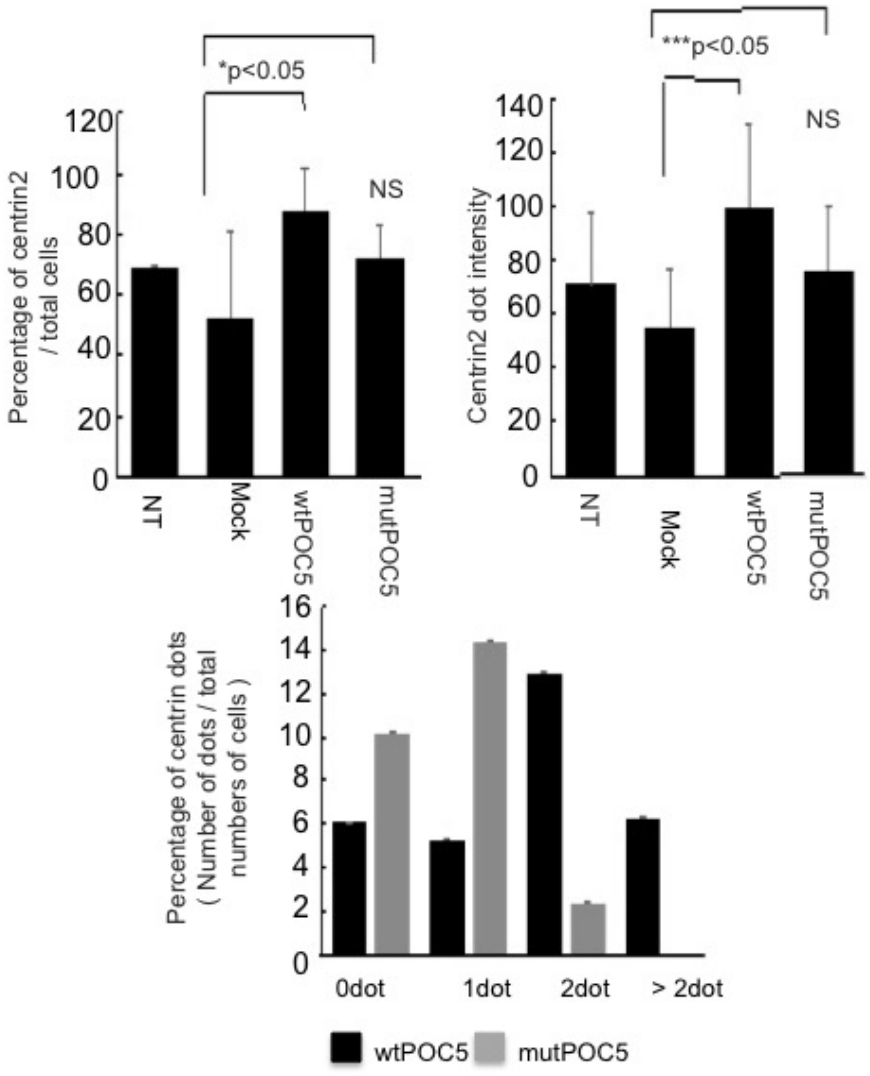
*p<0.05
NS
Percentage of centrin2 / total cells
120
100
80
60
40
20
0
NT
Mock
wtPOC5
mutPOC5
***p<0.05
NS
Centrin2 dot intensity
140
120
100
80
60
40
20
0
NT
Mock
wtPOC5
mutPOC5
Percentage of centrin dots (Number of dots / total numbers of cells)
16
14
12
10
8
6
4
2
0
0dot
1dot
2dot
> 2dot
wtPOC5
mutPOC5

Fig 6

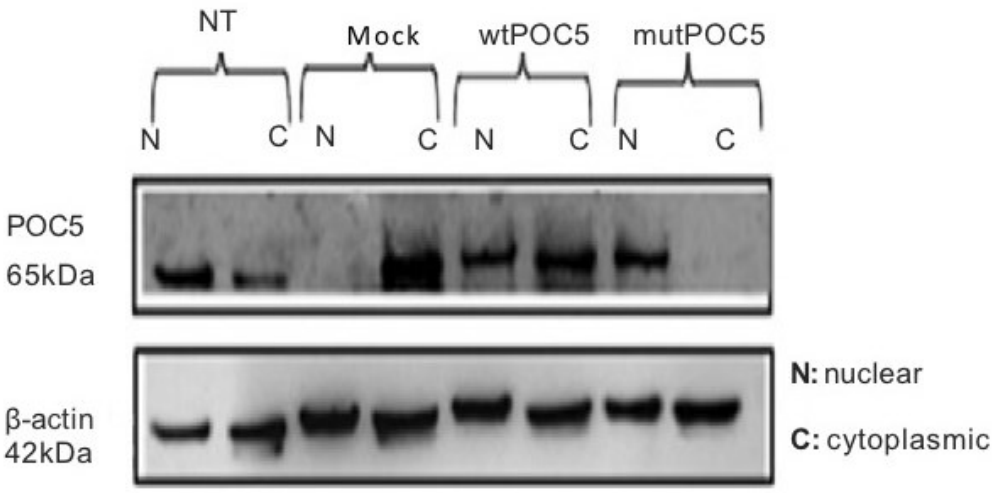
NT
Mock
wtPOC5
mutPOC5
N
C
N
C
N
C
N
C
POC5
65kDa
β-actin
42kDa
N: nuclear
C: cytoplasmic

Fig 7

wtpoc5

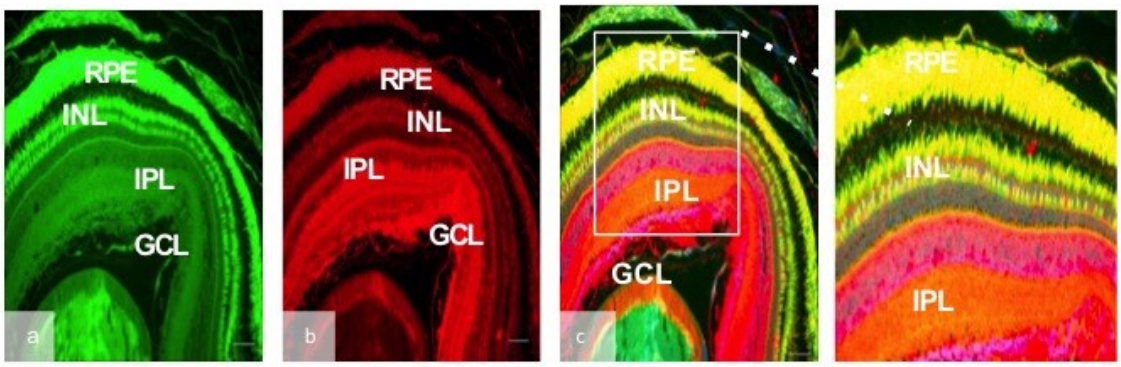

mutpoc5

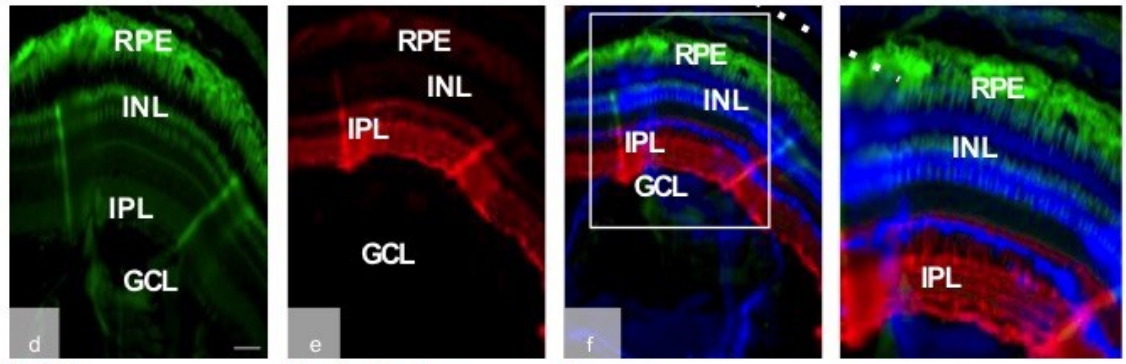

Fig 8

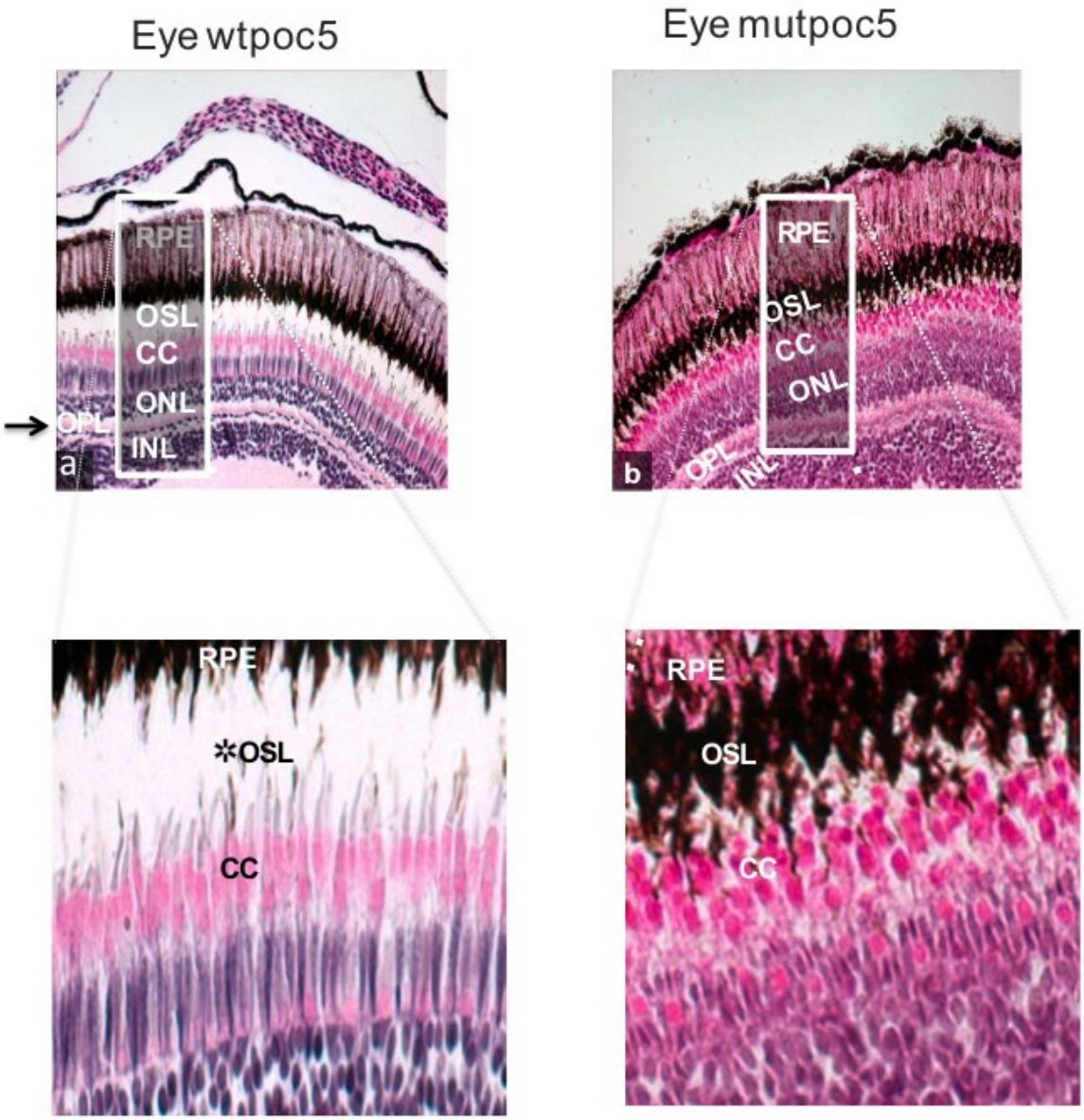
Eye wtpoc5
Eye mutpoc5
RPE
OSL
CC
ONL
OPL
INL
a
b
RPE
*OSL
CC
RPE
OSL
CC

Fig 9

wtpoc5

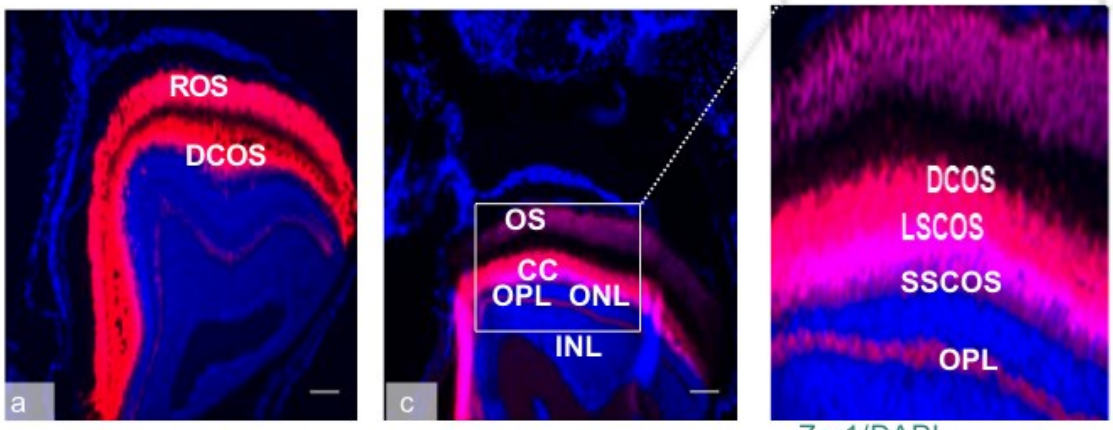

mutpoc5

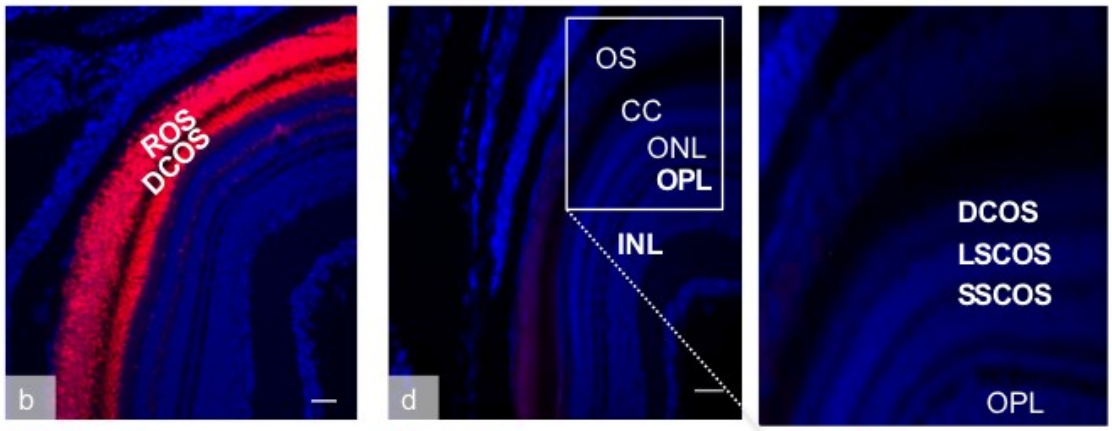

Fig 9

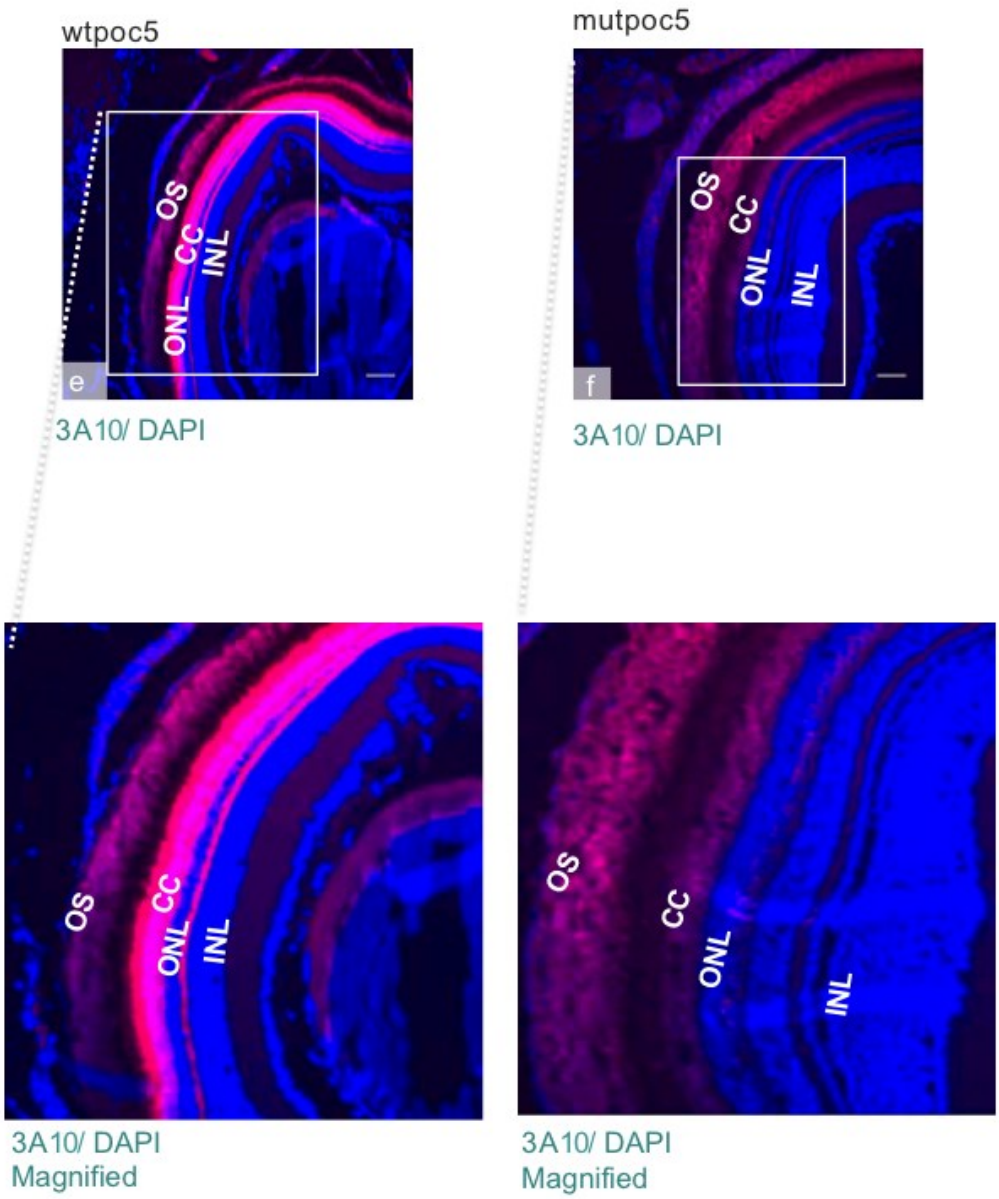
wtpoc5
OS
CC
INL
ONL
e
3A10/ DAPI
mutpoc5
OS
CC
ONL
INL
f
3A10/ DAPI
OS
CC
ONL
INL
3A10/ DAPI
Magnified
OS
CC
ONL
INL
3A10/ DAPI
Magnified

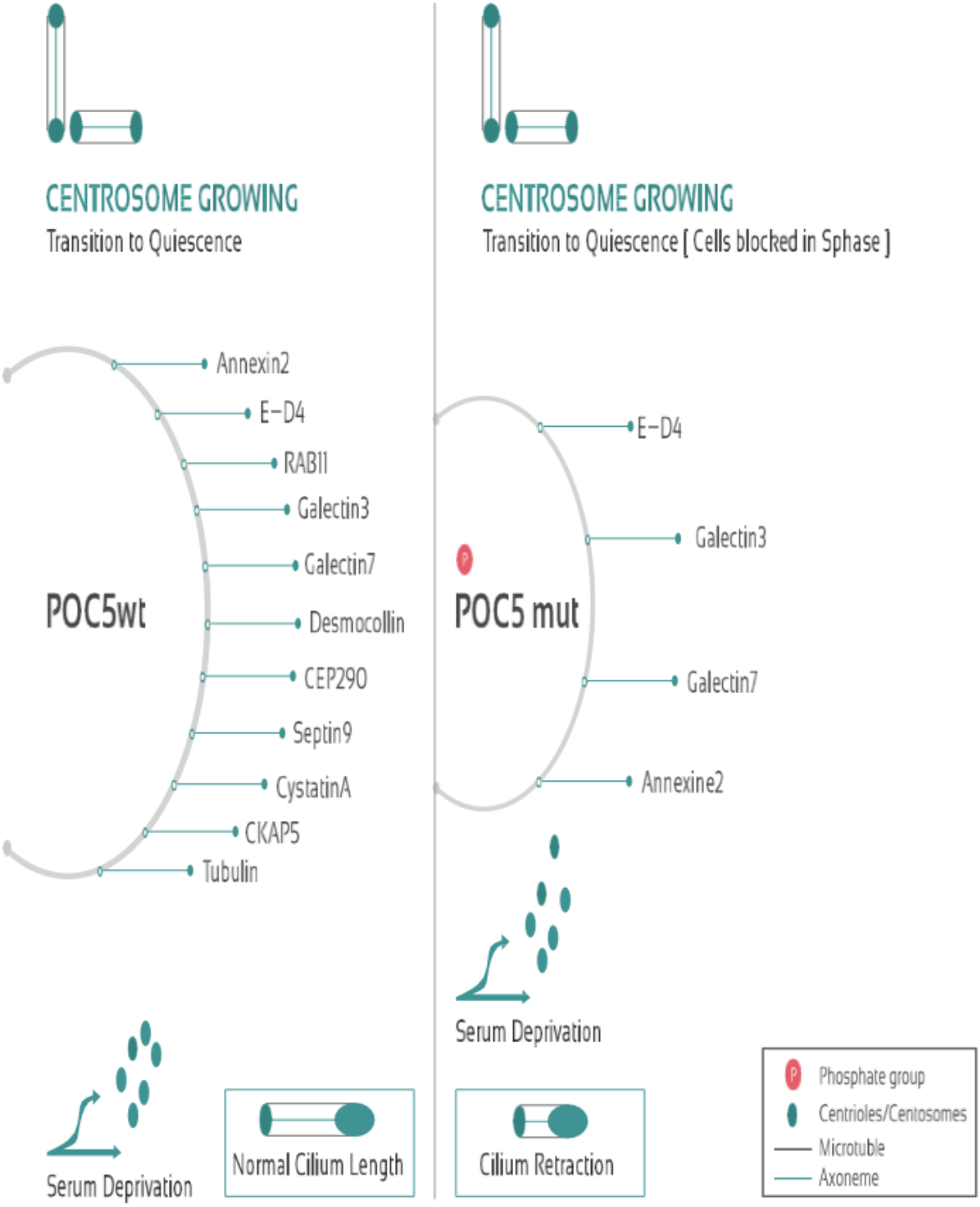
CENTROSOME GROWING
Transition to Quiescence
Annexin2
E-D4
RAB11
Galectin3
Galectin7
POC5wt
Desmocollin
CEP290
Septin9
CystatinA
CKAP5
Tubulin
Serum Deprivation
Normal Cilium Length
CENTROSOME GROWING
Transition to Quiescence [Cells blocked in Sphase]
E-D4
Galectin3
POC5 mut
Galectin7
Annexine2
Serum Deprivation
Cilium Retraction
Phosphate group
Centrioles/Centosomes
Microtuble
Axoneme

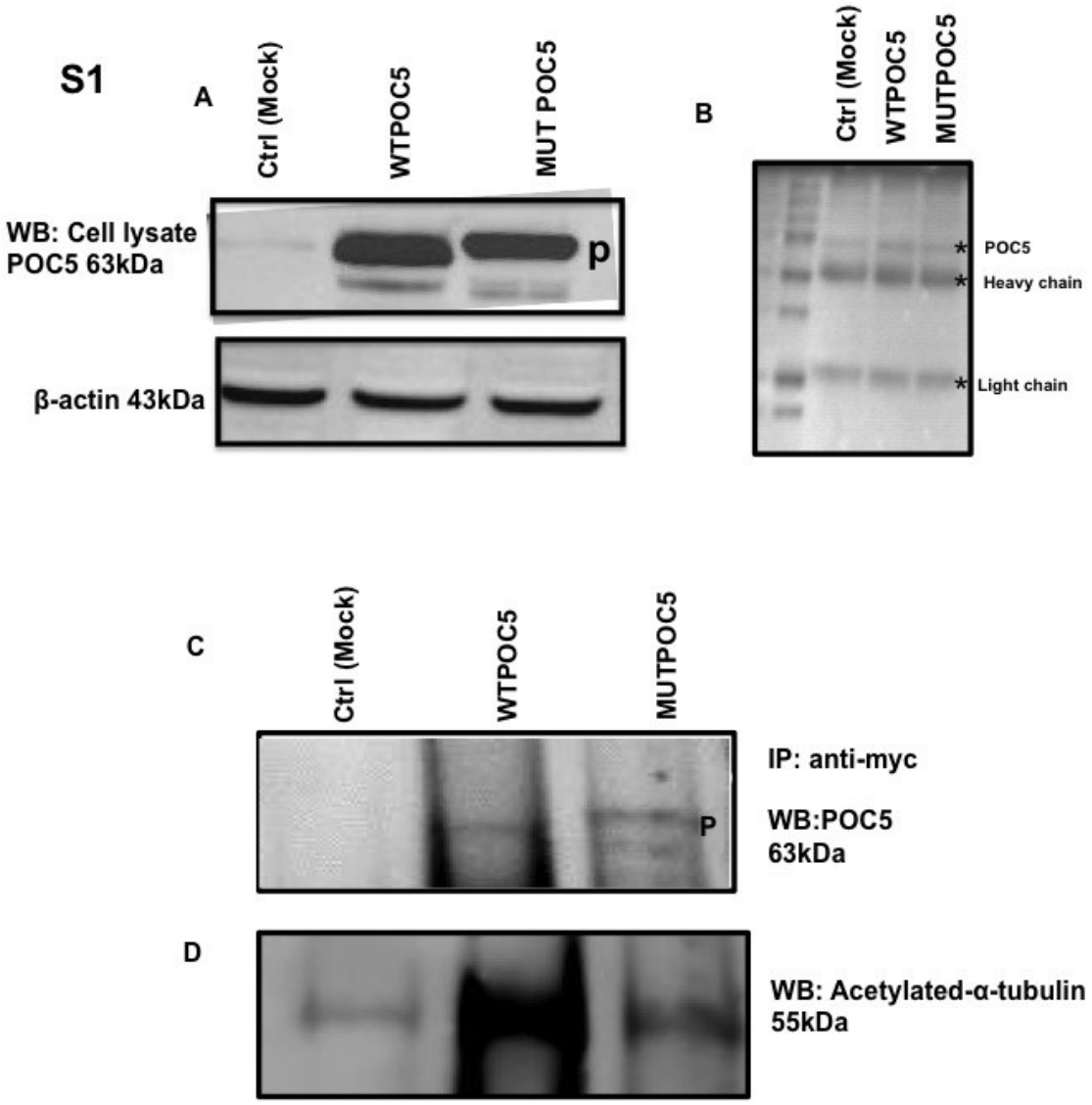
S1
A
Ctrl (Mock)
WTPOC5
MUT POC5
WB: Cell lysate
POC5 63kDa
p
β-actin 43kDa
B
Ctrl (Mock)
WTPOC5
MUTPOC5
* POC5
* Heavy chain
* Light chain
C
Ctrl (Mock)
WTPOC5
MUTPOC5
IP: anti-myc
P
WB:POC5
63kDa
D
WB: Acetylated-α-tubulin
55kDa

S2

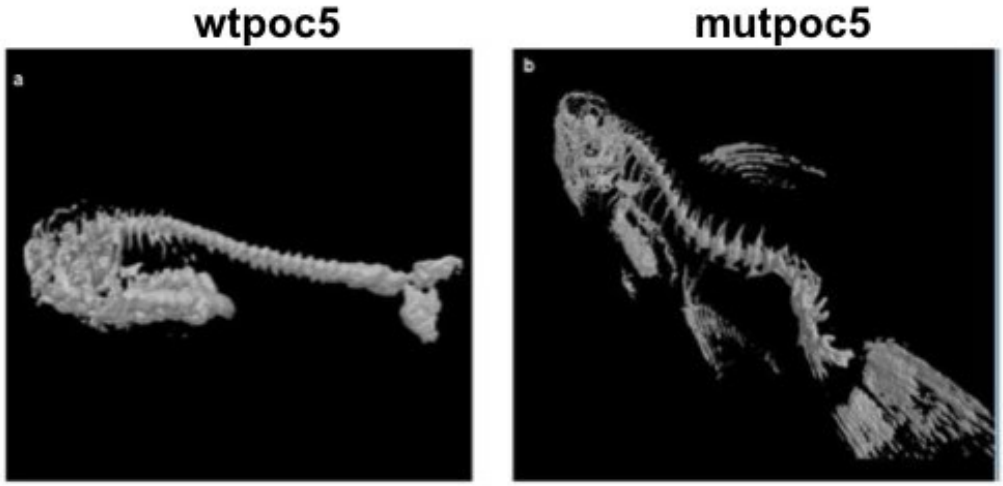

S3

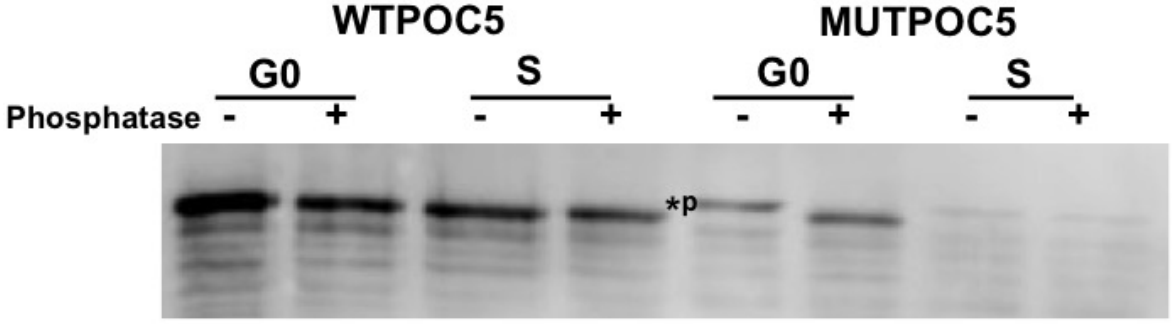

IP: anti-myc
WB:POC5 63kDa

S4

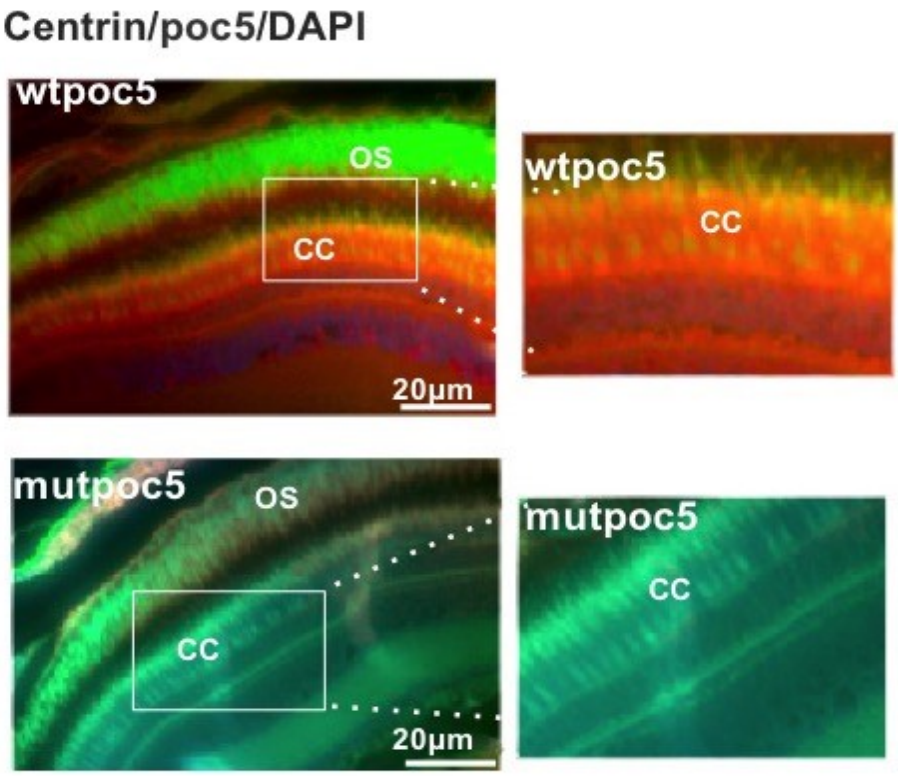
Centrin/poc5/DAPI
wtpoc5
OS
CC
20µm
wtpoc5
CC
mutpoc5
OS
CC
20µm
mutpoc5
CC

A

S5

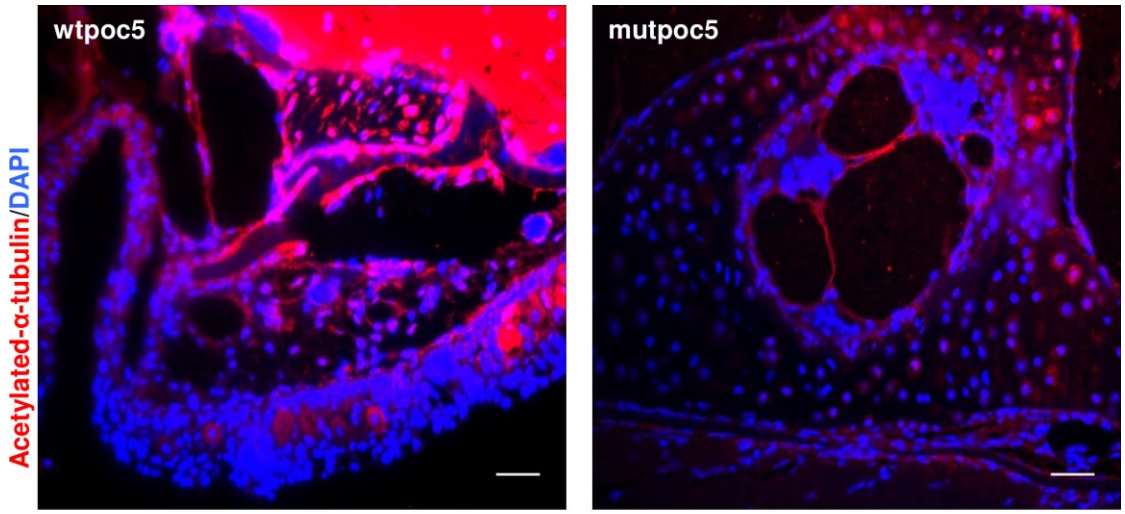
wtpoc5
mutpoc5
Acetylated-α-tubulin/DAPI

B

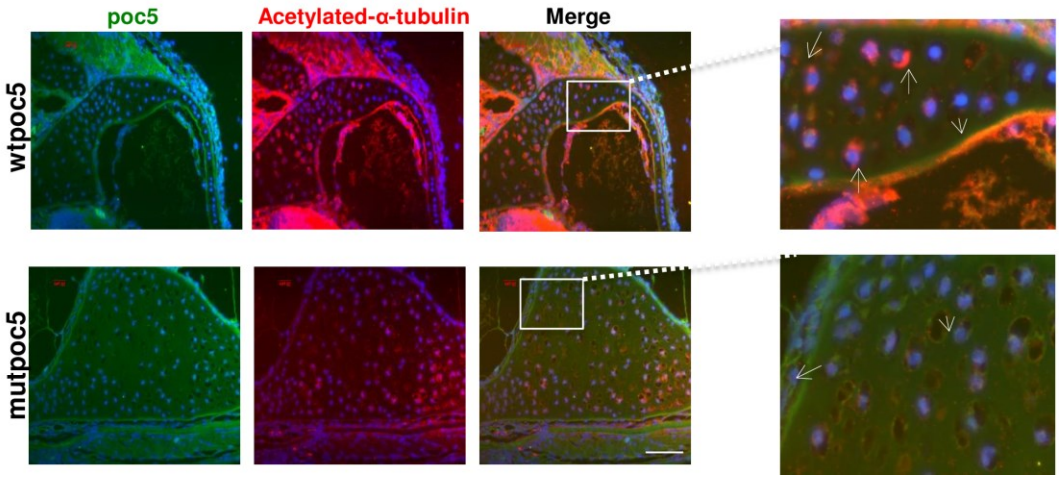
poc5
Acetylated-α-tubulin
Merge
wtpoc5
mutpoc5

III.2. MANUSCRIPT 2

The 17β-Estradiol induced upregulation of the Adhesion G-protein coupled receptor (ADGRG7) is modulated by ESRα and SP1 complex

Amani Hassan[1], Edward T. Bagu[2], Mathieu Levesque[1], Shunmoogum A. Patten[3], Samira Benhadjeba[1], Lydia Edjekouane[1], Isabelle Villemure[4], André Tremblay[1], Florina Moldovan[1,5].

[1]Research Center at Sainte-Justine University Hospital, Montreal, Canada.[2]Department of Biochemistry, College of Medicine, University of Saskatchewan, Saskatoon, Saskatchewan, Canada.[3]INRS-Institute Armand-Frappier, Laval, Canada.[4]Department of Mechanical Engineering, Ecole Polytechnique de Montreal, Montreal, Canada.[5]Department of Dental Medicine, University of Montreal, Montreal, Canada.

***Running title**: ADGRG7* regulation by 17β-Estradiol

***To whom correspondence should be addressed:** Dr. Florina Moldovan: florina.moldovan@umontreal.ca.

Keywords: Adhesion G-protein coupled Receptor protein G7, (ADGRG7); Specific Protein 1, (SP1); Estrogen Receptor alpha, (ESR-alpha/ ESRα); 17β-Estradiol, Estrogen, (E2); Osteoblasts; Adolescent idiopathic scoliosis, (AIS).

Abbreviations: 4-OHT: 4-hydroxy tamoxifen, ADGRG6: Adhesion G-protein coupled receptor, ADGRG7: Adhesion G-protein coupled Receptor protein G 7, AIS: Adolescent Idiopathic Scoliosis, AP1: Activator protein, bcl-2: B-cell lymphoma 2, BMD: bone mineral density, CELSR2: Cadherin EGF LAG seven-pass G-type receptor 2, ChIP: Chromatin Immunoprecipitation, COLIA1: collagen type I alpha 1 gene, CS-FBS: charcoal stripped fetal bovine serum, E2: Estrogen, ERE: Estrogen Response Element, ESR-alpha/ ESRα: Estrogen Receptor alpha, GEO: Gene Expression Omnibus, GPR128: G protein coupled receptor 128, h: hour, MAF: minor allele frequency, mut: mutant, NCBI: US National Center for Biotechnology Information, NOB: normal osteoblasts, PE: Pectus Excavatum, qPCR: quantitative polymerase chain reaction, SEM: standard error mean, SNP: single nucleotide

polymorphism, SP1: Specific Protein 1, TGFα: Transforming growth factor alpha, TSS: transcription start site.

Summary statement: Estrogen plays a significant role in AIS and studying the regulation of ADGRG7 by E2 in AIS cells is essential for understanding molecular mechanisms underlying AIS pathogenesis.

Abstract

The physiological role and the regulation of ADGRG7 are not yet elucidated. The functional involvement of this receptor was linked with different physiological process such as reduced body weight, gastrointestinal function and recently, a gene variant in *ADGRG7* was observed in patients with idiopathic scoliosis. The physiological role and the regulation of Adhesion G protein coupled receptor7 *(*ADGRG7) are not yet elucidated. The functional involvement of this receptor was linked with different physiological process such as reduced body weight, gastrointestinal function and recently, a gene variant in *ADGRG7* was observed in patients with adolescent idiopathic scoliosis (AIS). Here, we identify the *ADGRG7* as an estrogen-responsive gene under the regulation of estrogen receptor ERα in different cells lines. We found that *ADGRG7* expression was upregulated in response to estrogen (E2) in normal osteoblasts (NOB) but not in AIS cells. *ADGRG7* promoter studies indicate the presence of an ERα response half site in close vicinity of an SP1 binding site. Mutation of the SP1 site completely abrogated the response to E2, indicating its essential requirement. ChIP confirmed the binding of SP1 and ERα to the *ADGRG7* promoter. Our results identify the *ADGRG7* gene as an estrogen-responsive gene under the control of ERα and SP1 tethered actions, suggesting a possible role of estrogens in the regulation of *ADGRG7*.

Introduction:

Adolescent idiopathic scoliosis (AIS) is a complex three-dimensional deformity of the spine that mostly occurs during late childhood or puberty (Konieczny, Senyurt et al. 2013). Severe forms of AIS are more common in girls as compared to boys (Cheng, Castelein et al. 2015). The difference between girls and boys, as well as the etiology of AIS are still unclear. Several studies suggest that AIS could be an endocrinal disease and that various hormones, especially

estrogens, have a role in its onset, development and spinal curve progression (Barrios, Cortes et al. 2011). Lower peak bone mass and osteopenia at puberty have been reported in 27 % to 38 % of AIS patients, suggesting that AIS may be correlated with hormonal disturbance involving estrogen, melatonin, and leptin (Ishida, Aota et al. 2015). Estrogens (E2) and Estrogen receptors (ERs), including the ERα and ERβ isoforms are suspected of influencing AIS severity and delayed puberty which was directly associated with a higher prevalence of AIS in girls than in boys with an incidence ratio of 7.1:1 (Konieczny, Senyurt et al. 2013). Indeed, several *ER* polymorphisms were found in AIS (Stavrou, Zois et al. 2002), but the predisposition to and severity of AIS was not clearly demonstrated (Janusz, Kotwicka et al. 2014). Estradiol (E2) participation in puberty, spinal growth and bone metabolism are important factors to consider in AIS. Until now, it was not clear how E2 could affect the initiation or progression of AIS. However, estrogens interact with many physiopathological factors (including neuroendocrine, neurological, muscular, biochemical and structural) relevant to the etiology of scoliosis, and there is interdependence between the concentration of E2 and development of scoliosis (Leboeuf, Letellier et al. 2009).

E2 is the major hormonal regulator of puberty and bone metabolism and acts through genomic and non-genomic pathways. The genomic effects of E2 are exerted by it's binding to the ER in the cytoplasm. This is followed by the translocation to the nucleus and binding of the complex to target genes. In addition to the direct genomic signaling through ER (Dahlman-Wright, Cavailles et al. 2006, Prossnitz, Arterburn et al. 2008), ERs can also mediate their transcriptional potential through tethered interaction with other transcription factors, such as SP1 and activator protein (AP1). In these cases, most estrogen responsive genes are devoid of estrogen response elements (ERE) (Bjornstrom and Sjoberg 2005), suggesting enhanced recruitment of ER ligands to target promoters through protein-protein interaction such as SP1 (Safe 2001). SP1 is a ubiquitously expressed transcription factor that binds and acts through GC-rich elements to regulate gene expression in mammalian cells (Li, Mitchell et al. 2007, Keay and Thornton 2009).

The Adhesion G protein-coupled receptor 7 (ADGRG7), previously known as the G protein-coupled receptor 128 (GPR128), is a membrane bound protein encoded by *ADGRG7*

(Fredriksson, Lagerstrom et al. 2002, Bjarnadottir, Fredriksson et al. 2004, Arac, Aust et al. 2012). In humans and mice, the *ADGRG7* gene is on chromosome 3q12.2 and 16; 16 C1.1, respectively (Fredriksson, Lagerstrom et al. 2002, Bjarnadottir, Fredriksson et al. 2004, Arac, Aust et al. 2012). ADGRG7 is an orphan receptor that belongs to the family of proteins that consists of over 33 homologous proteins (Bjarnadottir, Fredriksson et al. 2004, Yona, Lin et al. 2008, Yona and Stacey 2010). Like most members of ADGRG family, the extracellular region often a N-terminal protein module is extended and linked to a transmembrane (TM) 7 region via the GPCR-autoproteolysis inducing (GAIN) domain (Arac, Aust et al. 2012). *ADGRG7,* which is phylogenetically related to *ADGRG2* and *ADGRG1,* lacks the conserved N-termini domains present in other GPCRs (Foord, Jupe et al. 2002, Bjarnadottir, Fredriksson et al. 2004, Huang, Chiang et al. 2012). ADGRG7 was shown to be expressed in the mucosa of the intestine restricted to the epithelial cells (Badiali, Cedernaes et al. 2012, Ni, Chen et al. 2014).

The physiological role of ADGRG7 remains mostly unclear. The GPCR family of proteins are mainly involved in cellular adhesion, migration, cell–cell and cell–matrix interactions (Yona, Lin et al. 2008). In mice, targeted deletions of the *Adgrg7* gene reduced weight gain and increased the frequency of peristaltic contractions of the small intestine, suggesting a role in intestinal absorption of nutrients (Badiali, Cedernaes et al. 2012). An important paralog of this gene is *ADGRG6*, which is suggested as playing a role in musculoskeletal disorders such as AIS and pectus excavatum (PE) (Kou, Takahashi et al. 2013, Karner, Long et al. 2015).

In humans, *ADGRG6* gene variants were first associated with AIS in the Japanese population and then a SNP in *ADGRG6* gene (rs657050) was replicated in Han Chinese and European-ancestry AIS population. In zebrafish, the *adgrg6* knockdown, causes delayed ossification of the developing spine (Kou, Takahashi et al. 2013), and in a mice model, the loss of *Adgrg6* in osteochondroprogenitor cells affects spinal column development and intervertebral disk morphogenesis (Karner, Long et al. 2015).

ADGRG7 was also suggested among the genetic causes or genetic contributors for the pathogenesis of AIS. The *ADGRG7* gene maps on the chromosome 3q12.2. Through linkage analysis, in multigenerational AIS families with dominant inheritance, this locus was reported as one of the two locations containing the gene for AIS (Edery, Margaritte-Jeannin et al. 2011). Our recent study by Patten et al. (Patten, Margaritte-Jeannin et al. 2015) identified by

exome sequencing two candidate gene variants (SNV) among the novel or rare (minor allele frequency [MAF] <5%) variants: one in *ADGRG7* and the other in *POC5* (Patten, Margaritte-Jeannin et al. 2015). The *ADGRG7* SNV (1274A>G) did not perfectly co-segregate with AIS in all the members of this multigenerational AIS family; consequently, the *ADGRG7* gene was concluded as a contributory/modifier gene in the pathogenesis of AIS. Based on these findings, and because *ADGRG7* is closely related to the *ADGRG6* (gene implicated in AIS), we hypothesized that *ADGRG7* is regulated by E2 and consequently can contribute to the cellular events in AIS.

To examine how *ADGRG7* is regulated at the transcriptional and protein level by E2, we conducted promoter and deletion analysis. We also conducted gene and protein expression study in human osteoblasts, Huh7 and MCF7 cells. Human *ADGRG7* gene was cloned and analyzed for functional *cis*-elements mediating the effects of E2. Deletion analysis of the promoter identified the SP1 site required for both basal activity and hormone-induced activation. Chromatin immunoprecipitation (ChIP) assay confirmed that SP1/ERα binds to *ADGRG7* promoter. Our study suggests that the regulation of ADGRG7 expression by E2 is due to the association of ERα and SP1 proteins to *ADGRG7* promoter.

Results

Gene expression profile of *ADGRG7* and *SP1* in multiple human tissues

The ADGRG7 has been poorly characterized in terms of function and tissue expression. We therefore analyzed the expression levels of *ADGRG7* and *SP1* in different tissues (Fig. 1A, B) using the Gene Expression Omnibus (GEO) database at the US National Center for Biotechnology Information (NCBI). We found that *ADGRG7* was highly expressed in the small intestine, as previously reported (Badiali, Cedernaes et al. 2012), However, unlike in mice, *ADGRG7* expression was not selective for the intestine, *ADGRG7* was also expressed in the liver, pancreas and placenta. The SP1 transcription factor was highly expressed in the pancreas with wide expression in all tissues tested except for the skin. Interestingly, *ADGRG7* and *SP1* were also expressed in the bone; this suggests a wider function than expected and an undetermined role of ADGRG7 in bone.

Dose dependent differential upregulation of *ADGRG7* by 17β-estradiol in NOB and AIS cells

To characterize changes in gene and protein expression in response to E2 treatment in normal control osteoblasts (NOB) and AIS osteoblasts, we performed qPCR and western blot on cells treated with E2. ADGRG7 was differentially regulated by E2 treatment in NOB and AIS cells. E2 upregulated ADGRG7 protein levels at 10^{-7} M E2 in normal osteoblasts with maximal response at 10^{-9}, 10^{-12} and 10^{-13} M (Fig. 2A). The response in AIS was non significant (Fig. 2B). In NOB cells there was a dose-dependent increase in steady-state levels of ADGRG7. The densitometry signals for the E2-treated control NOB and AIS cell samples were normalized to the β-actin signal and yielded normalized densitometry ratios. The data for the normalized ratios for the specific protein ADGRG7 are summarized in (Fig. 2A, B).

To test whether E2 affects ADGRG7 protein localization, we performed applied fluorescence imaging technique using ADGRG7 antibody. We observed low staining in untreated cells, enhanced staining after treatment with E2 in NOB cells (Fig. 2C), and low immunofluorescence in AIS cells. These results are consistent with the results of upregulation of ADGRG7 by E2 in Western blot (Fig. 2A, B).

The ability of ERα and SP1 to interact with each other and DNA along with the differential expressions of ERα in different normal and AIS patient cells (Leboeuf D. 2008), led us to examine the expression levels of SP1 and ERα in NOB and AIS cells. We observed by western blot differential expression patterns of both proteins. SP1 and ERα levels were higher in NOB than AIS cells (Fig. 2D).

These studies reveal that ADGRG7 is a cytoplasmic protein regulated by E2 in NOB osteoblasts and at lower levels in AIS cells (Fig. 2A, B, C). ERα and SP1 protein levels were also higher in NOB cells than AIS cells (Fig. 2D).

Transcriptional activation of *ADGRG7* and deletion analysis of the *ADGRG7* gene promoter

In order to address the regulation of *ADGRG7* gene expression in response to E2, we used Huh-7 cells, which have high transfection efficiency, and treated them at three different time points (3 h, 12 h and 24 h). Since Huh-7 cells have low levels of expression of ER, we overexpressed the estrogen receptor-construct or pcDNA3 mock vector as control. Cells were

either non-treated or treated with ethanol or E2. We found that ADGRG7 has maximal response to E2 after 3 h treatment. From 12 h and 24 h, we did not find differences between treated and untreated samples. This suggests an early response gene to E2 (Fig. 3A). At the protein level, ADGRG7 was upregulated with a 10^{-7} M treatment of E2 for 24 h (Fig. 3B). We assessed by luciferase assay if the regulation of ADGRG7 is through ERα or ERβ in Huh-7 cells, and we found that *ADGRG7* promoter (-2259/+55) is upregulated by E2 in the presence of ERα but not ERβ (Fig. 3C). Finally, we observed similar responses to E2 at 24 h and 48 h post treatment (Fig. 3D). *ADGRG7* is upregulated by E2 through ERα at 3 h and at lower levels at 24 h and 48 h post-treatments with E2.

Deletion analysis of the proximal region of the *ADGRG7* promoter

To determine the responsive region responsible for the estrogenic upregulation of the *ADGRG7* gene, we performed reporter gene assay in Huh-7 cells using a portion of 2.2kb proximal to the transcription start site (TSS) of the *ADGRG7* promoter. A schematic of the proximal promoter of the *ADGRG7* gene shows the presence of several putative ERE binding elements (Fig. 4A). The co-transfection of hERα and various truncations of the promoter series, of 5′- deletion constructs including the −2259 to +112, −1285 to +112, −474 to +112, -309 to +112, -283 to +112 and -44 to +112 regions of the *ADGRG7* gene promoter were used in transient transfection studies to identify specific E2-responsive elements within this region of the promoter (Fig. 4B). We found that the estrogenic induction was retained with the -474 construct and then lost with the -309 construct, suggesting that this region is essential for the E2 response of the promoter (Fig. 4B). Further deletions were not inducible by E2. These results indicate that (i) the stimulation of the promoter by E2 requires the presence of its receptor, and (ii) the region between 474 and 309bp encompasses potential regulatory elements sufficient to confer regulation by E2.

An essential role for SP1, ERE1/2 motif in signaling estrogen regulation of the *ADGRG7* promoter

Deletion analysis of the SP1xERE1/2 of the *ADGRG7* promoter was carried out to define further their role for functional interactions with ERα/SP1 (Fig. 5A). The 586bp and Δ67bp

were E2-responsive, and deletion analyses were used to determine contributions of the upstream SP1xERE1/2 binding sites. E2 did not significantly induce luciferase activity in cells transfected with 442bp fragment. To provide experimental evidence that the activation of *ADGRG7* by E2 is mediated by an Sp1-binding element, we choose MCF7 cells that have high expression levels of ESR and transiently transfected them with a luciferase reporter gene driven by a promoter carrying SP1mut. Relative luciferase activity data showed the absence of response to E2 treatment (Fig. 5B). Results obtained for these deletion/mutant constructs (Fig. 5A, B) indicate that the SP1xERE1/2 in the Δ67 region of the *ADGRG7* gene is important for hormonal activation by ERα/SP1. These studies support a role for the SP1xERE1/2 site in mediating estrogen responsiveness of the human *ADGRG7* gene.

Physical and functional interactions of SP1 and ERα

We studied the gene expression patterns induced in MCF7 ERα-positive, estrogen dependent, breast cancer cell line, grown in steroid-depleted medium or in the presence of E2. As observed in Huh-7 cells, E2-induced mRNA expression occured at 3 h and this response returned to basal levels after 12 h and 24 h (Fig. 6A). ADGRG7 protein levels were upregulated to 2.5 fold in MCF7 cells (Fig. 6B).

The recruitment of ERα and SP1 proteins with the proximal region of the ADGRG7 promoter indicated by arrows (−478 to -423) was investigated (Fig. 6C). The interaction of ERα and SP1 proteins with the *ADGRG7* gene promoter was investigated in MCF7 cells treated with 10^{-7} M E2 for 1 h using a chromatin immunoprecipitation (ChIP) assay in which cells were treated with formaldehyde to form DNA-protein cross-links. After sonication, and immunoprecipitation by SP1 or ERα antibodies, qPCR was used to determine binding (Fig. 6D). The results indicated that both ERα and SP1 antibodies immunoprecipitate this region of *ADGRG7* promoter. The qPCR products were migrated on gel to confirm the correct product size.

We showed that *ADGRG7* is also upregulated by E2 in MCF7 cells. Through a ChIP experiment, we confirmed the binding of SP1 and ERα to *ADGRG7* promoter after stimulation with E2 for 1 h.

ERα antagonists 4-hydroxy tamoxifen (4-OHT) and fulvestrant (ICI-182, 780) reverse the up-regulatory effects of E2 on *ADGRG7* expression and promoter activity

We tested the effect of 4-OHT, which is considered a context-dependent mixed agonist/antagonist of ERα (Fig. 7A). Interestingly, while 4-OHT was able to block the E2 activation of the *ADGRG7* promoter thus acting as an ERα antagonist, when used in absence of E2, 4-OHT was inducing *ADGRG7* promoter activity in MCF7 cells (Fig. 7A). This effect is consistent with the reported activity of 4-OHT as an ERα agonist in the context of SP1 and AP-1 regulated genes (Schultz, Petz et al. 2005), indicating that SP1is required in promoting *ADGRG7* promoter activation. ICI-182, 780 is known as a potent ERα antagonist that promotes ERα degradation and abolishes its transcriptional competence to E2 in responsive cells. We observed that increasing concentrations of ICI-182, 780 completely abolished the response of the *ADGRG7* promoter to E2, thus suggesting a direct role of ERα (Fig. 7B). We also tested the effect of ICI-182, 780 treatments on the SP1 mutant. Contrary to the inhibitory effects observed with ICI-182, 780, there was no response with the SP1 mutant (Fig. 7C).

We also tested the effects of ICI-182, 780 and 4-OHT on ADGRG7 protein levels (Fig. 7D, E). Both antagonists significantly downregulated the E2 induced ADGRG7 protein levels.

Based on the above results, both SP1 and ERα are responsible for the regulation of *ADGRG7*, and the mutation of SP1 prevents the response *of ADGRG7* to the ERα antagonists.

Discussion:

In the present study, we demonstrate *ADGRG7* regulation by E2. We observed that E2 increases ADGRG7 expression in different cell lines, Huh-7, MCF7, osteoblasts from normal control (NOB) and patients with scoliosis (AIS), with or without cotransfection with ERα. This is the first report demonstrating that ER signalling regulates ADGRG7 expression and activity. Additionally, we showed the mechanism of regulation of *ADGRG7* by E2 represented in Fig. 8.

Our results indicate that the activity of E2 on the *ADGRG7* promoter was significantly impaired by mutations that interrupt SP1 binding to the Δ67bp fragment (Fig. 5B). These data

suggest that SP1-binding sites in the promoter are the critical regulatory *cis*-acting elements that mediate the activation of *ADGRG7* transcription by ERα. ERα but not ERβ induced *ADGRG7* promoter upregulation. ERβ is thought to have weaker activity than ERα, although in some studies it was shown that the ERβ a better activator than ER-α on an ERE reporter (Fournier, Gutzwiller et al. 2001). Thus, ER-α and ER-β can regulate gene activity differentially depending on the promoter context and the ligand used. Also we found that in MCF7, the E2 antagonists 4-OHT and ICI-182, 780 inhibited E2-stimulated promoter activity as well as protein levels (Fig. 7), suggesting that also ERα is important in the *ADGRG7* regulation by E2. This was then confirmed by ChIP.

There is a classical pathway of ERα action where E2 induces the formation of a nuclear ER**α** homodimer that binds to 5'-regulatory estrogen response elements (EREs) in target gene promoters in response to E2, resulting in enhanced gene transcription. On the other hand, ERα can mediate E2 regulation through tethered interactions with SP1 protein to regulate genes and this occurs by the binding of SP1x ERE or SP1 x ERE half-site (1/2) motifs where both ERα and SP1 bind DNA elements (Safe 2001). As it seems to be the case for *ADGRG7*, there is activation through SP1(5)xERE1/2 that is located in the Δ67bp fragment of the *ADGRG7* promoter. Through ChIP, we showed that both proteins SP1 and ERα bind to the *ADGRG7* promoter fragment. It is generally accepted that E2 regulation of genes is mediated through EREs; however, several examples exist in literature for genes devoid of ERE having SP1 and ERE1/2 sites. The E2-responsive SP1(5)x ERE(1/2) motif regulation mechanism of *ADGRG*7 by E2 identified in this study is also shared with other E2-regulated genes, such as cathepsin D (Krishnan, Wang et al. 1994, Krishnan, Porter et al. 1995), TGFα (Vyhlidal, Samudio et al. 2000), heat shock protein 27 (Porter, Wang et al. 1996) and the progesterone receptor (Petz and Nardulli 2000). Cathepsin D doesn't contain a classical palindromic ERE. The promoter region between (-199 and -165) has an ERE1/2 and an SP1 binding that are mediating upregulatory E2 effects on cathepsin D expression (Krishnan, Wang et al. 1994, Krishnan, Porter et al. 1995). Similarly, TGFα promoter required SP1(30)xERE½ that had been characterized in the cathepsin D, progesterone receptor and heat shock protein 27 gene promoters; however, the number of nucleotides are 23, 10 and 16 respectively while for TGF α, they are 77. In our work, the SP1xERE1/2 in the *ADGRG7* promoter include 12 nucleotides (5 for ERE1/2 and 7 for SP1) distributed over one ERE1/2 and the SP1 site. Many other

examples of the SP1xERE1/2 in promoters of several E2-responsive genes, include cyclin D1, c-fos, retinoic acid receptor α1, E2F1, adenosine deaminase, insulin-like growth factor binding protein 4, creatine kinase B and bcl-2 (Khan, Abdelrahim et al. 2003).

The regulation of GPCRs by E2 has been described for several receptors. For instance, E2 can upregulate or downregulate the expression of mRNAs of several genes involved in lipid metabolism, transcription, and steroid metabolism that have a role in the control of reproductive behaviour (Snyder, Small et al. 2009). E2 also increases the expression of mRNA and protein levels of oxytocin receptor in human placenta cells (Kim, Lee et al. 2017).

No SP1 mutation association with scoliosis has yet been reported. However, mutation in in the binding site of SP1 transcription factor (G-->T mutation) in the *collagen type I alpha 1* gene (*COLIA1*) is a putative marker for low bone mineral density (Grant, Reid et al. 1996). Low mineral density (BMD) and osteopenia were previously described in AIS and considered as risk factors of spinal curve progression in AIS patients (Cheng, Tang et al. 2001, Peng, Liang et al. 2012, Sun, Wu et al. 2013). Based on these observations, it would be interesting to screen for SP1 binding site mutations in the *ADGRG7* gene in osteopenic scoliotic patients.

Interestingly, the upregulation of *ADGRG7* by E2 in NOB cells was higher and more significant than in AIS osteoblasts probably due to lower protein levels of SP1 (Fig. 2C). Ethanol was observed to increase the levels of ADGRG7 (non significant). It was found that ethanol induces bone loss by altering ER signaling and ER-p21 interaction and controls osteoblasts cell fate. In this study, ethanol stimulated the overexpression of ERs in bone in vivo and in osteoblasts in vitro and this effect was revered by ER agonist (Chen, Lazarenko et al. 2009). An E2 resistance mechanism in scoliosis was previously reported in humans with a mutation of the ERα gene. In exon 2 of ERα, a cytosine-to-thymine transition at codon 157 of both alleles, resulted in a premature stop codon (Smith, Boyd et al. 1994). The major phenotypic manifestations of this mutation were a severely under mineralized skeleton with biochemical evidence of increased bone resorption, evidence of continued slow linear growth, markedly delayed skeletal maturation, and osteoporosis. E2 resistance impact bone turnover (Quaynor, Stradtman et al. 2013) that could be connected to the molecular mechanisms underlying AIS. Since E2 is important for bone growth and mineralization, this could explain the low mineralization and osteopenia that was observed in patients with AIS (Li, Li et al. 2008). As mentioned earlier, little is known about the role of *ADGRG7* in general and

specifically in scoliosis, but our work identifies *ADGRG7* as a target gene of E2 regulation and suggests a possible involvement as a contributer gene in scoliosis.

The function of *ADGRG7* is poorly described in literature. Previously, a mouse model with targeted deletion of *Adgrg7* was generated. These mice had reduced body weight and increased intestinal contraction frequency, but the skeleton phenotype of these mice was not assessed (Ni, Chen et al. 2014). In humans, *ADGRG7* gene variants were observed in patients with idiopathic scoliosis (Patten, Margaritte-Jeannin et al. 2015). *ADGRG7* variant (*ADGRG7* 1274A>G) was found in several patients with familial form of idiopathic scoliosis in a multiplex French family. In a morpholino zebrafish model, this variant affected bone development resulting in very low calcification suggesting a role for this gene in bone formation and bone mineral density regulation in AIS.

Previously, through a stepwise association study, a susceptibility locus to AIS on chromosome 6q24.1 was reported in Japanese population. Interestingly, the most significantly associated Single Nucleotide Polymorphism (SNP) on this locus was rs6570507 that maps to another adhesion GPR receptor, *ADGRG6*. ADGRG6 is also connected with the reduced body mass index and its activity /function seems to be correlated with osteoblast metabolism and bone calcification (Kou, Takahashi et al. 2013) (both altered in idiopathic scoliosis). Recently, a rare variant of *CELSR2* was cosegregating with scoliosis in Swedish-Danish patients (Einarsdottir, Grauers et al. 2017). CELSR2 is an adhesion GPCR and plays a role in neuronal system development along with other physiological processes. The missense mutation in *CELSR2*, is located within the highly conserved GAIN domain. The consequences of this mutation on the structure of protein are not expected to be major; however, structure predictions of the mutant (mut) *CELSR2* indicates that it is located in close proximity to the H2355-T2357 autoproteolysis cut site. Homozygote loss of function mutations in *ADGRG6* was found to be associated with lethal arthrogryposis. Scoliosis occurrence in a patient with arthrogryposis was reported. The mutation (c. 2306T>A; p. Val769Glu) was located in the GAIN domain of ADGRG6, and results in a reduced but not a complete elimination of autoproteolytic activity (Ravenscroft, Nolent et al. 2015). The GAIN domain is highly conserved through evolution and it has a function in properly activating the receptor (Arac, Boucard et al. 2012). Interestingly, the mutation in *ADGRG7* (1274A>G) is also located in the GAIN domain. Since the mutation in *ADGRG7* is heterozygote, it doesn't significantly affect

the function of ADGRG7 protein, and it is possible that homozygote mutations would abolish ADGRG7 activity resulting in more severe phenotype of AIS. Future studies are thus needed to determine how *ADGRG7* mutation could disrupt the auto-proteolytic mechanism of the GAIN domain in ADGRG7.

Conclusion

This study reports the mechanism of *ADGRG7* regulation by E2, with differential response of normal and scoliotic osteoblasts, and suggests that *ADGRG7* is a contributor risk gene in AIS. The effect of E2 pointed out the disruption of the auto-proteolytic mechanism of the GAIN domain in the *ADGRG7*. The differential response of normal and scoliotic osteoblasts to E2 suggests that molecular mechanisms and pathways associated with AIS (progression and/or the onset) could be associated with the rise in sex-hormones (including E2). The functional consequences of *ADGRG7* upregulation as well as the gene variants of the adhesion subfamily of G-protein coupled receptors that are possibly contributing factors in the pathogenesis of AIS during the pubertal growth spurt merits further *in vivo* examination.

Materials and Methods:

In-Silico Analysis of Gene Expression

The expression profiles of target genes in normal and cancer samples generated from the affymetrix platform 133plus2 were downloaded using the GENT (gene expression across normal and tumor) software (Shin, Kang et al. 2011). GENT, (http://medicalgenome.kribb.re.kr/GENT/reference.php) uses data sets created by the Affymetrix platforms (U133A and U133plus2). The data of normal tissues was then analyzed using one-way analysis of variance performed.

Cell Culture and Treatments

The human hepatocellular carcinoma cell line Huh7 cells was a kind gift from Dr. M. Santo and cultured as previously published (Bagu and Santos 2011). Human breast cancer MCF-7 cells and cervical cancer HeLa cells were purchased from American Type Culture Collection (ATCC, Manassas, VA). The latter two cell lines were cultured in Dulbecco's modified Eagle's medium (Wisent) supplemented with 10% fetal bovine serum (Wisent) and 1% Penicillin-streptomycin antibiotic. Primary human osteoblasts were isolated and cultured as described (Fendri, Patten et al. 2013). For estrogen assays, cells were cultured in phenol red-free DMEM (Wisent) supplemented with 10% charcoal-stripped FBS (CS-FBS) for 3 days. The next day, the cells were treated with ethanol (vehicle) or 10^{-7} M E2 for 24 h. E2 and 4-hydroxy-tamoxifen (4-OHT) were purchased from Sigma-Aldrich, ICI-182, 780 was from Tocris Bioscience (Ellisville, MO). E2 along with its inhibitors ICI-182, 780 and 4-OHT were reconstituted in 100% ethanol as stock solutions of 2×10^{-2} M and stored at -20°C as indicated by manufacturer.

Patients

For AIS patients, at surgery, bone specimens were collected from the vertebrae (varying from T3 to L4 according to the surgical procedure performed). For control patients, all the tissues were collected with consent following approval by the Institutional Ethics Committee Board of CHU Sainte-Justine Hospital Montreal, Canada.

RNA Extraction and qPCR Analysis

Total RNA was isolated using TRizol as recommended by the manufacturer (Invitrogen Canada). RNA (2µg) was used as a template to synthesize the first strand-cDNA using Superscript reverse transcriptase (Bio-Rad). Total RNA was derived from cells and the cDNA was synthesized using iScript reverse transcriptase (Biorad). Quantification of gene expression was performed by 7900HT Fast Real-Time PCR System (Applied Biosystems Stratagene) with iQ™ SYBR® Green Supermix (Biorad). The oligonucleotides used to amplify *GAPDH* and *ADGRG7* are listed in Table S4. The generated PCR products were confirmed by agarose gel electrophoresis and sequencing (McGill University and Génome Québec Innovation

Centre, Montreal QC). Gene expression levels were normalized to *GADPH* expression and expressed as fold change compared to vehicle-treated cells derived from at least three separate experiments. All treatments were normalized to the control value, which was 1.

In-silico Analysis of *ADGRG7* Promoter

Multiple bio-informatics tools (Evolutionary Conserved Regions (ECR)-Browser, http://ecrbrowser.dcode.org determined putative regulatory elements (RE) in the *ADGRG7* promoter for ERα and SP1.

***ADGRG7* Promoter Constructs and Mutagenesis**

A 2204bp fragment corresponding to the proximal promoter (-2259 to +55) of *ADGRG7* was generated by PCR (primers listed in Table S1) from genomic DNA isolated from Huh7 cells. The fragment was then cloned into a pGL3 basic luciferase reporter plasmid vector (Promega, Madison, WI) to generate (-1285/+55) promoter construct. A series of deletion constructs (-474/+55; -309/+55 and -283/+55 and -44/+55) were generated by PCR amplification using the *ADGRG7* plasmid -1285/+55 as a template and primers are listed in (Table S1).
Mutated SP1 construct was obtained by site-directed mutagenesis using the QuikChange II XL mutation procedure (Stratagene, La Jolla, CA) with respective primer pairs (Table S2) according to manufacture's instructions. The constructs were validated by automated sequencing (McGill University and Genome Quebec Innovation Center). Expression vectors coding for GFP-flagged human estrogen receptor ERα (pEGFP-hERα) and ERβ (pEGFP-hERβ) were obtained from Addgene (#28230 and #28237).

Protein Lysate Preparation and Western Blotting

Whole cell protein lysates were prepared from cultured cells using RIPA buffer (Pierce thermoscientific) (25 mM TrisHCl pH 7.6, 150 mM NaCl, 1% NP-40, 1% sodium deoxycholate, 0.1% SDS,) supplemented with protease and phosphatase inhibitors (Roche Diagnostics, Mannheim, Germany). Samples were resolved by 10% SDS-PAGE and

transferred to nitrocellulose membranes (Millipore, Bedford, MA. Membranes were blocked with (20% skim milk) and probed with primary antibody (1:250) against ADGRG7 (Thermoscientific), SP1 (abcam), ERα (Santa Cruz) and β-actin (Santa Cruz Biotechnology). After being washed with phosphate-buffered saline containing 0.05% Tween 20, membranes were probed with a horseradish peroxidase-conjugated secondary antibody (1:10000; Thermoscientific) for 1 h. Signals were visualized with a chemiluminescent substrate (ECL Plus Western blotting detection system, Amersham Biosciences).

Transfection and Luciferase Reporter Assay

Transfections of Huh7 hepatoma cells and MCF7 were performed in 24 well plates using LipofectamineTM 2000 (Invitrogen, Burlington, ON, Canada) as recommended by the manufacturer. Briefly, on the day before transfection, approximately 9 x 10^4 cells (Huh7 and MCF7) were seeded per well in a 24 well plate in phenol red-free DMEM supplemented with 10%CS-FBS. Cells were co-transfected with 990 ng/ well of the different *ADGRG7* promoter constructs (-2259/+55; -1285/+55 -474/+55; -309/+55 and -283/+55 and -44/+55) along with 10 ng of phRL-TK vector (Renilla Luciferase; Promega) according to manufacture's protocol. The total DNA per well was kept at 750ng/ well in the 24-well plates by co-transfecting with the empty expression vector pCDNA3. When evaluating the effect of ERα on *ADGRG7* in the presence or absence of E2, ERα negative Huh7 cells were co-transfected with different *ADGRG7* promoter constructs along with either the expression vector encoding the full length human ERα protein (250 ng/ well) or the empty pCDNA-3 vector (Invitrogen, Burlington, ON, Canada). After a 24 h transfection, the cells were washed and treated for 24 h with fresh phenol red-free DMEM supplemented with 1% CS-FBS containing E2, 4-OHT or ICI-182, 780 only dissolved in ethanol, or ethanol alone as a vehicle control. The cells were harvested, and subsequently luciferase activity was determined with a luciferase assay system (Promega) according to the manufacturer's directions. Luciferase activity was normalized to the activity of co-transfected Renilla luciferase as an internal control for transfection efficiency. In order to evaluate the basal luciferase activity for each construct, controls for each full-length promoter construct were co-transfected with an empty pCDNA-3 vector (Invitrogen,

Burlington, ON, Canada) and then cultured in the vehicle. In all experiments, data reported represents the average of at least three experiments, done in triplicates.

Chromatin Immunoprecipitation (ChIP)

ChIP was performed as described (Edjekouane, Benhadjeba et al. 2016). Briefly, MCF7-ER**α** cells were cultured in phenol red-free medium and 10 % charcoal stripped FBS then treated with 10^{-7} M E2 or vehicle for 1 h. After fixation with 2% formaldehyde, cells were lysed and the precleared chromatin supernatants were immunoprecipitated with the respective antibodies specific anti-ERα (Santa Cuz) and anti-SP1 (abcam) or nonspecific IgG at 4**°**C. Bound DNA was purified with phenol/chloroform and used as a template for subsequent amplification using primers (see Table S3) that encompass respective specific binding elements within the proximal *ADGRG7* promoter region. Fold enrichment values were calculated using the Ct value of each ChIP sample compared to the Ct value of Input DNA. PCR products were resolved on a 2% agarose gel.

Fluorescence Microscopy

Osteoblasts from normal and AIS patients were seeded on Labtek (NUNC, Thermoscientific) and cultured overnight. On the second day, cells were treated with 10^{-7} M E2 for 24 h. On the third day, cells were fixed in 70% ethanol/0.1% triton on ice for 30 min. Cells were then washed with PBS and permeabilized with 0.1% Triton in PBS for 15 min. Cells were washed once with 0.5% BSA in PBS/Triton (PBT), blocked with 2% BSA in PBT for 45 min, and incubated with the anti-ADGRG7 antibody (Thermoscientific) at (1/200) for 1 h with gentle shaking at room temperature (RT). Cells were then incubated with Alexa Flour 555 (Life technologies USA) for 1 h. Cells were mounted and stained for nucleus at the same time using Prolong Gold antifade reagent with DAPI (Life technologies). Immunostaining was examined at magnification x 40. Scale bar 1.78 μm.

Statistical analysis

The Data collected were analyzed by a one-way analysis of variance (ANOVA; SigmaStat Version 2.0, Jadel Corporation, San Rafael, CA, USA). Multiple range comparisons of paired means were done using a Fishers LSD test or the Newman-Keuls test. Level of significance was set at $p<0.05$. Data is reported as mean ± SEM. Pearson's correlations were done to evaluate the consistence of the data and the relationship across gene expression profiles. For variables with the same letter, the difference is not statistically significant. Likewise, for variables with a different letter, the difference is statistically significant (Assaad, Hou et al. 2015). For luciferase and qPCR experiments, data are representative of at least three independent experiments in triplicates.

Acknowledgement

The authors would like to thank Heather Yampolsky for the help in editing and writing of the manuscript. We would like also to thank Dr. Stefan Parent, Madam Soraya Barchi and Mr. Francois Cereal for providing osteoblasts that were used in the study. We are also grateful for the lab of Dr. Santos for providing Huh-7 cells.

Funding:

This work was supported by the Fondation Yves Cotrel-Institut de France by grants to F.M., and S.A.P.; The Faculty of Dentistry, Université de Montréal, Fonds Ernest- Charron and The Network for Oral and Bone Health Research by grants to F.M.; We thank the MEDITIS program for the salary support (A.H) and FRQS to S.A.P.

Conflict of interest:

The authors declare that they have no conflicts of interest.

Author contribution:

A.H and E.T.B designed experiments and wrote the first version of the manuscript. AH performed the experiments. SB and LE helped in the design and performance of some

experiments. AH, ETB, AT, SAP and FM designed the study, interpreted the results and contributed to the writing of the manuscript. All authors approved the final version of this manuscript.

References

Arac, D., G. Aust, D. Calebiro, F. B. Engel, C. Formstone, A. Goffinet, J. Hamann, R. J. Kittel, I. Liebscher, H. H. Lin, K. R. Monk, A. Petrenko, X. Piao, S. Promel, H. B. Schioth, T. W. Schwartz, M. Stacey, Y. A. Ushkaryov, M. Wobus, U. Wolfrum, L. Xu and T. Langenhan (2012). "Dissecting signaling and functions of adhesion G protein-coupled receptors." Ann N Y Acad Sci **1276**: 1-25.

Arac, D., A. A. Boucard, M. F. Bolliger, J. Nguyen, S. M. Soltis, T. C. Sudhof and A. T. Brunger (2012). "A novel evolutionarily conserved domain of cell-adhesion GPCRs mediates autoproteolysis." EMBO J **31**(6): 1364-1378.

Assaad, H. I., Y. Hou, L. Zhou, R. J. Carroll and G. Wu (2015). "Rapid publication-ready MS-Word tables for two-way ANOVA." Springerplus **4**: 33.

Badiali, L., J. Cedernaes, P. K. Olszewski, O. Nylander, A. V. Vergoni and H. B. Schioth (2012). "Adhesion GPCRs are widely expressed throughout the subsections of the gastrointestinal tract." BMC Gastroenterol **12**: 134.

Bagu, E. T. and M. M. Santos (2011). "Friend of GATA suppresses the GATA-induced transcription of hepcidin in hepatocytes through a GATA-regulatory element in the HAMP promoter." J Mol Endocrinol **47**(3): 299-313.

Barrios, C., S. Cortes, C. Perez-Encinas, M. D. Escriva, I. Benet, J. Burgos, E. Hevia, G. Piza and P. Domenech (2011). "Anthropometry and body composition profile of girls with nonsurgically treated adolescent idiopathic scoliosis." Spine (Phila Pa 1976) **36**(18): 1470-1477.

Bjarnadottir, T. K., R. Fredriksson, P. J. Hoglund, D. E. Gloriam, M. C. Lagerstrom and H. B. Schioth (2004). "The human and mouse repertoire of the adhesion family of G-protein-coupled receptors." Genomics **84**(1): 23-33.

Bjornstrom, L. and M. Sjoberg (2005). "Mechanisms of estrogen receptor signaling: convergence of genomic and nongenomic actions on target genes." Mol Endocrinol **19**(4): 833-842.

Chen, J. R., O. P. Lazarenko, R. L. Haley, M. L. Blackburn, T. M. Badger and M. J. Ronis (2009). "Ethanol impairs estrogen receptor signaling resulting in accelerated activation of senescence pathways, whereas estradiol attenuates the effects of ethanol in osteoblasts." J Bone Miner Res **24**(2): 221-230.

Cheng, J. C., R. M. Castelein, W. C. Chu, A. J. Danielsson, M. B. Dobbs, T. B. Grivas, C. A. Gurnett, K. D. Luk, A. Moreau, P. O. Newton, I. A. Stokes, S. L. Weinstein and R. G. Burwell (2015). "Adolescent idiopathic scoliosis." Nat Rev Dis Primers **1**: 15030.

Cheng, J. C., S. P. Tang, X. Guo, C. W. Chan and L. Qin (2001). "Osteopenia in adolescent idiopathic scoliosis: a histomorphometric study." Spine (Phila Pa 1976) **26**(3): E19-23.

Dahlman-Wright, K., V. Cavailles, S. A. Fuqua, V. C. Jordan, J. A. Katzenellenbogen, K. S. Korach, A. Maggi, M. Muramatsu, M. G. Parker and J. A. Gustafsson (2006). "International Union of Pharmacology. LXIV. Estrogen receptors." Pharmacol Rev **58**(4): 773-781.

Edery, P., P. Margaritte-Jeannin, B. Biot, A. Labalme, J. C. Bernard, J. Chastang, B. Kassai, M. H. Plais, F. Moldovan and F. Clerget-Darpoux (2011). "New disease gene location and high genetic heterogeneity in idiopathic scoliosis." Eur J Hum Genet **19**(8): 865-869.

Edjekouane, L., S. Benhadjeba, M. Jangal, H. Fleury, N. Gevry, E. Carmona and A. Tremblay (2016). "Proximal and distal regulation of the HYAL1 gene cluster by the estrogen receptor alpha in breast cancer cells." Oncotarget **7**(47): 77276-77290.

Einarsdottir, E., A. Grauers, J. Wang, H. Jiao, S. A. Escher, A. Danielsson, A. Simony, M. Andersen, S. B. Christensen, K. Akesson, I. Kou, A. M. Khanshour, A. Ohlin, C. Wise, S. Ikegawa, J. Kere and P. Gerdhem (2017). "CELSR2 is a candidate susceptibility gene in idiopathic scoliosis." PLoS One **12**(12): e0189591.

Fendri, K., S. A. Patten, G. N. Kaufman, C. Zaouter, S. Parent, G. Grimard, P. Edery and F. Moldovan (2013). "Microarray expression profiling identifies genes with altered expression in Adolescent Idiopathic Scoliosis." Eur Spine J **22**(6): 1300-1311.

Foord, S. M., S. Jupe and J. Holbrook (2002). "Bioinformatics and type II G-protein-coupled receptors." Biochem Soc Trans **30**(4): 473-479.

Fournier, B., S. Gutzwiller, T. Dittmar, G. Matthias, P. Steenbergh and P. Matthias (2001). "Estrogen receptor (ER)-alpha, but not ER-beta, mediates regulation of the insulin-like growth factor I gene by antiestrogens." J Biol Chem **276**(38): 35444-35449.

Fredriksson, R., M. C. Lagerstrom, P. J. Hoglund and H. B. Schioth (2002). "Novel human G protein-coupled receptors with long N-terminals containing GPS domains and Ser/Thr-rich regions." FEBS Lett **531**(3): 407-414.

Grant, S. F., D. M. Reid, G. Blake, R. Herd, I. Fogelman and S. H. Ralston (1996). "Reduced bone density and osteoporosis associated with a polymorphic Sp1 binding site in the collagen type I alpha 1 gene." Nat Genet **14**(2): 203-205.

Huang, Y. S., N. Y. Chiang, C. H. Hu, C. C. Hsiao, K. F. Cheng, W. P. Tsai, S. Yona, M. Stacey, S. Gordon, G. W. Chang and H. H. Lin (2012). "Activation of myeloid cell-specific adhesion class G protein-coupled receptor EMR2 via ligation-induced translocation and interaction of receptor subunits in lipid raft microdomains." Mol Cell Biol **32**(8): 1408-1420.

Ishida, K., Y. Aota, N. Mitsugi, M. Kono, T. Higashi, T. Kawai, K. Yamada, T. Niimura, K. Kaneko, H. Tanabe, Y. Ito, T. Katsuhata and T. Saito (2015). "Relationship between bone density and bone metabolism in adolescent idiopathic scoliosis." Scoliosis **10**: 19.

Janusz, P., M. Kotwicka, M. Andrusiewicz, D. Czaprowski, J. Czubak and T. Kotwicki (2014). "Estrogen receptors genes polymorphisms and age at menarche in idiopathic scoliosis." BMC Musculoskelet Disord **15**: 383.

Karner, C. M., F. Long, L. Solnica-Krezel, K. R. Monk and R. S. Gray (2015). "Gpr126/Adgrg6 deletion in cartilage models idiopathic scoliosis and pectus excavatum in mice." Hum Mol Genet **24**(15): 4365-4373.

Keay, J. and J. W. Thornton (2009). "Hormone-activated estrogen receptors in annelid invertebrates: implications for evolution and endocrine disruption." Endocrinology **150**(4): 1731-1738.

Khan, S., M. Abdelrahim, I. Samudio and S. Safe (2003). "Estrogen receptor/Sp1 complexes are required for induction of cad gene expression by 17beta-estradiol in breast cancer cells." Endocrinology **144**(6): 2325-2335.

Kim, S. C., J. E. Lee, S. S. Kang, H. S. Yang, S. S. Kim and B. S. An (2017). "The regulation of oxytocin and oxytocin receptor in human placenta according to gestational age." J Mol Endocrinol **59**(3): 235-243.

Konieczny, M. R., H. Senyurt and R. Krauspe (2013). "Epidemiology of adolescent idiopathic scoliosis." J Child Orthop **7**(1): 3-9.

Kou, I., Y. Takahashi, T. A. Johnson, A. Takahashi, L. Guo, J. Dai, X. Qiu, S. Sharma, A. Takimoto, Y. Ogura, H. Jiang, H. Yan, K. Kono, N. Kawakami, K. Uno, M. Ito, S. Minami, H. Yanagida, H. Taneichi, N. Hosono, T. Tsuji, T. Suzuki, H. Sudo, T. Kotani, I. Yonezawa, D. Londono, D. Gordon, J. A. Herring, K. Watanabe, K. Chiba, N. Kamatani, Q. Jiang, Y. Hiraki, M. Kubo, Y. Toyama, T. Tsunoda, C. A. Wise, Y. Qiu, C. Shukunami, M. Matsumoto and S. Ikegawa (2013). "Genetic variants in GPR126 are associated with adolescent idiopathic scoliosis." Nat Genet **45**(6): 676-679.

Krishnan, V., W. Porter, M. Santostefano, X. Wang and S. Safe (1995). "Molecular mechanism of inhibition of estrogen-induced cathepsin D gene expression by 2,3,7,8-tetrachlorodibenzo-p-dioxin (TCDD) in MCF-7 cells." Mol Cell Biol **15**(12): 6710-6719.

Krishnan, V., X. Wang and S. Safe (1994). "Estrogen receptor-Sp1 complexes mediate estrogen-induced cathepsin D gene expression in MCF-7 human breast cancer cells." J Biol Chem **269**(22): 15912-15917.

Leboeuf, D., K. Letellier, N. Alos, P. Edery and F. Moldovan (2009). "Do estrogens impact adolescent idiopathic scoliosis?" Trends Endocrinol Metab **20**(4): 147-152.

Li, D., D. Mitchell, J. Luo, Z. Yi, S. G. Cho, J. Guo, X. Li, G. Ning, X. Wu and M. Liu (2007). "Estrogen regulates KiSS1 gene expression through estrogen receptor alpha and SP protein complexes." Endocrinology **148**(10): 4821-4828.

Li, X. F., H. Li, Z. D. Liu and L. Y. Dai (2008). "Low bone mineral status in adolescent idiopathic scoliosis." Eur Spine J **17**(11): 1431-1440.

Ni, Y. Y., Y. Chen, S. Y. Lu, B. Y. Sun, F. Wang, X. L. Wu, S. Y. Dang, G. H. Zhang, H. X. Zhang, Y. Kuang, J. Fei, M. M. Gu, W. F. Rong and Z. G. Wang (2014). "Deletion of Gpr128 results in weight loss and increased intestinal contraction frequency." World J Gastroenterol **20**(2): 498-508.

Patten, S. A., P. Margaritte-Jeannin, J. C. Bernard, E. Alix, A. Labalme, A. Besson, S. L. Girard, K. Fendri, N. Fraisse, B. Biot, C. Poizat, A. Campan-Fournier, K. Abelin-Genevois, V. Cunin, C. Zaouter, M. Liao, R. Lamy, G. Lesca, R. Menassa, C. Marcaillou, M. Letexier, D. Sanlaville, J. Berard, G. A. Rouleau, F. Clerget-Darpoux, P. Drapeau, F. Moldovan and P. Edery (2015). "Functional variants of POC5 identified in patients with idiopathic scoliosis." J Clin Invest **125**(3): 1124-1128.

Peng, Y., G. Liang, Y. Pei, W. Ye, A. Liang and P. Su (2012). "Genomic polymorphisms of G-protein estrogen receptor 1 are associated with severity of adolescent idiopathic scoliosis." Int Orthop **36**(3): 671-677.

Petz, L. N. and A. M. Nardulli (2000). "Sp1 binding sites and an estrogen response element half-site are involved in regulation of the human progesterone receptor A promoter." Mol Endocrinol **14**(7): 972-985.

Porter, W., F. Wang, W. Wang, R. Duan and S. Safe (1996). "Role of estrogen receptor/Sp1 complexes in estrogen-induced heat shock protein 27 gene expression." Mol Endocrinol **10**(11): 1371-1378.

Prossnitz, E. R., J. B. Arterburn, H. O. Smith, T. I. Oprea, L. A. Sklar and H. J. Hathaway (2008). "Estrogen signaling through the transmembrane G protein-coupled receptor GPR30." Annu Rev Physiol **70**: 165-190.

Quaynor, S. D., E. W. Stradtman, Jr., H. G. Kim, Y. Shen, L. P. Chorich, D. A. Schreihofer and L. C. Layman (2013). "Delayed puberty and estrogen resistance in a woman with estrogen receptor alpha variant." N Engl J Med **369**(2): 164-171.

Ravenscroft, G., F. Nolent, S. Rajagopalan, A. M. Meireles, K. J. Paavola, D. Gaillard, E. Alanio, M. Buckland, S. Arbuckle, M. Krivanek, J. Maluenda, S. Pannell, R. Gooding, R. W. Ong, R. J. Allcock, E. D. Carvalho, M. D. Carvalho, F. Kok, W. S. Talbot, J. Melki and N. G. Laing (2015). "Mutations of GPR126 are responsible for severe arthrogryposis multiplex congenita." Am J Hum Genet **96**(6): 955-961.

Safe, S. (2001). "Transcriptional activation of genes by 17 beta-estradiol through estrogen receptor-Sp1 interactions." Vitam Horm **62**: 231-252.

Schultz, J. R., L. N. Petz and A. M. Nardulli (2005). "Cell- and ligand-specific regulation of promoters containing activator protein-1 and Sp1 sites by estrogen receptors alpha and beta." J Biol Chem **280**(1): 347-354.

Shin, G., T. W. Kang, S. Yang, S. J. Baek, Y. S. Jeong and S. Y. Kim (2011). "GENT: gene expression database of normal and tumor tissues." Cancer Inform **10**: 149-157.

Smith, E. P., J. Boyd, G. R. Frank, H. Takahashi, R. M. Cohen, B. Specker, T. C. Williams, D. B. Lubahn and K. S. Korach (1994). "Estrogen resistance caused by a mutation in the estrogen-receptor gene in a man." N Engl J Med **331**(16): 1056-1061.

Snyder, E. M., C. L. Small, Y. Li and M. D. Griswold (2009). "Regulation of gene expression by estrogen and testosterone in the proximal mouse reproductive tract." Biol Reprod **81**(4): 707-716.

Stavrou, I., C. Zois, J. P. Ioannidis and A. Tsatsoulis (2002). "Association of polymorphisms of the oestrogen receptor alpha gene with the age of menarche." Hum Reprod **17**(4): 1101-1105.

Sun, X., T. Wu, Z. Liu, Z. Zhu, B. Qian, F. Zhu, W. Ma, Y. Yu, B. Wang and Y. Qiu (2013). "Osteopenia predicts curve progression of adolescent idiopathic scoliosis in girls treated with brace treatment." J Pediatr Orthop **33**(4): 366-371.

Vyhlidal, C., I. Samudio, M. P. Kladde and S. Safe (2000). "Transcriptional activation of transforming growth factor alpha by estradiol: requirement for both a GC-rich site and an estrogen response element half-site." J Mol Endocrinol **24**(3): 329-338.

Yona, S., H. H. Lin, W. O. Siu, S. Gordon and M. Stacey (2008). "Adhesion-GPCRs: emerging roles for novel receptors." Trends Biochem Sci **33**(10): 491-500.

Yona, S. and M. Stacey (2010). "Adhesion-GPCRs: structure to function. Preface." Adv Exp Med Biol **706**: v-vii.

FIGURES

Figure 1: *ADGRG7* and *SP1* expression in human tissues. *ADGRG7* (A) and *SP1* (B) microarray expression in normal human tissues were extracted from GEO database available from NCBI. The profiles of the target genes in human tissues were collected from different studies and the mean transcript levels determined. The data is presented as mean ± SD.

Figure 2: Upregulation of ADGRG7 expression in NOB and AIS osteoblasts by 17β-Estradiol (E2). A and B) NOB and AIS cells were treated with different doses of E2 (10^{-7}, 10^{-9},10^{-12}, 10^{-13} and 10^{-14} M) E2 for 24 h followed by analysis of whole cell extract by Western blotting using anti-ADGRG7 antibody. Anti-β-actin antibody was used as a loading control. Protein quantification was performed using the Image-J. The results are mean ± SD from two independent experiments (n=2). $p<0.05$ was considered statistically significant. C) Immunolocalization of ADGRG7 in NOB and AIS cells cultured without E2 (-E2) or with (+E2) overnight in CS-FBS medium. Cells were cultured on Labteck (as described in Material and Methods), fixed, permeabilized and analyzed for ADGRG7 positive immunostaining. Note the cytoplasmic staining of ADGRG7 in cells cultured overnight in defined medium and the increase in immunostaining after 24 h treatment with E2. Nucleus is stained with DAPI

(Blue). D) Western blot analysis of ERα and SP1 in NOB and AIS cells. Total cell lysates were isolated. Detections of ERα, SP1and β-actin were performed by immunoblotting as described in Materials and Methods. Protein quantification was done using Image-J. For variables with the same letter, the difference is not statistically significant. Likewise, for variables with a different letter, the difference is statistically significant. For western blot, data are the ±SD of two independent experiments (n=2). $p<0.01$ for ERα and $p<0.001$ for SP1.

Figure 3: ADGRG7 expression is upregulated by E2 in Huh-7 cells. A) E2 modulates *ADGRG7* gene expression. Human hepatocellular carcinoma cells, Huh7, were transiently transfected with either an expression plasmid vector that encodes the full length wild type estrogen receptor alpha (ERα) or with the empty expression vector back bone (pCDNA3 plasmid vector). The cells were then treated with E2 (10^{-7} M), and the control cells transfected with the empty pCDNA3 vector were treated with the vehicle (ethanol). The Huh7 cells were treated with E2 for 3 h, 12 h and 24 h. *ADGRG7* expression was measured by qPCR. The gene expression levels of *ADGRG7* in Huh7 cells following treatment with E2 were determined relative to that of a house keeping gene, *GAPDH* and the fold change was calculated relative to the controls for each time point. The controls at each time point were Huh7 cells transfected with pCDNA3 and treated with vehicle (ethanol) for 3 h, 12 h and 24 h. B) Western blot analysis of ADGRG7. Immunoblot analysis for ADGRG7 was performed following 24 h post treatment with E2 (10^{-7} M) or ethanol. The expression of ADGRG7 was determined relative to the house keeping gene β-actin that was used as a loading control. The mean relative protein expression levels were quantified by densitometry analysis of immunoblots using Image j. C) ERα but not ERβ mediates *ADGRG7* upregulation in Huh-7 cells. The *ADGRG7* promoter activity (-1285/+112; 500 ng/well) in Huh-7 cells was determined following co-transfection with an expression vector that encodes for the full length wild type estrogen receptor protein (ERα or ERβ) and treatment with E2 (10^{-7} M) for 24 h. D) Co-transfection with ERα**,** and then treatment with E2 (10^{-7} M) for 24 h or 48 h. Controls in each case were transfected with the empty pCDNA3 vector (Invitrogen) and then treated with the vehicle (ethanol). For variables with the same letter, the difference is not statistically significant. Likewise, for variables with a different letter, the difference is statistically significant. For western blot, data are the ± SD of two independent experiments (n=2). For luciferase and qPCR experiments, data are

representative of at least three independent experiments in triplicates and represented as fold activation over control (mean ± SD).

Figure 4: Regulation of the proximal promoter activity of *ADGRG7* by ERα. A) Schema representing the *ADGRG7* full length promoter with SP1 and ERE1/2 as well as elements and position with respect to transcription start site (TSS). B) Huh-7 cells were transfected with ERα in the presence of luciferase reporter construct containing the full- length promoter (-2259/+55) of *ADGRG7* and its serial deletions constructs (-1285/+55, -474/+55; -309/+55 and -283/+55 and -44/+55). Cells were then treated or not with 10^{-7} M E2 for 24 h. The arrow pointing to the right represents the transcription start site (TSS). Luciferase values were normalized to Renilla luciferase activity and expressed as relative fold response compared to vehicle-treated mock transfected cells set at 1. One-way ANOVA with Tukey B post hoc analysis was applied to determine significance among different treatment groups in this experiment. *P < 0.05 compared with vehicle treated control. Mean values (±SEM) of at least three separate transfections in triplicates are shown (n=3).

Figure 5: Localization of a functional region within *ADGRG7* promoter important for activation of *ADGRG7* transcription. A) *ADGRG7* wild-type (586bp), truncated (**Δ**67bp and 44bp) promoter activity was determined in MCF-7 cells treated with 10^{-7} M E2 or vehicle for 24 h. Cells were analyzed for luciferase activity. B) *ADGRG7* wild- type and mutant SP1 promoters were analyzed for luciferase activity as in A. Mean values (± SEM) of at least three separate transfections in triplicates are shown (n=3).

Figure 6: Specificity Protein 1 (SP1) and ERα binds to the *ADGRG7* proximal promoter in MCF-7 cells in the presence of E2. A) qPCR expression of *ADGRG7* in MCF7 cells in response to E2 at 3 different time points (3 h, 12 h and 24 h). B) Immunoblot analysis for ADGRG7 in control and cells treated E2 for 24 h. In the representative immunoblots, the protein was detectable at the expected size of 85 kDa for ADGRG7. Anti-β-actin antibody was used as a loading control. Protein quantification was performed using Image-J. Data are the ±SD of two independent experiments (n=2). C) Schematic representation of Δ67bp fragment of the *ADGRG7* showing approximate locations of ERE1/2 half-sites and SP1 binding sites. D) SP1 and ERα binding to the *ADGRG7* promoter. ChIP-qPCR validation of SP1xERE1/2

binding sites identified from ChIP-seq analysis in vicinity of the *ADGRG7*. The proximal region of the ADGRG7 promoter (−478 to -423) is indicated by arrows directed at the left and right of the sequence. MCF-7 cells were treated with 10-7 M E2 for 1 h. Results represent fold enrichment values obtained by comparing CT values of ChIP samples to the CT values of input. For qPCR experiments, data are representative of experiments in triplicates and represented as fold activation over control (mean ± SEM).

Figure 7: Effects of E2, ICI-182, 780 and 4-OHT on the induction of SP1- and ERα-driven reporter activities of *ADGRG7* in MCF7 cells. A) Dose response of *ADGRG7* promoter to 4-OHT. Cells were transiently transfected with 479bp luciferase reporter plasmid. After 24 h of transfection, cells were treated with vehicle only, 10^{-7} M estradiol (E2), and different doses 10^{-7}, 10^{-9}, and 10^{-11} M 4-OHT, or 10^{-7} M E_2 + 4-OHT (E2 + 4-OHT). After 24 h, cells were harvested and assayed for luciferase activity. Luciferase values were corrected for transfection efficiency by measuring the Renilla luciferase activity. Three individual experiments were performed. Data are presented as mean (columns) and standard mean error (bars). B**)** Dose response of ICI-182, 780 on *ADGRG7* promoter regulation. Transfection experiments were performed same as A. After 24 h of transfection, cells were treated with vehicle, 10^{-7} M estradiol (E2), 10^{-9} and 10^{-11} M ICI-182, 780, or 10^{-7} M E2 + ICI-182, 780 (E2 + ICI). C) Effects of 10^{-7} M E2 and 10^{-7} M ICI-182, 780 on SP1 mut reporter construct. Transfections were performed as in A and B (n=3 in triplicates). One-way ANOVA with Tukey B post hoc analysis was applied to determine significance among different treatment groups in this experiment. *$P < 0.05$ compared with vehicle treated control (n=3 in triplicates). D) Effect of E2 or ICI-182, 780 on ADGRG7 protein in MCF-7 cells. Cell lysates were prepared at the indicated treatment times with either 10^{-7} M E2 or 10^{-7} M ICI-182, 780. The ADGRG7 protein was detected using a primary polyclonal rabbit antibody and the immunocomplex was visualized using the enhanced chemiluminescence (ECL) detection system (Amersham). E) Western blot analysis of E2, ICI-182, 780 and 4-OHT effects on the expression of ADGRG7 protein. Protein expression was analysed in cells untreated or treated for 24 h with 10^{-7} M E2 or 10^{-7} M ICI-182, 780 or 10^{-7} M 4-OHT. Expression of β-actin was used as control. Protein quantification was performed using Image-J. For variables with the same letter, the difference is not statistically significant. Likewise, for variables with a

different letter, the difference is statistically significant. For western blot, data are the ±SD of three independent experiments (n=3). $p<0.05$ considered statistically significant.

Figure 8: Schematic representation of the effects of E2 in normal and AIS cells. The transcriptional regulation of *ADGRG7* is driven by both the genomic signalling (direct and indirect) of estrogen in conjunction with SP1.

Through promoter studies, we found that estrogen acts mostly through ERα to induce the expression of *ADGRG7* in cells through the distal promoter ERE half-site along with the SP1 binding site or response element (SP1-RE).

In AIS cells, there is decreased expression of SP1. The induction of the transcription of *ADGRG7* by E2 is non significant in AIS cells from scoliotic patients compared to the cells from normal control individuals.

Fig. 1A

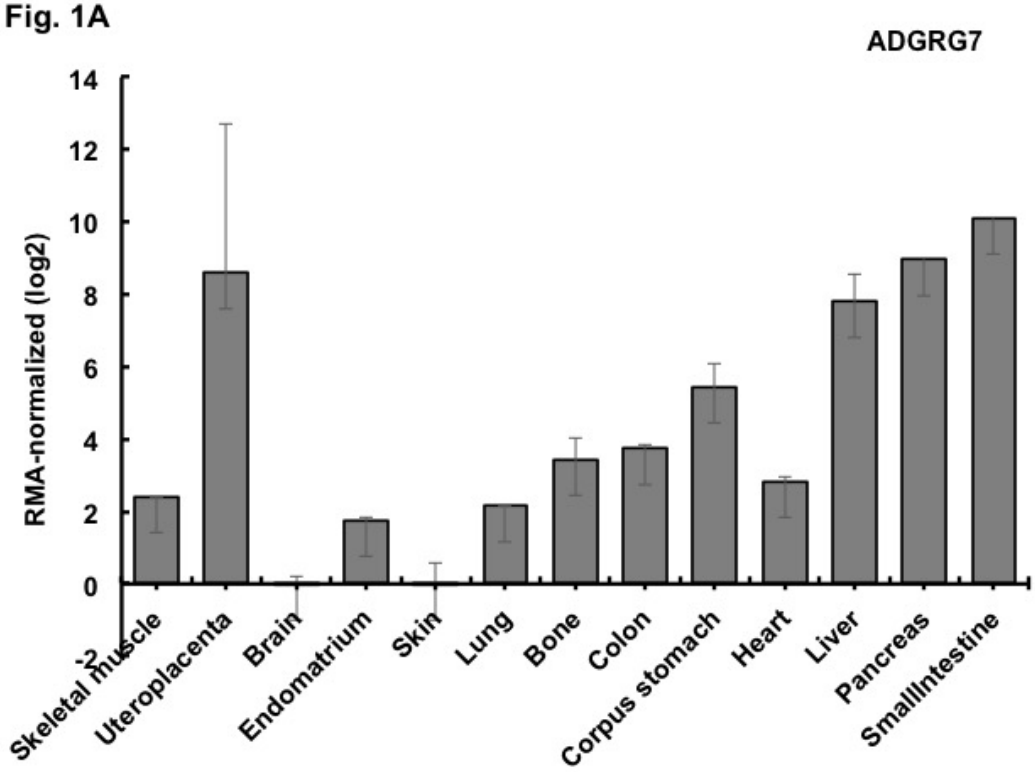
ADGRG7
RMA-normalized (log2)
14
12
10
8
6
4
2
0
-2
Skeletal muscle
Uteroplacenta
Brain
Endomatrium
Skin
Lung
Bone
Colon
Corpus stomach
Heart
Liver
Pancreas
SmallIntestine

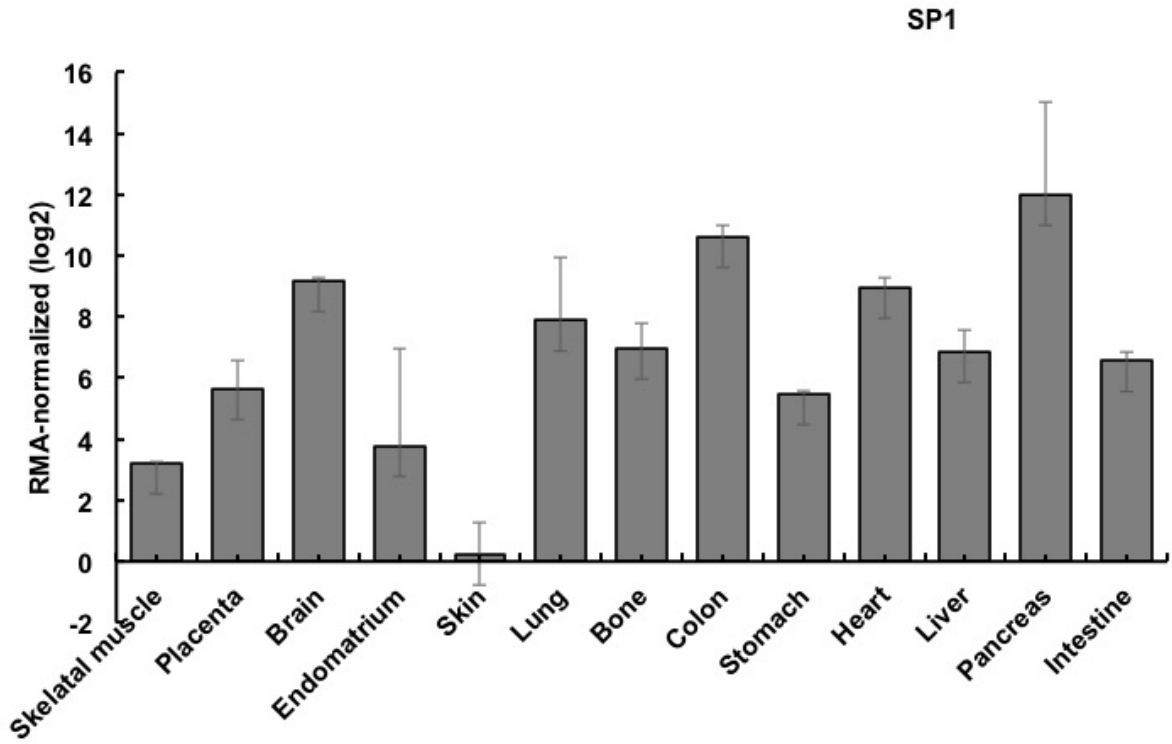
SP1
RMA-normalized (log2)
16
14
12
10
8
6
4
2
0
-2
Skelatal muscle
Placenta
Brain
Endomatrium
Skin
Lung
Bone
Colon
Stomach
Heart
Liver
Pancreas
Intestine

Fig. 2

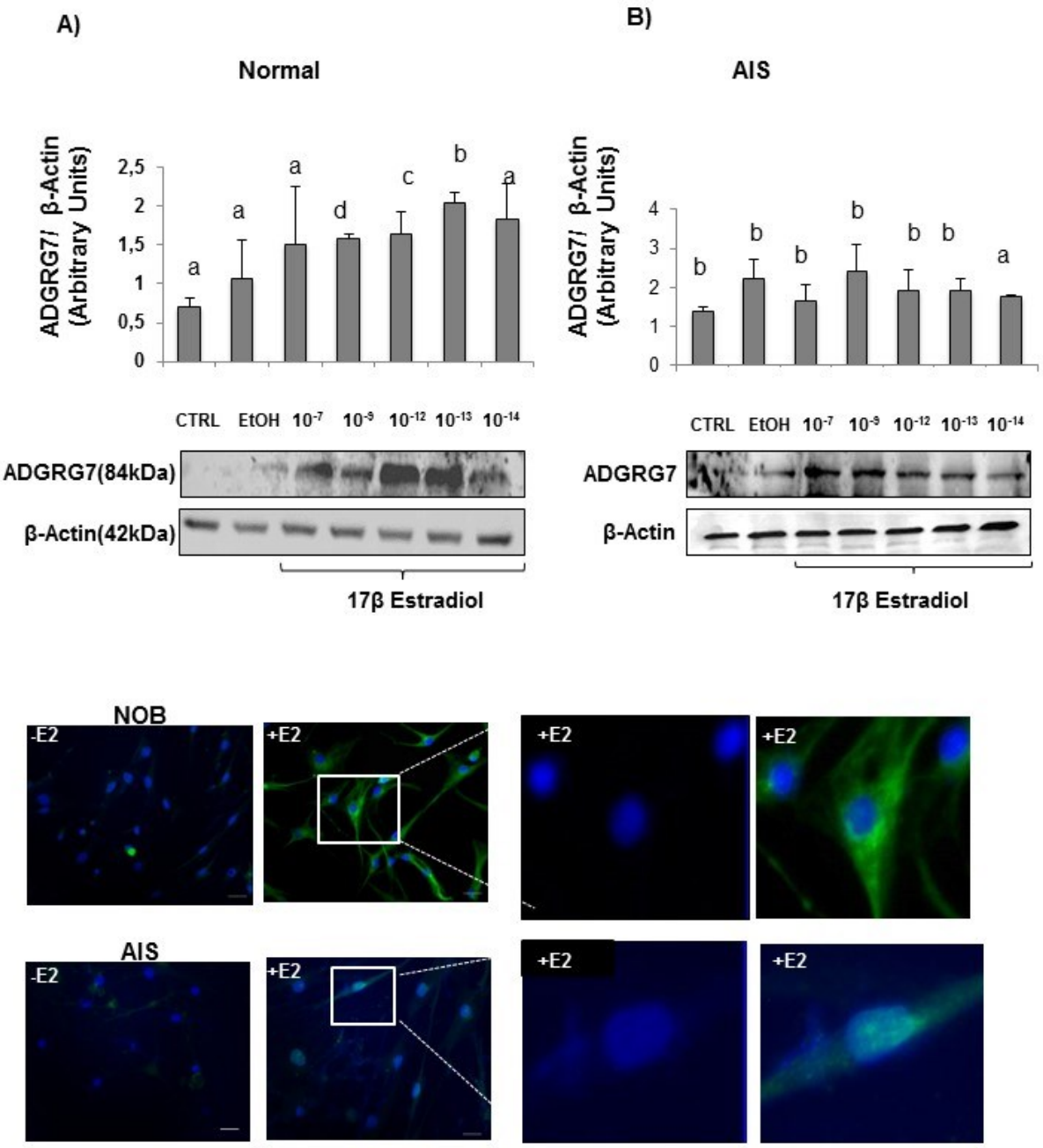
A)
Normal
ADGRG7/ β-Actin (Arbitrary Units)
2,5
2
1,5
1
0,5
0
a
a
a
d
c
b
a
CTRL
EtOH
10-7
10-9
10-12
10-13
10-14
ADGRG7(84kDa)
β-Actin(42kDa)
17β Estradiol
B)
AIS
ADGRG7/ β-Actin (Arbitrary Units)
4
3
2
1
0
b
b
b
b
b
b
a
CTRL
EtOH
10-7
10-9
10-12
10-13
10-14
ADGRG7
β-Actin
17β Estradiol
NOB
-E2
+E2
+E2
+E2
AIS
-E2
+E2
+E2
+E2

Fig. 3

D)

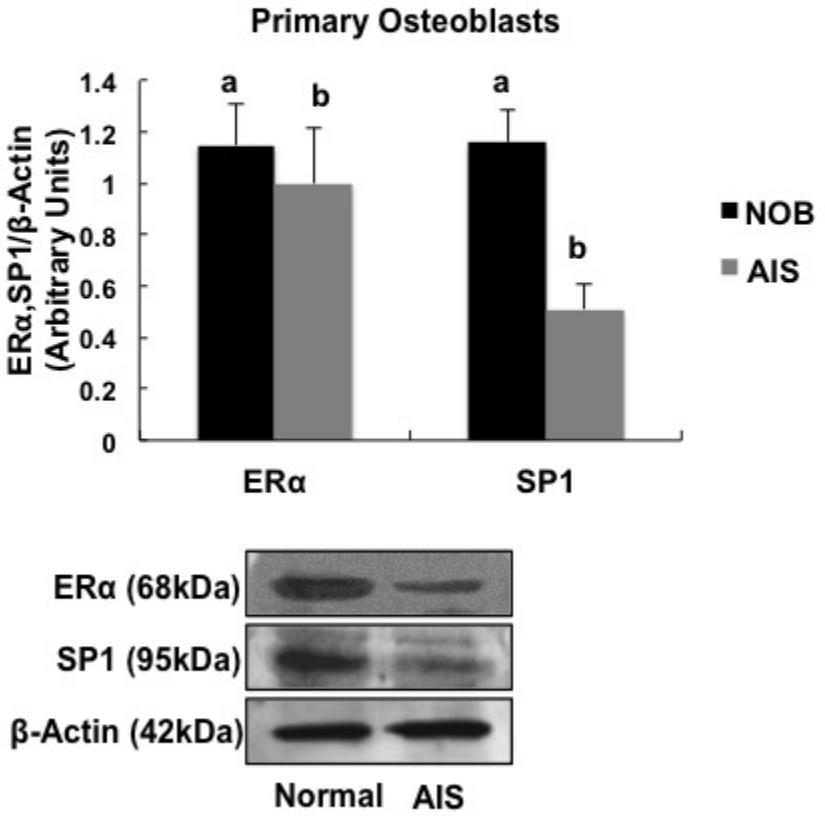
Primary Osteoblasts
ERα,SP1/β-Actin (Arbitrary Units)
1.4
1.2
1
0.8
0.6
0.4
0.2
0
a
b
a
b
ERα
SP1
NOB
AIS
ERα (68kDa)
SP1 (95kDa)
β-Actin (42kDa)
Normal
AIS

Fig. 3

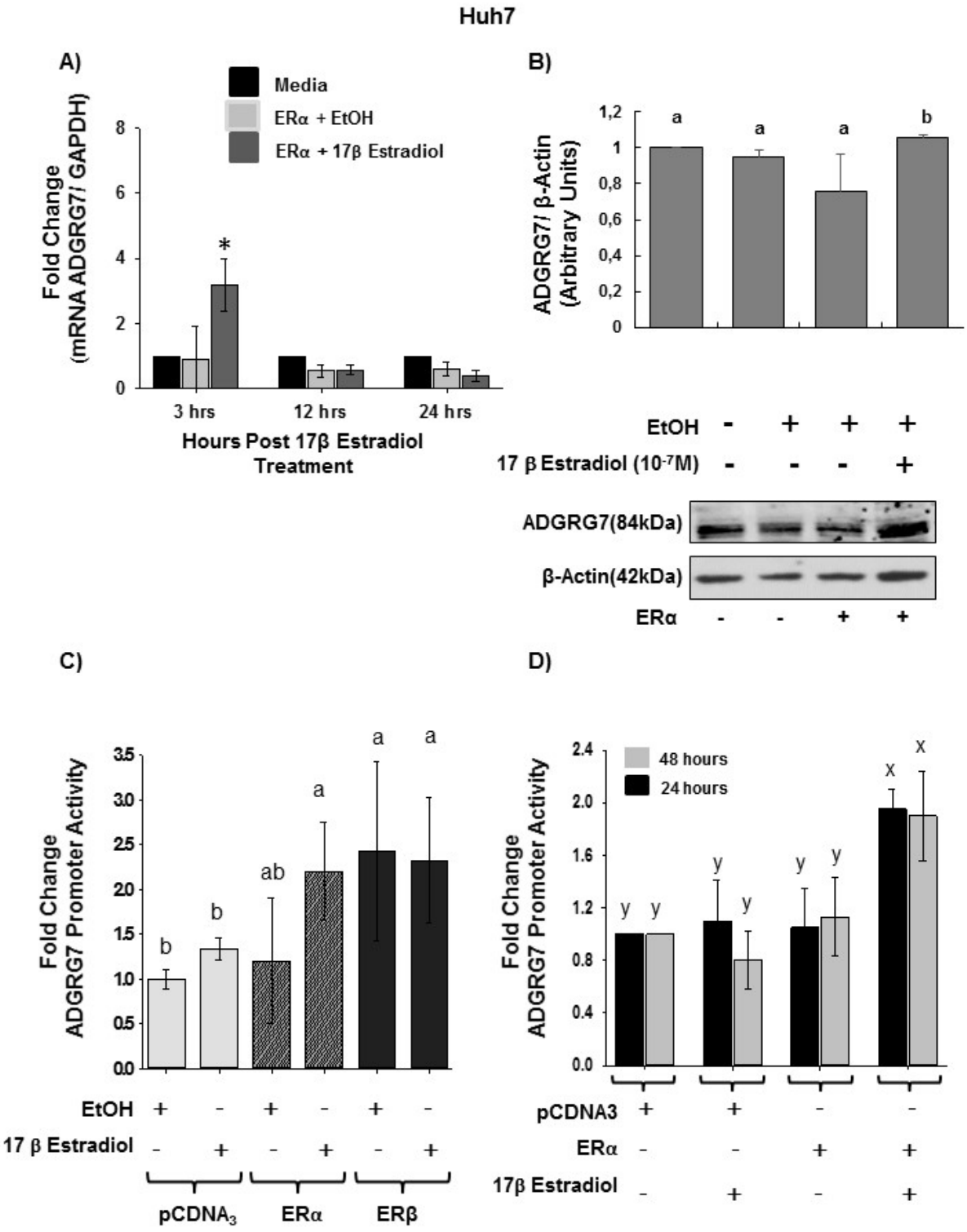
Huh7
A)
Media
ERα + EtOH
ERα + 17β Estradiol
Fold Change (mRNA ADGRG7/ GAPDH)
3 hrs
12 hrs
24 hrs
Hours Post 17β Estradiol Treatment
B)
ADGRG7/ β-Actin (Arbitrary Units)
EtOH
17 β Estradiol (10-7M)
ADGRG7(84kDa)
β-Actin(42kDa)
ERα
C)
Fold Change ADGRG7 Promoter Activity
EtOH
17 β Estradiol
pCDNA3
ERα
ERβ
D)
48 hours
24 hours
Fold Change ADGRG7 Promoter Activity
pCDNA3
ERα
17β Estradiol

Fig. 4

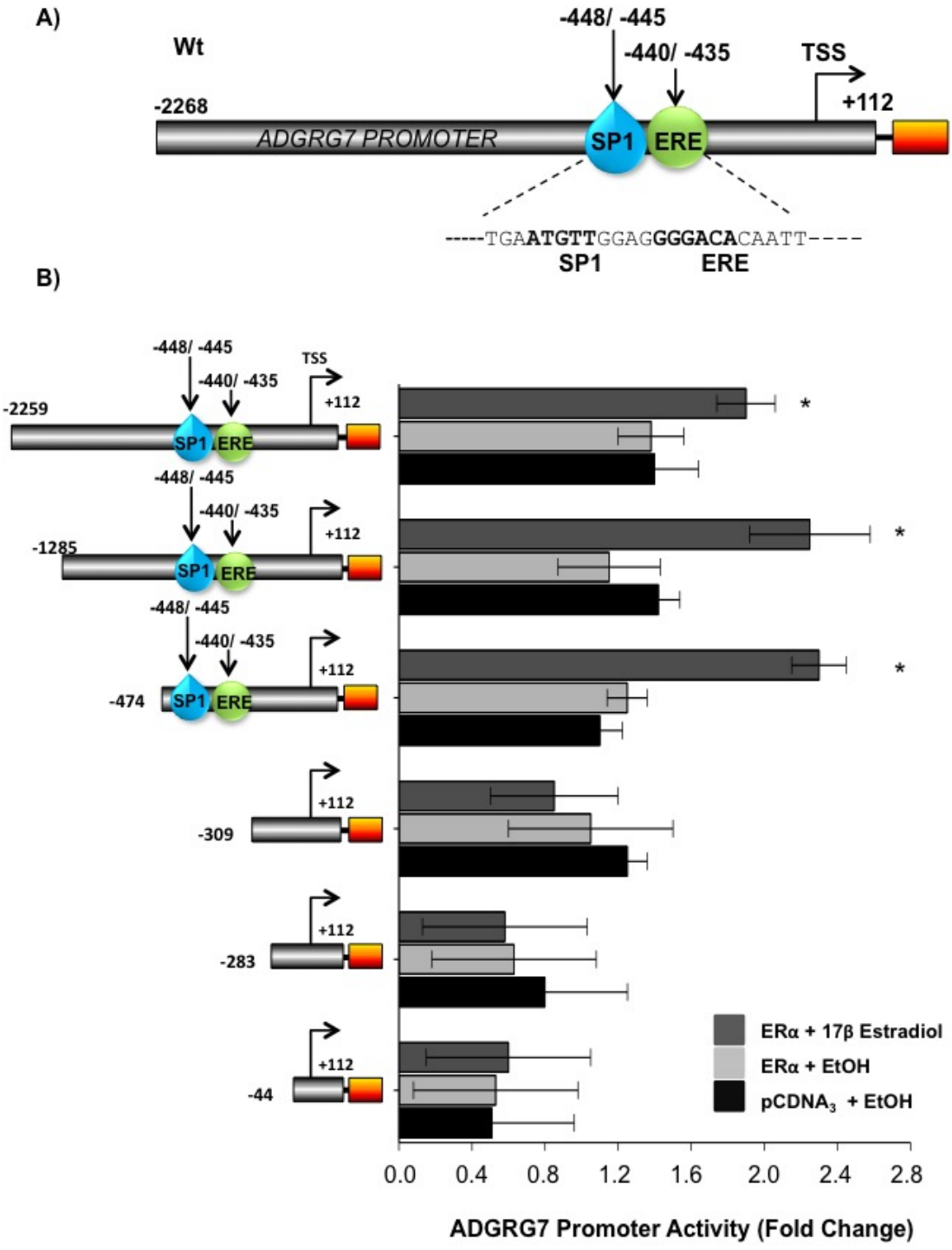
A)
Wt
-448/ -445
-440/ -435
TSS
+112
-2268
ADGRG7 PROMOTER
SP1
ERE
-----TGAATGTTGGAGGGGACACAATT----
SP1
ERE
B)
-448/ -445
-440/ -435
TSS
+112
-2259
-1285
-474
-309
-283
-44
*
ERα + 17β Estradiol
ERα + EtOH
pCDNA3 + EtOH
0.0
0.4
0.8
1.2
1.6
2.0
2.4
2.8
ADGRG7 Promoter Activity (Fold Change)

Fig. 5

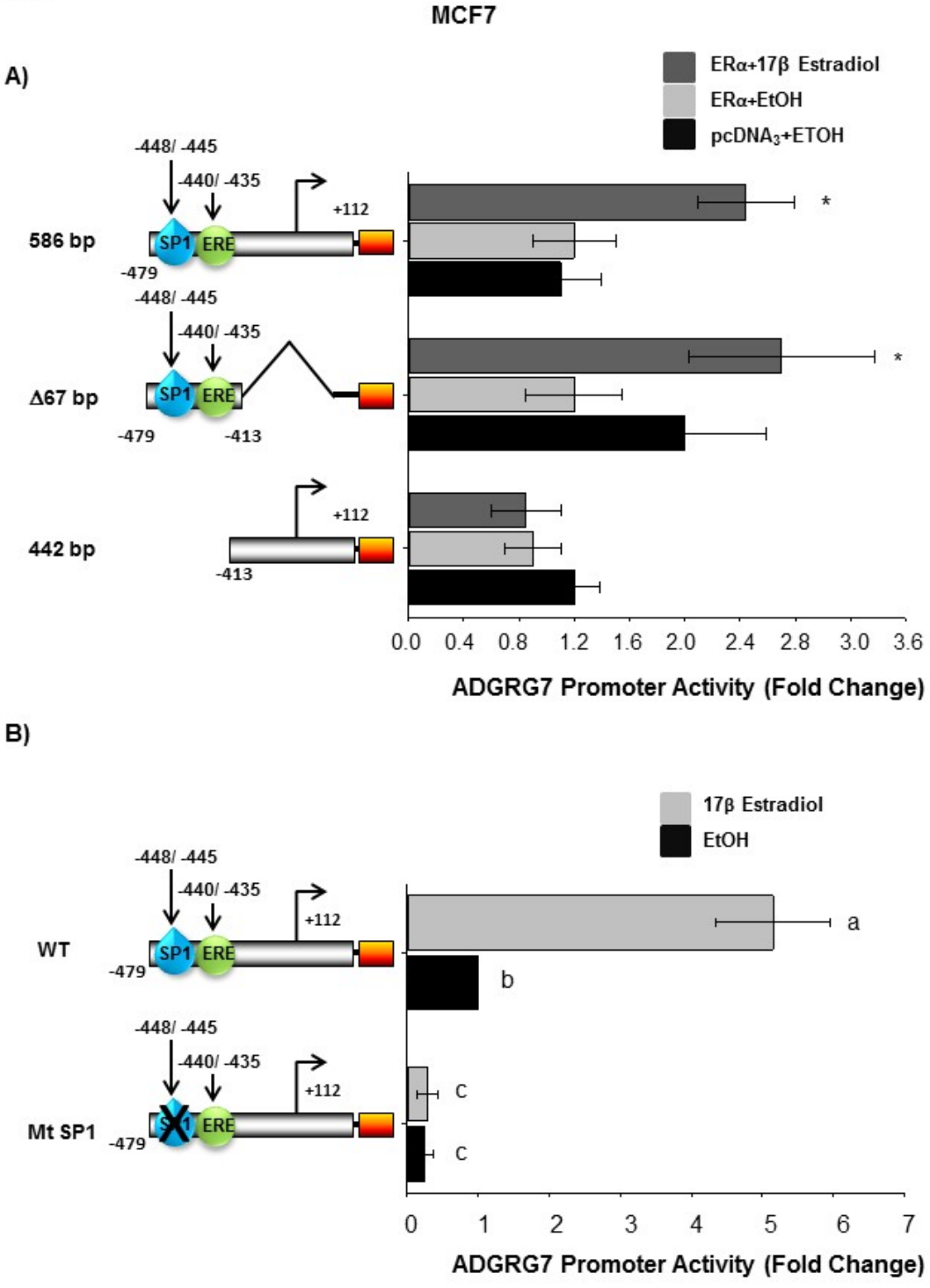
MCF7
A)
ERα+17β Estradiol
ERα+EtOH
pcDNA3+ETOH
-448/ -445
-440/ -435
+112
586 bp
SP1
ERE
-479
Δ67 bp
-413
442 bp
*
0.0 0.4 0.8 1.2 1.6 2.0 2.4 2.8 3.0 3.6
ADGRG7 Promoter Activity (Fold Change)
B)
17β Estradiol
EtOH
WT
Mt SP1
a
b
c
c
0 1 2 3 4 5 6 7
ADGRG7 Promoter Activity (Fold Change)

Fig. 6

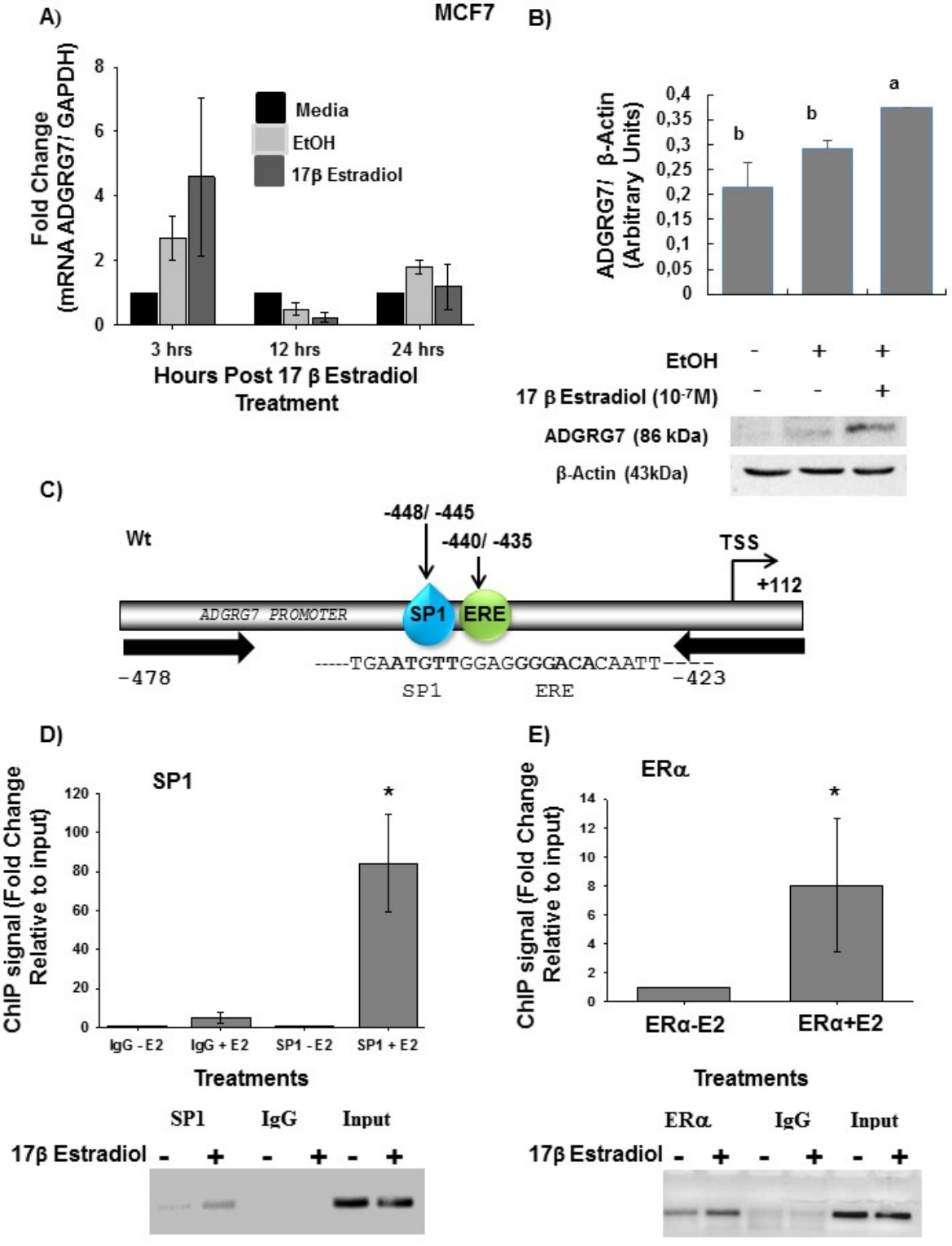
A)
MCF7
Fold Change (mRNA ADGRG7/ GAPDH)
Media
EtOH
17β Estradiol
3 hrs
12 hrs
24 hrs
Hours Post 17 β Estradiol Treatment
B)
ADGRG7/ β-Actin (Arbitrary Units)
a
b
b
EtOH
17 β Estradiol (10-7M)
ADGRG7 (86 kDa)
β-Actin (43kDa)
C)
Wt
-448/ -445
-440/ -435
TSS
+112
ADGRG7 PROMOTER
SP1
ERE
-----TGAATGTTGGAGGGGACACAATT-----
-478
-423
SP1
ERE
D)
SP1
ChIP signal (Fold Change Relative to input)
IgG - E2
IgG + E2
SP1 - E2
SP1 + E2
Treatments
SP1
IgG
Input
17β Estradiol
E)
ERα
ChIP signal (Fold Change Relative to input)
ERα-E2
ERα+E2
Treatments
ERα
IgG
Input
17β Estradiol

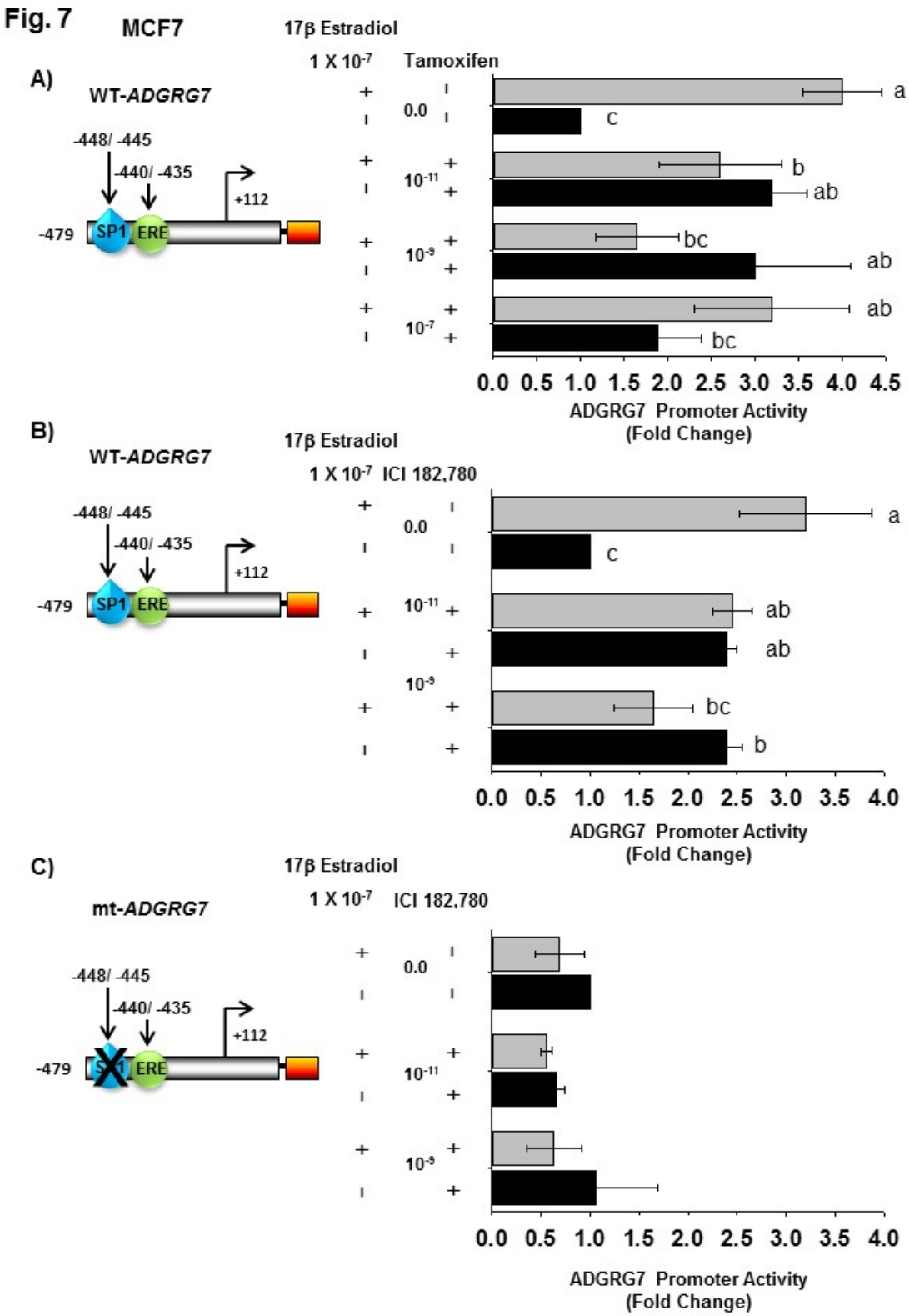
Fig. 7
MCF7
17β Estradiol
1 X 10-7
Tamoxifen
A)
WT-ADGRG7
-448/ -445
-440/ -435
+112
-479
SP1
ERE
0.0
10-11
10-9
10-7
a
c
b
ab
bc
ab
ab
bc
0.0 0.5 1.0 1.5 2.0 2.5 3.0 3.5 4.0 4.5
ADGRG7 Promoter Activity
(Fold Change)
B)
WT-ADGRG7
17β Estradiol
1 X 10-7 ICI 182,780
-448/ -445
-440/ -435
+112
-479
SP1
ERE
0.0
10-11
10-9
a
c
ab
ab
bc
b
0.0 0.5 1.0 1.5 2.0 2.5 3.0 3.5 4.0
ADGRG7 Promoter Activity
(Fold Change)
C)
17β Estradiol
1 X 10-7 ICI 182,780
mt-ADGRG7
-448/ -445
-440/ -435
+112
-479
ERE
0.0
10-11
10-9
0.0 0.5 1.0 1.5 2.0 2.5 3.0 3.5 4.0
ADGRG7 Promoter Activity
(Fold Change)

Fig. 7

MCF7

D)

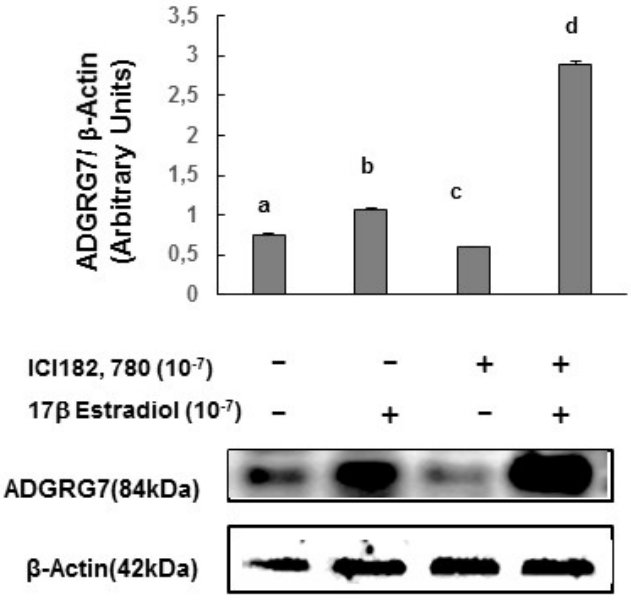
ADGRG7/ β-Actin (Arbitrary Units)
3,5
3
2,5
2
1,5
1
0,5
0
a
b
c
d
ICI182, 780 (10-7)
17β Estradiol (10-7)
ADGRG7(84kDa)
β-Actin(42kDa)

E)

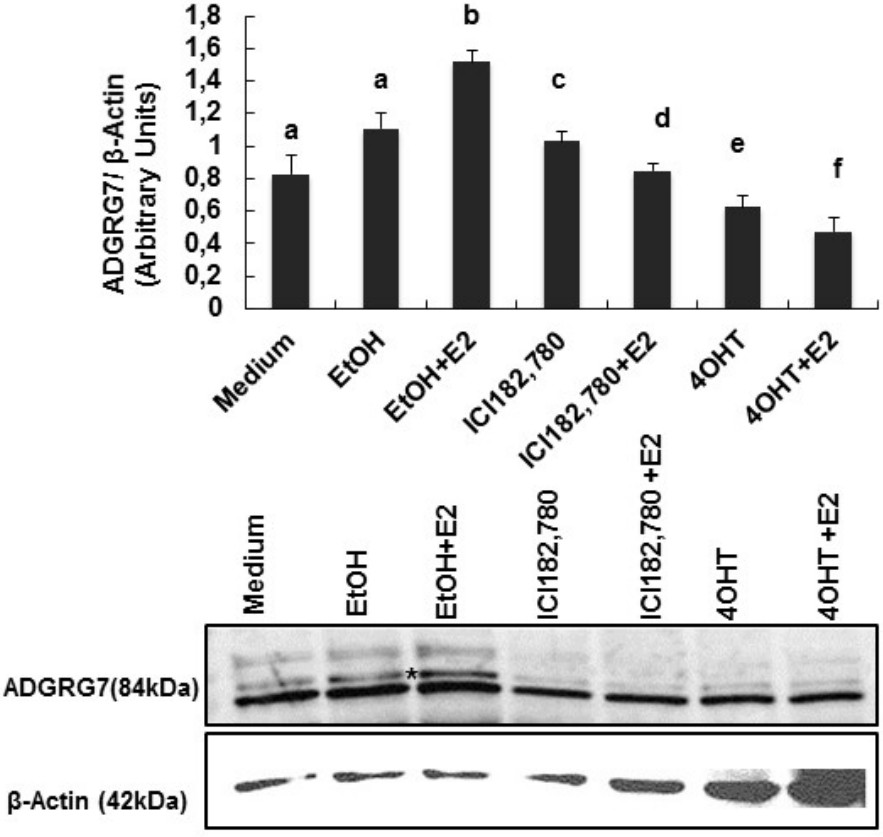
ADGRG7/ β-Actin (Arbitrary Units)
1,8
1,6
1,4
1,2
1
0,8
0,6
0,4
0,2
0
a
a
b
c
d
e
f
Medium
EtOH
EtOH+E2
ICI182,780
ICI182,780+E2
4OHT
4OHT+E2
Medium
EtOH
EtOH+E2
ICI182,780
ICI182,780 +E2
4OHT
4OHT +E2
ADGRG7(84kDa)
β-Actin (42kDa)

Fig. 8

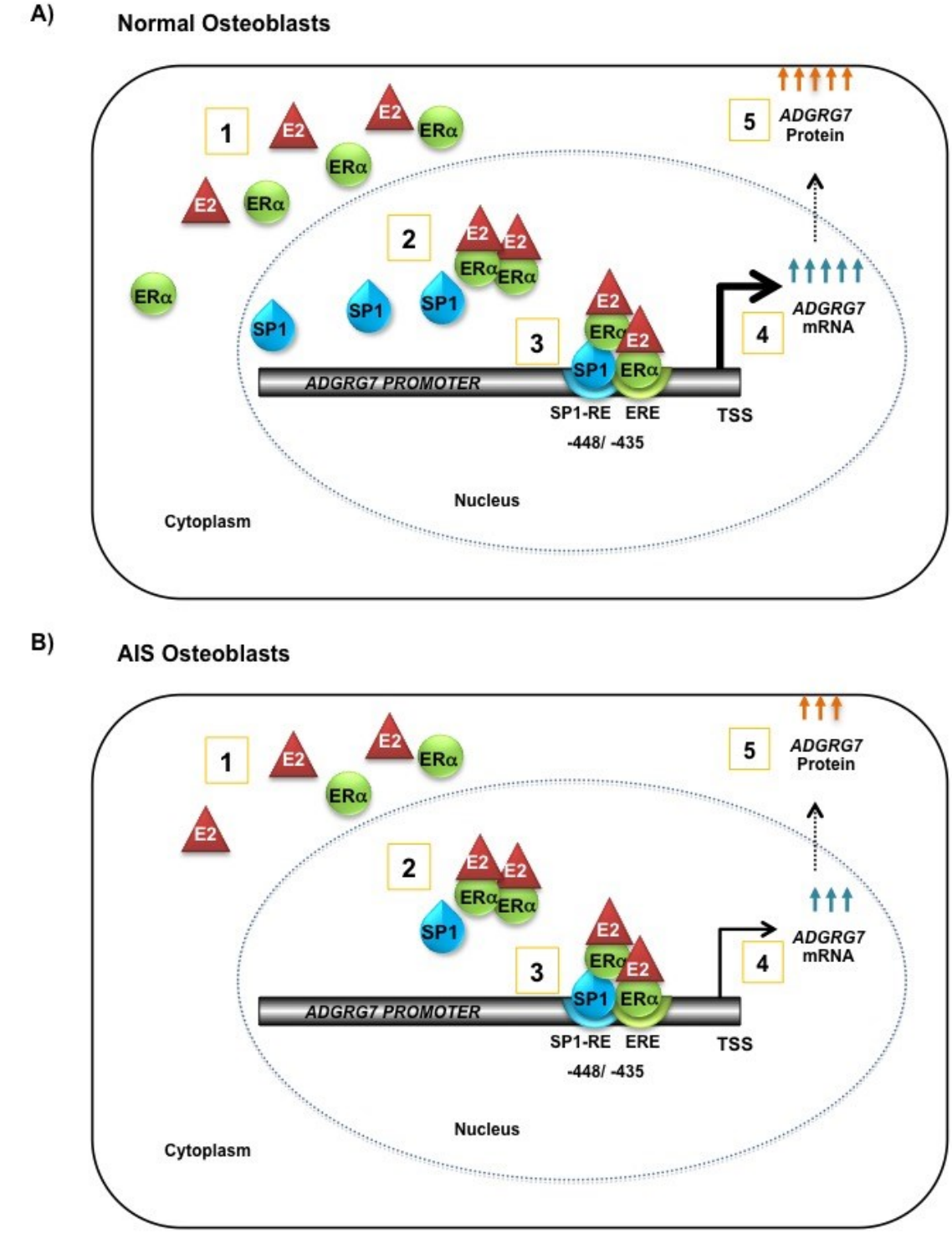
A)
Normal Osteoblasts
1
E2
ERα
2
SP1
3
ADGRG7 PROMOTER
SP1-RE
ERE
-448/ -435
TSS
4
ADGRG7
mRNA
5
ADGRG7
Protein
Nucleus
Cytoplasm
B)
AIS Osteoblasts

List of Tables:

Length (Bp)	Primer Position	Sequence
1397 (1/2)	-1318/-1291	F: 5'-GTATGTGTTTTGGGCACATTTAAGGTA-3'
	+82/ +112	R: 5'-TAGATCGCAGATCTCGAGGCTAATCCAGTAGGATGCAGTTTGAATC-3'
421 (3/2)	-309/ -285	F: 5'-GAAAT**GCTAG**CGCTAAAAACCATGTGTGGTGATT-3'
	+82/ +112	R: 5'-TAGATCGCAGATCTCGAGGCTAATCCAGTAGGATGCAGTTTGAATC-3'
283 (4/2)	-171/ -147	F: 5'-ATACAGCTAGCCGAGCCATAGGTGACTACTGGC-3'
	+82/ +112	R: 5'-TAGATCGCAGATCTCGAGGCTAATCCAGTAGGATGCAGTTTGAATC-3'
156 (5/2)	-44/ -22	F: 5'-CTTGTGGCTAGCCCCTCCCCTTCTTCTTTATTGC-3'
	+82/ +112	R: 5'-TAGATCGCAGATCTCGAGGCTAATCCAGTAGGATGCAGTTTGAATC-3'

S1: List of primers used to clone the A*DGRG7* promoter full length and deletion constructs. The primer direction was represented as Forward (F) and reverse (R). The first column from left indicting the amplicon length generated with the primer pairs in the raw and the second column indicating the beginning and end of the primer sequence with respect to the transcriptional start site.

Application	Position relative to TSS	Sequence
SP1 Mutant	-463 / -421	Forward: 5'-CTCCAACATATGAATGTTCCATGGGACACAATTCAGCCCATAG-3'
	-463 / -421	Reverse: 5'-CTATGGGCTGAATTGTGTCCCATGGAACATTCATATGTTGGAG-3'

S2: The forward and reverse primers that were used to mutate the SP1 response element in the *ADGRG7* promoter construct (-474/+112). The second column from the left indicates the beginning and end of the primer sequence with respect to the transcriptional start site.

Application	Position relative to TSS	Sequence
CHIP	SP1	Forward: 5'- GACCACCCTAACAAACTCG-3
		Reverse: 5'- GATAACCCACCTGCTATGG-3'
	ESRα	Forward: 5'- CCAACTTGGATTCTCCAGCTCC-3'
		Reverse: 5'- CAACAGGTCACCTCAAAACTTAGGG-3'

S3: List of primers used for Chromatin Immunoprecipitation (ChIP) of the SP1 and ESRα response element on the *ADGRG7* promoter. The third column indicates the beginning and end of the primer sequence with respect to the transcriptional start site.

Application	Description	Sequence
QPCR	GAPDH	Forward: 5'AGGAGTAAGACCCCTGGACC3'
		Reverse: 5'GGAGATTCAGTGTGGTGGGG3'
	ADGRG7	Forward: 5'TGAAAGCAGAGTATGCACCTT3'
		Reverse: 5'TCCTCCCCTCAGTGATCTGT3'

S4: Primers used for qPCR

III.3. MANUSCRIPT 3

POC5 is regulated by estradiol through direct genomic signaling by Estrogen Receptor α

Running title: POC5 regulation by estradiol

Hassan Amani[1], Bagu T. Edward [3], Shunmoogum A. Patten[4], Molidperee Sirinart[1], Parent Stefan[1], Barchi Soraya[1] and Moldovan Florina[1,2]*

1. CHU Sainte Justine Research center, 3175 Chemin de la Cote-Sainte-Catherine, Montréal, Quebec H3T1C5, Canada
2. Faculty of Dentistry-Stomatology, University of Montreal, 2900 Edouard Monpetit Boulevard, Montréal, Quebec, H3T1J4, Canada

*corresponding author: Florina Moldovan: CHU Sainte-Justine Research Center, Montréal, Canada; email address: florina.moldovan@umontreal.ca; Phone: 514-345-4931 # 5746; Fax: 514- 345-480

Acknowledgements :

This study is supported by the Yves Cotrel Foundation-Institute de France and the Faculty of Dentistry, Université de Montréal and the Scoliosis Research Society (SRS) grants to FM. We thank the MEDITIS program for the salary Support to A.H. and FRQS to S.A.P. We would like to thank Dr. Manouella Santos laboratory for providing the Huh-7 cells used in the study. The authors declare that they have no conflicts of interest.

Abstract

Adolescent idiopathic scoliosis (AIS) is a complex three-dimensional spinal deformity. During puberty, the incidence of AIS in females is 8.4 times higher than in males. POC5 is a

centriolar protein that was recently identified as a causative gene in AIS. The aim of this study was to determine the mechanism of transcriptional regulation of *POC5* by E2. Using promoter activity, gene and protein expression assays, we found that the expression of POC5 was upregulated by treatment of osteoblasts with E2 through direct genomic signaling. Through promoter studies, we found that the deletion of the estrogen response element (ERE) from the 552 bp fragment of *POC5* promoter resulted in the loss of the response to E2 stimulation. Finally, E2 treatments lead to multicentriole formation that colocalized with centrin. Collectively, these findings suggest that E2 is an etiological factor in scoliosis initiation through deregulation of POC5.

Keywords: Puberty; POC5; 17-β-estradiol, estrogen, E2; osteoblasts, NOB, human OB (c. C1286T; p. A429V) AIS; estrogen resistance; Estrogen receptor.

Introduction:

Scoliosis is a complex three-dimensional deformity of the spine, an unresolved disorder with 1.5 to 3% prevalence in the general population (Altaf, Gibson et al. 2013). The most common form of scoliosis is idiopathic scoliosis (IS), which can be classified according to the age of onset, as infantile, juvenile and adolescent (Altaf, Gibson et al. (2013). Adolescent idiopathic scoliosis (AIS) principally affects children over the age of 10 years during the course of skeletal maturation (Cheng, Castelein et al. (2015). AIS is more prevalent in girls as compared to boys and tends to be associated with more severe clinical deformities (Altaf, Gibson et al. 2013). At present, there isn't any consensus on the aetiology of AIS, although most experts do agree that it is due to a combination of multiple factors that have been grouped as biomechanical, genetic and metabolic factors (Leboeuf, Letellier et al. (2009).

In young females with scoliosis there is a decrease in bone density that coincides with the period when estrogen signaling is activated (Leboeuf, Letellier et al. (2009). Estrogen is the key endocrine contributor to growth, attainment of puberty, and maturation in females (Cheng, Qin et al. 2000, Cheng, Tang et al. 2001, Lam, Hung et al. 2011, Sun, Wu et al. 2013). Interestingly, patients with AIS were reported to harbor Estrogen Receptor isoforms (ESR) polymorphisms. It was suggested that the aberrant estrogen signaling in AIS patients was associated with the presence of these estrogen receptor (ESR) polymorphisms (Eastell (2005), (Zhang, Lu et al. 2009), Takahashi, Matsumoto et al. (2011). The coincidence of these endocrine signaling changes with bone abnormalities led to suggestion that AIS was an endocrine disease with estrogen deregulation as the main etiology (Yang, Li et al. 2014). At present, it is not clear how estrogen is involved in the pathogenesis of AIS; however, it is possible that estrogen may interact with other patho-physiological factors such as; melatonin, growth, biomechanical stress and metabolic stress that are believed to influence the development of scoliosis (Leboeuf, Letellier et al. 2009).

During puberty in girls, there is a rise in estrogen levels that is associated with the reduction in bone turnover markers (Eastell 2005). The latter subsequently causing the closure of the epiphyseal growth plates by decreasing periosteal apposition and endosteal resorption within cortical bone, and bone remodeling within cortical and cancellous bone (Grivas, Vasiliadis et al. 2006). These effects of estrogen on the bone are induced through promoting apoptosis of chondrocytes in the growth plate and osteoclasts within the cortical and cancellous bone. Based on the known effects of estrogen on bone formation, growth, maturation and turnover, it is believed to be an essential factor in the development and progression of scoliosis (Grivas, Vasiliadis et al. 2006) .

In a previous study of a multiplex family, three mutations; c. G1336A, c. G1363C, and c. C1286T were identified in the centriolar protein POC5 in patients with IS. In that study, it was concluded that *POC5* is a causative gene of AIS (Patten, Margaritte-Jeannin et al. 2015). The relationship between POC5 and AIS was later confirmed in a recent case-control study on Chinese patients (Xu, Sheng et al. 2017). POC5 is a centrin binding protein that is required for assembling the centriole and cellular proliferation. It is localized at the mother and daughter centrioles throughout the cell cycle. POC5 is a conserved protein coded for by the *POC5* gene located on chromosome 5q13.3 in humans (Azimzadeh, Hergert et al. 2009, Dantas, Daly et al. 2013).

In this work, we aim to study the regulation of POC5 by E2. We first checked POC5 synthesis at the gene and protein levels, cellular localization and multi centriole formation followed by in-silico analysis on Putative estrogen regulatory elements (ERE) in the *POC5* promoter for the estrogen receptor alpha (ERα). In this report, we show that in AIS human osteoblasts (c. C1286T, p. A429V) there is lower response to treatment with E2 as compared to the normal osteoblasts. We postulated that the aberrant E2 signaling in osteoblasts could be a driving factor for the development and progression of the spinal deformity. Our work helps understand the importance of E2 contribution to the AIS disease.

Materials and Methods:

Cell Culture:

Huh7 cells were cultured as previously published (Bagu and Santos 2011). MCF7, a breast cancer cell line was purchased from American Type Culture Collection (ATCC, Manassas, VA) and cultured as recommended by the vendor (ATCC). Human OB (c. C1286T; p. A429V) AIS and NOB cells were extracted from tissues and were collected with the consent

of patients after the approval by the Institutional Ethics Committee Board of CHU Sainte-Justine, Montreal, Canada. The primary osteoblasts were isolated as previously published (Letellier, Azeddine et al. 2008).

When evaluating the effect of 17β-estradiol, 4-hydroxy-Tamoxifen (4-OHT) and Fulvestrant (ICI-182, 780) on the expression of POC5 in Huh7, MCF7 and osteoblasts, the cells used were cultured in their respective media devoid of the phenol red, containing 10% FBS that was previously stripped with charcoal.

RNA isolation, reverse transcription, PCR, and real-time PCR:

Total RNA from Huh7 (Hepatocytes), MCF7 (breast cancer cells), osteoblasts was isolated using TRizol as recommended by the manufacturer (Invitrogen Canada). The RNA (2 µg) was used as a template to synthesize the first-strand cDNA using iscript reverse transcriptase from Bio-Rad (Mississauga, ON Canada). Quantification of gene expression was performed by 7900HT Fast Real-Time PCR System with iQ™ SYBR® Green Supermix. The oligonucleotides used are listed in table 3. Fold change was calculated using the delta CT method.

Cell Treatments

The 17β-estradiol (E2), and 4-hydroxy-Tamoxifen (4-OHT) were purchased from Sigma-Aldrich, Oakville, ON, Canada. Fulvestrant (ICI-182, 780) was purchased from TOCRIS (USA) and were separately reconstituted with 100% ethanol into solutions of 2×10^{-2} M stock concentration then stored at -20°C until use.

Plasmids Constructs

Two promoter fragments -3653/-1561 and -1481/+48 base pairs from the transcriptional start sites, upstream of the 5'-flanking end of the *POC5* un-translated region, were generated by

PCR using primers listed in table 1 and genomic DNA that was isolated from the Huh7 cell lines. The fragments were then cloned into separate pGL3 basic luciferase reporter plasmid vectors (Promega, Madison, WI), after restriction digestion with Nhe I/ Bgl II and Nhe I/ Xho I, respectively. Deletion constructs of the 1529 bp fragments -555/+48 and -248/+48 were generated using the primers listed in Table 1 using the *POC5* plasmid -1481/+48 as a template. All plasmids were verified by digestion with restriction enzymes and sequencing (McGill University and Génome Québec Innovation Centre). Expression vectors that were used to code for the full length wild type human ER-alpha (pEGFP-hERα) was acquired from Add gene (#28230).

In-silico analysis

Putative regulatory elements (RE) in the *POC5* promoter for the estrogen receptor alpha (*ESR1*) were determined by the multiple bio-informatics tools [http://biogrid-lasagna.engr.uconn.edu/lasagna_search/]. In the -3653/-1561 fragment of *POC5* promoter covering 3 Estrogen response elements (EREs) sites 1 (-3638 /-3541), 2 (-3407/-3400) 3 (-1845/ -1838) and the -1481/+48 fragment has 3 EREs sites 1(-1012/-1005), 2 (-845/-837), 3 (-755/-747).

Protein Lysate Preparation and Western Blotting

Whole cell protein lysates were prepared from cell lines using RIPA buffer from Pierce thermoscienitfic (ca 89900) (25 mM Tris•HCl pH 7.6, 150 mM NaCl, 1% NP-40, 1% sodium deoxycholate, 0.1% SDS, pierce) supplemented with protease and phosphatase inhibitors (Roche Diagnostics, Mannheim, Germany). To perform western blot, equal amounts of protein were resolved using SDS/polyacrylamide gel electrophoresis. Afterwards, proteins were transferred onto a nitrocellulose membrane and blocked in phosphate buffered saline

containing 0,05 % Tween-20 and 20% skim milk powder. Membranes were incubated with primary antibody (POC5, abcam, # ab1888330) and (β-actin, Santa Cruz, # sc-47778) overnight at 4ºC and then washed with phosphate-buffered saline Tween-20. Afterwards, membranes were incubated with secondary antibody conjugated with horseradish peroxidase (Anti rabbit, thermofisher # 31462) for 1 hour (h) at room temperature (RT). After incubation, proteins were visualized by enhanced chemo-luminescence.

Transient Transfection Assays

Transfections of Huh7 hepatoma cells were performed in 24 well plates using the Lipofectamine^{TM} 2000 (Invitrogen, Burlington, ON, Canada) as was recommended by the manufacturer. When cell attained 80% confluence, they were co-transfected with 990 ng/ well of the different *poc5* promoter constructs (-1481, -552, -248) along with 10 ng of phRL-TK (Renilla Luciferase). The total DNA per well was kept at 750 ng/ well in the 24 well plates by co-transfecting with the empty expression vector pCDNA3. When evaluating the effect of ER-α on *hPOC5* in the presence or absence of 17β-estradiol, ERα negative Huh7 cells were co-transfected with different *poc5* promoter constructs along with either the expression vector encoding the full length human ERα - protein (250 ng/ well) or the empty pCDNA-3 vector (Invitrogen, Burlington, ON, Canada). Five hours following transfection, the media in which cells were cultured was replaced with serum free media. After 12 h, cells were then cultured in fresh serum free media with or without one of the following treatments, E2, 4-OHT or ICI-182, 780 over 24 h. In order to evaluate the basal luciferase activities for each construct, controls for each full-length promoter construct were co-transfected with an empty pCDNA-3 vector (Invitrogen, Burlington, ON, Canada) and then cultured in the vehicle. In all

experiments, data reported represents the average of at least three experiments, done in triplicate, using at least three different DNA preparations.

Immunofluorescence

NOB and Human OB (c. C1286T; p. A429V) AIS osteoblasts were cultured in vitro to attach to the Labtek (NUNC, Thermoscientific) overnight. On the second day, cells were fixed in 70% ethanol / 0.1% triton on ice for 30 min. Cells were then washed with PBS and permeabilized with 0.1% Triton in PBS for 15 minutes (min). Cells were washed once with 0.5% BSA in PBS / Triton (PBT) and then blocked with 2% BSA in PBT for 45 min. Cells were washed after that and incubated with the anti-POC5 (Abcam, # ab1888330) and anti-centrin antibodies (LifeSpan Biosciences, # LS C482434) at (1/200) ON at 4 °C with gentle shaking. Cells were then incubated with Alexa Flour 555 (Life technologies USA, # A21422) and Alexa Flour 488 (Life technologies USA, # A11008) for one h. Cells were mounted and stained for nucleus at the same time using Prolong Gold antifade reagent with DAPI (Life technologies). Immunostaining was observed at Magnification X40.

Chromatin Immunoprecipitation (ChIP)

ChIP was performed as described (Edjekouane, Benhadjeba et al. 2016). Briefly, MCF7-ERα cells were cultured in phenol red-free medium and 10 % charcoal stripped FBS then treated with 10^{-7} M E2 or vehicle for 1 h. After fixation with 2% formaldehyde, cells were lysed and the precleared chromatin supernatants were immunoprecipitated with the respective antibodies specific anti-ERα (Santa-Cruz, # Sc-542) or nonspecific IgG at 4°C. Bound DNA was purified with phenol/chloroform and used as a template for subsequent amplification using primers (Table 2) that encompass respective specific binding elements within the proximal *POC5* promoter region. Fold enrichment values were calculated using the Ct value of each ChIP

sample compared to the Ct value of Input DNA. PCR products were resolved on a 2% agarose gel.

Statistical analysis

Statistical significance of the results was determined by Student's t-test for experiment. For luciferase and qPCR experiments, it was performed in triplicates three times (n=3). $P<0.05$ was accepted as statistically significant. Pearson's correlations were done to evaluate the consistence of the data and the relationship across gene expression profiles. For variables with the same letter, the difference is not statistically significant. Likewise, for variables with a different letter, the difference is statistically significant (Assaad, Hou et al. 2015).

Results

Centriolar protein POC5 is upregulated by E2:

First, we checked the expression levels of POC5 (gene and protein) in normal and in human OB (c. C1268T; p. A429V) AIS osteoblasts. At the gene level, POC5 was highly expressed in normal osteoblasts (NOB) and this expression was significantly downregulated in human OB (c. C1286T; p. A429V) AIS cells ($p<0.01$) (Fig. 1A). Fold change with respect to NOB cells was calculated using the delta cT method ($2^{-\Delta CT}$). Also, at the protein level, quantification of the difference in expression between both cells was highly significant ($p<0.001$) (Fig. 2B). The expression of POC5 in NOB cells is much higher than (c. C1286T; p. A429V) AIS cells. To determine if there is any effect of E2 treatment on subcellular localization of POC5 and if there is differential effects on NOB and human OB (c. C1286T; p. A429V) AIS osteoblasts, we performed immunofluorescence on NOB and human OB (c. C1286T; p. A429V) AIS cells after treatment with E2. There was up-regulation of centriolar protein POC5 as detected by

POC5 staining and multicentriole formation in both cells confirmed by centrin2 staining (Fig. 1C).

Estrogen treatment upregulates POC5 expression in a dose dependent manner in NOB but not AIS cells:

We examined the regulation of mRNA expression levels of *POC5* in response to E2 at 3 different time points in NOB and human OB (c. C1286T; p. A429V) AIS cells. NOB and human OB (c. C1286T; p. A429V) AIS cells had maximal response to E2 after 3h time treatment, and the response decreases at 12 and 24 h in both cells, which suggests an early response to E2 (Fig. 2A left and 2B left panels). *POC5* gene expression analysis shows that there is very strong induction of *POC5* by E2 in NOB after 3h treatment (1200 fold) (Fig. 2A left panel). However, there is lower induction in AIS cells at the same time point (250 fold) (Fig. 2B left panel). POC5 protein levels in response to different doses of E2 were tested in NOB and in human OB (c. C1286T; p. A429V) AIS cells. E2 upregulates POC5 expression in NOB starting at 10-7 M E2 and reaches a significant maximal response at 10-13 M (Fig. 2A right panel). In human OB (c. C1286T; p. A429V) AIS cells, the difference between control and E2 treated samples was statistically non significant (Fig. 2B right panel).

E2 upregulates POC5 gene and protein expressions in MCF7 and Huh-7 cells:

At the gene levels, *POC5* expression was induced by E2 treatments (12 folds versus control) after 3h in MCF7 cells (Fig. 3A left panel). The expression levels of *POC5* were downregulated afterwards at 12 and 24h. In Huh-7 cells, *POC5* expression levels were slightly induced at 3h, and it increases to 1.5 fold at 12h (Fig. 3B left panel), to be down regulated at 24h. We also tested the protein expression of POC5 in MCF7 (Fig. 3A right) and huh-7 cells (Fig. 3B right). POC5 protein levels were significantly upregulated in both tested cell lines.

Promoter region in the 552 bp fragment of *POC5* promoter is significant for activation by E2 through ER α

In silico analysis of the *POC5* promoter shows that the -1481 promoter fragment has 3 EREs, -455/ -432, -410/ -389, -291/ -272 (Fig. 4A). In order to determine the estrogen response element in the *POC5* promoter that is responsible for the regulation of *POC5* by E2, we generated deletion constructs of the downstream fragment of the *POC5* promoter (-1561-3653) and tested in luciferase assay. The POC5 promoter was activated to 1.8 fold with the full length -1561 to -3653 and to 2.3 folds with the -1481 to +48 fragment. The response was also upregulated (2.5 fold) with the -552/+48 fragment. This response was lost using the -248/+48 fragment of the promoter that is missing the EREs -455/ -432 and -410/-398. This suggests that EREs in the -552/+48 fragment is important for the induction of estrogen response of *POC5* (Fig. 4B).

Physical Interaction of ERα with POC5 promoter

We next determined the interactions of ERα proteins with the *POC5* gene promoter in MCF7 cells treated with 10^{-7} M E2 for 1 h using a chromatin immunoprecipitation (ChIP) assay in which cells were treated with formaldehyde to form DNA-protein cross-links. After sonication, and immunoprecipitation by ERα antibody, qPCR was used to determine binding to EREs -455/-432 and -410/-389 designated as A and B. The recruitment of ERα proteins with the proximal region of the *POC5* promoter (−478 to -423) was investigated and the results indicated that ERα immunoprecipitates this region of *POC5* promoter as determined by qPCR (Fig. 5 B). The highest recruitment of ERα (110 fold) was obtained with the ERE -455/-432 (designated by A) and at lower levels (2 fold and 4 fold) with the -410/-389 alone or both

sites respectively. The qPCR products were migrated on gel to confirm the correct product size.

ERα antagonists attenuate E2 induced regulation of POC5

To determine if the regulation of POC5 by E2 is through direct genomic signalling through the Estrogen receptor (ERα), we treated MCF-7 cells with the ER antagonists Fulvestrant (ICI-182, 780) and 4-hydroxy tamoxifen (OHT) for 24 h. At the protein level, there was no significant difference between E2 and antagonist treated cells (Fig. 6A). At the mRNA levels, *POC5* was downregulated after exposure to ICI-182, 780 (Fig. 6B).

E2 upregulates bone markers and ERs in NOB but not in human OB (c. C1286T; p. A429V) AIS cells

Given the role that E2 plays in the growth and maturation of bone, we next sought to see if there are differential effects of E2 on bone markers in NOB and human OB (c. C1286T; p. A429V) AIS cells. ALP and RUNX2 were significantly upregulated in NOB ($p<0.05$) and no significant change was observed for osteopontin and osteocalcin. In human OB (c. C1286T; p. A429V) AIS cells, there was no significant change in response to E2 (Fig. 7A). We also checked the regulation of ERα and ERβ by E2. The ERα was highly upregulated in NOB and human OB (c. C1286T; p. A429V) AIS cells ($p<0.05$). ERβ was downregulated by E2 in NOB cells ($p<0.01$) and no change in human OB (c. C1286T; p. A429V) AIS cells (Fig. 7B).

Discussion:

The principal finding of our study is that the centriolar protein POC5 was up regulated by E2 and estrogen induced up regulation of POC5 was dependent on the presence of estrogen receptor, which suggests that the regulation of *POC5* is through direct genomic signaling where the estrogen receptor directly binds to the estrogen response element that was found to

be located within the -552/+48 fragment of *POC5* promoter. In this work, we have used different cell lines MCF7, Huh-7 and osteoblasts to study regulation of POC5 by E2. In different cells, we might have variable mode of regulation by E2 at the gene and protein levels, that's why we expanded our study by using more than one cell type to confirm the upregulation of POC5 by E2. In all tested cells, the POC5 was upregulated after 3hr of E2 treatments and this was dependent on the presence of ERα. Also, we used Huh-7 cells that have low expression levels of ERα which requires cotransfection of ERα, and cells that are highly expressing ERα like MCF7 cells and osteoblasts. This allowed us to determine the expression patterns modulated by E2 in these cells and perform comparisons.

At the gene level, E2 highly induced *POC5* expression in NOB cells at significantly higher levels than human OB (c. C1286T; p. A429V) AIS cells. At the protein level, there was a dose response to E2 in NOB cells and no significant change in human OB (c. C1286T; p. A429V) AIS cells. Also bone formation markers was induced by E2 in NOB cells while human OB (c. C1286T; p. A429V) AIS cells were non responsive. Interestingly, ethanol induced POC5 expression in human OB (c. C1286T; p. A429V) AIS cells and E2 attenuated the effects of ethanol. Ethanol was found to control the cell fate of osteoblasts by altering ER signaling and ER-p21 interaction and hence induced bone loss. In this study, ethanol upregulated ERs expression in bone in vivo and in osteoblasts in vitro and this effect was revered by ER agonist (Chen, Lazarenko et al. 2009).

The estrogen insensitivity (or estrogen resistance) in AIS cells appears to be an interesting and clinically relevant observation, since delayed puberty and lower levels of estradiol were previously reported in girls with AIS. In progressive scoliosis, the clinical features include the absence of pubertal growth spurt. This is also associated with significant osteopenia (or

reduced mineral density), and clearly delayed bone maturation that have been identified as a risk factor for curve progression. POC5 genetically contribute to the scoliosis predisposition and is an etiological factor in scoliosis initiation, while the suggested resistance mechanism to E2 treatment would rather be a factor that contribute to the curve aggravation. Most probably, the mutation in *POC5* would be affecting the response to E2. To our knowledge, our work is the first to report the effect of E2 on *POC5* synthesis and regulation. There is little work on the role of POC5. In humans, POC5 localizes to the distal portion of centrioles and its recruitment to procentrioles is essential for the full centriolar maturation and normal cell-cycle processing. This centrosomal protein interacts with centrin and inversin (Azimzadeh, Hergert et al. 2009), both involved in cell division, polarity, and motility. More recently, POC5 variants were reported in Chinese scoliotic population; although this recent case-control study reported a common variant (rs6892146) of *POC5* to be associated with the susceptibility of AIS (Xu, Sheng et al. 2017), this study also shows significantly higher mRNA expression of *POC5* in the muscles of patients with scoliosis, compared to the controls.

There are several studies on the role of genetic factors in AIS, where mutations in several genes have been associated with the development, and progression of AIS (Zhu, Tang et al. 2015), however, little data is available on the role of estrogens in AIS. Our study come out with altered regulation of POC5 in normal and AIS cells and introduces POC5 as a gene regulated by E2 (beyond this disorder). Interestingly, ChIP experiments revealed that the A site had the highest enrichment levels (120 fold). The presence of the B site reduces the recruitment of ERα (4 fold). The B site has 3 CpG sites. It's possible that the B site is methylated and as a consequence this impedes the binding of ERα. This need to be addressed in future studies.

Another interesting finding was observed in this study; we found that treatment with E2 induces the amplification of POC5 expression and probably multi centriole formation. Several mechanisms has been described that lead to centrosome amplification including cytokinesis failure, mitotic slippage, cell–cell fusion, over duplication of centrioles and de novo centriole assembly. Centrosome amplification may result from centriole over duplication, for example through the overexpression of centriolar proteins which is most probably the mechanism that explains why the overexpression of POC5. This goes along with the work on Plk4 which associates with centrioles, either in basal bodies or centrosomes. Over-expression of Plk4 during development led to increased numbers of centrosomes in the basal epidermis. These findings complement our results on POC5. The centriole numbers are under tight cell-cycle control in most proliferating cells, however, exceptions exist. For example, the cells that line the epithelia of the respiratory and reproductive tracts form hundreds of centrioles in order to provide the basal bodies for the formation of beating cilia (Coelho, Bury et al. 2015). Hence, the observation of centrosome amplification might confer some unknown advantage to the cells. Future work should focus on the impact of centriole amplification on cell cycle in normal and AIS cells.

References

Altaf, F., A. Gibson, Z. Dannawi and H. Noordeen (2013). "Adolescent idiopathic scoliosis." BMJ **346**: f2508.

Assaad, H. I., Y. Hou, L. Zhou, R. J. Carroll and G. Wu (2015). "Rapid publication-ready MS-Word tables for two-way ANOVA." Springerplus **4**: 33.

Azimzadeh, J., P. Hergert, A. Delouvee, U. Euteneuer, E. Formstecher, A. Khodjakov and M. Bornens (2009). "hPOC5 is a centrin-binding protein required for assembly of full-length centrioles." J Cell Biol **185**(1): 101-114.

Bagu, E. T. and M. M. Santos (2011). "Friend of GATA suppresses the GATA-induced transcription of hepcidin in hepatocytes through a GATA-regulatory element in the HAMP promoter." J Mol Endocrinol **47**(3): 299-313.

Chen, J. R., O. P. Lazarenko, R. L. Haley, M. L. Blackburn, T. M. Badger and M. J. Ronis (2009). "Ethanol impairs estrogen receptor signaling resulting in accelerated activation of senescence pathways, whereas estradiol attenuates the effects of ethanol in osteoblasts." J Bone Miner Res **24**(2): 221-230.

Cheng, J. C., R. M. Castelein, W. C. Chu, A. J. Danielsson, M. B. Dobbs, T. B. Grivas, C. A. Gurnett, K. D. Luk, A. Moreau, P. O. Newton, I. A. Stokes, S. L. Weinstein and R. G. Burwell (2015). "Adolescent idiopathic scoliosis." Nat Rev Dis Primers **1**: 15030.

Cheng, J. C., L. Qin, C. S. Cheung, A. H. Sher, K. M. Lee, S. W. Ng and X. Guo (2000). "Generalized low areal and volumetric bone mineral density in adolescent idiopathic scoliosis." J Bone Miner Res **15**(8): 1587-1595.

Cheng, J. C., S. P. Tang, X. Guo, C. W. Chan and L. Qin (2001). "Osteopenia in adolescent idiopathic scoliosis: a histomorphometric study." Spine (Phila Pa 1976) **26**(3): E19-23.

Coelho, P. A., L. Bury, M. N. Shahbazi, K. Liakath-Ali, P. H. Tate, S. Wormald, C. J. Hindley, M. Huch, J. Archer, W. C. Skarnes, M. Zernicka-Goetz and D. M. Glover (2015). "Over-expression of Plk4 induces centrosome amplification, loss of primary cilia and associated tissue hyperplasia in the mouse." Open Biol **5**(12): 150209.

Dantas, T. J., O. M. Daly, P. C. Conroy, M. Tomas, Y. Wang, P. Lalor, P. Dockery, E. Ferrando-May and C. G. Morrison (2013). "Calcium-binding capacity of centrin2 is required for linear POC5 assembly but not for nucleotide excision repair." PLoS One **8**(7): e68487.

Eastell, R. (2005). "Role of oestrogen in the regulation of bone turnover at the menarche." J Endocrinol **185**(2): 223-234.

Edjekouane, L., S. Benhadjeba, M. Jangal, H. Fleury, N. Gevry, E. Carmona and A. Tremblay (2016). "Proximal and distal regulation of the HYAL1 gene cluster by the estrogen receptor alpha in breast cancer cells." Oncotarget **7**(47): 77276-77290.

Grivas, T. B., E. Vasiliadis, V. Mouzakis, C. Mihas and G. Koufopoulos (2006). "Association between adolescent idiopathic scoliosis prevalence and age at menarche in different geographic latitudes." Scoliosis **1**: 9.

Lam, T. P., V. W. Hung, H. Y. Yeung, Y. K. Tse, W. C. Chu, B. K. Ng, K. M. Lee, L. Qin and J. C. Cheng (2011). "Abnormal bone quality in adolescent idiopathic scoliosis: a case-control study on 635 subjects and 269 normal controls with bone densitometry and quantitative ultrasound." Spine (Phila Pa 1976) **36**(15): 1211-1217.

Leboeuf, D., K. Letellier, N. Alos, P. Edery and F. Moldovan (2009). "Do estrogens impact adolescent idiopathic scoliosis?" Trends Endocrinol Metab **20**(4): 147-152.

Letellier, K., B. Azeddine, S. Parent, H. Labelle, P. H. Rompre, A. Moreau and F. Moldovan (2008). "Estrogen cross-talk with the melatonin signaling pathway in human osteoblasts derived from adolescent idiopathic scoliosis patients." J Pineal Res **45**(4): 383-393.

Patten, S. A., P. Margaritte-Jeannin, J. C. Bernard, E. Alix, A. Labalme, A. Besson, S. L. Girard, K. Fendri, N. Fraisse, B. Biot, C. Poizat, A. Campan-Fournier, K. Abelin-Genevois, V. Cunin, C. Zaouter, M. Liao, R. Lamy, G. Lesca, R. Menassa, C. Marcaillou, M. Letexier, D. Sanlaville, J. Berard, G. A. Rouleau, F. Clerget-Darpoux, P. Drapeau, F. Moldovan and P. Edery (2015). "Functional variants of POC5 identified in patients with idiopathic scoliosis." J Clin Invest **125**(3): 1124-1128.

Sun, X., T. Wu, Z. Liu, Z. Zhu, B. Qian, F. Zhu, W. Ma, Y. Yu, B. Wang and Y. Qiu (2013). "Osteopenia predicts curve progression of adolescent idiopathic scoliosis in girls treated with brace treatment." J Pediatr Orthop **33**(4): 366-371.

Takahashi, Y., M. Matsumoto, T. Karasugi, K. Watanabe, K. Chiba, N. Kawakami, T. Tsuji, K. Uno, T. Suzuki, M. Ito, H. Sudo, S. Minami, T. Kotani, K. Kono, H. Yanagida, H. Taneichi, A. Takahashi, Y. Toyama and S. Ikegawa (2011). "Replication study of the association between adolescent idiopathic scoliosis and two estrogen receptor genes." J Orthop Res **29**(6): 834-837.

Xu, L., F. Sheng, C. Xia, Y. Li, Z. Feng, Y. Qiu and Z. Zhu (2017). "Common variant of POC5 is associated with the susceptibility of adolescent idiopathic scoliosis." Spine (Phila Pa 1976).

Yang, M., C. Li and M. Li (2014). "The estrogen receptor alpha gene (XbaI, PvuII) polymorphisms and susceptibility to idiopathic scoliosis: a meta-analysis." J Orthop Sci **19**(5): 713-721.

Zhang, H. Q., S. J. Lu, M. X. Tang, L. Q. Chen, S. H. Liu, C. F. Guo, X. Y. Wang, J. Chen and L. Xie (2009). "Association of estrogen receptor beta gene polymorphisms with susceptibility to adolescent idiopathic scoliosis." Spine (Phila Pa 1976) **34**(8): 760-764.

Zhu, Z., N. L. Tang, L. Xu, X. Qin, S. Mao, Y. Song, L. Liu, F. Li, P. Liu, L. Yi, J. Chang, L. Jiang, B. K. Ng, B. Shi, W. Zhang, J. Qiao, X. Sun, X. Qiu, Z. Wang, F. Wang, D. Xie, L. Chen, Z. Chen, M. Jin, X. Han, Z. Hu, Z. Zhang, Z. Liu, F. Zhu, B. P. Qian, Y. Yu, B. Wang, K. M. Lee, W. Y. Lee, T. P. Lam, Y. Qiu and J. C. Cheng (2015). "Genome-wide association study identifies new susceptibility loci for adolescent idiopathic scoliosis in Chinese girls." Nat Commun **6**: 8355.

List of figures:

Figure 1: Effects of E2 on POC5 subcellular localization in normal control and human (OB c. C1286T; p. A429V) AIS cells

A) qPCR of the expression of *POC5* in NOB and human (OB c. C1286T; p. A429V) AIS cells. The level of expression of *POC5* is higher in NOB cells than in human (OB c. C1286T; p. A429V) AIS cells. *GAPDH* was used as endogenous control. Fold change with respect to NOB cells was calculated using the delta cT method (2-ΔCT). For qPCR, error bars represent ± S.D in triplicates ($p<0.01$). B) Western blot quantification shows that the expression difference of endogenous protein levels of POC5 in normal and human OB (c. C1286T; p. A429V) AIS cells in the absence of E2 was significant ($p<0.001$). β-actin was used as loading control.. Band intensity was measured using Image J and the ratio of POC5 to β-actin was calculated. The results are mean ± SD from two independent experiments (n=2). C) Immunofluorescence to study the localization of POC5 in response to E2 using anti-POC5 and anti-centrin antibodies. POC5 cellular localization in both normal and human (OB c. C1286T; p. A429V) AIS cells in the absence and presence of 10^{-7} M E2. Centrin (green) POC5 (red) and DAPI (blue). Scale bar 20μm.

Figure 2: Dose dependent regulation of POC5 by E2 in normal and human OB (c. C1286T; p. A429V) AIS osteoblasts

A) qPCR and WB for normal osteoblasts treated with E2. qPCR on NOB treated with E2 at different time points (3h, 12h, 24h) using specific primers for *POC5* and *GAPDH* (used as endogenous control). Maximal response to E2 obtained at 3h (left). WB was performed on NOB treated with different doses of E2 ranging from (10^{-7} M, 10^{-14} M). E2 upregulated POC5 expression in a dose dependent manner. Maximal response is obtained at 10^{-12} M (right).,**B)** qPCR on human OB (c. C1286T; p. A429V) AIS cells treated with E2 as described above.

The response to E2 reached maximum levels after 3h of induction (left). WB expression of POC5 at different doses of E2 (10^{-7} M, 10^{-14} M) in human OB (c. C1286T; p. A429V) AIS cells. No significant change was observed after treatment with different doses of E2. Bands corresponding to the correct molecular weight are indicated for both POC5 (63kDa) and β actin (42kDa). For qPCR, error bars represent ± S.D in triplicates. For quantification of band intensity, Image j was used and ratio of POC5 to β-actin was calculated (n=2). The results are mean ± SD from two independent experiments.

Figure 3: Regulation of POC5 by E2 in MCF7 and Huh-7 cells

A) qPCR on RNA extracted from MCF7 exposed to 10^{-7} M E2 for different time points (3h, 12h, 24h) using specific primers for *POC5* and *GAPDH*. Data is represented as fold change with respect to vehicle treated. Maximal response was obtained at 3h post treatment with E2. The levels go back to basal levels at 12 and 24h (left). POC5 protein expression in MCF7 exposed and non exposed to E2. 10^{-7} M E2 upregulates POC5 expression (right). B) qPCR was performed in Huh-7 cells treated with 10^{-7} M E2 for different time points (3h, 12h, 24h) as described above. At 3h, slight increase in POC5 expression. At 12 h, there was higher induction that is decreased at 24h (left). Protein expression of POC5 in response to 10^{-7} M E2, there was increase in the protein levels of POC5 (right). For qPCR, error bars represent ± S.D in triplicates. For quantification of band intensity, Image j was used and ratio of POC5 to β-actin was calculated (n=2). The results are mean ± SD from two independent experiments.

Figure 4: Regulation of POC5 by E2 at the promoter level through ER

A) Schematic representation of the promoter fragment with the corresponding EREs. The -1481/+48 fragment has three EREs. B) Luciferase assay was performed using different deletion promoter fragments that were transfected in Huh-7 cells. The estrogen receptor was

transfected along the promoter coding vector and Renilla luciferase vector for normalizing. There is up regulation of *POC5* promoter by E2 with the -1481/+48 and -552/+48 . With the -284/+48 fragment, response to E2 is lost. The data are expressed as the mean ± SD of three experiments in triplicates (n=3).

Figure 5: Estrogen receptor binds to the POC5 promoter.

A) Schematic presentation showing the two EREs (A and B) present in the 552bp fragment of *POC5* promoter. **B)** Chromatin was isolated from MCF-7 cells non treated or treated with 10^{-7} M E2 for one h prior to ChIP and immunoprecipitations were performed with antibody specific to ESR1 and a non specific IgG. qPCR reactions were carried out with the various ChIP samples (ER-E2, ER+E2, IgG-E2, IgG+E2, Input-E2, Input+E2). Primers that amplify either the region with ERE1, ERE2 separately (designated by A and B) or both sites (AB) were used. The fold change in the values for E2- and E2+ were calculated and graphed. Error bars represent ± S.D in triplicates.

Figure 6: ERα antagonists reverse the up-regulatory effects of E2 on *POC5* expression.

A) MCF7 cells were treated with either ETOH (0.1%), 10^{-7} M E2, or the estrogen receptor antagonists 10^{-7} M ICI-182, 780, 10^{-7} M 4-OHT and then western blot using POC5 antibody. β-actin was used as loading control. ICI-182, 780 and 4-OHT treatments inhibit the E2 induced upregulation of POC5. B) ICI182, 780 treatment strongly downregulated the mRNA levels of *POC5* and reversed the upregulatory effect of E2 on POC5. For quantification of band intensity, Image j was used and ratio of POC5 to β-actin was calculated (n=2). The results are mean ± SD from two independent experiments. For qPCR, error bars represent ± S.D in triplicates. $p<0.05$.

Figure 7: qPCR of gene expression of different markers of differentiation and ERs in osteoblasts. A) RNA was extracted from NOB and human OB (c. C1286T; p. A429V) AIS treated with vehicle or 10^{-7} M 17-β-estradiol (E2) for 24 hrs. ALP and RUNX2 were upregulated by E2 in NOB cells. No significant change was observed in human OB (c. C1286T; p. A429V) AIS cells. Expression was normalized to GAPDH and is plotted as fold increase from the vehicle treated sample. ALP: alkaline phosphatase; RUNX2: Runt-related transcription factor 2; B) qPCR of expression of ERα and ERβ. NOB and human OB (c. C1286T; p. A429V) AIS cells were exposed to vehicle or 10^{-7} M E2 for 24 hrs. ERα expression was induced by E2 in NOB and human OB (c. C1286T; p. A429V) AIS cells. ERβ was downregulated in NOB. Expression was normalized to GAPDH and is plotted as fold increase from the vehicle treated sample. Error bars represent ± S.D in triplicates.

Footnotes

Current address for Edward T. Bagu[3] and Shunmoogum A. Patten[4]:

3. Department of Basic Biomedical Sciences, Sanford Medical School, University of South Dakota, Vermillion SD 57069, United States of America
4. INRS Center Armand–Frappier, 531 DES Prairies Boulevard Laval, Quebec H7V1B7, Canada

Figure 1

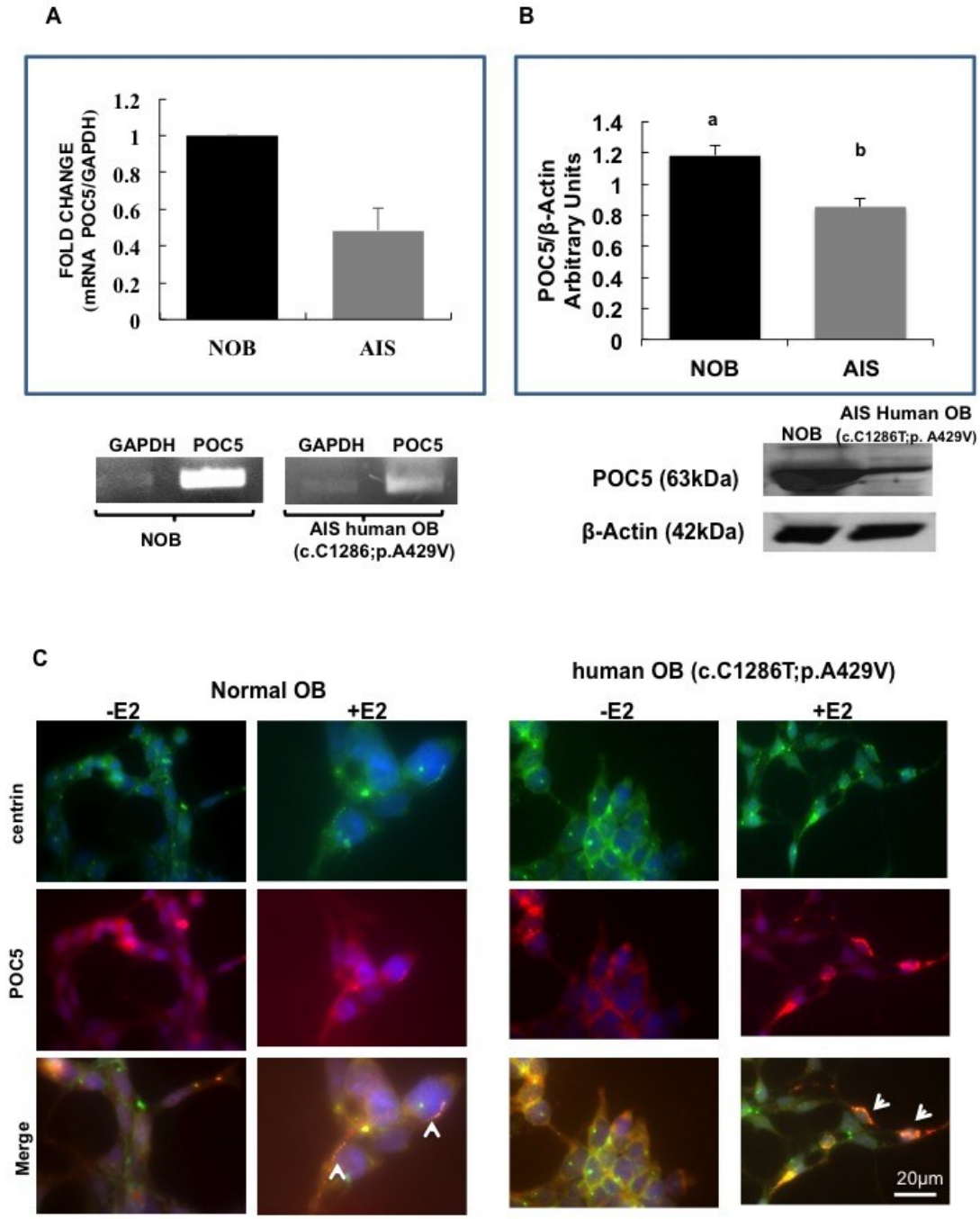
A
B
FOLD CHANGE (mRNA POC5/GAPDH)
1.2
1
0.8
0.6
0.4
0.2
0
NOB
AIS
POC5/β-Actin Arbitrary Units
1.4
1.2
1
0.8
0.6
0.4
0.2
0
a
b
NOB
AIS
GAPDH
POC5
GAPDH
POC5
NOB
AIS human OB (c.C1286;p.A429V)
AIS Human OB (c.C1286T;p. A429V)
NOB
POC5 (63kDa)
β-Actin (42kDa)
C
Normal OB
human OB (c.C1286T;p.A429V)
-E2
+E2
-E2
+E2
centrin
POC5
Merge
20μm

Figure 2

A

NOB

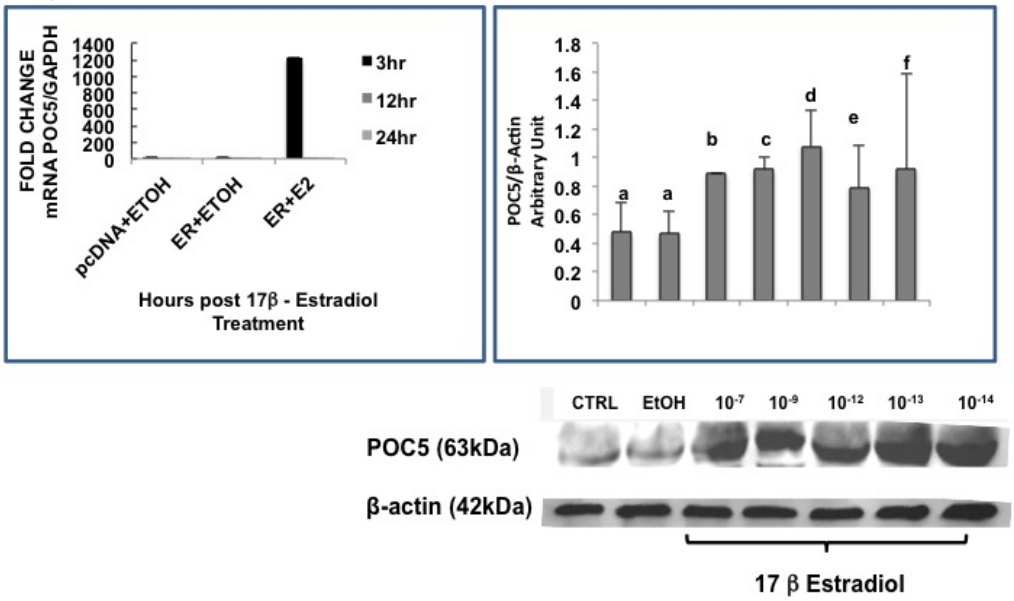

B

AIS human OB (c. C1286T; A429V)

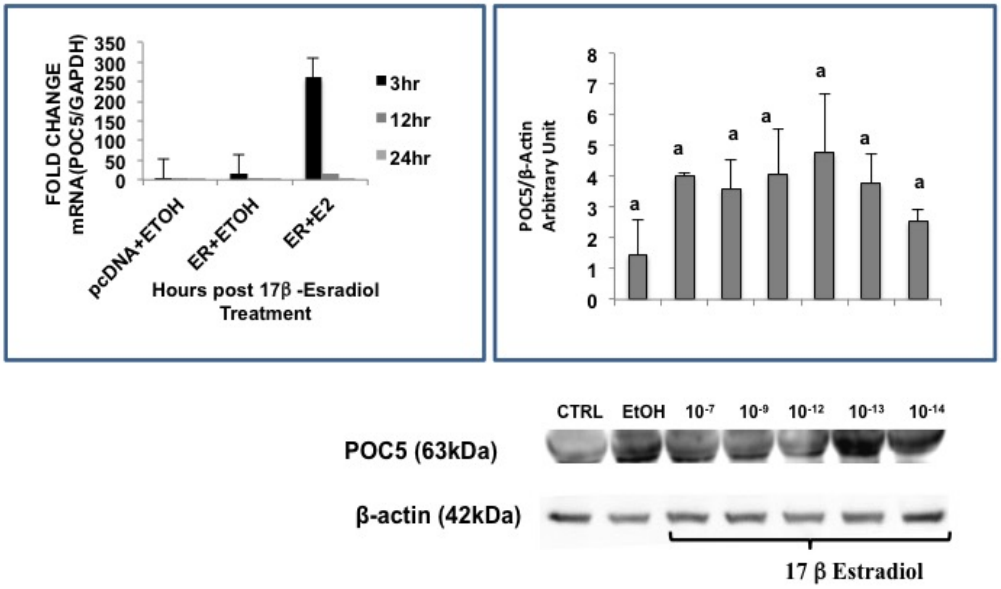

Figure 3

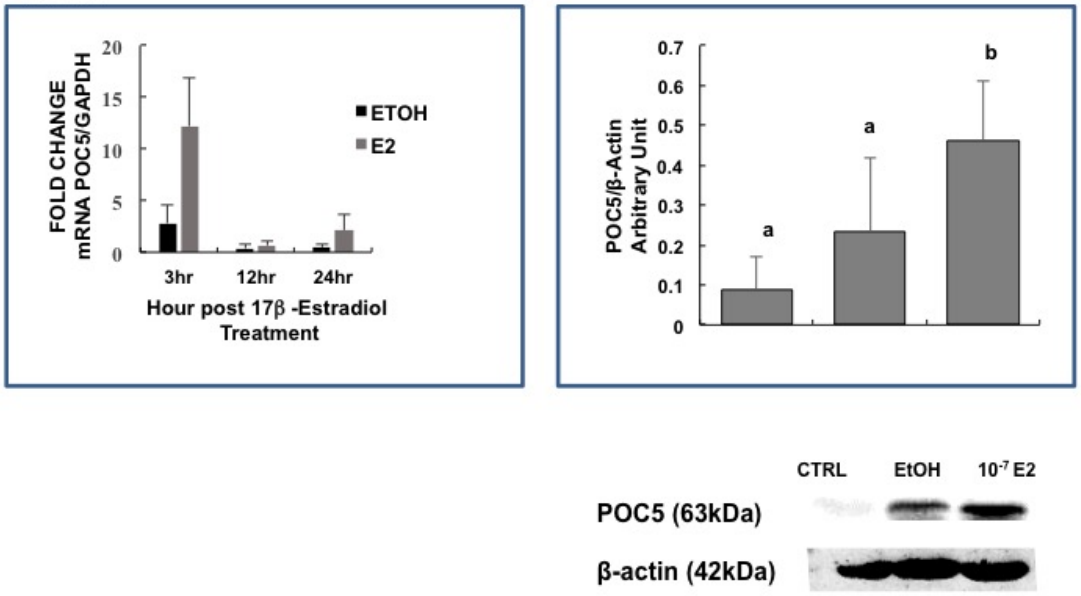
A
MCF-7
FOLD CHANGE mRNA POC5/GAPDH
20
15
10
5
0
ETOH
E2
3hr
12hr
24hr
Hour post 17β -Estradiol Treatment
POC5/β-Actin Arbitrary Unit
0.7
0.6
0.5
0.4
0.3
0.2
0.1
0
a
a
b
CTRL
EtOH
10-7 E2
POC5 (63kDa)
β-actin (42kDa)
B
Huh7
pcDNA+ETOH
ER+ETOH
ER+E2
FOLD CHANGE mRNA(POC5/GAPDH)
2
1.5
1
0.5
0
3hr
12hr
24hr
Hour post 17β -Estradiol Treatment
POC5/β-Actin Arbitrary Unit
1
0.8
0.6
0.4
0.2
0
a
b
a
c
Estradiol (10-7)
pcDNA3
ER
ER
-
-
-
+
POC5 (63kDa)
β-actin (42kDa)

Figure 4

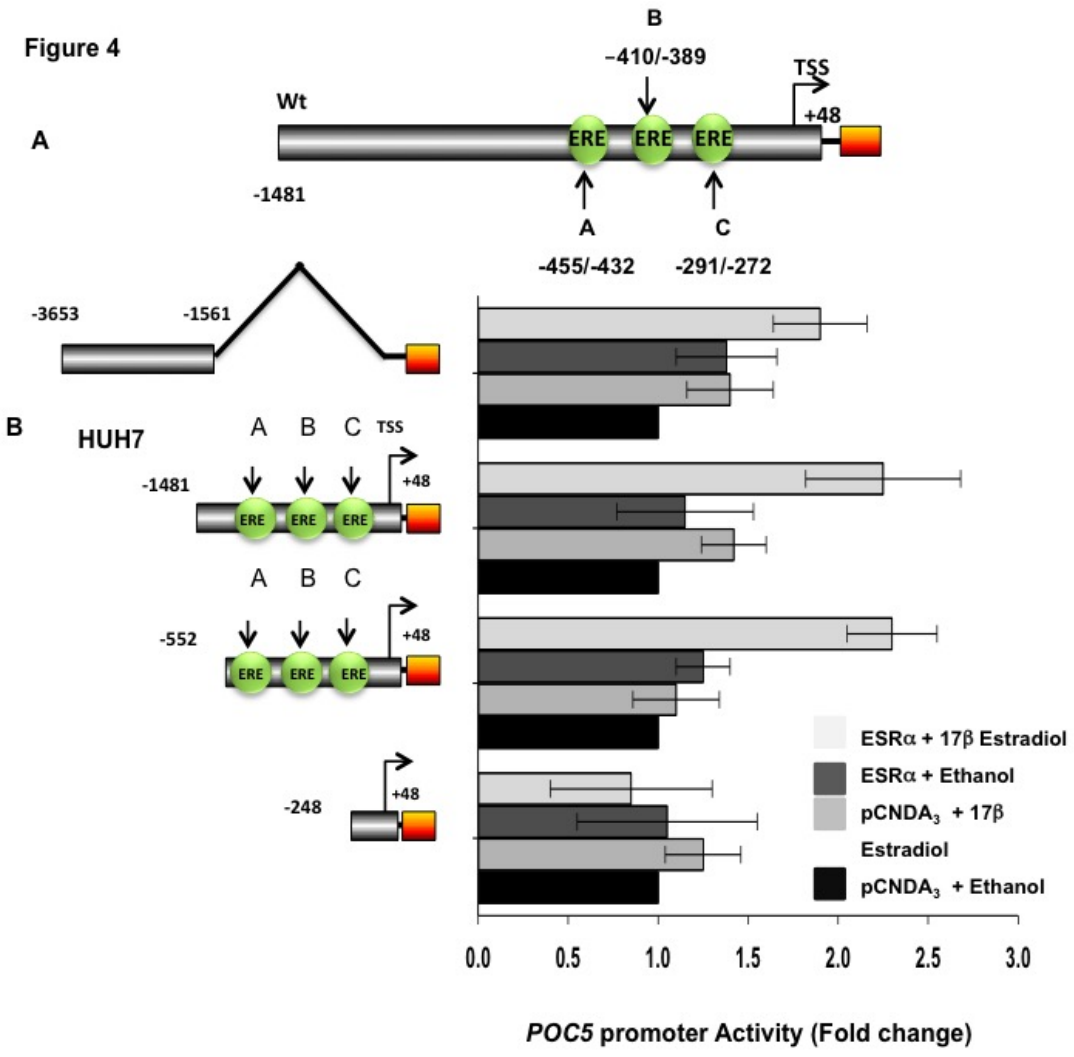
A
Wt
B
−410/-389
TSS
+48
ERE
ERE
ERE
-1481
A
C
-455/-432
-291/-272
-3653
-1561
B
HUH7
A B C TSS
-1481
+48
A B C
-552
+48
-248
+48
ESRα + 17β Estradiol
ESRα + Ethanol
pCNDA3 + 17β Estradiol
pCNDA3 + Ethanol
0.0
0.5
1.0
1.5
2.0
2.5
3.0
POC5 promoter Activity (Fold change)

Figure 5

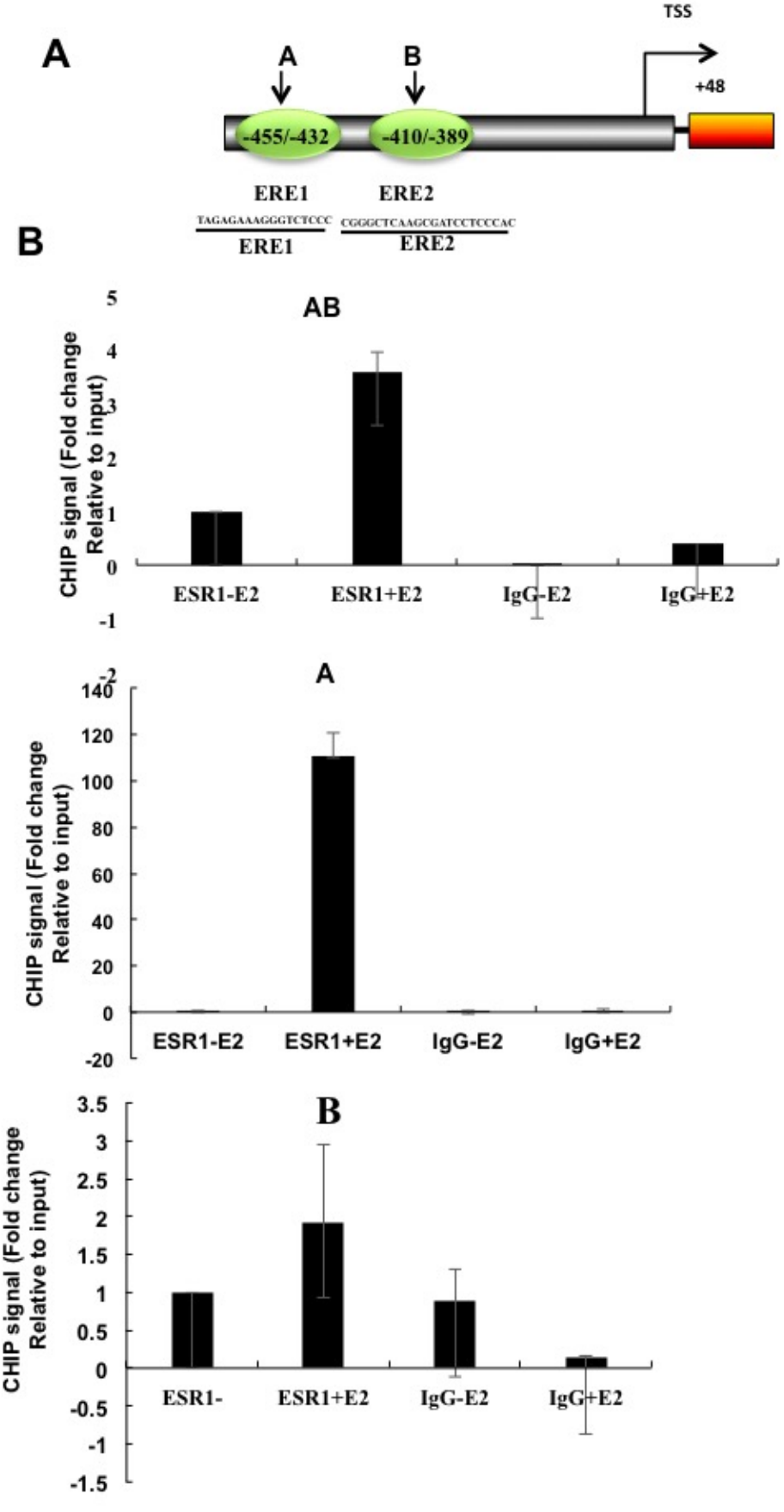
A
TSS
A
B
+48
-455/-432
-410/-389
ERE1
ERE2
TAGAGAAAGGGTCTCCC
ERE1
CGGGCTCAAGCGATCCTCCCAC
ERE2
B
AB
CHIP signal (Fold change Relative to input)
5
4
3
2
1
0
-1
-2
ESR1-E2
ESR1+E2
IgG-E2
IgG+E2
A
CHIP signal (Fold change Relative to input)
140
120
100
80
60
40
20
0
-20
ESR1-E2
ESR1+E2
IgG-E2
IgG+E2
B
CHIP signal (Fold change Relative to input)
3.5
3
2.5
2
1.5
1
0.5
0
-0.5
-1
-1.5
ESR1-
ESR1+E2
IgG-E2
IgG+E2

Figure 6

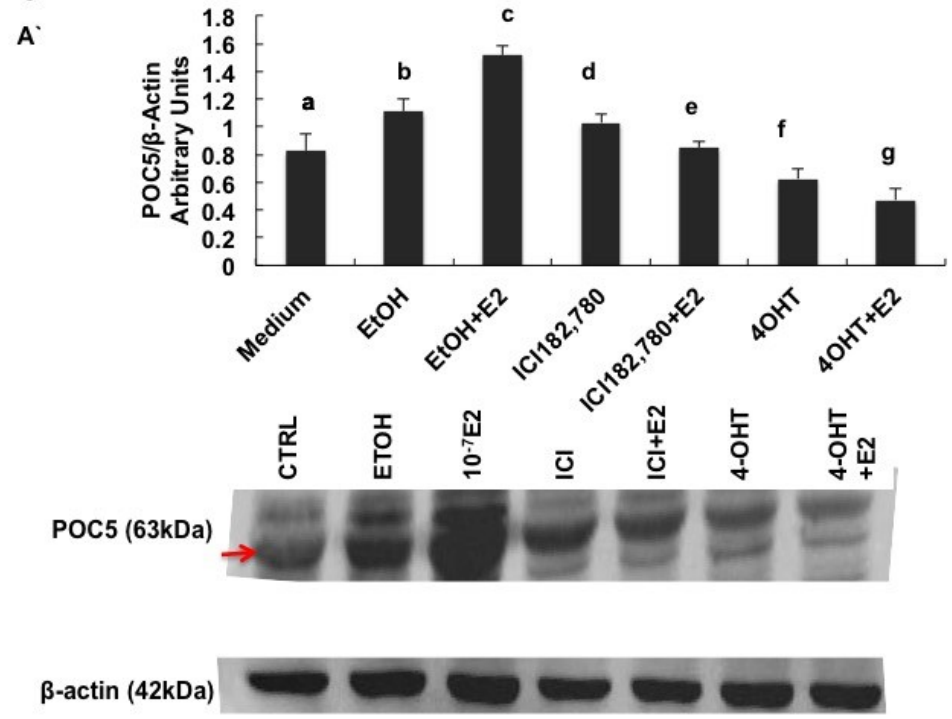
A`
POC5/β-Actin Arbitrary Units
1.8
1.6
1.4
1.2
1
0.8
0.6
0.4
0.2
0
a
b
c
d
e
f
g
Medium
EtOH
EtOH+E2
ICI182,780
ICI182,780+E2
4OHT
4OHT+E2
CTRL
ETOH
10-7E2
ICI
ICI+E2
4-OHT
4-OHT +E2
POC5 (63kDa)
β-actin (42kDa)

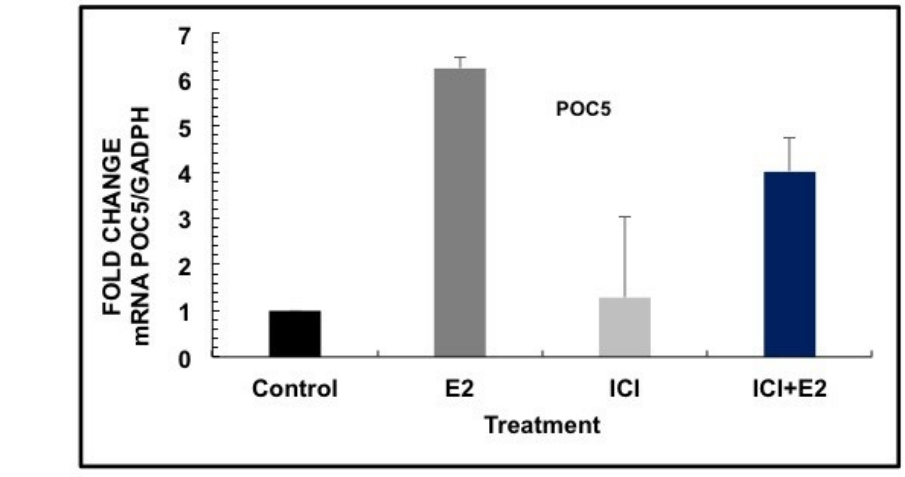
B
FOLD CHANGE mRNA POC5/GADPH
7
6
5
4
3
2
1
0
POC5
Control
E2
ICI
ICI+E2
Treatment

Figure 7

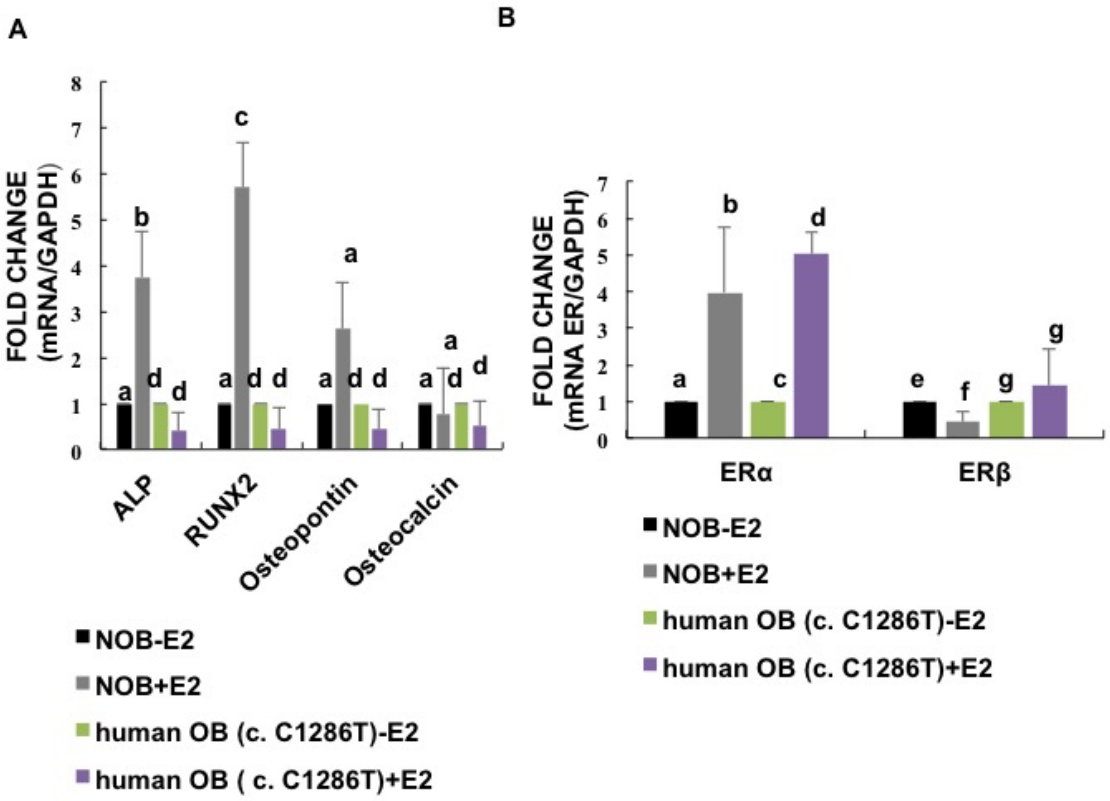
A
FOLD CHANGE (mRNA/GAPDH)
ALP
RUNX2
Osteopontin
Osteocalcin
B
FOLD CHANGE (mRNA ER/GAPDH)
ERα
ERβ
NOB-E2
NOB+E2
human OB (c. C1286T)-E2
human OB (c. C1286T)+E2
NOB-E2
NOB+E2
human OB (c. C1286T)-E2
human OB (c. C1286T)+E2

List of tables:

Primer Name	Position Relative to TSS	Primer Sequence
Sense	-3661/-3641	5CCAGCAGGCTAGCCCAGGCGT3
Anti-sense	-1478/-1448	5GTCTTTCAACTTACATTGGCAACAGATAGGC3
Sense	-1481/-1455	5CATACCTGCTAGCCTATCTGTTGCCAATGTAAGTT3
Sense	-555/-536	5CTGCACACCAGCCTGGACGGGCTAGCAAGACTCCATCTCAAAA3
Sense	-248/-230	5GAAAGCCAACAGCACACGGCGCTAGCCAACTTCAGCCCTGC3
Anti-sense	+21/+48	5CTGCAGGCTCGAGGAATTAAGGACCGCCCTGGGC3

Table 1: List of primers used to clone the *POC5* promoter full length and deletion constructs. The FOR and REV represent the forward and reverse directions respectively. The second column indicating the beginning and end of the primer sequence with respect to the transcriptional start site

.

Primer Name	Sequence
POC5_CHIP__EREAB_S	5 GGGATCTGTGGATGATGCAG 3
POC5_CHIP_EREAB_AS	5 GGCCTCCCAAAGTGCCGGG 3
POC5_CHIP__EREA_S	5GGGATCTGTGGATGATGCAG 3
POC5_CHIP_EREA_AS	5GAGTTCGAGACTAGTCTGGG3
POC5_CHIP__EREB_S	5CCCAGACTAGTCTCGAACTC3
POC5_CHIP_EREB_AS	5CCCGGCACTTTGGGAGGCC3

Table 2: List of primers used in ChIP experiment. List of primers used for ESRα response element on the *POC5* promoter.

Primer Name	Primer Sequence	Product Size
GAPDH_S	5AGGAGTAAGACCCCTGGACC3	111bp
GAPDH_AS	5GGAGATTCAGTGTGGTGGGG3	
POC5_S	5CATGTCAGAGCCAGACAGGA3	96bp
POC5_AS	5GGAACGCCAGACTTTCCAGA3	
ALP_S	5ACACCTGGAAGAGCTTCAAACCGA3	401bp
ALP_AS	5TCCACCAAATGTGAAGACGTGGGA3	
OSTEOCALCIN_S	5ACACTCCTCGCCCTATTG3	249bp
OSTEOCALCIN_AS	5GATGTGGTCAGCCAACTC3	
RUNX2_S	5TCCGGAATGCCTCTGCTGTTATGA3	239bp
RUNX2_AS	5ACTGAGGCGGTCAGAGAACAAACT3	
OSTEOPONTIN_S	5CAGCCATGAATTTCACAGCC3	307bp
OSTEOPONTIN_AS	5GGGAGTTTCCATGAA GCCAC3	

Table 3: List of primers used in qPCR.

III.4. MANUSCRIPT 4

The role of TRPV4 in osteoblasts during mechanical stress

A. Hassan[1], C. Zaouter[1], S. Parent[1], S. Barchi[1], I. Londono[1], I. Villemure [1,4], S.A. Patten[2], F. Moldovan[1,3*]

1. CHU Sainte-Justine Research Center, Montréal, Québec, Canada

2. INRS-Institute Armand-Frappier Research Centre | INRS, Montréal, Québec, Canada

3. Faculty of Dentistry, Université de Montréal, Montréal, Québec, Canada

4. Department of Mechanical Engineering, École Polytechnique de Montréal, Québec, Canada

key-words: Scoliosis, TRPV4, osteoblast, cilia, biomechanical stress, POC5

* Codirected work

Corresponding author: Dr. Florina Moldovan, CHU Sainte Justine, 3175 Côte Sainte-Catherine, 2nd floor, room (217.315.7), Montréal, Québec, Canada, H3T 1C5 Tel: 1-514 -345-4931 ext: 5746; Fax: +1 (514) 345-4801; email: florina.moldovan@umontreal.ca

Abstract

Adolescent idiopathic scoliosis is the most common form of scoliosis, a three-dimensional spinal deviation whose etiology remains unexplained. Several factors have been associated with the initiation and progression of AIS. The concept of a multifactorial pathology is generally accepted. There exists a strong correlation between abnormal mechanical loading and AIS progression, where it can lead to altered bone growth and subsequent deformity, a phenomenon known as the mechanical modulation of bone growth. Transient receptor potential vanilloid 4 (TRPV4) is a receptor operated ion channel activated by mechanical stress. In osteoblasts, during cell differentiation, TRPV4 expression is enhanced and changes in response to mechanical load. Mutations in *TRPV4* channel (R616Q and V620I) have been associated with a skeletal dysplasia named Brachyilmias, where scoliosis is a secondary phenotype. In the present work, normal control osteoblasts and mutant*POC5* (mut*POC5*) cells were treated in vitro with TRPV4 antagonist (RN-1737) or TRPV4 agonist (RN-1747) or PKA

antagonist (H-89) after cells were exposed to mechanical stress. Then, we studied the response in these cells with respect to MAPKinase p38 signalling pathways and NFκB, osteoblast mineralization, cell proliferation, viability and cilia expression pattern. We further performed in vivo work, on wt*poc5* and mut*poc5* zebrafish retina. The retinas were either stained with a combination of trpv4 and acetylated-α-tubulin or poc5 and annexin5. Our results showed strong implication of TRPV4 channel in the stress response of both normal control osteoblasts and mut*POC5* expressing cells. The *POC5* mutation has consequences on TRPV4 localization and expression in vitro and in vivo.

Introduction:

Scoliosis is a complex three-dimensional deformity of the spine, with 1.5–3% prevalence in the general population. The most commonly known type of scoliosis is idiopathic scoliosis (IS), including adolescent idiopathic scoliosis (AIS), which affects principally girls (Altaf, Gibson et al. 2013). Its prevalence is 1% to 2% among adolescents; it develops in otherwise healthy, pre-adolescent children. AIS primarily occurs and progresses in girls during growth spurts (2). Abnormal mechanical loading lead to altered bone growth and subsequent deformity, a phenomenon known as the mechanical modulation of bone growth. This phenomenon is strongly implicated in scoliosis progression, including in AIS (Villemure and Stokes 2009). One of the hypothesis for the progression of scoliosis is that it results from abnormal mechanical loading conditions influencing longitudinal growth prior to skeletal maturity (Villemure and Stokes 2009).

Bone cells (osteoblasts) are recruited in an organized manner through matrix vesicles and cell-produced growth and differentiation factors (GDFs) (Shapiro, Landis et al. 2015) from mesenchymal stem cells. Once these cells are incorporated in the bone matrix, they become osteocytes that communicate with each other and with surface layer osteoblasts by the cell processes which line the canaliculi that permeate the matrix. The type I collagen is highly crosslinked and constitute the organic matrix of bone which is very dense. The bone also contains small amounts of osteopontin and osteocalcin, which are important in coordinating the organic matrix and bone mineral (Blair, Larrouture et al. 2017). Bone synthesis is determined by bone alkaline phosphatase (ALP) that is a critical factor providing phosphate

for bone mineralization. Not only ALP, but also osteoblasts secrete large amounts of type I collagen and smaller amounts of matrix organizing proteins, including osteocalcin and osteopontin. Osteocalcin is an indicator of osteoblast synthetic activity (Young, Kerr et al. 1992).

Several gene mutations have been described in AIS, among which are the ciliary genes POC5 and TRPV4. It was recently found that scoliosis may be caused by variants in genes related to cellular mechanotransduction, but is not restricted to ciliary genes. Given the fact that POC5 (Patten, Margaritte-Jeannin et al. 2015, Weisz Hubshman, Broekman et al. 2017, Xu, Sheng et al. 2017) and TRPV4 (Nilius and Voets 2013) are ciliary genes that have been associated with scoliosis, this makes them interesting factors to investigate.

Considering POC5 gene, mutations in POC5 were identified in AIS patients (Patten, Margaritte-Jeannin et al. 2015) and confirmed, using a zebrafish model, as the leading cause to spinal curvature. POC5 is a centrosomal protein that is localized at the mother and daughter centrioles throughout the cell cycle. The recruitment of POC5 into centrioles occurs late in the duplication phase of the cell cycle, G2/M phase. Through knockdown studies, hPOC5 was found to be essential for the assembly of full length centrioles and for cellular proliferation (Azimzadeh, Hergert et al. 2009).

Unlike *POC5* that has been identified as the primarily cause of AIS in patients, mutations in *TRPV4* was leading to scoliosis as a secondary rather than a primary phenotype in patients. Cilia plays an essential role in mechanotransduction, and this makes TRPV4 an important factor to consider in studying mechanical factors involved in the mechanism of AIS pathogenesis. The transient receptor potential vanilloid 4 (TRPV4) channel is a Ca2+-preferred membrane ion channel, which is widely implicated in transducing external environmental signals into specific metabolic responses via the generation of intracellular Ca2+ transients (Liedtke 2007, Everaerts, Nilius et al. 2010, Moore, Cevikbas et al. 2013). Mutations in the *TRPV4* gene are known to be causative of several human diseases affecting the skeletal and the peripheral nervous systems. Scoliosis is a secondary phenotype in several TRPV4 associated diseases. One of the TRPV4 mediated skeletal disease includes the

autosomal dominant brachyolmia type 3, which is primarily characterized by brachyolmia. Patients have normal length at birth, but develop short trunk and stature during childhood, mainly due to platyspondyly (flattening (platy-) of the vertebrae (spondyl-) throughout the axial skeleton. The common phenotype in patients with this disease includes kyphoscoliosis (abnormal spinal curvatures in both coronal and sagittal planes) and slightly short limbs (Everaerts, Nilius et al. 2010). Parastremmatic dysplasia is an autosomal dominant dysplasia, which is characterized typically by a severe distortion and twisting of the limbs and extreme dwarfism. The disease is congenital (apparent at birth) and patients develop progressive kyphoscoliosis, distortion and bowing of the extremities and contractures of the large joints during the first years of life. The malformations are attributed to a deficit in bone mineralization (Nilius and Voets 2013).

TRPV4 channel localizes in the primary cilium, onto which the flow-induced intracellular calcium ion (Ca2+) increase depends. The primary cilium is a protrusion from the surface of most eukaryotic cells, except for hematopoietic cells. It plays an essential role in chemosensation and mechanosensation in cartilage, bone and kidney. It was previously reported that primary cilium plays a role in osteocyte mechanotransduction, but the molecular mechanisms involved in this process are not fully understood (Lee, Guevarra et al. 2015).

Defects in mechanotransduction was associated with IS. Elongated cilia was identified in idiopathic scoliosis patient bone cells (Oliazadeh, Gorman et al. 2017). In the present work, we studied the differential effects of mechanical stress on bone cells from normal and cells with *POC5* (*c. C1286T* (p. A429V)) mutation including pathways activated by mechanical stress in the presence of TRPV4 antagonist RN-1734, TRPV4 agonist RN-1747 and the PKA antagonist H-89. We also studied the impact of mechanical stress on cell proliferation and apoptosis and bone differentiation in vitro. In vivo work was also conducted to study the differential expression of trpv4 in wt*poc5* and mut*poc5* zebrafish retina. Overall, our results indicate that the TRPV4 channel is implicated in the response of osteoblasts to mechanical stress and that mechanical stress induces differential response and signalling pathway in normal and mut*POC5* osteoblasts.

Materials and methods

A. In vitro study

Patients

Bone specimens were collected from vertebrae of AIS patients undergoing surgery (varying from T3 to L4 according to the surgical procedure performed). For control and AIS patients, all tissues were collected with the consent of patients following approval by the Institutional Ethics Committee Board of CHU Sainte-Justine.

Osteoblast extraction and cell culture

Bone fragments were reduced to smaller pieces with bone cutter in sterile conditions. The fragments were incubated at 37°C in 5% CO2 in a 100-mm culture dish in the presence of Alpha Modified Eagle Medium containing 10% fetal bovine serum (FBS) (Wisent) and 1% penicillin and streptomycin (Invitrogen, Burlington, ON, Canada). After a 28-day period, the osteoblasts derived from the bone pieces were separated at confluence from the remaining bone fragments by trypsinization.

Transient transfection assays

Transfections of osteoblasts were performed in 12 well plates using LipofectamineTM 2000 (Invitrogen, Burlington, ON, Canada) as recommended by the manufacturer. Briefly, on the day before transfection, cells were seeded in a 12 well plate-using 0.5ml of media. When cell attained 80% confluence, they were transfected with 1600 ng/ well of mut*POC5* construct. On the second day, cells were exposed or not to 1g/cm^2 mechanical stress for 6h. For TRPV4 subcellular localization study, HeLa cells were used and they were either transfected with mock (myc-tagged empty vector), myc-wt*POC5* (origene) or myc- mut*POC5* vectors (generated by site directed mutagenesis as described in (Patten, Margaritte-Jeannin et al. 2015). Cells were transfected as described above and then serum starved for 24h followed by immunofluorescence.

Cell treatments

Osteoblasts were treated with TRPV4 agonist RN-1747 or TRPV4 antagonist RN-1734 or PKA antagonist H-89 for 24h at 10μm final concentration. Agonists and antagonists were purchased from (Tocris) and were separately reconstituted with DMSO and stored at -20^{o}C.

Induction of mechanical stress

We have developed a method to induce mechanical stress on cells by applying weight. This weight is represented by coins that will exert a mechanical force of 1g/cm2 of strength. The stress can be equated to the load per unit area or the force applied per cross-sectional area perpendicular to the force. The coins were sterilized by autoclaving and then washed with ethanol and water before being applied to cells.

Protein Lysate Preparation and Western Blotting

Whole cell protein lysates were prepared from cultured cells using RIPA buffer from Pierce thermoscientific (25 mM Tris•HCl pH 7.6, 150 mM NaCl, 1% NP-40, 1% sodium deoxycholate, 0.1% SDS,) supplemented with protease and phosphatase inhibitors (Roche Diagnostics, Mannheim, Germany). To perform western blot, equal amounts of protein (40ug) were resolved using 10 % SDS/polyacrylamide gel electrophoresis. Afterwards, proteins were transferred onto a nitrocellulose membrane and blocked in Tris buffered saline containing 1% Tween-20 or Phosphate buffered saline with 0.05% Tween-20 as recommended by manufacturer and 20% skim milk powder. Membranes were incubated with primary antibody overnight at 4^{o}C (list of antibodies table 2). Afterwards, membranes were incubated with a secondary antibody conjugated with horseradish peroxidase for 1h at RT. After incubation, proteins were visualized by Syngene G: BOX Chemi XRQ.

RNA isolation, reverse transcription, PCR, and real-time PCR:

Total RNA was extracted from osteoblasts using TRIzol®reagent (Invitrogen), in accordance with the manufacturer's instructions (Invitrogen Canada). The extracted RNA was quantified spectrophotometrically. RNA (1 μg) was used as a template to synthesize cDNA using iscript reverse transcriptase (Diamed). Quantification of gene expression was performed by RT-PCR light cycler 96 System (company) with SYBR® Green with ROX Supermix (Diamed). Primers for different genes are listed in table1. The PCR products generated were confirmed

by agarose gel electrophoresis. Gene expression levels in all cells assayed were represented relative to the expression of the housekeeping gene *GAPDH* (List of primers table 1). Fold change was calculated using the delta CT method ($2^{-\Delta CT)}$.

Alkaline phosphatase (ALP)

Osteoblasts were cultured in DMEM/F12 until confluency (2x105 cells). Three days before alkaline phosphatase staining, medium was replaced with MEM supplied with 10% FBS, 1% PS in addition to ascorbic acid 50µg/ul, dexamethasone 10nM and β-glycerophosphate 2.5 mM. After 72h, cells were washed with PBS and then fixed with 3.7% PFA. The cells were then washed with PBS 1X and incubated with a solution of 1,25 mg of naphtol AS-MX phosphate (Sigma, Ontario, Canada), 2,5 mg of fast red TR (Sigma, Ontario, Canada), and 62,5 µL ethylene glycol monoethylether in 6 ml of TBS 0,1 M pH 9,5 (Tris 0,1 M, NaCl 0,15 M, pH 9,5) for 1 h at room temperature (RT). The cells were then washed with water and observed under light microscope. For quantification, cells were washed with PBS and then the absorbance was measured at 405 nm together with the standard curve samples using micro plate reader. ALP concentration (mg/ml) of non treated and stress treated was determined using the standard curve.

Alizarin Red Staining

Osteoblasts were cultured untill confluency (2x105) in 24 well plates using alpha MEM. When the cells reached confluency, mineralization medium was started by adding ascorbic acid 50ug/ml, dexamethasone 10nM and glycerophosphate 2.5mM. The medium was changed every other day. Cells were fixed with PFA 10% for 15 minute and then 1ml of alizarin red 40mM (pH=4.1) was added and incubated 20 minutes at RT. The cells were washed with water and left untill dried. At this stage, photos were acquired using light microscope at 20x. For quantification using microplate reader, 800ul acetic acid 10% was added and incubated with agitation for 30 minutes. The samples were then transferred to ependorf tubes. Samples were incubated at 85°C for 10 minutes and transferred on ice for 5 minutes. Samples were centrifuged at 20,000g for 15 minutes. 500ul of each sample was added to 500ul ammonium hydroxide 10%. The absorbance was measured at 405nm.

For preparing the standard curve, a mixture of acetic acid 10% and ammonium hydroxide 10% was prepared and then a mixture of alizarin red and the above mixture was added in a ratio (5 to 1) to have a stock solution 1mg/ml. Serial dilutions were prepared from this mixture (500, 250, 100, 50, 25, 10, 5, 0 μg/ml).

Propidium iodide staining

Osteoblasts were left to attach on coverslips overnight (ON). Before cell seeding, the coverslips were treated with poly-L-lysine for 1h at 37ºC and then washed with ethanol and water. Cells were transfected or not with mut*POC5* expressing vectors, and then on the second day were exposed to stress for 24 h. 33.33 ul of PI (1mg/ml) was diluted in 10 ml PBS and then cells were incubated with PI for 30 mins at 37ºC. Cells were counterstained with DAPI and were visualized by fluorescence microscope.

Immunofluorescence and Acetylated-α-tubulin staining

Osteoblasts were left to attach to coverslips (coated with polylysine) in 12 well plate ON. On the second day, cells were transfected with myc tag-mut*POC5*. On the third day, cells were subjected to mechanical stress for 24h and on the other day, cells were fixed in 70% ethanol/0.1% triton on ice for 30 mins. Cells were then washed with PBS and permeabilized with 0.1% Triton in PBS for 15 mins. Cells were washed once with 0.5%BSA in PBS/Triton (PBT) and then blocked with 2% BSA in PBT for 45 mins. Cells were washed after that and incubated with Acetylated-α-tubulin (Sigma-Aldriche) ON at 4ºC. On the second day, cells were washed and then incubated with Alexa Flour 555 (Life technologies USA) for 1h at RT. Cells were mounted and stained for nucleus at the same time using Prolong Gold antifade reagent with DAPI (Life technologies). Immunostaining was observed at magnification x40. For the measurement of the cilium length and cilium number, we used the ZEN software. Immunofluorescence was also performed in HeLa cells, the same protocol was followed as described above but staining for TRPV4 (proteintech) was performed.

B. In vivo study

Immunostaining on zebrafish:

Immunolocalization of trpv4 and colocalization with the cilia were performed by double immunofluorescence carried out by mixture of anti-trpv4 antibody (proteintech) and anti-acetylated-α-tubulin (Sigma-Aldrich). Tissue sections of eye (1.5µm) were deparaffinized in xylene, rehydrated in a graded series of ethanol, washed several times in PBS and permeabilized for 30 mins in 4% Triton-X 100 containing 2% bovine serum albumin (BSA) and 10% goat serum. Following permeabilization, retinal sections were incubated with the primary antibody trpv4 (1/250) and acetylated-α-tubulin (1/2000) simultaneously during 24h at 4°C. Tissue sections were washed several times in PBS/0.5%Triton, and then incubated with the secondary antibody conjugated with Alexa Fluor 488 (life technologies 1/500) and Alexa Flour 555 (Life technologies 1/500) for 1 h at RT. Nucleus staining was performed using Prolong Gold antifade reagent with DAPI (Life technologies). Images were acquired using confocal microscope Zeiss under 40x objective. Staining for annexin 5 was performed using the same protocol described above but with annexin 5 antibody (Santa Cruz).

Statistical analysis:

All values are expressed as mean SD. All the data from experiments were analyzed using a two-tailed Student's t test ($P < 0.05$) comparing the means of non stress and stress treated samples. Student's paired and unpaired t-tests were performed by Microsoft excel. Values of $P<0.05$ were considered statistically significant.

Results:

Regulation of *Acetylated-α-tubulin, POC5* and *TRPV4* expression in response to stress:

Considering the requirement for TRPV4 in stimulating the response to mechanical stress and given the role of cilium in mechanotransduction, we investigated the TRPV4 activity in stress induced gene and protein expression of ciliary genes by applying different treatments of TRPV4 agonist and antagonists to normal control osteoblasts and to cells overexpressing the mut*POC5*. We studied expression levels of *POC5, Acetylated-α-tubulin* and *TRPV4*. At the gene level, in NOB cells, *Acetylated-α-tubulin* was downregulated in response to stress ($p<0.01$) and no significant difference was observed with the other treatments (NS). In mut*POC5* cells, we observed upregulation in response to stress ($p<0.05$) and this effect was

significantly enhanced with RN-1747 treatment ($p<0,05$) (Fig. 1A). *POC5* was significantly downregulated in mut*POC5* cells in response to stress ($p<0.01$) and upregulated in response to stress in the presence of RN-1747 in NOB ($p<0.05$) and in mut*POC5* cells ($p<0.05$) (Fig. 1B). *TRPV4* was upregulated with RN-1734 treatment ($p<0.05$) in NOB. In mut*POC5* cells, TRPV4 was highly upregulated with RN-1747 treatments ($p<0.01$) and at lower levels with RN-1734 ($p<0.05$) (Fig. 1C). At the protein level, Acetylated-α-tubulin was upregulated in response to stress in both cells. Treatment with H-89 and RN-1734 enhanced Acetylated- α-tubulin in mutPOC5 cells. RN-1747 downregulated Acetylated-α-tubulin levels in NOB while no effect was observed in mutPOC5 cells. POC5 was downregulated in mutPOC5 cells in response to stress while no effect was observed on NOB cells. Treatment with RN-1747 downregulated POC5 levels in both cells. The TRPV4 was upregulated in response to stress and in the presence of H-89 in NOB and downregulated in mutPOC5 cells. RN-1747 treatment highly downregulated levels of TRPV4 in mutPOC5 cells, at lower levels with RN-1734 while no change was observed in NOB cells (Fig. 1D).

MAPKs and p38 were activated by mechanical stress:

The molecular mechanisms underlying the response of cells to stress need to be clarified. p38 MAPK signaling is activated in response to stress, and blocking the p38 MAPK inhibits cytoskeletal reorganization. To explore the roles of p38 MAPK pathways in the mechanical stress response, the effect of mechanical stimulation on the phosphorylation of ERK1/2, p38 and NFκB was analyzed following the 6h loading period. Mechanical stress induced downregulation of ERK1/2, p38 and NFκB in mutPOC5 cells. We observed that in the absence of stress, the ratio of phosphorylated ERK1/2, p38 and NFκB to the total protein expression was higher in mutPOC5 cells than in NOB cells. When exposed to stress, ERK1/2 was strongly downregulated in NOB cells and to lesser extent in mutPOC5 cells. When treated with RN-1734 and RN-1747, ERK1/2 was upregulated in NOB and mutPOC5 cells (Fig. 2 A). Interestingly, there was higher upregulation with RN-1747 than with RN-1734 treatment in both cells.

P38 was upregulated in response to stress in NOB cells but downregulated in mutPOC5 cells. Treatment with RN-1747 induced the activation of p38 as detected by phosphorylation (Fig. 2 B).

We also checked for the regulation of NFκB expression in response to mechanical stress. When exposed to stress, NFκB was downregulated in mutPOC5 cells and slightly upregulated in NOB cells. No effect of the agonist and antagonist treatments on NFκB levels on both cells (Fig. 2 C).

Mechanical stress regulation of mRNA levels of bone formation markers:

We first characterized the gene expression profile of bone markers in NOB and mutPC5 cells by qPCR (alkaline phosphatase (ALP), osteopontin, osteocalcin, Runt-related transcription factor 2 (RUNX2) and collagen A1 (Col A1)) in NOB and mutPOC5 cells. The results show that NOB cells have higher expression of all markers except for osteocalcin (Fig. 3A). We then studied the mRNA expression levels of osteopontin, osteocalcin and Runt-related transcription factor 2 (RUNX2) in response to stress in NOB and mutPOC5 cells in the presence or absence of RN-1743, RN-1734 and H-89 after 6h of exposition to mechanical stress. Osteopontin levels were significantly induced upon stress in NOB ($p<0.05$) but no significant changes in mutPOC5. In mutPOC5 cells, mechanical stress downregulated osteopontin levels after treatment with RN-1734 ($p<0.01$) (Fig. 3B). No change was observed for osteocalcin levels upon different treatments in NOB except with RN-1734, there was significant induction of osteocalcin ($p<0.01$). Treatment with stress significantly reduced osteocalcin expression in mutPOC5 cells ($p<0.05$) (Fig. 3C). *Osteocalcin* expression was increased with H-89 treatment ($p<0.05$) and significant induction of *osteocalcin* expression was obtained with RN-1734 treatment ($p<0.01$). As for *Runx2* expression, no significant effects of mechanical stress was observed in NOB, however, in mut*POC5* cells, treatment with RN-1734 upregulated *RUNX2* expression ($p<0.01$) with higher upregulation with treatment with RN-1747 ($p<0.01$) (Fig. 3D).

Mechanical stress induces higher ALP activity in normal osteoblasts than in mutPOC5 cells:

To study the effect of mechanical stress on ALP, we performed alkaline phosphatase assay on NOB and on cells transfected with mut*POC5*. There were higher levels of ALP expression in normal cells exposed to stress (b) than in mut*POC5* cells (d). There was low and almost no

effect on ALP in mut*POC5* cells (Fig. 4A and 4B). ALP concentration was determined as described in the section of materials and methods.

Mechanical stress induces osteoblast mineralization:

Since mechanical load is able to accelerate differentiation and enhance osteoblast communication and function during the differentiation process, we next sought to study the effect of mutation in altering the mineralization of osteoblasts in response to mechanical stress. In our model, mechanical stress significantly induced mineralization as detected by alizarin staining and quantification ($p<0.003$) in NOB cells. However, in mutPOC5 cells, there was significantly lower mineralization rate compared to NOB ($p<0.0008$). The cells were still able to mineralize but at lower levels (Fig. 5A and B).

Effect of mechanical stress on mineralization factors:

Since mechanical stress had effect on osteoblast differentiation as determined by ALP, we next sought to investigate the expression of mineralization and ciliary genes in mineralizing cells in the presence of stress. TRPV4 was highly downregulated in mutPOC5 cells exposed to stress ($p<0.001$) while no significant change was observed in NOB. *Acetylated-α-tubulin* was downregulated in response to stress in NOB ($p<0.01$) but upregulated in mut*POC5* cells ($p<0.05$) (Fig. 6A). In order to study the differential expression of bone mineralization factors between normal and mut*POC5* cells, we studied the mRNA levels in mineralizing osteoblasts. Interestingly, mechanical stress induced upregulation of most of the analyzed factors including *RUNX2 ($p<0.05$)*, *ALP ($p<0.01$)* and *osteocalcin ($p=0.05$)* in NOB cells, however, they were downregulated in mut*POC5* cells ($p<0.001$) (Fig. 6B).

COX2 mRNA expression levels in response to stress:

Since signalling through TRPV4 channel has an impact on ERK1/2 and p38 that eventually end up with the upregulation of *COX-2* gene, we investigated the effect of mechanical stress on *COX2* mRNA levels in NOB and AIS cells. There was strong upregulation of *COX2* in NOB and, to lesser extent, in AIS cells when cells were exposed to stress (Fig. 7).

Mechanical stress effects on apoptosis:

To determine the effects of mechanical stress on osteoblast apoptosis, cells were treated with stress for 24h and apoptosis was assessed using propidium iodide. Mechanical stress induced osteoblast apoptosis in NOB ($p<0.05$) and mut*POC5* cells ($p<0.05$) (Fig. 8). Interestingly, mut*POC5* cells non exposed to stress had initially higher apoptosis rate than NOB ($p<0.01$).

Cilia length and number are regulated by mechanical stress in normal and mut*POC5* cells:

To identify if primary cilia is involved in cell response to stress and if there exists differences in NOB and mut*POC5* cells , cells were exposed to mechanical stress for 24h and then labeled with Acetylated-α-tubulin, a marker for cilia. Acetylated-α-tubulin-positive primary cilia were visualized as small bright protrusions (red) emanating from most cells located close to the cell nucleus (stained with DAPI) (Fig. 9A). When exposed to stress, number of cilia expressing cells (Fig. 9B) was reduced in both NOB ($p<0.01$) and mut*POC5* cells ($p<0.05$). The difference in cilia length was not significant.

Differential subcellular localization of TRPV4 in wt and mut*POC5* expressing cells after mechanical stress application: We checked whether there was a difference in subcellular localization of TRPV4 in wt*POC5* and mut*POC5* expressing cells after exposure to mechanical stress. In wt*POC5* cells, when exposed to stress, TRPV4 shifted to cytoplamic localization. Unlike mut*POC5* cells, when exposed to stress, there was nuclear expression of TRPV4 as punctate pattern (Fig. 10).

TRPV4 immunoreactivity in wt*poc5* and mut*poc5* zebrafish retina: We were also interested in studying differences of trpv4 expression in wt and mut*poc5* scoliotic zebrafish retina. In wt*poc5* retina, trpv4 was strongly expressed in the outer segment layer (OS) and in the connecting cilium (CC) (Fig. 11 a and c), as well as in the ganglion cell layer (GCL) (Fig. 11 e and g) where it was found surrounding the glial cells. In mut*poc5* retina, there was less staining of TRPV4 in the outer segment layer (OS) and CC layers (Fig. 11 b and d) and absence of staining in the GCL as well as absence of glial cells (Fig. 11 f and h) suggesting degeneration of the retina. In wt retina and mut*poc5* retina, trpv4 and acetylated-α-tublin colocalized in the CC and inner plexiform layer (IPL), however, the colocalization was absent

in the outer plexiform layer (OPL). The cilium length was shorter in mut*poc5 (*10.7 μm) than in wt*poc5* retina (13.5 μm) ($p<0.00001$) (Fig. 11 i).

Increased apoptosis in mu*tpoc5* retina: Confirming the in vitro work, we also checked the expression of apoptotic marker annexin5 in the retinas of wt*poc5* and mut*poc5* zebrafish. There was very strong expression of annexin5 in the mut*poc5* retina in the OS, in the CC and GCL as compared to wt*poc5* retina (Fig.12).

Discussion

Here in, we reported the effect of mechanical stress on POC5, Acetylated-α-tubulin and TRPV4 expression in normal osteoblasts and mut*POC5* expressing cells as well as expression of MAPKinase p38 signalling pathway and NF-κB, mineralization, proliferation, viability and cilia expression patterns. Our results show a strong implication of TRPV4 channel in the mechanical stress activated signalling pathways with variations in both osteoblasts derived from AIS patients and cells overexpressing mut*POC5*.

Signal transduction pathways are activated by mechanical signals; these pathways include the MAPK signal pathway. The extracellular signal-regulated kinase (ERK), c-Jun N-terminal kinase (JNK), and p38 MAPK (p38), play an essential role in osteoblastic cell proliferation and differentiation. Specifically, ERK1/2 is involved in cell transformation, proliferation, and the survival of several cell types, including osteoblasts. Until now, it's not clear how the cells convert the mechanical signal into a biological signal (Yan, Gong et al. 2012).

In the present study, we found dissimilarity in the response to mechanical stress of POC5 expression, Acetylated-α-tubulin and TRPV4 (Fig. 1 A, B, C, D), MAPK signalling pathways (Fig. 2), mineralization (Fig. 5) and proliferation (Fig. 7), in NOB control osteoblasts and cells transfected with mut*POC5* gene. The impact of mechanical stress on cell signalling was established by checking the activation of ERK1/2, p38 MAPK and NF-κB in osteoblasts. Overall, the results of western blot and gene expression in the NOB and mut*POC5* expressing cells confirm the differential responses of these cells to mechanical stress and also the implication of TRPV4 signalling pathways in osteoblast response to stress. An interesting observation was that in mut*POC5* cells, in absence of mechanical loads, the levels of ERK1/2, p38 and NF-κB were higher than in normal cells. Moreover, in mut*POC5* cells non exposed to

stress, there was higher level of apoptosis than in normal cells (Fig. 8). Hence, expression of mut*POC5* could be inducing inflammatory response in osteoblasts and this response is augmented when exposed to stress. We also observed dissimilarity in the mode of activation of p38, ERK1/2 and NFκB pathways in NOB and mut*POC5* cells. The mut*POC5* expressing osteoblasts showed a higher downregulation in, p38, NF-κB activity than NOB cells when exposed to stress. There were differences in the effects of agonists and antagonist used on the signalling pathways examined in this study. Different degrees of stimulus could have different outcomes in the NF-κB activation, low tension inhibits while high stress activates the pathway. Not only the strength of the stimulus but also the type of stimulus, tonic vs oscillatory, determines the effect on NF-κB pathways. Mechanical forces are an important factor in the maintenance of bone mass (12), hence, NF-κB-mediated response to shear stress might be an important component. It was found that in the presence of shear stress, NF-κB stimulates osteoblastic differentiation via the prostaglandin synthesis (Granet, Boutahar et al. 2001, Chen, Geist et al. 2003). NF-κB was upregulated in NOB cells but downregulated in mutPOC5 cells (Fig. 2) and this explains why there was more apoptosis observed in mut*POC5* expressing cells (Fig. 8).

An important aspect of mechanical loading is that it regulates the bone structure and bone mass. It was shown that mechanical loading have anabolic effects while unloading of bone have bone resorbing effects. Our results show that there was increased mineralization of osteoblasts (Fig. 5) as well as increase in osteogenic markers (Fig. 6B). The mineralization of mut*POC5* cells was lower than in NOB cells. The pertinence of these observations lies in the possible connection of the mechanical stress with signalling pathways involved and the possible role of TRPV4 channel in AIS. In this work, we propose a model for the different effects of mechanical stress on normal and mut osteoblasts cells (Fig. 13). The mutation in POC5 affects the response to stress and induces different signalling pathways as compared to control cells.

Osteoblast exposure to mechanical stress also induced changes in the expression of Acetylated-α-tubulin. Application of mechanical stress on osteoblasts caused downregulation of cilia length as compared to non-treated cells and similarly in mut*POC5* cells. These findings go along with previous work studying the effect of mechanical stress on cilia, where

primary cilia were found to be shorter and less in number after exposure to periods of OFF compared with static controls (Delaine-Smith, Sittichokechaiwut et al. 2014). However, in our work mechanical stress induced osteogenesis and mineralization as detected by ALP staining (Fig. 4) and alizarin red staining (Fig. 5) as well as by studying the expression of bone forming factors (Fig. 6B). It's worth to note that mineralization and ALP were higher in NOB than in mut*POC5* cells. Also, *TRPV4* mRNA levels were strongly reduced in mut*POC5* differentiating cells in response to stress. TRPV4 has a role in the effects of force stimuli on calcium in osteoblasts (Suzuki, Notomi et al. 2013). *TRPV4* mRNA levels are increased throughout osteoblastic differentiation of primary osteoblast-enriched cell cultures and the osteoblastic cell line MC3T3-E1 (McNulty, Leddy et al. 2015) which goes along with our results.

There is increasing hypothesis about the primary cilium functions as mechanosensor in bone. However, little is known about the ability of primary cilium and the sensation of mechanical stress and bone formation. Defects in sensory function of the primary cilium is associated with a number of disease such as musculoskeletal diseases, like osteoarthritis (Temiyasathit, Tang et al. 2012) and osteoporosis (Wann and Knight 2012).

It was reported that loading causes Ca2+ increase and *COX-2* mRNA increase in osteocyte primary cilia (Lee, Guevarra et al. 2015). It was found that this effect of loading is initiated by TRPV4. By immunocytochemistry, it was found that TRPV4 mutant channel is a stretch-activated Ca2+-permeable channel and it localizes to the primary cilium and plasma membrane. The knockdown of TRPV4 channel lowered the Ca2+ release in the cilium induced by loading. These findings make TRPV4 as an interesting pharmacologic target for bone loss disease (Lee, Guevarra et al. 2015). Available agonists: 4α-PDD, GSK1016790A, and RN-1747 and antagonist: RN-1734. Mechanical strain plays a critical role in the proliferation, differentiation and maturation of bone cells. This prompted us to investigate the effect of mechanical load on cell apoptosis. The observation that apoptosis was induced in normal osteoblasts (Fig. 8) (as detected by propidium iodide staining) goes along with previous finding where large magnitude stretch induced apoptosis of osteoblasts (Song, Wang et al. 2016).

We were also interested in studying the impact of mechanical stress on subcellular localization of TRPV4. There were different effects of mechanical load on localization of TRPV4 in wt*POC5* and mut*POC5* expressing cells. TRPV4 had cytoplasmic localization in wt*POC5* but nuclear punctate pattern in mut*POC5* cells (Fig. 10). This suggests that the mutation in POC5 affects the subcellular locatization of TRPV4 which could be problematic in AIS. The TRPV4 channel translocates under shear stress as it was reported by Loot et al where TRPV4 translocated from the Golgi apparatus to the cell membrane in cultured human endothelial cells (Loot, Popp et al. 2008). Moreover, Cuajungco et al found that there was increased ratio of plasma membrane-associated versus cytosolic TRPV4 when they co-expressed TRPV4 and PACSIN 3. PACSIN 3 is a binding protein of TRPV4 and a of the PACSIN family (Cuajungco, Grimm et al. 2006). In addition to that, the membrane expression of TRPV4 was found to be enhanced by the microfilament-associated protein 7 (Suzuki, Hirao et al. 2003) as well as by kinases of the WNK family that have been reported to influence the function and localization of TRPV4 (Fu, Subramanya et al. 2006).. In the present study, TRPV4 protein was shown with unusual distribution profiles, dominant in the nuclear region in non stressed cells and within the cytoplasmic region in stressed wtPOC5 expressing cells. More importantly, TRPV4 protein moved out of the nucleus in response to stress in wtPOC5 but failed to translocate in mutPOC5 expressing cells. These results strongly suggested that TRPV4 protein could shuttle into and out of the nucleus.

TRPV4 null mice have no staining for TRPV4 in retinal ganglion cell layer (RGCL) (Ryskamp, Witkovsky et al. 2011). Defect in cilia was found to reduce the number of RGC with respect to photoreceptors. The impairment of cilia result in RGCL generation and/or differentiation (Lepanto, Davison et al. 2016). As both POC5 and TRPV4 are ciliary proteins, we hypothesized that the knockdown of poc5 has similar consequences on the GCL as in the case of the absence of trpv4 channel. We observed disorganization and reduction of staining of trpv4 in the connecting cilium (CC) of mutpoc5 retina. The cilium of the CC in mutpoc5 retina was significantly shorter than wtpoc5. Evidence supports the role of the primary cilia as pressure-sensing organelles in the retina. The defect at the level of the cilium causes improper

functioning of the TRP vanilloid 4 (TRPV4) channel. This leads to increased intraocular pressure (IOP) (Luo, Conwell et al. 2014).

Also, We successfully showed degeneration of retinal ganglion cell layer (RGCL) in mutpoc5 retina by annexin 5 staining (Fig. 11, 12). In healthy RGCL, TRPV4 plays as an essential osmoreceptor. It is possible that TRPV4 channel is implicated in the initiation and progression of glaucomatous remodeling. Glaucoma is an optic neuropathy which is characterized by elevated IOP, the cause of irreversible blindness in the world (Kwon, Fingert et al. 2009, Quigley 2011). Lowering the eye pressure is the only way to treat glaucoma (Zhang, Zhang et al. 2012). The degeneration of retinal ganglion cells is the major cause of vision loss. The elevated IPO is due to defects in the function of the Trabecular meshwork (TM) that is in charge of the drainage of the majority of aqueous fluid (Nickells, Semaan et al. 2008, Kaufman and Rasmussen 2012). The mechanism through which the elevated pressure leads to aberrant mechanosensory signaling that leads to vision loss is not well described. In this work, we postulate that the defect in mechanosensation would be a contributing factor in glaucoma. The normal expression of POC5, a ciliary protein, is important factor for the formation of normal cilia length (in the CC) and for ganglion cell layer. It was found that the trabecular meshwork cell cilia are essential for the regulation of pressure (Luo, Conwell et al. 2014). When these cilia are defective, this will contribute to the pathogenesis of glaucoma. In mutpoc5 retina, we observed lower staining of acetylated-α-tubulin in the OPL and INL. This defect might contribute to high pressure in the eye and as a consequence increased apoptosis as detected by annexin 5 staining. .

The presented work contributes to the understanding of the molecular mechanisms underlying AIS. Specifically, it focuses on the differential pathways activated in normal and patient cells. Untill now, there is no connection between scoliosis and the retinal phenotype that we observed. Thus, future work should focus on studying functional consequences of the degeneration of RGCL in the mutpoc5 zebrafish. The progressive loss of RGCL causes glaucoma through apoptosis. The increased apoptosis is the primary step of glaucoma disease and it’s associated with severity of disease (Ryskamp, Witkovsky et al. 2011). In this study, we didn't study vision problems. Hence, it would be necessary in future work to consider studying visual motor response (VMR), as a measurement of retinal function in zebrafish.

References:

Altaf, F., A. Gibson, Z. Dannawi and H. Noordeen (2013). "Adolescent idiopathic scoliosis." BMJ **346**: f2508.

Azimzadeh, J., P. Hergert, A. Delouvee, U. Euteneuer, E. Formstecher, A. Khodjakov and M. Bornens (2009). "hPOC5 is a centrin-binding protein required for assembly of full-length centrioles." J Cell Biol **185**(1): 101-114.

Blair, H. C., Q. C. Larrouture, Y. Li, H. Lin, D. Beer-Stoltz, L. Liu, R. S. Tuan, L. J. Robinson, P. H. Schlesinger and D. J. Nelson (2017). "Osteoblast Differentiation and Bone Matrix Formation In Vivo and In Vitro." Tissue Eng Part B Rev **23**(3): 268-280.

Chen, N. X., D. J. Geist, D. C. Genetos, F. M. Pavalko and R. L. Duncan (2003). "Fluid shear-induced NFkappaB translocation in osteoblasts is mediated by intracellular calcium release." Bone **33**(3): 399-410.

Cuajungco, M. P., C. Grimm, K. Oshima, D. D'Hoedt, B. Nilius, A. R. Mensenkamp, R. J. Bindels, M. Plomann and S. Heller (2006). "PACSINs bind to the TRPV4 cation channel. PACSIN 3 modulates the subcellular localization of TRPV4." J Biol Chem **281**(27): 18753-18762.

Delaine-Smith, R. M., A. Sittichokechaiwut and G. C. Reilly (2014). "Primary cilia respond to fluid shear stress and mediate flow-induced calcium deposition in osteoblasts." FASEB J **28**(1): 430-439.

Everaerts, W., B. Nilius and G. Owsianik (2010). "The vanilloid transient receptor potential channel TRPV4: from structure to disease." Prog Biophys Mol Biol **103**(1): 2-17.

Fu, Y., A. Subramanya, D. Rozansky and D. M. Cohen (2006). "WNK kinases influence TRPV4 channel function and localization." Am J Physiol Renal Physiol **290**(6): F1305-1314.

Granet, C., N. Boutahar, L. Vico, C. Alexandre and M. H. Lafage-Proust (2001). "MAPK and SRC-kinases control EGR-1 and NF-kappa B inductions by changes in mechanical environment in osteoblasts." Biochem Biophys Res Commun **284**(3): 622-631.

Kaufman, P. L. and C. A. Rasmussen (2012). "Advances in glaucoma treatment and management: outflow drugs." Invest Ophthalmol Vis Sci **53**(5): 2495-2500.

Kwon, Y. H., J. H. Fingert, M. H. Kuehn and W. L. Alward (2009). "Primary open-angle glaucoma." N Engl J Med **360**(11): 1113-1124.

Lee, K. L., M. D. Guevarra, A. M. Nguyen, M. C. Chua, Y. Wang and C. R. Jacobs (2015). "The primary cilium functions as a mechanical and calcium signaling nexus." Cilia **4**: 7.

Lepanto, P., C. Davison, G. Casanova, J. L. Badano and F. R. Zolessi (2016). "Characterization of primary cilia during the differentiation of retinal ganglion cells in the zebrafish." Neural Dev **11**: 10.

Liedtke, W. B. (2007). TRPV Channels' Function in Osmo- and Mechanotransduction. TRP Ion Channel Function in Sensory Transduction and Cellular Signaling Cascades. W. B. Liedtke and S. Heller. Boca Raton (FL).

Loot, A. E., R. Popp, B. Fisslthaler, J. Vriens, B. Nilius and I. Fleming (2008). "Role of cytochrome P450-dependent transient receptor potential V4 activation in flow-induced vasodilatation." Cardiovasc Res **80**(3): 445-452.

Luo, N., M. D. Conwell, X. Chen, C. I. Kettenhofen, C. J. Westlake, L. B. Cantor, C. D. Wells, R. N. Weinreb, T. W. Corson, D. F. Spandau, K. M. Joos, C. Iomini, A. G. Obukhov and Y. Sun (2014). "Primary cilia signaling mediates intraocular pressure sensation." Proc Natl Acad Sci U S A **111**(35): 12871-12876.

McNulty, A. L., H. A. Leddy, W. Liedtke and F. Guilak (2015). "TRPV4 as a therapeutic target for joint diseases." Naunyn Schmiedebergs Arch Pharmacol **388**(4): 437-450.

Moore, C., F. Cevikbas, H. A. Pasolli, Y. Chen, W. Kong, C. Kempkes, P. Parekh, S. H. Lee, N. A. Kontchou, I. Yeh, N. M. Jokerst, E. Fuchs, M. Steinhoff and W. B. Liedtke (2013). "UVB radiation generates sunburn pain and affects skin by activating epidermal TRPV4 ion channels and triggering endothelin-1 signaling." Proc Natl Acad Sci U S A **110**(34): E3225-3234.

Nickells, R. W., S. J. Semaan and C. L. Schlamp (2008). "Involvement of the Bcl2 gene family in the signaling and control of retinal ganglion cell death." Prog Brain Res **173**: 423-435.

Nilius, B. and T. Voets (2013). "The puzzle of TRPV4 channelopathies." EMBO Rep **14**(2): 152-163.

Oliazadeh, N., K. F. Gorman, R. Eveleigh, G. Bourque and A. Moreau (2017). "Identification of Elongated Primary Cilia with Impaired Mechanotransduction in Idiopathic Scoliosis Patients." Sci Rep **7**: 44260.

Patten, S. A., P. Margaritte-Jeannin, J. C. Bernard, E. Alix, A. Labalme, A. Besson, S. L. Girard, K. Fendri, N. Fraisse, B. Biot, C. Poizat, A. Campan-Fournier, K. Abelin-Genevois, V. Cunin, C. Zaouter, M. Liao, R. Lamy, G. Lesca, R. Menassa, C. Marcaillou, M. Letexier, D. Sanlaville, J. Berard, G. A. Rouleau, F. Clerget-Darpoux, P. Drapeau, F. Moldovan and P. Edery (2015). "Functional variants of POC5 identified in patients with idiopathic scoliosis." J Clin Invest **125**(3): 1124-1128.

Quigley, H. A. (2011). "Glaucoma." Lancet **377**(9774): 1367-1377.

Ryskamp, D. A., P. Witkovsky, P. Barabas, W. Huang, C. Koehler, N. P. Akimov, S. H. Lee, S. Chauhan, W. Xing, R. C. Renteria, W. Liedtke and D. Krizaj (2011). "The polymodal ion channel transient receptor potential vanilloid 4 modulates calcium flux, spiking rate, and apoptosis of mouse retinal ganglion cells." J Neurosci **31**(19): 7089-7101.

Shapiro, I. M., W. J. Landis and M. V. Risbud (2015). "Matrix vesicles: Are they anchored exosomes?" Bone **79**: 29-36.

Song, F., Y. Wang, D. Jiang, T. Wang, Y. Zhang, H. Ma and Y. Kang (2016). "Cyclic Compressive Stress Regulates Apoptosis in Rat Osteoblasts: Involvement of PI3K/Akt and JNK MAPK Signaling Pathways." PLoS One **11**(11): e0165845.

Suzuki, M., A. Hirao and A. Mizuno (2003). "Microtubule-associated [corrected] protein 7 increases the membrane expression of transient receptor potential vanilloid 4 (TRPV4)." J Biol Chem **278**(51): 51448-51453.

Suzuki, T., T. Notomi, D. Miyajima, F. Mizoguchi, T. Hayata, T. Nakamoto, R. Hanyu, P. Kamolratanakul, A. Mizuno, M. Suzuki, Y. Ezura, Y. Izumi and M. Noda (2013). "Osteoblastic differentiation enhances expression of TRPV4 that is required for calcium oscillation induced by mechanical force." Bone **54**(1): 172-178.

Temiyasathit, S., W. J. Tang, P. Leucht, C. T. Anderson, S. D. Monica, A. B. Castillo, J. A. Helms, T. Stearns and C. R. Jacobs (2012). "Mechanosensing by the primary cilium: deletion of Kif3A reduces bone formation due to loading." PLoS One **7**(3): e33368.

Villemure, I. and I. A. Stokes (2009). "Growth plate mechanics and mechanobiology. A survey of present understanding." J Biomech **42**(12): 1793-1803.

Wann, A. K. and M. M. Knight (2012). "Primary cilia elongation in response to interleukin-1 mediates the inflammatory response." Cell Mol Life Sci **69**(17): 2967-2977.

Weisz Hubshman, M., S. Broekman, E. van Wijk, F. Cremers, A. Abu-Diab, K. Samer, S. Tzur, I. Lagovsky, P. Smirin-Yosef, D. Sharon, L. Haer-Wigman, E. Banin, L. Basel-Vanagaite and E. de Vrieze (2017). "Whole-exome sequencing reveals POC5 as a novel gene associated with autosomal recessive retinitis pigmentosa." Hum Mol Genet.

Xu, L., F. Sheng, C. Xia, Y. Li, Z. Feng, Y. Qiu and Z. Zhu (2017). "Common variant of POC5 is associated with the susceptibility of adolescent idiopathic scoliosis." Spine (Phila Pa 1976).

Yan, Y. X., Y. W. Gong, Y. Guo, Q. Lv, C. Guo, Y. Zhuang, Y. Zhang, R. Li and X. Z. Zhang (2012). "Mechanical strain regulates osteoblast proliferation through integrin-mediated ERK activation." PLoS One **7**(4): e35709.

Young, M. F., J. M. Kerr, K. Ibaraki, A. M. Heegaard and P. G. Robey (1992). "Structure, expression, and regulation of the major noncollagenous matrix proteins of bone." Clin Orthop Relat Res(281): 275-294.

Zhang, K., L. Zhang and R. N. Weinreb (2012). "Ophthalmic drug discovery: novel targets and mechanisms for retinal diseases and glaucoma." Nat Rev Drug Discov **11**(7): 541-559.

Figure 1. Different regulatory mechanisms of the expression of ciliary genes in NOB and mut*POC5* expressing osteoblasts. Expression of ciliary genes *POC5* (A), *Acetylated-α-tubulin* (B) and *TRPV4* (C) were examined by qPCR in response to stress (1g/cm2) in the absence or presence of different agonists and antagonists for TRPV4 10μM (RN-1747), 10 μM (RN-1734) and 10 μM PKA antagonist (H89) (*p<0.05, **p<0.01). (D) Protein expression of Acetylated-α-tubulin, POC5 and TRPV4 was assessed by western blot. β-actin was used as loading control. For quantification of band intensity, Image j was used and the fold change with respect to control (-stress) was calculated (n=3). The results are mean ± SD from three independent experiments.

Figure 2. Mechanical stress induces changes in ERK1/2, and p38α and NFκB through TRPV4. A) Western blot was performed on osteoblast cells, NOB and cells overexpressing the mut*POC5*, and then exposed and non exprosed to 1g/cm2 of stress for 6h in the presence of TRPV4 agonist (RN-1747) and antagonist (RN-1734). Total p38 and ERK1/2 as well as phosphorylated ERK1/2 and p38 was determined by specific antibodies. The ERK1/2 activation was detected by the phosphorylation of Thr202/Tyr204 residues and for p38 by the phosphorylation of Thr180/Tyr182. Activation of NF-κB was determined by studying the phosphorylation p65 (Ser536). β-actin was used as loading control. Relative intensities are represented as the fold changes of the phosphorylated protein levels normalized to the total protein levels. Data are presented as the mean ± SD of three independent experiments (n=3).

Figure 3. Different regulatory mechanisms of gene expression on osteogenic factors in NOB and mut*POC5* osteoblasts. A) Gene expression analysis of bone formation markers in NOB and mutPOC5 cells. (B, C, D) Osteoblasts that are expressing the mutPOC5 and non expressing were exposed to 1g/cm2 stress in the absence and presence of antagonists of different pathways, H-89 for PKA and RN-1734 for TRPV4, as well TRPV4 agonist RN-1747. Markers for bone formation like the genes for *osteopontin* (B), *osteocalcin* (C*)* and *RUNX2* (D) were examined. There exists a difference in the pathways induced in response to stress in normal NOB and mut*POC5* expressing cells. *GAPDH* was used as endogenous control for the normalization of expression levels of different genes. Experiment was performed in triplicates and data are presented as the mean ± SD *p<0.05, **p<0.01.

Figure 4. Mechanical stress induces osteoblast differentiation in both NOB and mut*POC5* expressing cells with lower levels in mut*POC5* cells. A) Normal Osteoblasts (NOB) and mut*POC5* expressing cells were exposed to stress. Morphology of primary osteoblasts and mut*POC5* cells and alkaline phosphatase (ALP) activity was analyzed in determination of optimal effects of stress. Induction with mechanical stress significantly upregulated alkaline phosphatase expression in normal osteobalsts but not mut*POC5*

expressing cells. B) Quantification of ALP concentration (mg/ml) for different conditions at wavelength 405nm. Reading was performed in triplicates. *p<0.01, ** p<0.005,***p<0.001.

Figure 5. Increased deposition of bone mineral (calcium phosphate) by osteoblasts stimulated with mechanical stress. A) Red color is a marker for the reaction between calcium ions and alizarin red dye. There was increased mineralization in response to stress in both NOB and mutPOC5 cells. B) Quantification of alizarin staining using microplate reader at 405 nm. Reading was performed in triplicates. p-values < 0.05 were considered as statistically significant

Figure 6. Up regulation of bone differentiation markers in mineralized normal cells but not mut*POC5* cells. A) *TRPV4* and *Acetylated-α-tubulin* gene expression in mineralizing cells was examined in response to stress in NOB and mut*POC5* cells. B) Gene expression of different osteogenic markers (*osteocalcin (OS), Runt-related transcription factor 2 (RUNX2), alkaline phosphatase (ALP)* and *osteopontin (OP)* in normal (NOB) and mut*POC5* cells exposed and non exposed to stress by qPCR. *GAPDH* was used as endogenous housekeeping gene. Data are presented as the mean ± SD in triplicates. *p<0.05, **p<0.01,***p<0.001

Figure 7. Induction of *COX-2* expression by 1.5g/cm2 of mechanical stress in NOB and to lesser extent in mut*POC5* osteoblasts. Expression levels of *COX2* was studied in NOB and mut*POC5* expressing cells non exposed and exposed to 1.5g/cm2 of mechanical load. Very strong induction of *COX2* was obtained in normal NOB and to lesser extent in mut*POC5* cells in response to stress. Expression level of *COX2* was normalized to *GAPDH*. PCR products were run on gel to confirm the product expected size and for the quantification of the band intensity. Data are presented as the mean ± SD in triplicates. ***p<0.001.

Figure 8. Mut*POC5* expressing cells undergo apoptosis in response to stress at higher level than NOB. 1g/cm2 of stress was applied to NOB and mut*POC5* osteoblasts and then apoptosis was detected by propidium iodide staining (PI). In the absence of mechanical stress, mut*POC5* cells have higher apoptosis levels (c) than NOB (a). Application of stress strongly induces apoptosis in mut*POC5* cells (d) as detected by PI staining in red and to lesser extent in NOB (b). PI in red and DAPI in blue.

Figure 9: Mechanical stress induces ciliary retraction in NOB and mut*POC5* expressing osteoblasts. A) Staining for cilia was performed using specific antibody that stains cilia which is Acetylated-α-tubulin. Osteoblasts (NOB) and cells overexpressing mut*POC5*, were exposed to mechanical stress of weight of 1g/cm2. In NOB and in mut*POC5* cells, cilia were observed as protrusion from the nucleus (a, c) (red), although its shorter in mut*POC5* expressing cells (c). When exposed to stress, cilia were retracted, and almost lost in both NOB and mut*POC5* osteoblasts (b, d). Acetylated-α-tubulin (red) and DAPI as counterstain (blue). Scale bar 20μm. Magx40. B) Cilia length in NOB and mut*POC5* cells non exposed and exposed to stress. Mechanical stress significantly affected NOB and mut*POC5* cilia length. In the absence of stress, NOB had longer cilia than cells exposed to stress (*$p < 0.01$). Mut*POC5* expressing cells non exposed to stress had initially shorter cilia than NOB cells (***$p < 0.001$). Mechanical stress significantly reduced cilia length in mut*POC5* cells (**$p < 0.005$). B) Quantitation of changes in percentage of ciliated cells. The histogram shows the percentage of

total cilia in NOB and mut*POC5* cells non exposed and exposed to stress. Application of mechanical stress on NOB didn't significantly reduce cilia number. However, in mut*POC5* cells, following mechanical stress both the number of cilia was strongly reduced (***p<0.001). The cilia number and length was measured by ZEN software. Measurements were taken for at least 6 images. NS: non significant.

Figure 10: Mechanical stress induced differential subcellular localization of TRPV4. HeLa cells that are either expressing mock empty vector (a, b), wt*POC5*-myc tagged vector (c, d) and mut*POC5*-myc (e, f) tagged vector were induced by stress and the subcellular localization of TRPV4 was studied. In wt*POC5* expressing cells, mechanical stress application induced cytoplasmic localization of TRPV4 (d). However, in mut *POC5* expressing cells, TRPV4 has nuclear expression as punctate pattern (f). Scale bar 20µm. Magx40.

Figure 11: Altered staining of TRPV4 in the CC and RGCL in mut*poc5* zebrafish retina. a, b) In vivo, zebrafish retina of wt*poc5* and mut*poc5* were stained with trpv4 and acetylated-α-tubulin. Both proteins colocalizes in the outer segment layer (OS) and cone cell layer (CC) in both zebrafish as shown in the merged images. Zoomed images (c, d) shows less and disorganized staining of TRPV4 expression in mut retina in the CC (e, f, g, h). The staining shows absence of retinal ganglion cell layer (RGC) in the mut*poc5* retina. i) Diagram representing the length of connecting cilium (CC) in the retina of wt and mutpoc5 retina. Reduced cilium length in mutpoc5 retina (****p<0.0001). Cilium length was measured using ZEN software. P values was determined using t-test. OS: outer segment layer, CC: connecting cilium , RGCL: retinal ganglion cell layer.

Figure 12: Annexin 5 staining confirm the degeneration in the RGCL. Retinas of wt*poc5* and mut*poc5* zebrafish were stained with annexin5, a marker for apoptosis. There is strong expression of annexin 5 in the outer segment layer (OS), connecting cilium (CC) and retinal ganglion cell layer (RGCL) in the mut*poc5* retina. Very low expression of annexin 5 was detected in the OS, CC of wt*poc5* zebrafish. Scale bar 20µm. Magx40.

Figure 13: Proposed model for the differential effects of mechanical stress on different signalling pathways in wt*POC5* and mut*POC5* cells. In normal cells, mechanical stress activates the TRPV4 and as a consequence several pathways are activated including MAPK, PKA and NF-κB. These pathways regulate apoptosis, mineralization and activation of the COX2. All of this is important for the maintenance of normal bone density. However, in mut*POC5* expressing cells, there is deregulation of the MAPK pathways that causes increased apoptosis, lower mineralization due to downregulated osteopontin levels that end up in lower bone density.

Tables:

Primer Name	Primer Sequence	Product Size
GAPDH_S	5AGGAGTAAGACCCCTGGACC3	111bp
GAPDH_AS	5GGAGATTCAGTGTGGTGGGG3	
TRPV4_S	5ATGAGAGTGGCACCCCAGG3	285bp
TRPV4_AS	5GGTGACGATAGGTGCCGTAG3	
POC5_S	5CATGTCAGAGCCAGACAGGA3	96bp
POC5_AS	5GGAACGCCAGACTTTCCAGA3	
TUBA_S	5ACGTGCCTTTGTTCACTGGT 3	180bp
TUBA_AS	5AGCAGCACCTTTGTGACGTTT 3	
ALP_S	5ACACCTGGAAGAGCTTCAAACCGA3	401bp
ALP_AS	5TCCACCAAATGTGAAGACGTGGGA3	
OSTEOCALCIN_S	5ACACTCCTCGCCCTATTG3	249bp
OSTEOCALCIN_AS	5GATGTGGTCAGCCAACTC3	
RUNX2_S	5TCCGGAATGCCTCTGCTGTTATGA3	239bp
RUNX2_AS	5ACTGAGGCGGTCAGAGAACAAACT3	
OSTEOPONTIN_S	5CAGCCATGAATTTCACAGCC3	307bp
OSTEOPONTIN_AS	5GGGAGTTTCCATGAA GCCAC3	

Table 1: List of primers used in qPCR.

Antibody name	Species	Source	Dilution factor	Product size
Anti-POC5 antibody [EPR14000-76] - N-terminal	Rabbit	Abcam	1/250	63kDa
GPR128	Rabbit	Thermo scientific	1/250	83kDa
Acetylated-α-tubulin	Mouse	Sigma-aldriche	1/1000	55kDa
NFκB p65 (C-20)	Mouse	Santa Cruz	1/1000	65kDa
Phospho-NF-κB p65 (Ser536) (93H1)	Rabbit	Cell signalling technology	1/500	65kDa
Phospho-p44/42 MAPK (Erk1/2) (Thr202/Tyr204)	Rabbit	Cell signalling technology	1/500	42/44 kDa
Phospho-p38 MAP Kinase (Thr180/Tyr182)	Rabbit	Cell signalling technology	1/500	43kDa
TRPV4	Rabbit	Protein tech	1/500	98kDa
ESRβ	Rabbit	Santa Cruz	1/500	60kDa
β-actin	Mouse	Santa Cruz	1/500	42kDa

Table 2: List of Antibodies

Fig 1

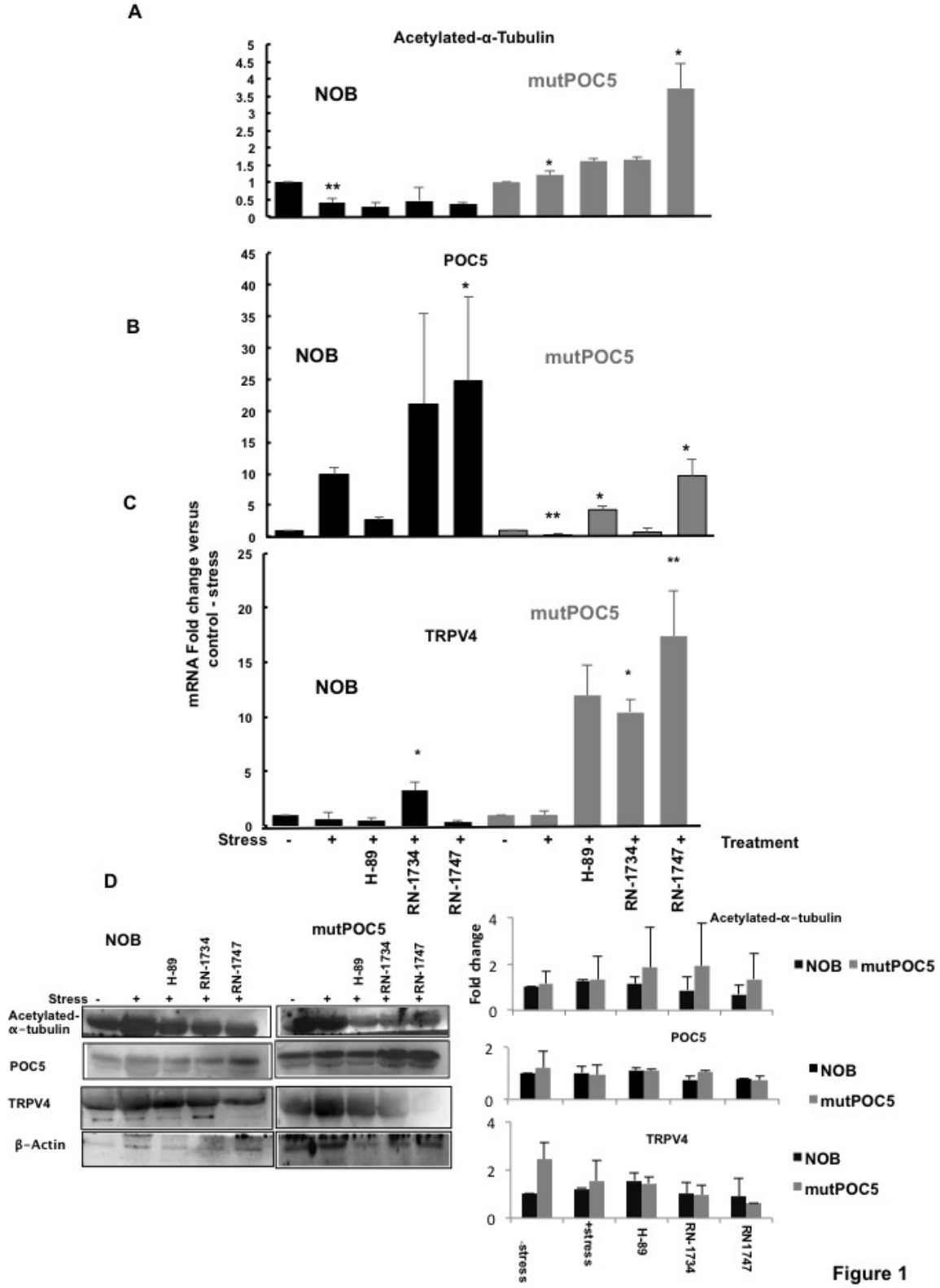

Figure 1

Fig 2

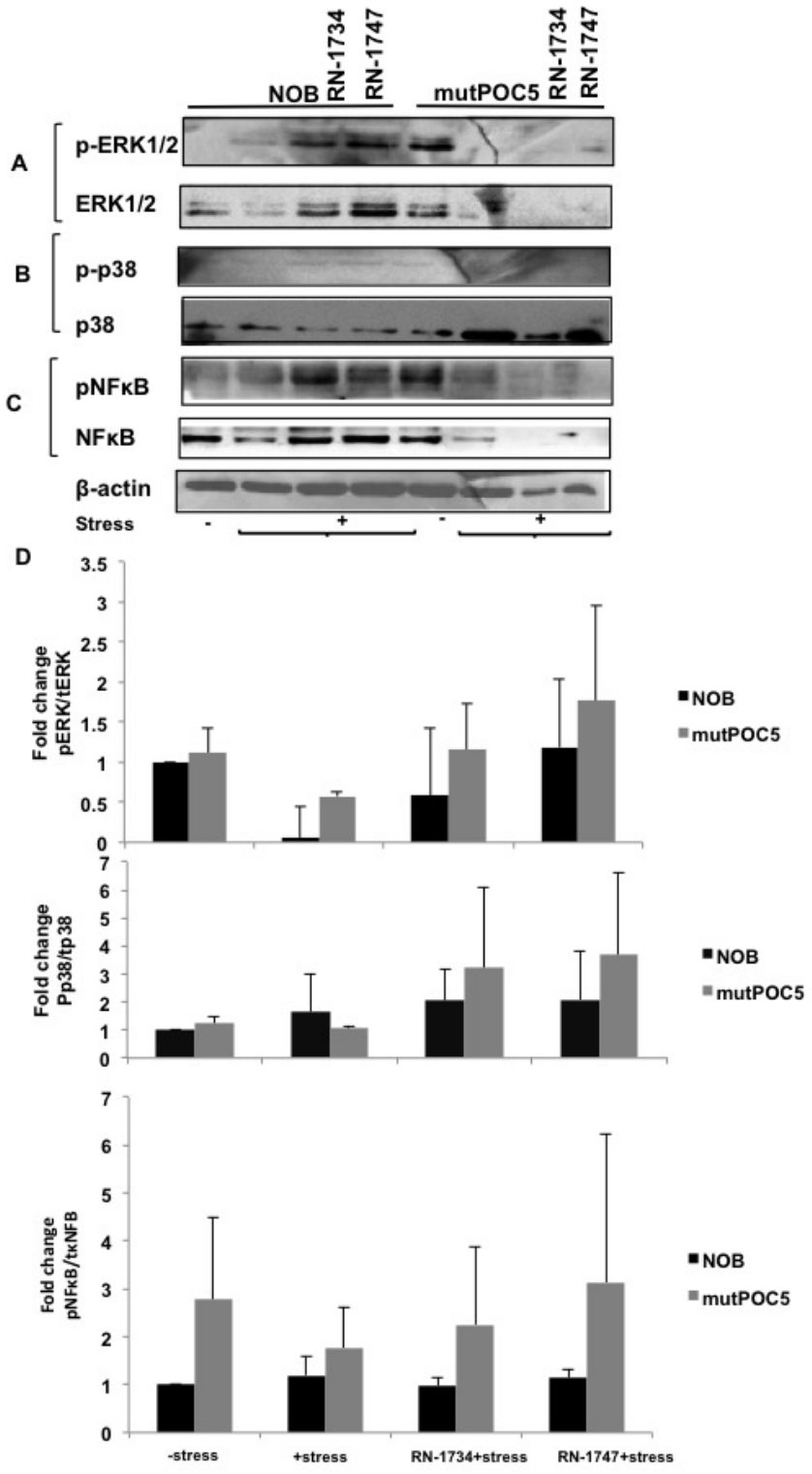
NOB
RN-1734
RN-1747
mutPOC5
RN-1734
RN-1747
A
p-ERK1/2
ERK1/2
B
p-p38
p38
C
pNFκB
NFκB
β-actin
Stress
-
+
-
+
D
Fold change pERK/tERK
Fold change Pp38/tp38
Fold change pNFκB/tκNFB
NOB
mutPOC5
-stress
+stress
RN-1734+stress
RN-1747+stress

Fig 3

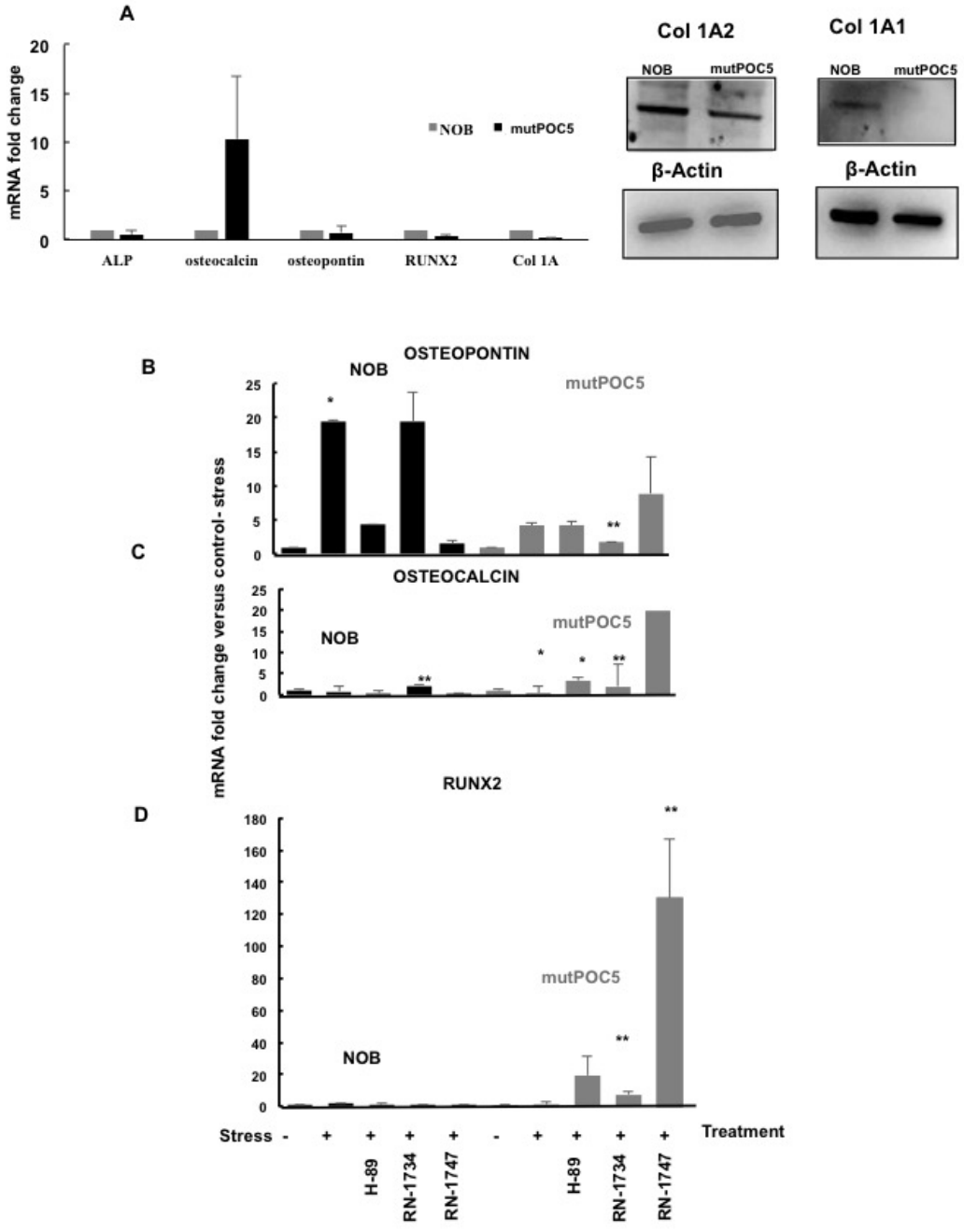
A
mRNA fold change
NOB
mutPOC5
ALP
osteocalcin
osteopontin
RUNX2
Col 1A
Col 1A2
Col 1A1
β-Actin
B
OSTEOPONTIN
C
OSTEOCALCIN
mRNA fold change versus control - stress
D
RUNX2
Stress
Treatment
H-89
RN-1734
RN-1747

Fig 4

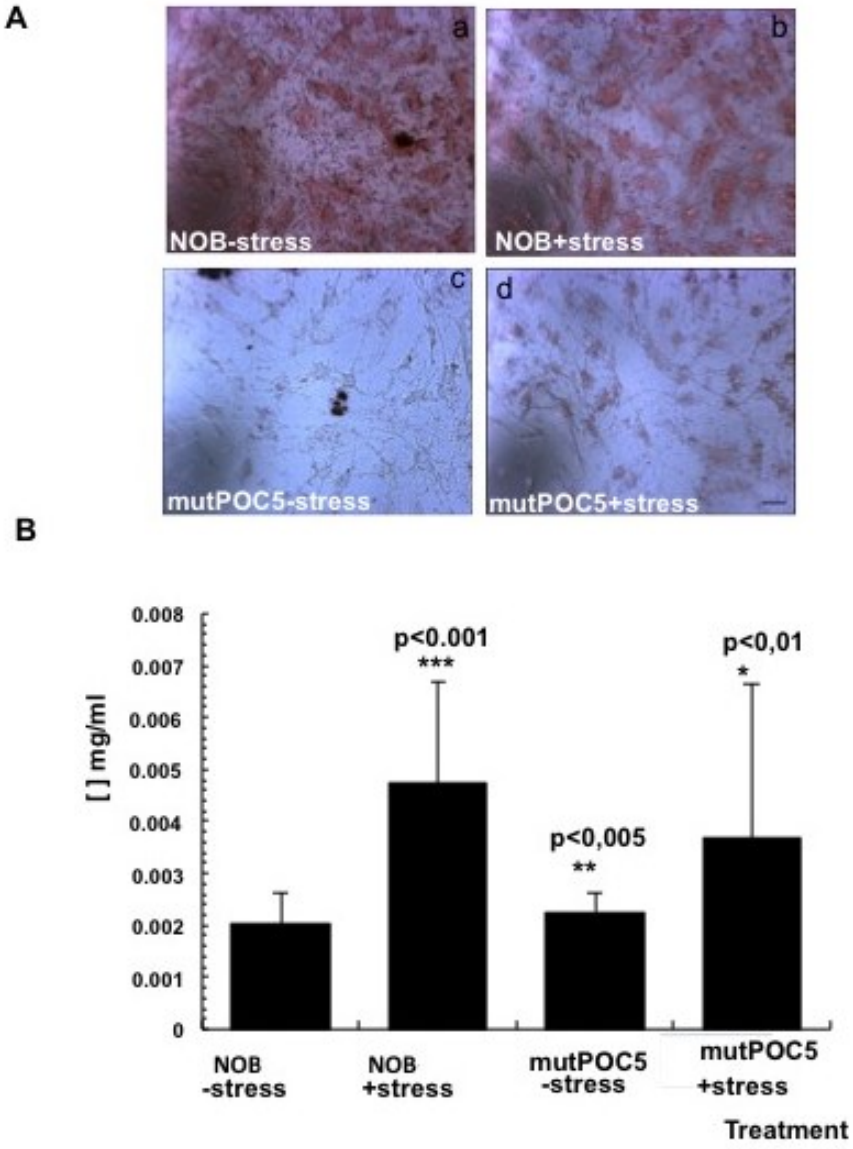
A
a
NOB-stress
b
NOB+stress
c
mutPOC5-stress
d
mutPOC5+stress
B
[ ] mg/ml
0.008
0.007
0.006
0.005
0.004
0.003
0.002
0.001
0
p<0.001
***
p<0,005
**
p<0,01
*
NOB -stress
NOB +stress
mutPOC5 -stress
mutPOC5 +stress
Treatment

Fig 5

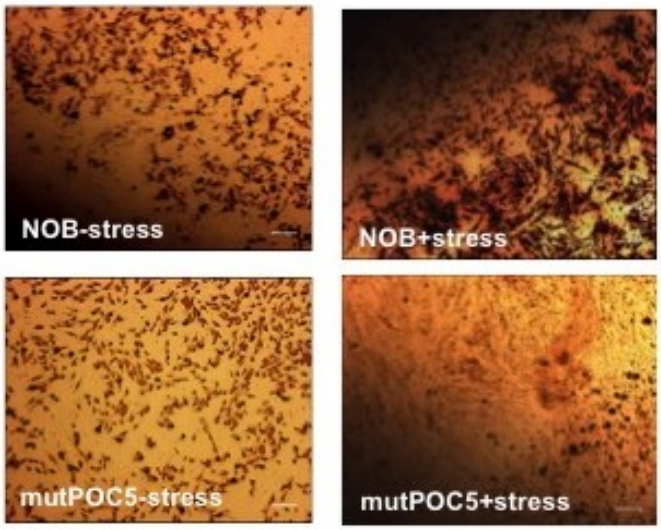
NOB-stress
NOB+stress
mutPOC5-stress
mutPOC5+stress

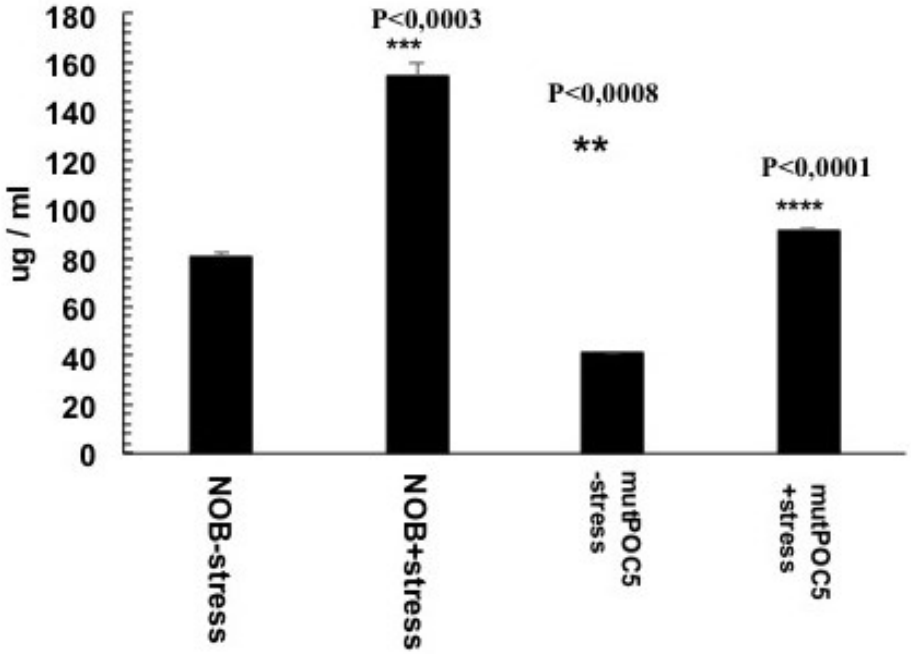
ug / ml
180
160
140
120
100
80
60
40
20
0
P<0,0003
***
P<0,0008
**
P<0,0001
****
NOB-stress
NOB+stress
mutPOC5 -stress
mutPOC5 +stress

Fig 6

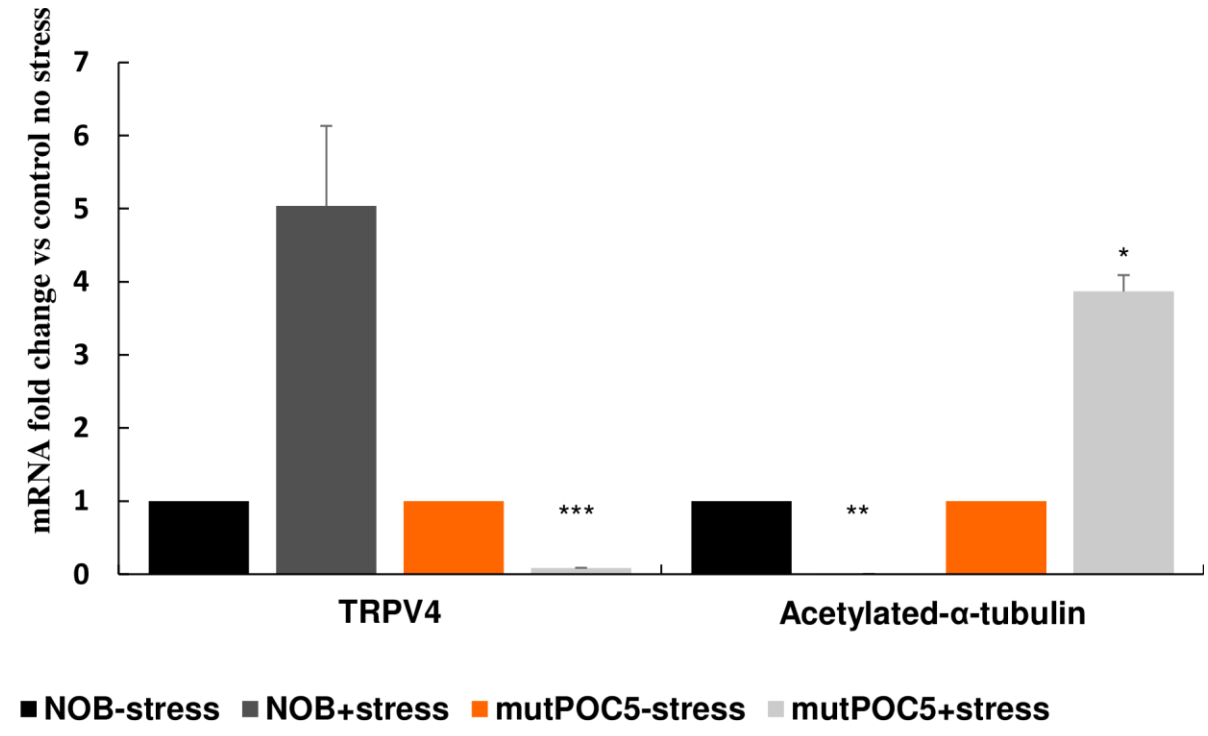
mRNA fold change vs control no stress
7
6
5
4
3
2
1
0
***
**
*
TRPV4
Acetylated-α-tubulin
NOB-stress
NOB+stress
mutPOC5-stress
mutPOC5+stress

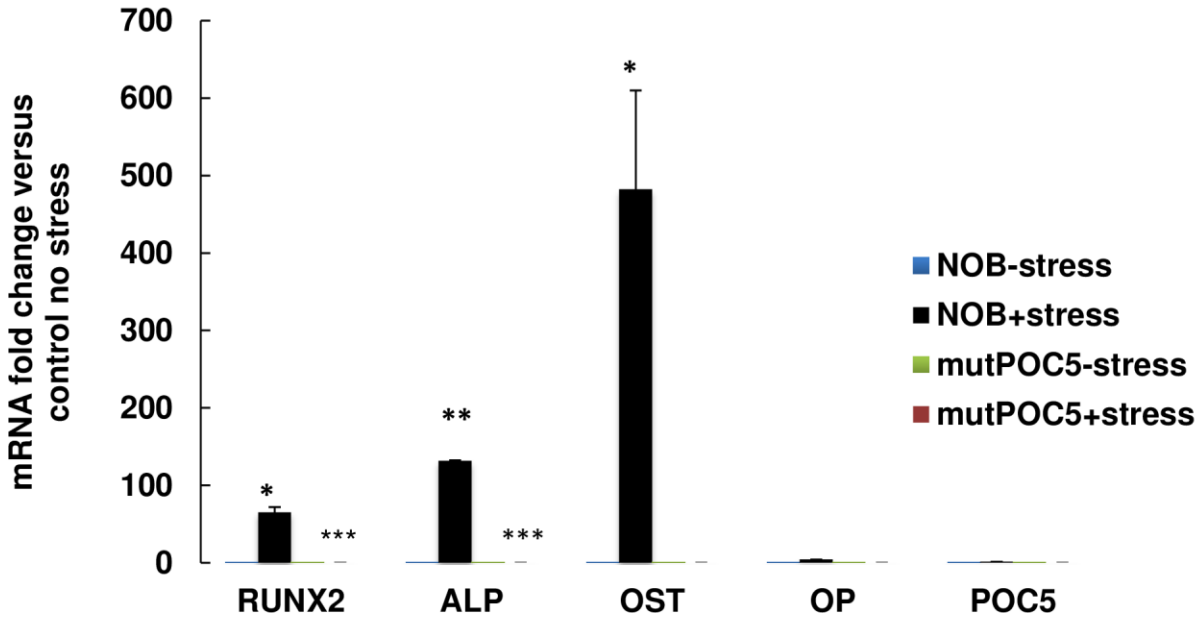
mRNA fold change versus control no stress
700
600
500
400
300
200
100
0
*
***
**
***
*
RUNX2
ALP
OST
OP
POC5
NOB-stress
NOB+stress
mutPOC5-stress
mutPOC5+stress

Fig 7

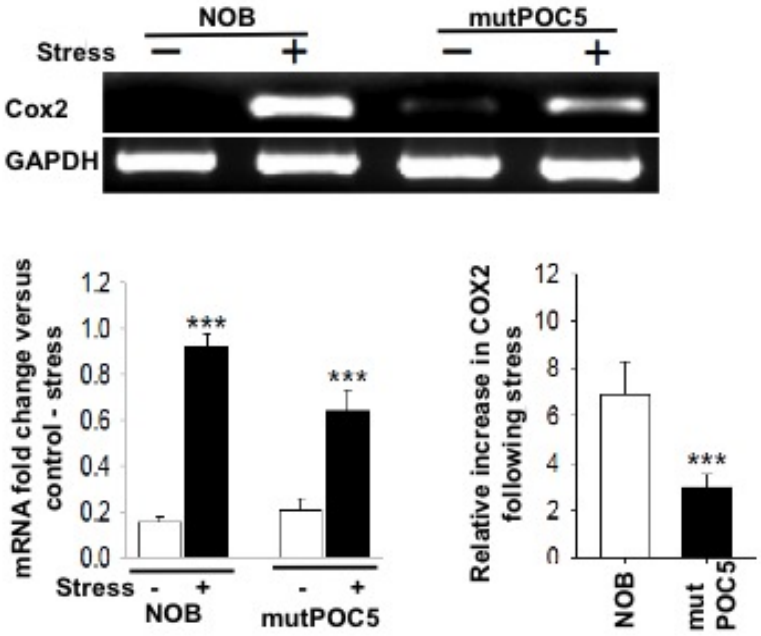
NOB
mutPOC5
Stress
–
+
–
+
Cox2
GAPDH
mRNA fold change versus control - stress
1.2
1.0
0.8
0.6
0.4
0.2
0.0
***
***
Stress
-
+
-
+
NOB
mutPOC5
Relative increase in COX2 following stress
12
10
8
6
4
2
0
***
NOB
mut POC5

Fig 8

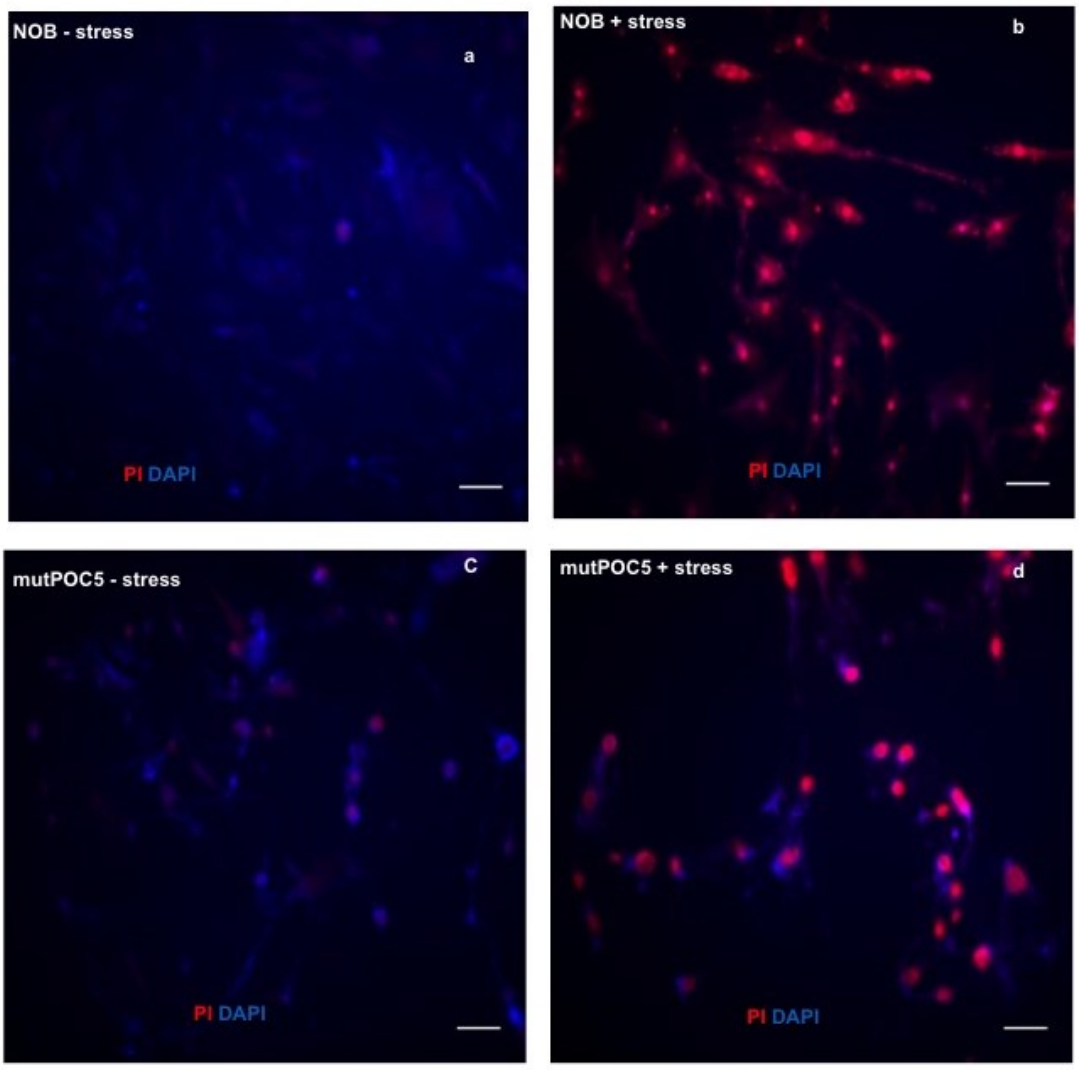
NOB - stress
a
PI DAPI
NOB + stress
b
PI DAPI
mutPOC5 - stress
c
PI DAPI
mutPOC5 + stress
d
PI DAPI

Fig 9

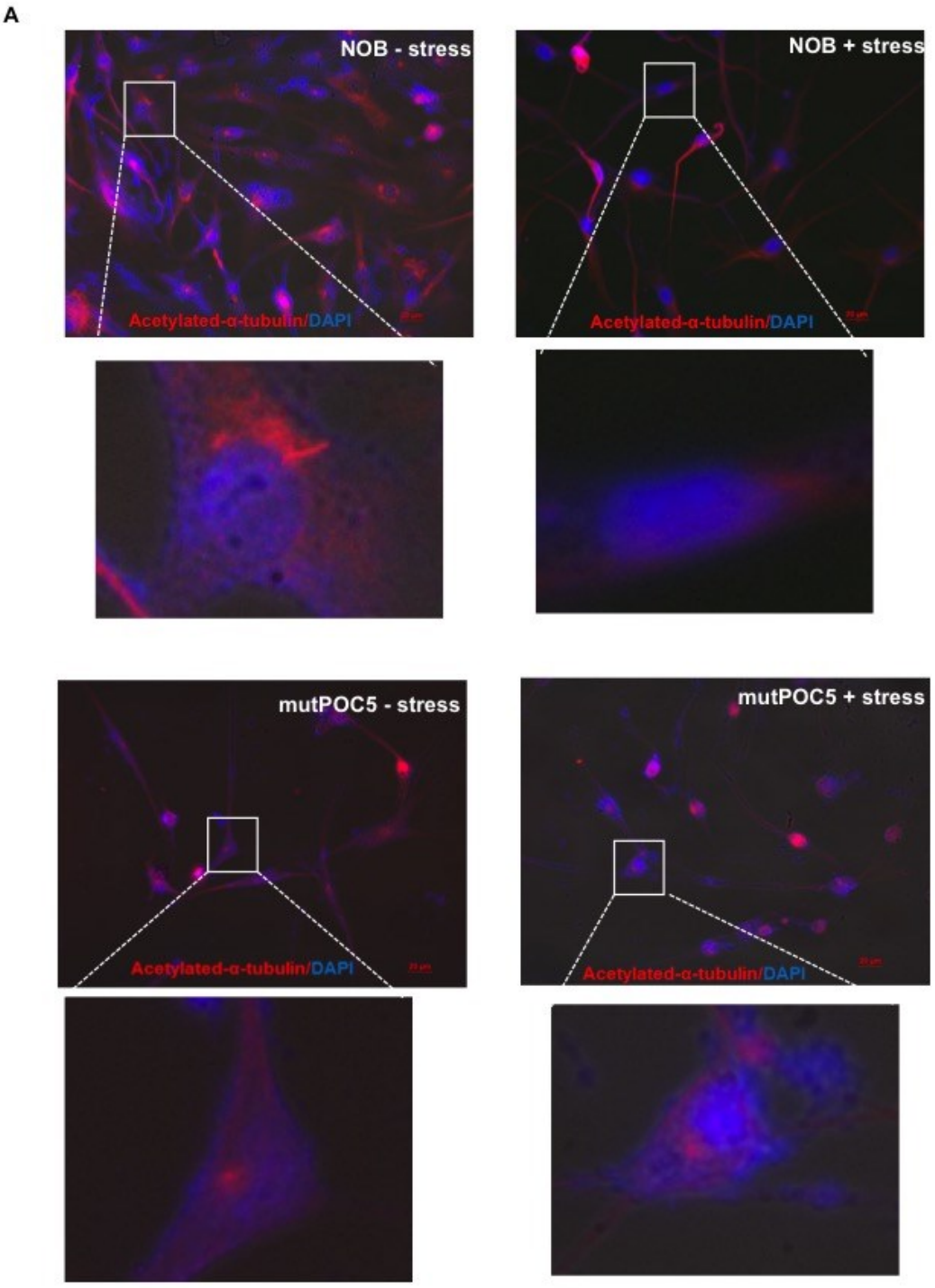
A
NOB - stress
Acetylated-α-tubulin/DAPI
NOB + stress
Acetylated-α-tubulin/DAPI
mutPOC5 - stress
Acetylated-α-tubulin/DAPI
mutPOC5 + stress
Acetylated-α-tubulin/DAPI

Fig 9

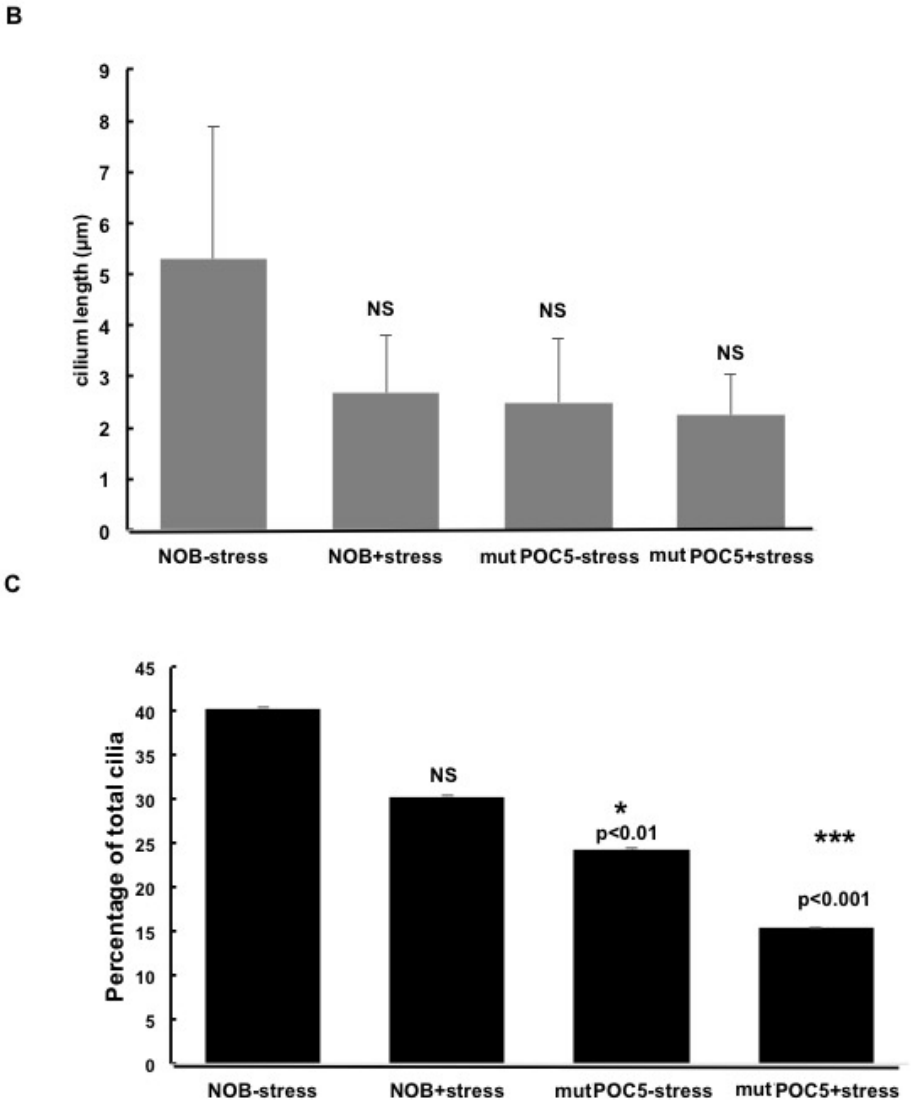
B
cilium length (µm)
9
8
7
6
5
4
3
2
1
0
NS
NS
NS
NOB-stress
NOB+stress
mut POC5-stress
mut POC5+stress
C
Percentage of total cilia
45
40
35
30
25
20
15
10
5
0
NS
*
p<0.01
***
p<0.001
NOB-stress
NOB+stress
mutPOC5-stress
mut POC5+stress

Fig 10

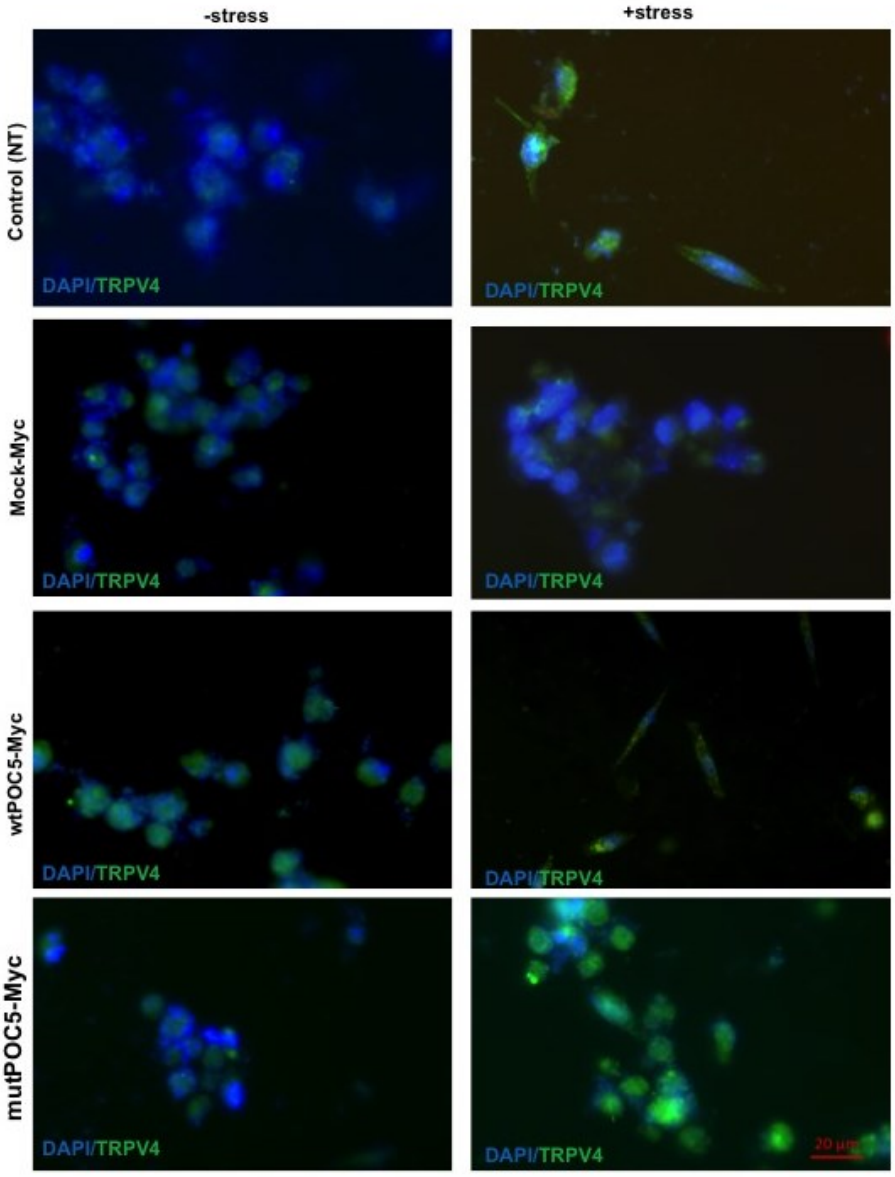
-stress
+stress
Control (NT)
Mock-Myc
wtPOC5-Myc
mutPOC5-Myc
DAPI/TRPV4
DAPI/TRPV4
DAPI/TRPV4
DAPI/TRPV4
DAPI/TRPV4
DAPI/TRPV4
DAPI/TRPV4
DAPI/TRPV4

Fig 11

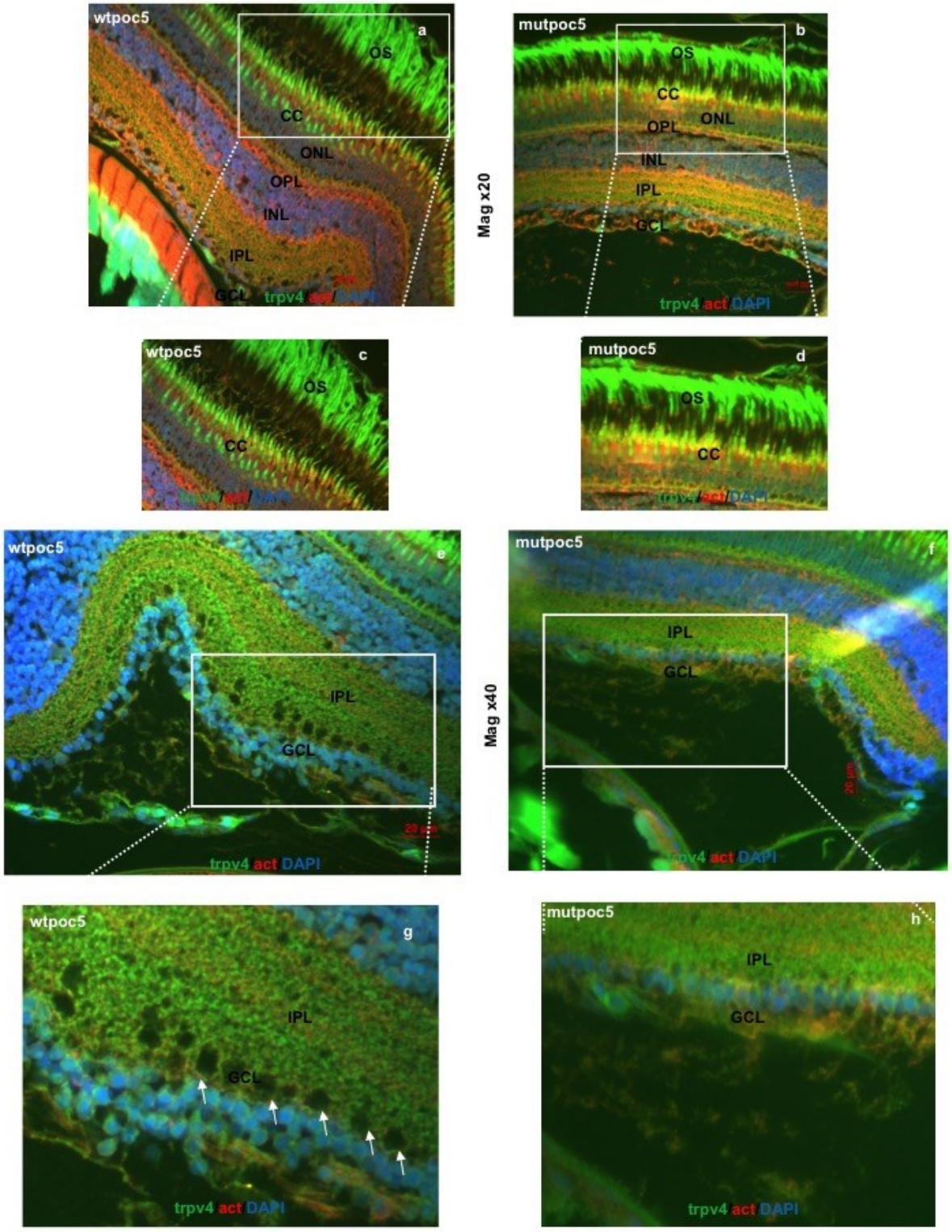
wtpoc5
a
OS
CC
ONL
OPL
INL
IPL
GCL
trpv4 act DAPI
mutpoc5
b
OS
CC
ONL
OPL
INL
IPL
GCL
trpv4 act DAPI
Mag x20
wtpoc5
c
OS
CC
mutpoc5
d
OS
CC
wtpoc5
e
IPL
GCL
trpv4 act DAPI
mutpoc5
f
IPL
GCL
trpv4 act DAPI
Mag x40
wtpoc5
g
IPL
GCL
trpv4 act DAPI
mutpoc5
h
IPL
GCL
trpv4 act DAPI

Fig 11

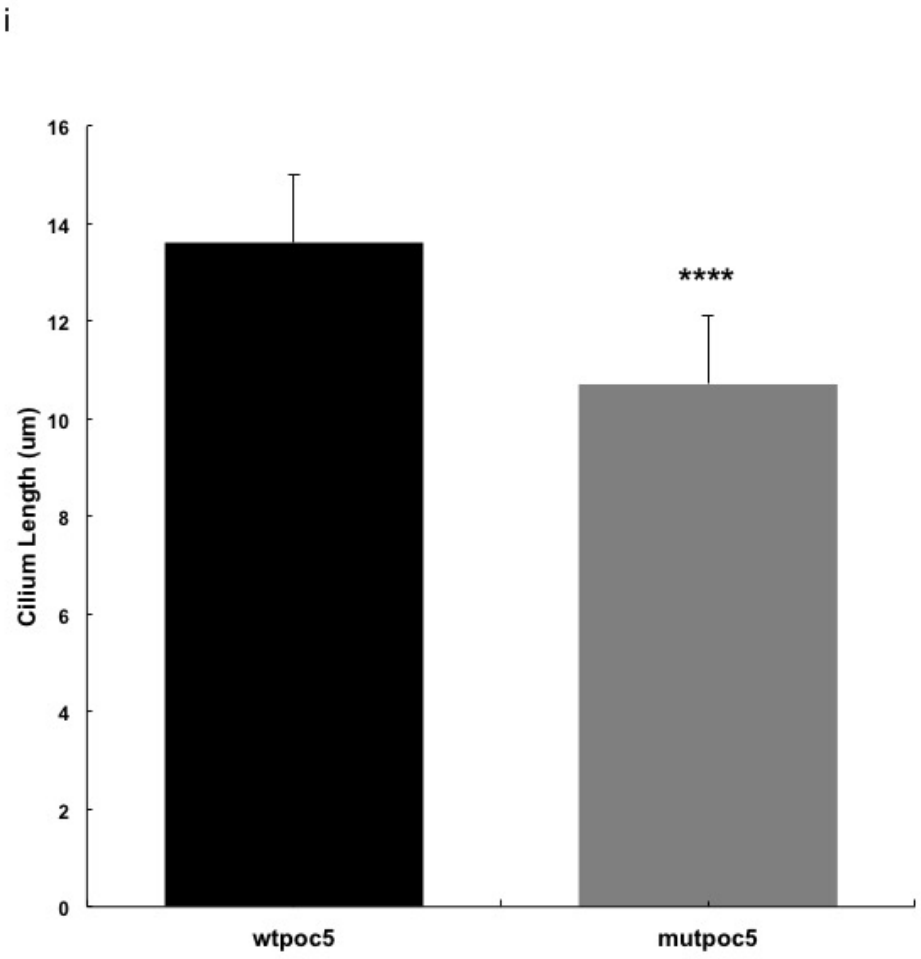

Fig 12

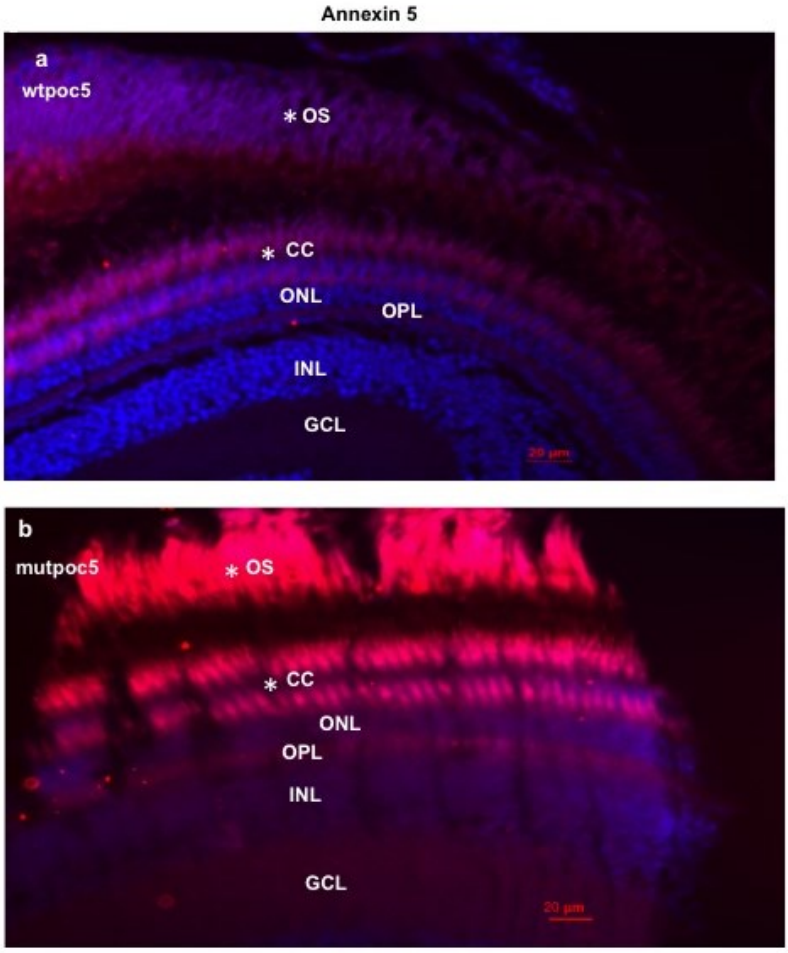
Annexin 5
a
wtpoc5
OS
CC
ONL
OPL
INL
GCL
b
mutpoc5
OS
CC
ONL
OPL
INL
GCL

Fig 13

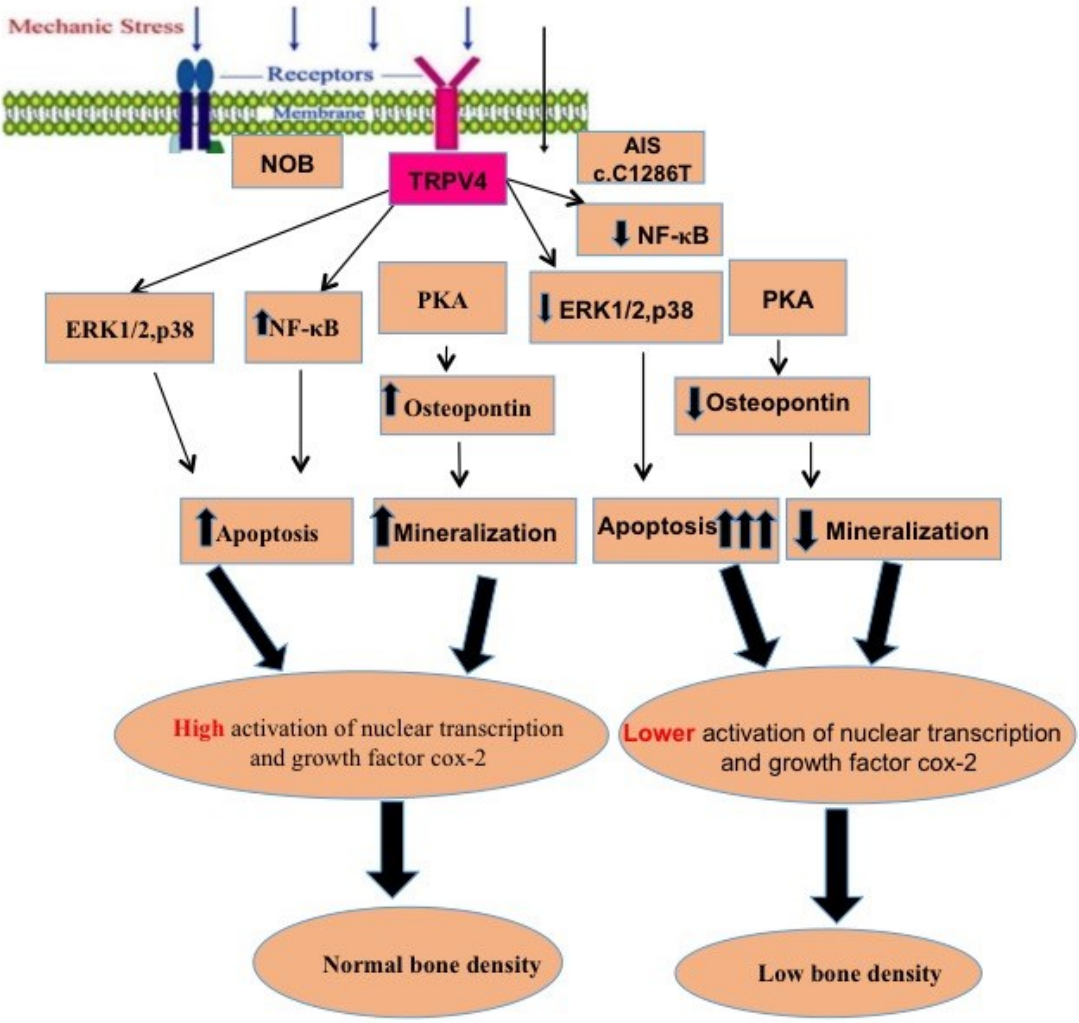
Mechanic Stress
Receptors
Membrane
NOB
TRPV4
AIS
c.C1286T
NF-κB
ERK1/2,p38
NF-κB
PKA
ERK1/2,p38
PKA
Osteopontin
Osteopontin
Apoptosis
Mineralization
Apoptosis
Mineralization
High activation of nuclear transcription and growth factor cox-2
Lower activation of nuclear transcription and growth factor cox-2
Normal bone density
Low bone density

CHAPTER IV: GENERAL DISCUSION

AIS is the most common form of scoliosis (more common in girls than in boys), and understanding the molecular pathways involved in AIS pathogenesis remains controversial and challenging. Our study revealed the contribution of two genes (*POC5* and *ADGRG7*) with regards to their regulation by E2 and to their expression in normal and AIS osteoblasts. This thesis demonstrated the role of mutated *POC5* in a ciliopathy underlying AIS pathogenesis.

In this thesis, I investigated the possible role of E2 and mechanical stress on human osteoblasts derived from AIS and normal patients. The two genes, *POC5* and *ADGRG7,* were selected for this study based on a recent publication from our lab where *POC5* and *ADGRG7* variants were identified in French families with scoliosis (Patten, Margaritte-Jeannin et al. 2015). The role of E2 in AIS is not clear, but seems to be critical given that E2 interplays with several factors participating in the initiation, development and progression of AIS; E2 affects 1) melatonin signaling, where there is a crosstalk between estrogen melatonin signalling, also, 2) E2 impact bone formation and resorption; 3) E2 amplify the response to strain and hence can modulate the loads of the spine and vertebral growth alteration; and 4) gene defects at the level of estrogen receptors (e.g. polymorphisms of *ESR1* gene [ERα]).

In this work, we reported the role of POC5 in AIS cells (Manuscript 1 and 3) and the regulation of ADGRG7 by E2 (Manuscript 2). We found that the two genes are upregulated by E2 at the gene and protein levels in normal and in osteoblasts from patients with scoliosis with the c. C1268T (p. A429V) in *POC5*. This work is important since it sheds light on two genes, *POC5* which is a centriolar protein that interacts with centrin and inversin genes (Azimzadeh, Hergert et al. 2009, Dantas, Daly et al. 2013) and *ADGRG7* whose function is not well described yet. *ADGRG7* is an adhesion GPCR where the function of this gene is poorly known. While no data confirms the causative relation between ADGRG7 and AIS, our hypothesis is that *ADGRG7* is a contributer gene in AIS.

We describe a new possible connection between E2 signalling pathway and the two genes in AIS. Through promoter studies, we identified the specific regions responsible for the

regulation of *ADGRG7* and *POC5*. *ADGRG7* was found to be regulated through indirect genomic signalling by SP1 and ESRα, while *POC5* is regulated though direct genomic signalling through ESRα. Both genes were upregulated in normal osteoblasts and to lesser extent in AIS cells with the mutation (c. C1268T; p. A429V).

Herein, we propose estrogen resistance mechanism in AIS. The idea of estrogen resistance is not original but the work on this topic is limited since previous reports found an estrogen resistance mechanism in humans carrying the mutation of the *ESR* gene. This mutation exists in exon 2 of *ESR*, a cytosine-to-thymine transition at codon 157 of both alleles, that results in a premature stop codon (Smith, Boyd et al. 1994). Male patients with this mutation had problems in bone development with clinical manifestations ranging from severely under mineralized skeleton with biochemical evidence of increased bone resorption and evidence of continued slow linear growth, markedly delayed skeletal maturation, and osteoporosis. On the other hand, in female, estrogen resistance resulted in the increased bone turnover (Quaynor, Stradtman et al. 2013). In our work, we found that cells overexpressing the *POC5* mutation (c. C1268T (p. A429V) had lower mineralization rate than control cells (data not shown). This goes along with the fact that patients with AIS have low bone mineralization and osteopenia (Cheng, Qin et al. 2000).

Overall, there is no data in literature that addresses the regulation of *POC5* and *ADGRG7* by E2, nor in the context of AIS or other skeletal disease.

The progression of spinal deformity in AIS patients progresses mainly during puberty. During this period of life, there is significant fluctuation of E2 levels. E2 increased with age and pubertal stage, more in girls than in boys, and there is a correlation with the increased growth velocity (Eastell 2005). Both puberty and growth are interrelated and it is well known that the influence of E2 on puberty and growth is very complex. The levels of GH and E2 have positive correlation with prepuberty in girls and boys. The sensitivity of GH is upregulated in pubertal children by endogenous E2. Indeed, there is strong link between GH and E2 throughout the female puberty period.

E2 exerts its effects through ESR whose expression was present in all maturation zones of the human growth plate during development and puberty. Increased secretion of estrogens and androgens are responsible for the pubertal growth spurt. The pubertal bone growth in females is induced by the hormone estrogen (Perry, Farquharson et al. 2008). Skeletal maturation and puberty affect curve progression and it's associated with genetic variations. Both human osteoblasts and osteoclasts express the *ESR* gene and mutation in this gene is associated with bone loss and delayed skeletal growth in humans. Hence, this suggests that the estrogen response to skeletal and sexual growth is determined by *ESR* gene polymorphism, this can be reflected by several findings that *ESR* polymorphisms is related to curve progression in IS (Smith, Boyd et al. 1994, Inoue, Minami et al. 2002, Nikolova, Yablanski et al. 2015). This in turn strongly supports the hypothesis that E2 is indeed involved in the etiology of AIS indirectly through regulating genes like *POC5* and *ADGRG7* in addition to other genes to be investigated.

We found that when we treat osteoblasts with E2, this caused multiPOC5 foci and POC5 amplification as well as loss of cilia (Manuscript 3, Fig. 1). This goes along with the work on Plk4 which associates with centrioles, either in basal bodies or centrosomes. Over-expression of Plk4 during development led to increased numbers of centrosomes in the basal epidermis and a loss of primary cilia. A primary cilium was still able to form alongside additional centrosomes in some hair follicle cells after *PLK4* overexpression but these primary cilia are abnormal in structure (Coelho, Bury et al. 2015). These findings complement our results on POC5. E2 treatment to osteoblasts causes POC5 amplification as well as the formation of abnormal cilia (Fig. 5)

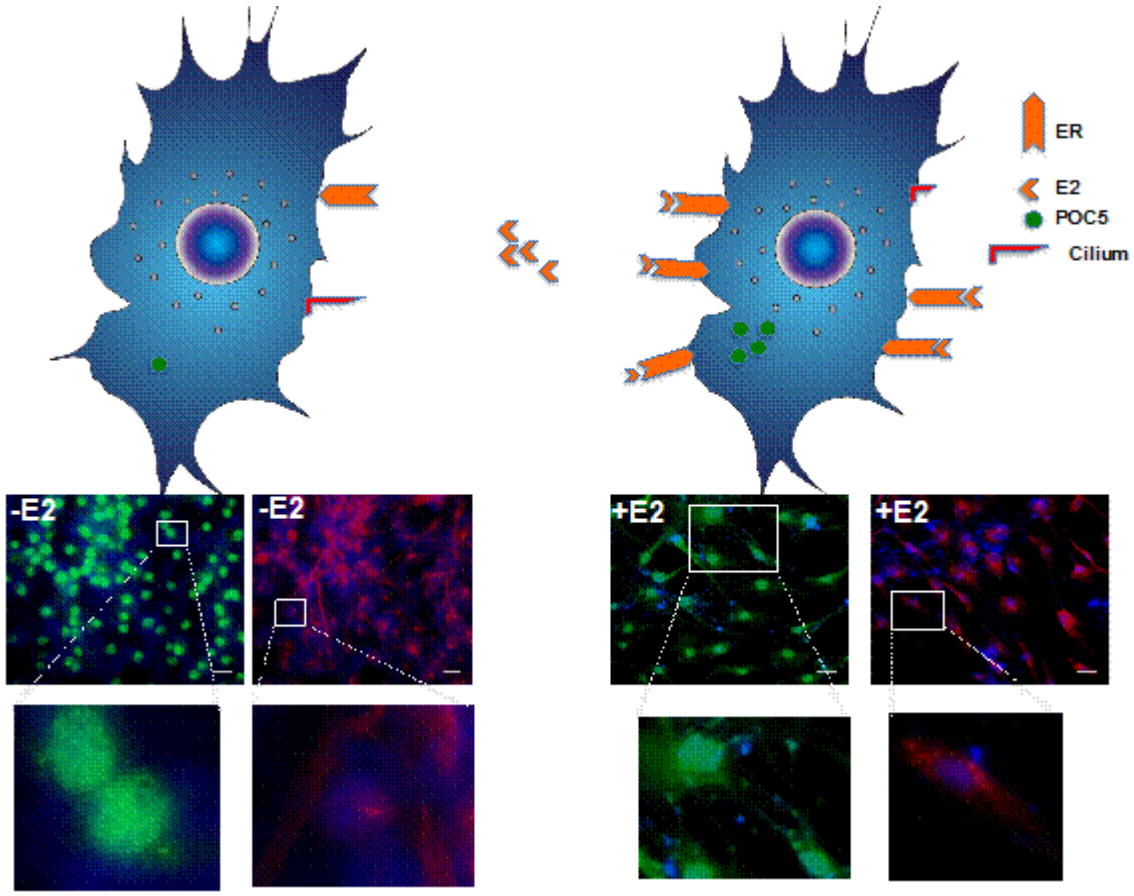

Figure 5: Scheme showing the effects of E2 on POC5 expression and cilia. E2 treatment to osteoblasts causes an upregulation of POC5 expression detected as multi foci. In E2 treated cells, there is centriole amplification and ciliary retraction (acetylated-α-tubulin). Dapi in blue, POC5 in green, Cilia in red. Scale bar 20 μm.

Our finding corresponding to the regulation of POC5 and ADGRG7 regulation by E2 (Manuscript 2 and 3) reflects the participation of E2 in AIS. Possibly, during puberty, E2 regulate several genes, including *POC5* and *ADGRG7* in osteoblasts and given the role of POC5 in cell cycle, this might lead to defects in cell cycle and contribute to the pathogenesis of AIS. The disregulation of gene expression of *POC5* and *ADGRG7* in AIS could be one of the many contributing factors in AIS pathogenesis. SP1 mutations in collagen was found in osteopenic patients (Grant, Reid et al. 1996). Estrogen regulates collagen 1 expression, where in osteoblasts, E2 upregulates collagen 1 expression (Ernst, Schmid et al. 1988, Ireland, Bord

et al. 2002). We showed that both genes are expressed in control osteoblasts at higher level than in AIS cells. Both genes are upregulated by E2 (Fig. 6), but the significance of this upregulation and the exact roles of these genes in bone and skeletal development are still obscure. Our results suggest the implication of both POC5 and ADGRG7 in a role of the differentiation of skeletal elements and structural integrity of the vertebrae.

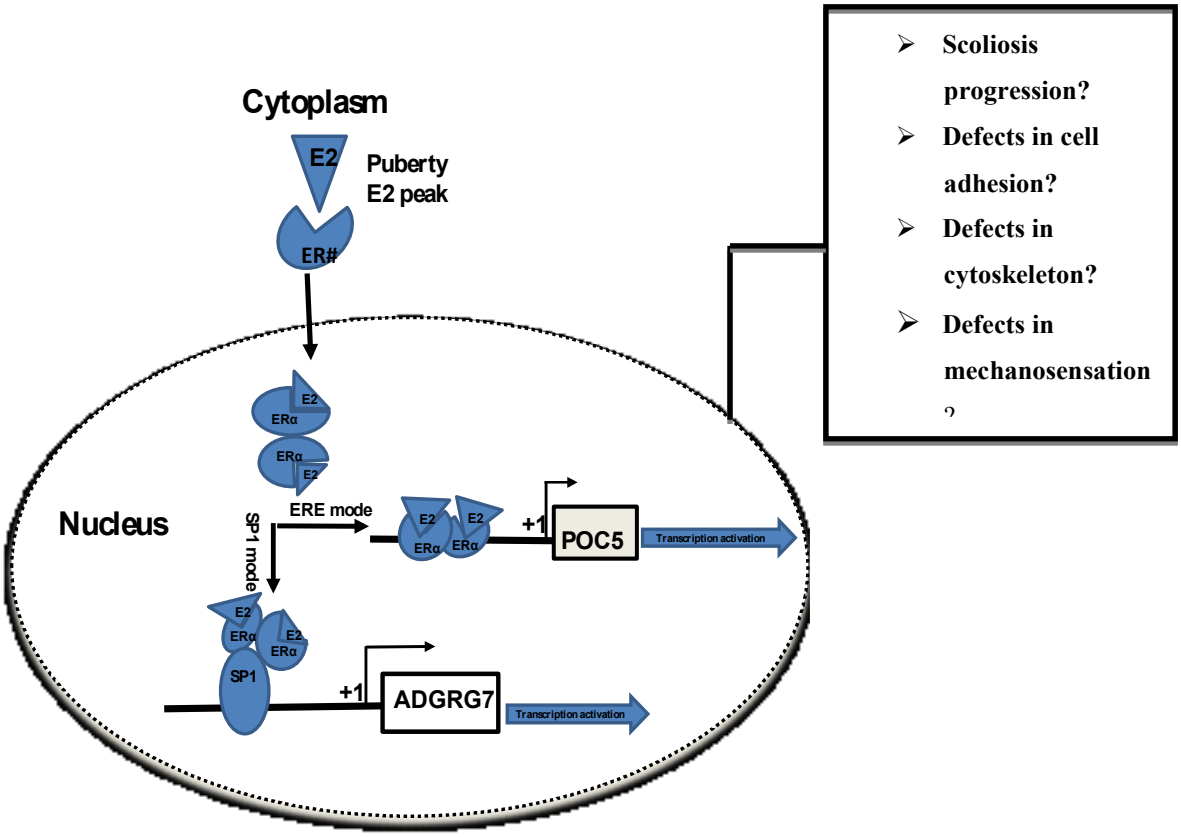

Figure 6: Model of *POC5* and *ADGRG7* transcriptional up-regulation following E2 exposure. Upon E2 exposure, ERα is activated and binds to the *ADGRG7* promoter through Sp1 binding sites. For *POC5*, there is direct binding of ERα promoter. The outcome is upregulation of *ADGRG7* and *POC5*. The physiological impact of upregulation of *POC5* and *ADGRG7* are yet to be investigated.

An important finding of our work is that POC5 is a ciliary protein and the mutation (c. C1286T; p. A429V) that was found in scoliotic patients affects the subcellular localization of POC5 with respect to cilia (Manuscript 1). The wtPOC5 was found to be located at the base of the cilium as detected by immunoflourescence. High expression level of acetylated-α-tubulin (cilia marker) was associated with wtPOC5 but not mutPOC5. By cell fractionation of cytoplasmic and nuclear proteins, we showed that wtPOC5 is expressed in both nuclear and cytoplasmic fractions with higher expression in the cytoplasm, while the mutPOC5 is solely expressed in the nucleus (Manuscript 1, Fig. 6). Several ciliary proteins were found to be interacting with wtPOC5 and not with mutPOC5. POC5 is known as a centriolar protein interacting with centrin (Azimzadeh, Hergert et al. 2009), however its role in cilium is not very well described. The importance of our work is that it introduces *POC5* as a ciliary gene that is located at the base of the cilium (as confirmed by centrin2 staining, Manuscript 1, Fig. 5). POC5 wt localized with centrin but the POC5 mut was detached from centrin. Not only in vitro, but also in vivo in zebrafish, we observed defect in colocalization between centrin and poc5 in mutpoc5 zebrafish retina (Manuscript 1, S6). Also, we confirm by CoIP several ciliary proteins interacting with POC5. Our work is the first work to address the function of POC5 and the effect of gene mutations in *POC5*. Recently, several work was focused in identifying the role of *POC5* in scoliosis. Recent work from our lab identified *POC5* gene as a causative gene in AIS (Patten, Margaritte-Jeannin et al. 2015). POC5 knockdown in zebrafish generated scoliosis. However, the impact of mutation at the level of protein was not investigated.

Further work also investigated the correlation of *POC5* with retinitis pigmentosa (Weisz Hubshman, Broekman et al. 2017). In zebrafish with *poc5* knockdown, there was retinal dysfunction, no scoliosis phenotype was reported in this study. It is very possible that different mutations in the same gene have different phenotype outcomes. This is a typical feature of ciliopathy diseases. Ciliopathies are characterized by having a broad range of phenotypic variability and many clinical features with renal, retinal, hepatic as well as skeletal defects and central nervous system developmental defects. Phenotypic variability is explained by the fact that mutation in some genes can result in a number of clinically different outcomes where at the same time mutation in many genes can give rise to the same ciliopathy. Moreover phenotypic variability is also explained by the fact that different ciliopathic diseases share the

same phenotype (Satir 1995). In our work, we connect the ciliary abnormalities association with *POC5* mutations described in scoliotic patients. We also describe the differential proteins interacting with wtPOC5 or mutPOC5. Indeed, there is a link between cilia, POC5 and scoliosis which we investigated in this study that have not been identified before.

The effect of mutations on protein structure can modify the protein-protein binding. Usually these modifications result in an abnormal protein interaction. Thus, the POC5 protein structure and biological function could be affected by functional mutations that were found in AIS patients. In our study, several ciliary proteins were found to be associated with wt but not mutPOC5 such as CEP 290, Desmocollin 1, Isoform 2 of Annexin A2, Tubulin beta chain, Septin 9, Cystatin-A and CKAP5 protein. These proteins have well described functions with respect to cilia (McEwen, Koenekoop et al. 2007, Tsang, Bossard et al. 2008, Papon, Perrault et al. 2010, Anand and Khanna 2012, Rachel, Li et al. 2012, Kobayashi, Kim et al. 2014, Rachel, Yamamoto et al. 2015). This emphasizes the finding that POC5 is a ciliary protein. Other proteins were also found interacting exclusively with wtPOC5 but not mutPOC5. Some of these proteins are cell adhesion proteins like Seprin B5, Zinc –alpha-2-glycoprotein and ribosomal L1 domain–containing protein 1. Other proteins are RNA processing like nuclear RNA export factor 1, nuclear protein 58, splicing factor 3A subunit 1 and 2, ATP-dependent DNA helicase Q1. Some proteins are involved in cell cycle and cytokinesis like E3 ubiquitinin/ISG15 ligase TRIM 25. There were also extracellular protein like lacritin, collagen type IV and suprabasin (Manuscript 1, Table 1). With respect to the proteins interacting with mutPOC5, only 5 proteins were found to be interacting exclusively with mutPOC5. Two proteins are involved in inflammation like Amino peptidase B and poly (ADP-ribose) polymerase family, member 1 (PARP1) (Soderling, Knuttila et al. 1977, Altmeyer and Hottiger 2009). Golgi resident protein GCP60 which is involved in apoptosis and regulation of asymmetric cell division and another protein partner protein disulfide isomerase A4 that is related to neuro degenerative disease involving protein misfolding and is upregulated following ER stress, (Fan, Liu et al. 2010, Galligan and Petersen 2012, Kaplan, Gaschler et al. 2015) were found to be interacting with mutPOC5 only which suggests that AIS pathogenesis could be due to POC5 protein misfolding. Another interesting protein was found among proteins exclusively interacting with mut POC5: DNA FLJ53595. DNA FLJ53595 is highly

similar to iduronate 2-sulfatase that was reported to be related to Hunter syndrome. Hunter syndrome is a very rare, inherited genetic disorder caused by a missing or malfunctioning enzymes, characterized by orthopaedic manifestations such as scoliosis and kyphosis (Wilson, Morris et al. 1990, Roberts and Tsirikos 2016) (Manuscript 1, Table 2).

The originality of our work presented in the Manucript 1 is the revelation of *POC5* as a ciliary gene, and its localization at the base of the cilium. We also found that the mutation in *POC5* (c. C1268T; p. A429V) affects the type of proteins interacting with the protein. Little is known about the localization of POC5 with respect to cilia and the effect of mutation that was described in Patten et al (Patten, Margaritte-Jeannin et al. 2015) on the protein POC5. In this work, we identified new binding partners for POC5 in addition to the already known partners (Fig.7) (Szklarczyk, Morris et al. 2017). Also, we found that the mutation of *POC5* (c. C1268T; p. A429V) affects its interaction with ciliary proteins. Most of the proteins that we identified in our work interacting with POC5 are novel. Little is known about the proteins partners of POC5. POC5 is known to interact with centrin 2 and centrin 3 (Azimzadeh, Hergert et al. 2009). The significance of our work is that it helps understand the function of POC5. The fact that POC5 interacts at high levels with ciliary proteins shedslight on the possible roles of POC5 in ciliogenesis as some of these proteins like RAB11 are essential for the formation of cilia (Westlake, Baye et al. 2011). Other proteins like galectin 3 and 7 have important functions in the biogenesis and function of cilia (Rondanino, Poland et al. 2011). An important partner of POC5 identified in this study is CEP290. Mutation in the gene *CEP290* results in different disease outcomes like JBS, Joubert syndrome, and MKS, a Meckel–Gruber syndrome and BBS, Bardet–Biedl syndrome. CEP290 is known to be an important component of the primary cilium, localizing to the Y-links of the ciliary transition zone and having a role in the regulation of transport in and out of the ciliary compartment (Craige, Tsao et al. 2010). MKS and JBTS are ciliopathies caused by mutations in genes encoding proteins that are components of the primary cilium and basal body. Common phenotypes observed in both syndromes are retinal disease and scoliosis. Septin 9 wih other septins were found to colocalize along the axoneme in the primary cilium and control ciliary length (Ghossoub, Hu et al. 2013). All of these facts shedlight on the significance of our finding, and help understand

the mechanisms through which scoliosis develops in patients with *POC5* mutations. This in turn opens new avenues to uncover in the future.

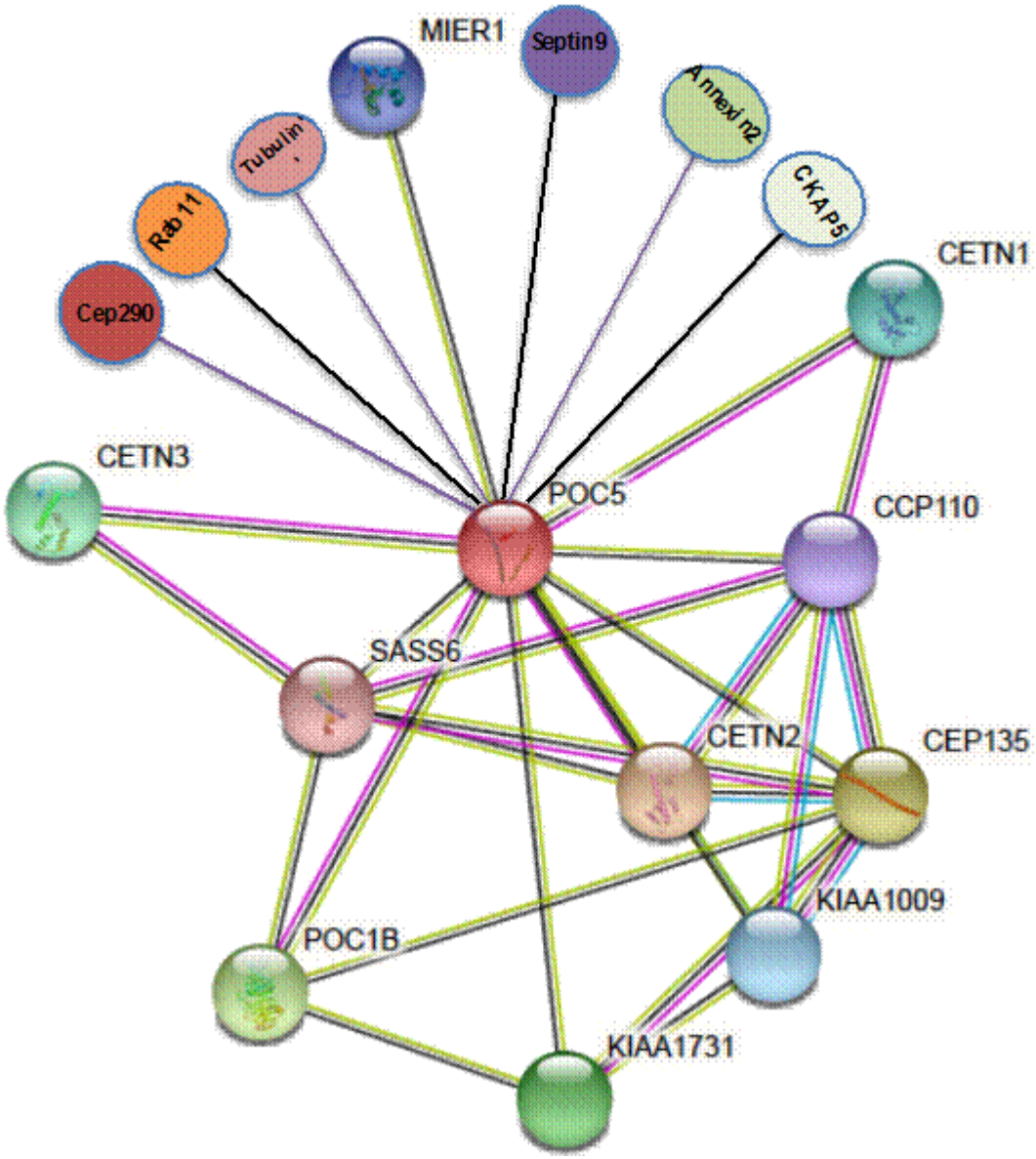

Figure 7: Proteins interacting with POC5 as determined with string database in addition to proteins we identified in this study. Under normal conditions, POC5 is located at the base of the cilium and interacting with other ciliary proteins like CEP290, RAB11, CKAP5, SEPTIN9 and tubulin. The mutation in *POC5* (c. C1286T; p. A429V) affects the interaction and causes detachment of these proteins and the overall consequence is the retraction of cilia. Adapted from Szklarczyk et al. (Szklarczyk, Morris et al. 2017).

We also performed *in vivo* work, in zebrafish wt*poc5* and mut*poc5*. Our work focused on identifying defects in the retina in scoliotic zebrafish. Indeed, we found that, retina of mut*poc5* zebrafish had missing outer segment layer and several defects at the level of rods, cones and retinal pigmented epithelium. By immunofluoresence using specific marker, for the cone layer, we found that cones are absent from the mut*poc5* retina, rod layer has reduced thickness while no defect was observed in wt*poc5* retina. We are not the first to present retinal defects in mut*poc5* retinas. Very recently, work by Weisz et al (Weisz Hubshman, Broekman et al. 2017), *POC5* nonsense mutation (c.304_305delGA [p. D102*]) was found to be associated with retinitis pigmentosa (RP). Retinitis pigmentosa is a retinal degeneration disease characterized by the loss of rods and then followed by cone loss and blindness. In the work by Weisz et al, zebrafish with the morpholino knockdown of *poc5* a shorter outer segment layer in the retina concomitant with the decreased visual motor response (VMR) was observed, a measurement of retinal function. In this last work, retina structure (histology) was not shown and the spinal deformity was absent. In contrast, the zebrafish model expressing mut*POC5* mRNAs, of any of the 3 human IS-associated POC5 variant mRNAs resulted in spine deformity (spine curvature and rotation reminiscent of IS), without affecting other skeletal structures (Patten, Margaritte-Jeannin et al. 2015). In our model, the defect was not only at the level of outer segment layer but also there was clear absence of cones but the exact significance of these observations needs to be further clarified, particularly with respect to the primary cilia that display a highly dynamic behavior during the early retinal differentiation. Also, recently, mutations in *ptk7* in zebrafish model was found to cause scoliosis and these mutant zebrafish revealed defects in cerebrospinal fluid and abnormalities in motile cilia (Grimes, Boswell et al. 2016).

The zebrafish represents a valuable model organism for studying scoliosis and also for the human ocular disease; it is utilized in eye research to understand underlying developmental processes, and it is well known that zebrafish eyes are functionally, physiologically and morphologiclay similar to humans eyes. Unlike mice, the larval zebrafish at 15 days post fertilization (dpf) or younger is also considered cone-dominant as its rods do not contribute to vision. Based on absorption spectra and morphology, cones are distributed into red- and green sensitive cones are fused at the level of the inner segment and form double cones, while the

ultraviolet (UV) and blue sensitive cones are separate and function as short and long single cones, respectively. Therefore zebrafish are, in contrast to humans, tetrachromats that are sensitive to light in the ultraviolet range. The cones mediate vision at bright light levels, while rods being functional at low light conditions (Gestri, Link et al. 2012) (Fig. 8). In the upcoming paragraph, I will elaborate the function of cones specifically the double cones. I will focus on double cones because they appeared to be defective in our zebrafish model of scoliosis and it is necessary to discuss the function of this retinal structure in vision in zebrafish.

DCs, consist of pairs of closely apposed principal and accessory members which act as a single functional unit and are thought to mediate luminance detection that is used for motion perception. Double cones are absent from placental mammals and they use a single set of cones for both functional purposes. However, DCs dominate the cone photoreceptors in fish, reptiles and birds. Based on several studies, DCs do not participate in colour vision. In fish, while single cones (SCs) certainly contribute to colour vision, DCs are likely to be involved in achromatic tasks, such as luminance, motion and polarization vision. The analysis of colour thresholds in some birds suggests that DCs do not participate in colour vision and it has been demonstrated that the long wavelength-sensitive visual pigment housed in DCs are responsible for the motion vision in goldfish and chickens (Pignatelli, Champ et al. 2010). Summation of the signals of individual members of DCs would be beneficial for luminance vision, as this would broaden the spectral sensitivity and improve the ability of fish to detect targets contrasting to background in different parts of the spectrum (Fig. 8) (Pignatelli, Champ et al. 2010). Based on these facts, it explains why our zebrafish didn't have vision problems. In our model, we observed absence of double cones and this suggests that the problem in scoliosis is not vision but rather the perception of environment. Confirming this hypothesis, AIS patients were found to have problems in stability in standing position and maintaining postural sway (Nault, Allard et al. 2002). The instability in body balance could be corrolated to alteration in sensory signal processing (Machida, Dubousset et al. 1994, Guo, Chau et al. 2006, Lao, Chow et al. 2008). Also, when compared to healthy children, the scoliotic patients were found to have significantly poorer postural control suggesting that postural disequilibrium could be a causative factor in AIS (Sahlstrand, Ortengren et al. 1978).

In our work, we found that cilia are retracted in scoliotic osteoblasts (Manuscript 1, Fig.2). Control cells had normal cilia while scoliotic cells expressing the mutation in *POC5* (c. C1268T; p. A429V) showed retracted cilium (Fig. 9) and the cells were blocked in S phase. In recent work by Oliazadeh et al, it was found that cilia in IS cells are significantly longer (Oliazadeh, Gorman et al. 2017). In this work, exome sequencing was performed and several genes that are involved in mechanotransduction were identified like *CLASP1*, *CD1B* and *LYN*, *SUGT1* and *HNRNPD*. The identified genes have roles connected to actin, cell cycle and proliferation, and centrosome organization (Oliazadeh, Gorman et al. 2017). Our work reveals the consequence of *POC5* mutation at the cellular level.

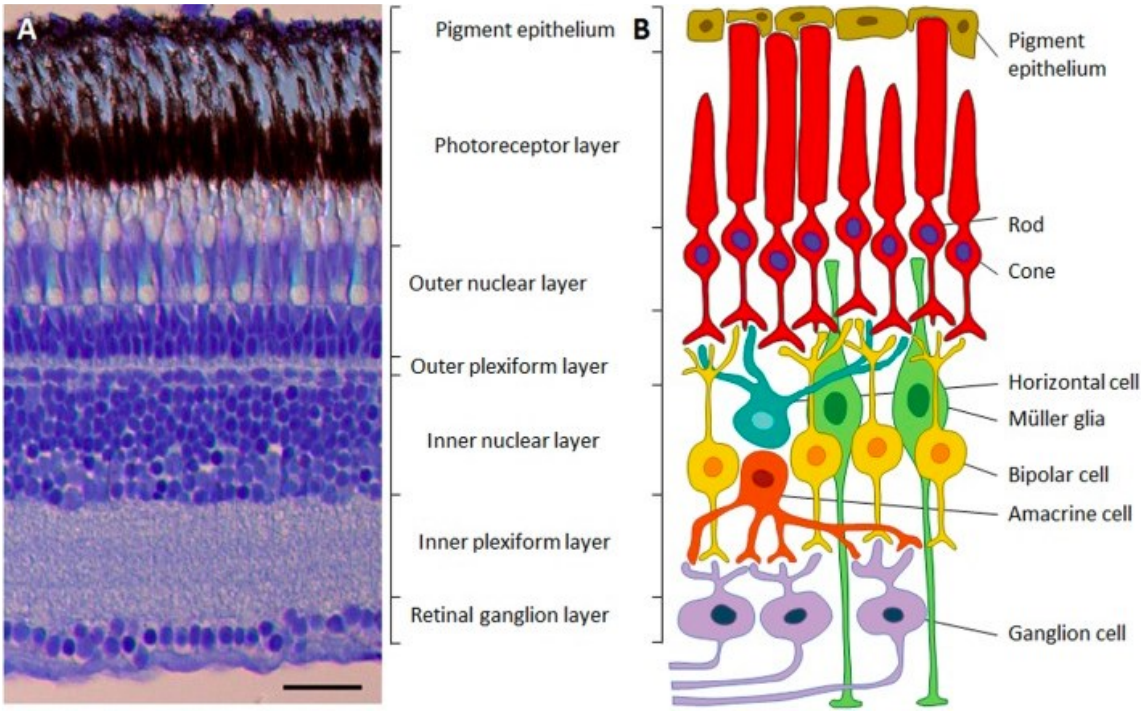

Figure 8: Structure of adult zebrafish retina. A) Microphotograph of a cross-section through the retina of an adult zebrafish. The figure shows different layers of the retina. B) Diagram representing the neural circuit of the retina. The diagram shows the six neuronal cell types and the two supporting cell types (Müller glia and retinal pigmented epithelium). Adapted from Gramage et al. (Gramage, Li et al. 2014). In A, the scale bar = 25µm.

As a possible effect of mutation in *POC5*, scoliotic cells are blocked in S phase as detected by the staining of POC5. Recently, it was found that hPOC5-depleted HeLa cells are blocked in S phase. The cells were treated with hPOC5 siRNA and as a consequence there was an increase in the proportion of S-phase cells (46% compared with ~30% in controls Brdu incorporation assay) confirming thus, the abnormal cell cycle progression. The defect in S-phase progression was not observed after simultaneous depletion of hCen2 and hCen3 or after depletion of hSfi1, which is the human homologue of yeast Sfi1p, suggesting that progression through S phase is specifically affected by hPOC5 depletion (Azimzadeh, Hergert et al. 2009). Interestingly, in addition to the arrest of cells expressing the mut*POC5* in S phase, these cells displayed apoptotic and inflammatory proteins interacting with mutPOC5 (mass spectroscopy results, Manuscript 1, Table 2)

It is well known that ciliogenesis initiation occurs when the cell enters quiescence, while the cilia retraction occurs once the cell enters the cell cycle (Inaba, Goto et al. 2016). The human enhancer of filamentation1-Aurora A-histone deacetylase-6 (a scaffolding protein) (HEF1-Aurora A-HDAC6)-dependent mechanism is responsible for cilia resorption and it just proceeds cell cycle re-entry. Centrosomal protein CP110 interacts with Cep97, CEP290, and Rab8a to suppress ciliogenesis or centriolar length through interactions with centromere protein J (CENPJ also known as CPAP).

CP110 and CENPJ are expressed in a cell cycle-dependent manner. Missing-in-Metastasis (MIM) is a protein that is regulated by cell cycle, and it functions antagonistically to the actin regulator cortactin to keep a normal level of ciliogenesis. Finally, a subset of centrosomal proteins have been shown to be required for both cell cycle progression and ciliogenesis (Kim, Zaghloul et al. 2011). The fact that scoliotic osteoblasts are blocked in S phase as detected by the subnuclear expression of POC5, could explain why cilia is retracted in these cells (Fig. 9). Also, we found that scoliotic osteoblasts have lower mineralization rate and delayed proliferation than normal osteoblasts (Data not shown).

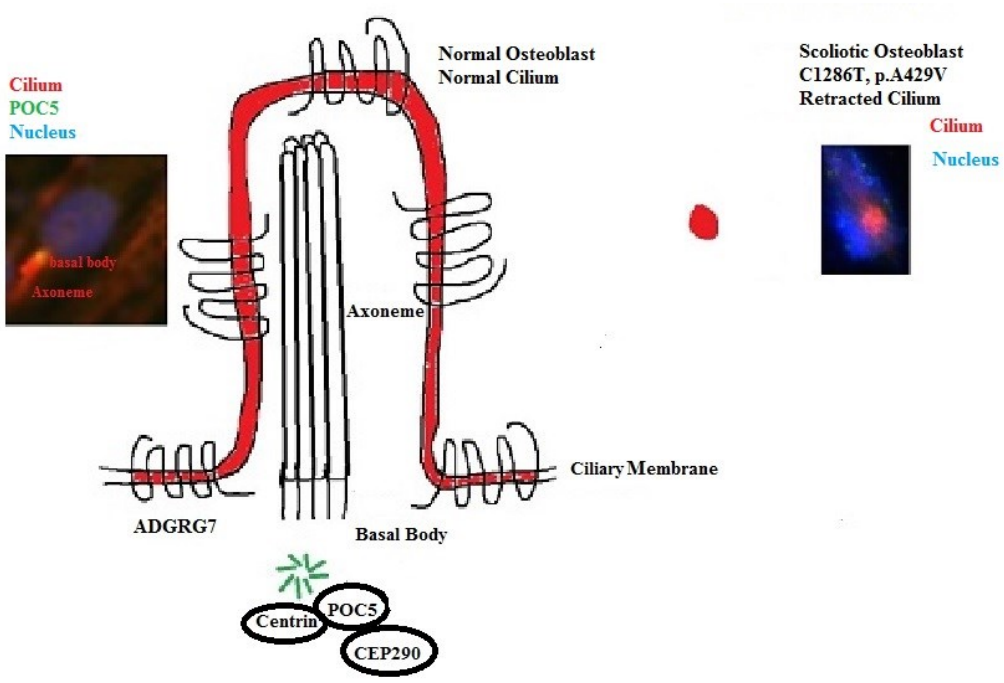

Figure 9: Comparison of the cilium structure between normal and AIS osteoblasts (c. C1286T; p. A429V). Our hypothesis is that POC5 is localized in normal osteoblasts at the base of the cilium and co-localize with other ciliary proteins such as CEP290 and centrin. Like other adhesion GPCRs, ADGRG7 is expressed at the membrane of the cilium and has a function in mechanosensation. In human osteoblasts expressing *POC5* mutation (c. C1286T; p. A429V), there is defect in the structure of the cilium. The organization and orientation of the cilium is affected in AIS patients. (Red: Acetylated tubulin; green: POC5; blue: DAPI).

In addition to the defects detected at the retina level, we also observed anomalies in the steriocilia. POC5 and acetylated-α-tubulin colocalize in the ear of wt*poc5* and shows strong staining. However, in mut*poc5* ear, there was lower staining observed for both proteins. Also, the cellularity of the ear was decreased in mut*poc5* as compared to wt*poc5* (Manuscript1, S5). Supporting the possible role of vestibular system in AIS, another intriguing *in vivo* mutant zebrafish model was reported; *kif6* mutant zebrafish, new zebrafish mutant, called skolios, were shown to develop spinal deformity that parallels many aspects of human idiopathic scoliosis. This mutant had abnormalities in otolith number (Buchan, Gray et al. 2014). In several animal models, including guinea pigs, tadpole, frog, rabbits, chicken and lambs

(Monticelli, Ascani et al. 1975, De Waele, Graf et al. 1989), research was focused on identifying possible links between vestibular system and AIS. The vestibular system includes the cochlea and the labyrinth that is included in the otic capsule of the temporal bones. The inertial sensors of the vestibular system include the three semicircular canals and two otolith organs.

The utricle and saccule are present within the vestibule and their function is the sense linear accelerations of the head, steriocilia act as mechanosensing organelles of hair cells and play a role in the response to fluid motion in numerous types of animals for various functions, including hearing and balance. In Xenopus, vestibular asymmetry was linked to the scoliosis (Lambert, Malinvaud et al. 2009). In this animal model, scoliosis was experimentally induced by unilateral removal of the vestibular organs in larval Xenopus, clearly showing the causal link between imbalance and spinal deformity.

Idiopathic scoliosis patients were found to have defects in the morphology of semicircular canal that is part of the inner ear (Patten and Moldovan 2011). This in turn might have an effect on the way the body responds to sensory signals, thus resulting in imbalance of the neuronal circuit. The overall consequence would be the initiation of spine curvature. Indeed, our observation (ear cilia defect in the ear of mutpoc5) also suggests a link between the ciliary defects/vestibular system and AIS. We have performed staining for acetylated tubulin and poc5 in the zebrafish and we found colocalization of both proteins in wt but not mutpoc5 ear as well as reduced cellularity in mutpoc5 zebrafish (Manuscript 1, S5).

Another important aspect of the project was the understanding of the molecular mechanisms of mechanical stress on gene regulation in AIS (Manuscript 4). There exist a strong correlation between bone morphology and mechanical load described by Wolff's law. The regular loading in the bone ensures that maintenance of its integrity and the repair of any damage. However, in scoliosis, curvature of the spine leads to asymetrical loading on the spine and as a consequence results in asymmetrical growth and progression of scoliosis during skeletal growth (Stokes 2008). There are several benefits for the biomechanical signals. Biomechanical signals are essential for bone homeostasis, growth, adaptation, healing and remodeling. Signal

transduction pathways are activated by mechanical signals, these pathways include the MAPK signal pathway. The extracellular signal-regulated kinase (ERK), c-Jun N-terminal kinase (JNK), and p38 MAPK (p38), play an essential role in osteoblastic cell proliferation and differentiation. Specifically, ERK1/2 is involved in cell transformation, proliferation, and the survival of several cell types, including osteoblasts. Until now, it's not clear how the cells convert the mechanical signal into a biological signal (Yan, Gong et al. 2012).

Indeed, in this work, we found differences in the signalling pathways (MAPK p38, NF-κB) activation in normal control cells and cells expressing the *POC5* mutation (c. C1286T; p. A429V). We also report the involvement of the TRPV4 channel in the regulation of the described pathways. We propose a model for the difference in the signalling pathways activation in the response to stress in normal situation and in AIS (Manuscript 4, Fig. 12).
For the application of mechanical stress, we have developed a method in the lab to apply mechanical force on cells using weight of 1g/cm2. TRPV4 seems to play an essential role in the activation of different signalling pathways tested.

Mechanical stress also had effects on the ciliary length and subcellular localization of TRPV4 channel that go along previous work studying the effect of mechanical stress on cilia, where primary cilia were found to be shorter and less in number after exposure to periods of OFF compared with static controls (Delaine-Smith, Sittichokechaiwut et al. 2014). There is increasing hypothesis that the primary cilium functions as mechanosensor in bone. However, little is known about the connection between primary cilium and its ability of sensation of mechanical stress and bone formation. Defects in sensory function of the primary cilium were associated with a number of musculoskeletal diseases, including osteoarthritis (Temiyasathit, Tang et al. 2012) and osteoporosis (Delaine-Smith, Sittichokechaiwut et al. 2014).

Our work presented in manuscript 4 shows the possible involvement of TRPV4 in scoliosis. The TRPV4 is a receptor operated ion channel activated by mechanical stress. In osteoblasts, during cell differentiation, TRPV4 expression is enhanced and changes in response to mechanical load (Liedtke 2007). Mutations in *TRPV4* channel (R616Q and V620I) have been associated with a skeletal dysplasia named Brachyilmias, where scoliosis is a secondary

phenotype (Everaerts, Nilius et al. 2010, Nilius and Voets 2013). By immunocytochemistry, it was found that TRPV4 channel is a stretch-activated Ca^{2+}-permeable channel and it localizes to the primary cilium and plasma membrane. The knockdown of *TRPV4* channel lowered the Ca^{2+} release in the cilium induced by loading. These findings make TRPV4 as an interesting pharmacologic target bone loss disease (Lee, Guevarra et al. 2015). Because mechanical strain plays a critical role in the proliferation, differentiation and maturation of bone cells, we were interested in studying the effect of mechanical load on cell apoptosis. Our finding shows that there was induced apoptosis in normal osteoblasts (Manuscript 4, Fig. 8) and it goes along with previous finding where large magnitude stretch induced apoptosis of osteoblasts (Song, Wang et al. 2016).

An important aspect of mechanical loading is that it regulates the bone structure and bone mass. It was shown that mechanical loading have anabolic effects while unloading of bone have bone resorbing effects (Villemure and Stokes 2009, Klein-Nulend, Bacabac et al. 2012). The mechanical forces exerted on the bone during physical activity are the consequence of both ground reaction forces and by the contractile activity of muscles. As a result, this not only contributes to the maintenance or gain of bone mass, but also to the adaptation of bone structure. On the other hand, in the absence of loading, there is loss of bone mass, in situations like bed rest (Klein-Nulend, Bacabac et al. 2012). As mentioned earlier in the introduction that one of the contributing factors to scoliosis progression is mechanical forces. The vicious cycle theory describes the cause of the progression of scoliosis that is the result of biomechanical factors modulating spinal growth. As described by Stokes, the asymmetrical load on the spine can result in small lateral curvature of the spine and as a consequence leads to asymmetrical growth (Stokes 2008). Given the fact that scoliotic patients have low bone density and the significance of the mechanical factor, this prompted us to study the impact of the mutation in *POC5* in the response of osteoblasts to mechanical stress precisely on osteoblast mineralization. Our results (Manuscript 4, Fig. 4 and 5) show that there was increased mineralization of osteoblasts as well as increase in osteogenic markers. The mineralization of mut*POC5* cells was lower than in normal osteoblasts (NOB). This in turn helps us understand the impact of mutation in patients with AIS on bone. Hence, under normal conditions, mechanical load induces bone formation. However, in AIS, in patients carrying the *POC5*

mutation (c. C1286T; p. A429V), we observed low response of bone cells to the mechanical load.

In the present thesis, we have presented work on the role of estrogens (Manuscript 2 and 3) and mechanical stress (Manuscript 4) in AIS cells, and we propose a possible connection between these two factors. For E2, there was differential effects of E2 on the regulation of both ADGRG7 and POC5 at the protein and gene levels in NOB and AIS cells. On the other hand, studying the effects on mechanical stress, there were also different effects of stress on NOB and mut*POC5* cells. This suggests that E2 and mechanical stress activated pathways are different in NOB and AIS different signalling pathways activated by E2. We have studied both factors independently, although there are studies showing that these factors are connected to each other (Rodan 1991, Joldersma, Klein-Nulend et al. 2001, Yeh, Chiu et al. 2010). The difference in the action of mechanical stress acting locally while E2 as a systemic hormone makes E2 as a significant modulator of bone mass where it can upregulate the effect of local loading and downregulate the effect of unloading. The signalling pathway through which E2 exerts its effects on bone is still unclear (Joldersma, Klein-Nulend et al. 2001). However, previous findings show that weight-bearing exercises did not increase bone mass in amenorrheic female athletes and in postmenopausal women which confirms the relationship between E2 and mechanical load (Rodan 1991). Supportive evidence was obtained from patients with osteoporosis where the mechanosensitivity of osteocytes is low and E2 deficiency causes reduced response to stress (Rodan 1991). It was found that E2 modulates bone cell mechanosensitivity. This occurs through different pathways through upregulation of prostaglandin E2 (PGE2) independently from COX1. E2 increased the sensitivity of the bone cells to mechanical loading and enhanced cell signalling in osteoblasts induced by mechanical load (Joldersma, Klein-Nulend et al. 2001). Also, E2 alleviated the response of signal transduction and gene expression to shear stress in MG63 cells (Yeh, Chiu et al. 2010). An interplay between both E2 and mechanical stress factors in the pathogenesis of AIS, could be proposed. Scoliotic osteoblasts response to E2 and to mechanical stress was lower than the response of control normal cells, and we hypothesize that scoliotic cells carrying the mutation (c. C1286T; p. A429V) in *POC5* have reduced response to the mechanical stress (load).

However, is still unclear how these mechanisms occurs, and what is the impact of POC5 mutation on these pathways.

CHAPTER V: GENERAL CONCLUSION

In this work, we have addressed several factors that have been described to be possibly contributing factors in AIS. These factors included ciliary defects (Manuscript 1), hormonal (E2) (Manuscript 2 and 3) factors and biomechanical factors (Manuscript 4).

Manuscript 1: Our work defined the ciliary location of wtPOC5 together with other ciliary proteins and the significance of the role that the cilia plays in the pathogenesis of AIS. There seems to be an important influence of ciliary defects on cell cycle fate. Not only *in vitro* but also *in vivo* studies confirm the ciliary defects in AIS at the retinal system. The connecting cilium of the retina is retracted in mut*poc5* zebrafish. Hence, these results suggest that it is possible that the sensation of environment and balance in AIS patients could be impaired.

Manuscripts 2 and 3: Up to now, several groups tried to understand the involvement of E2 in AIS pathogenesis. The most interesting question asked over decades is why girls are more affected than boys and why is puberty the period during which AIS is predominantly progressing in girls. This thesis reports the effects of E2, with respect to the gene regulations, human cells from normal (control) and AIS patients. In the presented thesis, we showed that estrogen plays an important role in the regulation of two genes *POC5* and *ADGRG7*. The role of *POC5* in AIS is growing and developing while the involvement of *ADGRG7* in AIS is still missing. However, based on our findings, there seems to be a differential regulation of POC5 and ADGRG7 by E2 in normal and AIS osteoblasts, suggesting a phenomenon of E2 resistance in AIS.

Manuscript 4: Finally, we studied the influence of mechanical stress on normal osteoblasts and cells expressing the mutation in *POC5*. Our results suggest differential impact of mechanical stress on normal and mut*POC5* cells. At the cellular level, we revealed differential response of mut*POC5* cells to the stress. This supports the implication of biomechanics in cellular response of bone cells, and we postulated a resistance mechansism in AIS.

To generally conclude, our work unravels some of the critical aspects of the molecular mechanisms involved in AIS pathogenesis. Based on the results presented in this thesis, we conclude that cellular mechanisms of this multifactorial pathology are still complex; defective genes, differential response of normal osteoblasts and cells with mutation in POC5 to E2 and to mechanical stress as well as ciliary defects would all contribute to AIS. We focused on two genes (*ADGRG7* and *POC5*) and their regulation by E2 and mechanical stress. Also, we emphasize the role of *POC5* as a ciliary gene that as well as the contribution of *POC5* gene variant (c. C1286T; p. A429V) to the primary cilia anomalies in scoliosis.

E2 deficiency was reported in girls with AIS and there was correlation between E2 levels and AIS (Esposito, Uccello et al. 2009, Kulis, Gozdzialska et al. 2015). Identification of the contribution of E2 would help to understand how AIS develops during skeletal growth and the improvement of new therapeutic interventions. Thus, this clinically put emphasis on the role that estrogen hormone plays in AIS. Examination of estradiol would help in the diagnosis and prognosis spinal pathologies associated with AIS.

On the other hand, the mechanical factor has several effects on the growth plate and its structural proteins biocomposition (Valteau, Grimard et al. 2011, Benoit, Mustafy et al. 2016, Kaviani, Londono et al. 2018). Understanding the mechanism of action of mechanical stress at the cellular level, and the impact of mutation of POC5 in AIS is an important step in the development of fusionless treatment of scoliosis.

Finally, as discussed in the following thesis, several symptoms in AIS patients like problem in environment perception are not well understood. Deffects in the cilia of retina and ear can help understand the cause behind these phenotypes. Developing tests for the assessment of the ciliary defects would be a great tool for the diagnosis of AIS severity. We have discussed each of these points (mentioned above) separately in different manuscripts, however, there is correlation between all these factors, between mechanical stress, E2 and cilia. Thus, understanding how they contribute to AIS will help unravel the puzzle of AIS, and improve treatment options.

CHAPTER VI: FUTURE PERSPECTIVES AND LIMITATIONS

The work of this thesis covers different aspects of the pathogenesis of AIS and discussed factors that have been suggested to play roles in the onset and/or the progression of AIS. In addition to the results presented here, this thesis opens new avenues: Future investigations are needed in order to confirm the exact role of *POC5* and *ADGRG7* in AIS, *in vivo*, in a more robust animal model of AIS, in AIS patient-derived cells and by clinical investigation of AIS patients.

To further study the regulation of *POC5* and *ADGRG7* by E2 *in vivo*, a mouse or zebrafish model, could be developed, through the generation of a knock-in model. The goal of these forthcoming research should be to ascertain the consequences of the genetic abnormalities in the cilia, centrosome and the organization of microtubules, to ultimately clarify the mechanisms responsible for the AIS development and how E2 is a factor in this disorganization. The generation of knock-in mice carrying the same pathogenic mutations present in AIS patients represents the best approach (i.e in mutant zebrafish or mice to be created using the Clustered Regularly Interspaced Short Palindromic Repeats (CRISPR/cas9 approach). Since mice are mammals, this will give the opportunity to also study hormonal factors that will not be applicable in zebrafish. The CRISPR/Cas9 is well known for its simplicity and efficiency. CRISPR/Cas9 reduces the time required to modify target genes compared to gene targeting technologies based on the use of embryonic stem (ES) cells.

Also, since there is interplay between E2 and mechanical stress pathways, it would be interesting to study the combined effects of both factors in AIS. Would both factors induce a higher resistence in AIS as compared to control? This question to be answered in *in vitro*, and *in vivo* in mouse or zebrafish model of AIS.

Since POC5 is essential for the assembly of the distal half of centrioles required for centriole elongation, and since this assembly defect can lead to the cilia defects and gene instability, another hypothesis can be proposed and explored: the critical role of *POC5* mutations for the embryonic development. Defects in left–right asymmetry, the expression patterns of axial

patterning genes involved in anterior–posterior polarity gene, segmentation clock genes, and genes of anterior–posterior polarity of the individual somites shoud also be examined. This research could be a major step towards the understanding pathogenesis of scoliosis, and clarifying the role of centrosome, cilia and microtubules organization in AIS.

Epigenetic aspect is another plausible mechanism for investigation, more particularly in AIS patient-derived cells. Epigenetic modifications are an additional mode of regulation that expands capability of the human genome. Little evidence exists regarding the relative contribution of hormonal factors during the pubertal growth, which is a critical (precarious) period for the onset of AIS. There are no reported studies about the possible contribution of E2 to *POC5* gene expression in AIS, nor with respect to the pattern of methylation. Because regulatory consequences of DNA methylation and histone modifications can provoke induction, suppression or no effect on gene expression, it is therefore important to consider the genomic location and the protein factors associated with, to obtain a better understanding of its function and effects. Indeed, we can propose to investigate whether E2 could modulate *POC5* and *ADGRG7* promoter and their expression by epigenetic mechanisms. We can also postulate that E2 could modulate expression of several centrosome and cilia genes in AIS, through the epigenetic modifications, DNA methylation in *POC5* promoter, and *ADGRG7* or by modulating its expression (mRNA and protein levels).

Finally, in patients with AIS, some aspects of clinical manifestations i.e. the vision and the space perception are the research direction opened by this thesis. To confirm the causality of the mutations in *POC5* and their part for retinal defects in patients, retinal dysfunction could be evaluated. Electrophysiological retinal abnormalities in children with scoliosis and controls can be examined as well as the dysfunction of the vestibular system that may be a contributing factor to the development or to the progression of AIS. Also, the cortical sensorimotor information processing associated with postural control merits to be further examined in patients with AIS, and age and sex matched controls.

Throughout the work of this thesis there were some limitations that I would like to discuss.

One of the major limitations of the presented work is that our mut*poc5* zebrafish had retinal defects that were described in paper 1, but vision was not investigated in this animal model. To support these anomalies, it would be also interesting to explore the retinal function in AIS patients.

We presented the functional consequences of one of the mutations (c. C1286T; p. A429V). In this work, a transient transfection of *POC5* gene expression was used. This method was useful for short-term expression of genes and protein post-transfection changes that we analysed by mass spectroscopy experiments. Stable transfection with a longer and more stable complex process of long-term genetic regulation was not performed during this thesis. This will be a valuable approach and could be applied to other described mutations of *POC5.*

Herein, we hypothesize that the localization of POC5 at the base of the cilium and ciliary retraction phenotype in mut expressing cells. For all these experiments we used acetylated-α-tubulin as a marker for cilia. Acetylated-α-tubulin is not specific for the base of the cilium. Hence for future work, other specific markers for the base of cilium like ARL3 should be used.

For the estrogen effects on gene regulation, most of the experiments were done in overexpression systems. Hence, it would be necessary to perform these experiments (promoter study) on endogenous promoter. Also, knockdown of SP1 and ERα by crisper in osteoblasts would be interesting to confirm the importance of these factors in gene and protein regulation of ADGRG7 and POC5 by E2.

Confirming the exact role of several candidate genes of AIS in patient-derived cells and creating better animal model of AIS will be a major step towards the understanding of the molecular and cellular mechanisms responsible for AIS.

REFERENCES

Acaroglu, E., I. Akel, A. Alanay, M. Yazici and R. Marcucio (2009). "Comparison of the melatonin and calmodulin in paravertebral muscle and platelets of patients with or without adolescent idiopathic scoliosis." Spine (Phila Pa 1976) **34**(18): E659-663.

Akel, I., G. Demirkiran, A. Alanay, S. Karahan, R. Marcucio and E. Acaroglu (2009). "The effect of calmodulin antagonists on scoliosis: bipedal C57BL/6 mice model." Eur Spine J **18**(4): 499-505.

Akel, I., O. Kocak, G. Bozkurt, A. Alanay, R. Marcucio and E. Acaroglu (2009). "The effect of calmodulin antagonists on experimental scoliosis: a pinealectomized chicken model." Spine (Phila Pa 1976) **34**(6): 533-538.

Akoume, M. Y., B. Azeddine, I. Turgeon, A. Franco, H. Labelle, B. Poitras, C. H. Rivard, G. Grimard, J. Ouellet, S. Parent and A. Moreau (2010). "Cell-based screening test for idiopathic scoliosis using cellular dielectric spectroscopy." Spine (Phila Pa 1976) **35**(13): E601-608.

Allen, D. B. (1996). "Safety of human growth hormone therapy: current topics." J Pediatr **128**(5 Pt 2): S8-13.

Altaf, F., A. Gibson, Z. Dannawi and H. Noordeen (2013). "Adolescent idiopathic scoliosis." BMJ **346**: f2508.

Altmeyer, M. and M. O. Hottiger (2009). "Poly(ADP-ribose) polymerase 1 at the crossroad of metabolic stress and inflammation in aging." Aging (Albany NY) **1**(5): 458-469.

Anand, M. and H. Khanna (2012). "Ciliary transition zone (TZ) proteins RPGR and CEP290: role in photoreceptor cilia and degenerative diseases." Expert Opin Ther Targets **16**(6): 541-551.

Andersen, M. O., K. Thomsen and K. O. Kyvik (2007). "Adolescent idiopathic scoliosis in twins: a population-based survey." Spine (Phila Pa 1976) **32**(8): 927-930.

Andersen, M. R., M. Farooq, K. Koefoed, K. W. Kjaer, A. Simony, S. T. Christensen and L. A. Larsen (2016). "Mutation of the planar cell polarity gene VANGL1 in adolescent idiopathic scoliosis." Spine (Phila Pa 1976).

Arac, D., G. Aust, D. Calebiro, F. B. Engel, C. Formstone, A. Goffinet, J. Hamann, R. J. Kittel, I. Liebscher, H. H. Lin, K. R. Monk, A. Petrenko, X. Piao, S. Promel, H. B. Schioth, T. W. Schwartz, M. Stacey, Y. A. Ushkaryov, M. Wobus, U. Wolfrum, L. Xu and T. Langenhan (2012). "Dissecting signaling and functions of adhesion G protein-coupled receptors." Ann N Y Acad Sci **1276**: 1-25.

Arac, D., A. A. Boucard, M. F. Bolliger, J. Nguyen, S. M. Soltis, T. C. Sudhof and A. T. Brunger (2012). "A novel evolutionarily conserved domain of cell-adhesion GPCRs mediates autoproteolysis." EMBO J **31**(6): 1364-1378.

Assaad, H. I., Y. Hou, L. Zhou, R. J. Carroll and G. Wu (2015). "Rapid publication-ready MS-Word tables for two-way ANOVA." Springerplus **4**: 33.

Aubin, C. E., J. Clin and J. Rawlinson (2018). "Biomechanical simulations of costo-vertebral and anterior vertebral body tethers for the fusionless treatment of pediatric scoliosis." J Orthop Res **36**(1): 254-264.

Aulisa, L., P. Papaleo, E. Pola, F. Angelini, A. G. Aulisa, F. C. Tamburrelli, P. Pola and C. A. Logroscino (2007). "Association between IL-6 and MMP-3 gene polymorphisms and adolescent idiopathic scoliosis: a case-control study." Spine (Phila Pa 1976) **32**(24): 2700-2702.

Avikainen, V. J., A. Rezasoltani and H. A. Kauhanen (1999). "Asymmetry of paraspinal EMG-time characteristics in idiopathic scoliosis." J Spinal Disord **12**(1): 61-67.

Axenovich, T. I., A. M. Zaidman, I. V. Zorkoltseva, I. L. Tregubova and P. M. Borodin (1999). "Segregation analysis of idiopathic scoliosis: demonstration of a major gene effect." Am J Med Genet **86**(4): 389-394.

Azimzadeh, J., P. Hergert, A. Delouvee, U. Euteneuer, E. Formstecher, A. Khodjakov and M. Bornens (2009). "hPOC5 is a centrin-binding protein required for assembly of full-length centrioles." J Cell Biol **185**(1): 101-114.

Badiali, L., J. Cedernaes, P. K. Olszewski, O. Nylander, A. V. Vergoni and H. B. Schioth (2012). "Adhesion GPCRs are widely expressed throughout the subsections of the gastrointestinal tract." BMC Gastroenterol **12**: 134.

Bae, J. W., C. H. Cho, W. K. Min and U. K. Kim (2012). "Associations between matrilin-1 gene polymorphisms and adolescent idiopathic scoliosis curve patterns in a Korean population." Mol Biol Rep **39**(5): 5561-5567.

Bagnall, K. M., V. J. Raso, D. L. Hill, M. Moreau, J. K. Mahood, H. Jiang, G. Russell, M. Bering and G. R. Buzzell (1996). "Melatonin levels in idiopathic scoliosis. Diurnal and nocturnal serum melatonin levels in girls with adolescent idiopathic scoliosis." Spine (Phila Pa 1976) **21**(17): 1974-1978.

Bagu, E. T. and M. M. Santos (2011). "Friend of GATA suppresses the GATA-induced transcription of hepcidin in hepatocytes through a GATA-regulatory element in the HAMP promoter." J Mol Endocrinol **47**(3): 299-313.

Baker, L., K. K. Meldrum, M. Wang, R. Sankula, R. Vanam, A. Raiesdana, B. Tsai, K. Hile, J. W. Brown and D. R. Meldrum (2003). "The role of estrogen in cardiovascular disease." J Surg Res **115**(2): 325-344.

Baker, M. E. (2002). "Recent insights into the origins of adrenal and sex steroid receptors." J Mol Endocrinol **28**(3): 149-152.

Barrios, C., S. Cortes, C. Perez-Encinas, M. D. Escriva, I. Benet, J. Burgos, E. Hevia, G. Piza and P. Domenech (2011). "Anthropometry and body composition profile of girls with nonsurgically treated adolescent idiopathic scoliosis." Spine (Phila Pa 1976) **36**(18): 1470-1477.

Benoit, A., T. Mustafy, I. Londono, G. Grimard, C. E. Aubin and I. Villemure (2016). "In vivo dynamic compression has less detrimental effect than static compression on newly formed bone of a rat caudal vertebra." J Musculoskelet Neuronal Interact **16**(3): 211-220.

Bilal, I., A. Chowdhury, J. Davidson and S. Whitehead (2014). "Phytoestrogens and prevention of breast cancer: The contentious debate." World J Clin Oncol **5**(4): 705-712.

Bjarnadottir, T. K., R. Fredriksson, P. J. Hoglund, D. E. Gloriam, M. C. Lagerstrom and H. B. Schioth (2004). "The human and mouse repertoire of the adhesion family of G-protein-coupled receptors." Genomics **84**(1): 23-33.

Bjornstrom, L. and M. Sjoberg (2005). "Mechanisms of estrogen receptor signaling: convergence of genomic and nongenomic actions on target genes." Mol Endocrinol **19**(4): 833-842.

Blair, H. C., Q. C. Larrouture, Y. Li, H. Lin, D. Beer-Stoltz, L. Liu, R. S. Tuan, L. J. Robinson, P. H. Schlesinger and D. J. Nelson (2017). "Osteoblast Differentiation and Bone Matrix Formation In Vivo and In Vitro." Tissue Eng Part B Rev **23**(3): 268-280.

Boot, A. M., I. M. van der Sluis, S. M. de Muinck Keizer-Schrama, J. B. van Meurs, E. P. Krenning, H. A. Pols and A. G. Uitterlinden (2004). "Estrogen receptor alpha gene polymorphisms and bone mineral density in healthy children and young adults." Calcif Tissue Int **74**(6): 495-500.

Braun, J. T., J. W. Ogilvie, E. Akyuz, D. S. Brodke and K. N. Bachus (2004). "Fusionless scoliosis correction using a shape memory alloy staple in the anterior thoracic spine of the immature goat." Spine (Phila Pa 1976) **29**(18): 1980-1989.

Brodner, W., P. Krepler, M. Nicolakis, M. Langer, A. Kaider, W. Lack and F. Waldhauser (2000). "Melatonin and adolescent idiopathic scoliosis." J Bone Joint Surg Br **82**(3): 399-403.

Brooks, M. D., R. D. Bennett, A. L. Weaver, T. J. Sebo, S. E. Eckert, E. E. Strehler and A. B. Carr (2013). "Human Calmodulin-Like Protein CALML3: A Novel Marker for Normal Oral Squamous Mucosa That Is Downregulated in Malignant Transformation." Int J Dent **2013**: 592843.

Buchan, J. G., D. M. Alvarado, G. E. Haller, C. Cruchaga, M. B. Harms, T. Zhang, M. C. Willing, D. K. Grange, A. C. Braverman, N. H. Miller, J. A. Morcuende, N. L. Tang, T. P. Lam, B. K. Ng, J. C. Cheng, M. B. Dobbs and C. A. Gurnett (2014). "Rare variants in FBN1

and FBN2 are associated with severe adolescent idiopathic scoliosis." Hum Mol Genet **23**(19): 5271-5282.

Buchan, J. G., R. S. Gray, J. M. Gansner, D. M. Alvarado, L. Burgert, J. D. Gitlin, C. A. Gurnett and M. I. Goldsmith (2014). "Kinesin family member 6 (kif6) is necessary for spine development in zebrafish." Dev Dyn **243**(12): 1646-1657.

Buckingham, M. and F. Relaix (2007). "The role of Pax genes in the development of tissues and organs: Pax3 and Pax7 regulate muscle progenitor cell functions." Annu Rev Cell Dev Biol **23**: 645-673.

Burke, J. G., G. W. RW, D. Conhyea, D. McCormack, F. E. Dowling, M. G. Walsh and J. M. Fitzpatrick (2003). "Human nucleus pulposis can respond to a pro-inflammatory stimulus." Spine (Phila Pa 1976) **28**(24): 2685-2693.

Burwell, R. G., R. K. Aujla, M. P. Grevitt, P. H. Dangerfield, A. Moulton, T. L. Randell and S. I. Anderson (2009). "Pathogenesis of adolescent idiopathic scoliosis in girls - a double neuro-osseous theory involving disharmony between two nervous systems, somatic and autonomic expressed in the spine and trunk: possible dependency on sympathetic nervous system and hormones with implications for medical therapy." Scoliosis **4**: 24.

Burwell, R. G. and P. H. Dangerfield (2006). "Pathogenesis of progressive adolescent idiopathic scoliosis. Platelet activation and vascular biology in immature vertebrae: an alternative molecular hypothesis." Acta Orthop Belg **72**(3): 247-260.

Burwell, R. G., P. H. Dangerfield and B. J. Freeman (2008). "Etiologic theories of idiopathic scoliosis. Somatic nervous system and the NOTOM escalator concept as one component in the pathogenesis of adolescent idiopathic scoliosis." Stud Health Technol Inform **140**: 208-217.

Burwell, R. G., P. H. Dangerfield, A. Moulton and S. I. Anderson (2008). "Etiologic theories of idiopathic scoliosis: autonomic nervous system and the leptin-sympathetic nervous system concept for the pathogenesis of adolescent idiopathic scoliosis." Stud Health Technol Inform **140**: 197-207.

Burwell, R. G., N. J. James, F. Johnson, J. K. Webb and Y. G. Wilson (1983). "Standardised trunk asymmetry scores. A study of back contour in healthy school children." J Bone Joint Surg Br **65**(4): 452-463.

Caron, A., X. Xu and X. Lin (2012). "Wnt/beta-catenin signaling directly regulates Foxj1 expression and ciliogenesis in zebrafish Kupffer's vesicle." Development **139**(3): 514-524.

Carr, A. J. (1990). "Adolescent idiopathic scoliosis in identical twins." J Bone Joint Surg Br **72**(6): 1077.

Chang, C. W., W. B. Hsu, J. J. Tsai, C. J. Tang and T. K. Tang (2016). "CEP295 interacts with microtubules and is required for centriole elongation." J Cell Sci **129**(13): 2501-2513.

Chen, H. Y., C. T. Wu, C. C. Tang, Y. N. Lin, W. J. Wang and T. K. Tang (2017). "Human microcephaly protein RTTN interacts with STIL and is required to build full-length centrioles." Nat Commun **8**(1): 247.

Chen, J. R., O. P. Lazarenko, R. L. Haley, M. L. Blackburn, T. M. Badger and M. J. Ronis (2009). "Ethanol impairs estrogen receptor signaling resulting in accelerated activation of senescence pathways, whereas estradiol attenuates the effects of ethanol in osteoblasts." J Bone Miner Res **24**(2): 221-230.

Chen, N. X., D. J. Geist, D. C. Genetos, F. M. Pavalko and R. L. Duncan (2003). "Fluid shear-induced NFkappaB translocation in osteoblasts is mediated by intracellular calcium release." Bone **33**(3): 399-410.

Chen, S., L. Zhao, D. M. Roffey, P. Phan and E. K. Wai (2014). "Association of rs11190870 near LBX1 with adolescent idiopathic scoliosis in East Asians: a systematic review and meta-analysis." Spine J **14**(12): 2968-2975.

Chen, Z., N. L. Tang, X. Cao, D. Qiao, L. Yi, J. C. Cheng and Y. Qiu (2009). "Promoter polymorphism of matrilin-1 gene predisposes to adolescent idiopathic scoliosis in a Chinese population." Eur J Hum Genet **17**(4): 525-532.

Cheng, J. C., R. M. Castelein, W. C. Chu, A. J. Danielsson, M. B. Dobbs, T. B. Grivas, C. A. Gurnett, K. D. Luk, A. Moreau, P. O. Newton, I. A. Stokes, S. L. Weinstein and R. G. Burwell (2015). "Adolescent idiopathic scoliosis." Nat Rev Dis Primers **1**: 15030.

Cheng, J. C. and X. Guo (1997). "Osteopenia in adolescent idiopathic scoliosis. A primary problem or secondary to the spinal deformity?" Spine (Phila Pa 1976) **22**(15): 1716-1721.

Cheng, J. C., L. Qin, C. S. Cheung, A. H. Sher, K. M. Lee, S. W. Ng and X. Guo (2000). "Generalized low areal and volumetric bone mineral density in adolescent idiopathic scoliosis." J Bone Miner Res **15**(8): 1587-1595.

Cheng, J. C., S. P. Tang, X. Guo, C. W. Chan and L. Qin (2001). "Osteopenia in adolescent idiopathic scoliosis: a histomorphometric study." Spine (Phila Pa 1976) **26**(3): E19-23.

Cheskis, B. J., J. G. Greger, S. Nagpal and L. P. Freedman (2007). "Signaling by estrogens." J Cell Physiol **213**(3): 610-617.

Cheung, C. S., W. T. Lee, Y. K. Tse, K. M. Lee, X. Guo, L. Qin and J. C. Cheng (2006). "Generalized osteopenia in adolescent idiopathic scoliosis--association with abnormal pubertal growth, bone turnover, and calcium intake?" Spine (Phila Pa 1976) **31**(3): 330-338.

Coelho, P. A., L. Bury, M. N. Shahbazi, K. Liakath-Ali, P. H. Tate, S. Wormald, C. J. Hindley, M. Huch, J. Archer, W. C. Skarnes, M. Zernicka-Goetz and D. M. Glover (2015). "Over-expression of Plk4 induces centrosome amplification, loss of primary cilia and associated tissue hyperplasia in the mouse." Open Biol **5**(12): 150209.

Cowell, H. R., J. N. Hall and G. D. MacEwen (1972). "Genetic aspects of idiopathic scoliosis. A Nicholas Andry Award essay, 1970." Clin Orthop Relat Res **86**: 121-131.

Craige, B., C. C. Tsao, D. R. Diener, Y. Hou, K. F. Lechtreck, J. L. Rosenbaum and G. B. Witman (2010). "CEP290 tethers flagellar transition zone microtubules to the membrane and regulates flagellar protein content." J Cell Biol **190**(5): 927-940.

Crean, J. K., S. Roberts, D. C. Jaffray, S. M. Eisenstein and V. C. Duance (1997). "Matrix metalloproteinases in the human intervertebral disc: role in disc degeneration and scoliosis." Spine (Phila Pa 1976) **22**(24): 2877-2884.

Cuajungco, M. P., C. Grimm, K. Oshima, D. D'Hoedt, B. Nilius, A. R. Mensenkamp, R. J. Bindels, M. Plomann and S. Heller (2006). "PACSINs bind to the TRPV4 cation channel. PACSIN 3 modulates the subcellular localization of TRPV4." J Biol Chem **281**(27): 18753-18762.

Czeizel, A., A. Bellyei, O. Barta, T. Magda and L. Molnar (1978). "Genetics of adolescent idiopathic scoliosis." J Med Genet **15**(6): 424-427.

Dahlman-Wright, K., V. Cavailles, S. A. Fuqua, V. C. Jordan, J. A. Katzenellenbogen, K. S. Korach, A. Maggi, M. Muramatsu, M. G. Parker and J. A. Gustafsson (2006). "International Union of Pharmacology. LXIV. Estrogen receptors." Pharmacol Rev **58**(4): 773-781.

Dantas, T. J., O. M. Daly, P. C. Conroy, M. Tomas, Y. Wang, P. Lalor, P. Dockery, E. Ferrando-May and C. G. Morrison (2013). "Calcium-binding capacity of centrin2 is required for linear POC5 assembly but not for nucleotide excision repair." PLoS One **8**(7): e68487.

Day, G., K. Frawley, G. Phillips, I. B. McPhee, R. Labrom, G. Askin and P. Mueller (2008). "The vertebral body growth plate in scoliosis: a primary disturbance of growth?" Scoliosis **3**: 3.

de Seze, M. and E. Cugy (2012). "Pathogenesis of idiopathic scoliosis: a review." Ann Phys Rehabil Med **55**(2): 128-138.

De Waele, C., W. Graf, P. Josset and P. P. Vidal (1989). "A radiological analysis of the postural syndromes following hemilabyrinthectomy and selective canal and otolith lesions in the guinea pig." Exp Brain Res **77**(1): 166-182.

Deak, F., R. Wagener, I. Kiss and M. Paulsson (1999). "The matrilins: a novel family of oligomeric extracellular matrix proteins." Matrix Biol **18**(1): 55-64.

Delaine-Smith, R. M., A. Sittichokechaiwut and G. C. Reilly (2014). "Primary cilia respond to fluid shear stress and mediate flow-induced calcium deposition in osteoblasts." FASEB J **28**(1): 430-439.

Demirkiran, G., O. Dede, N. Yalcin, I. Akel, R. Marcucio and E. Acaroglu (2014). "Selective estrogen receptor modulation prevents scoliotic curve progression: radiologic and histomorphometric study on a bipedal C57Bl6 mice model." Eur Spine J **23**(2): 455-462.

Doi, T., K. Harimaya, H. Mitsuyasu, Y. Matsumoto, K. Masuda, K. Kobayakawa and Y. Iwamoto (2011). "Right thoracic curvature in the normal spine." J Orthop Surg Res **6**: 4.

Drivas, T. G. and J. Bennett (2014). "CEP290 and the primary cilium." Adv Exp Med Biol **801**: 519-525.

Dubousset, J. and M. Machida (2001). "[Possible role of the pineal gland in the pathogenesis of idiopathic scoliosis. Experimental and clinical studies]." Bull Acad Natl Med **185**(3): 593-602; discussion 602-594.

Eastell, R. (2005). "Role of oestrogen in the regulation of bone turnover at the menarche." J Endocrinol **185**(2): 223-234.

Edery, P., P. Margaritte-Jeannin, B. Biot, A. Labalme, J. C. Bernard, J. Chastang, B. Kassai, M. H. Plais, F. Moldovan and F. Clerget-Darpoux (2011). "New disease gene location and high genetic heterogeneity in idiopathic scoliosis." Eur J Hum Genet **19**(8): 865-869.

Edjekouane, L., S. Benhadjeba, M. Jangal, H. Fleury, N. Gevry, E. Carmona and A. Tremblay (2016). "Proximal and distal regulation of the HYAL1 gene cluster by the estrogen receptor alpha in breast cancer cells." Oncotarget **7**(47): 77276-77290.

Eick, G. N. and J. W. Thornton (2011). "Evolution of steroid receptors from an estrogen-sensitive ancestral receptor." Mol Cell Endocrinol **334**(1-2): 31-38.

Einarsdottir, E., A. Grauers, J. Wang, H. Jiao, S. A. Escher, A. Danielsson, A. Simony, M. Andersen, S. B. Christensen, K. Akesson, I. Kou, A. M. Khanshour, A. Ohlin, C. Wise, S. Ikegawa, J. Kere and P. Gerdhem (2017). "CELSR2 is a candidate susceptibility gene in idiopathic scoliosis." PLoS One **12**(12): e0189591.

Engesaeth, V. G., J. O. Warner and A. Bush (1993). "New associations of primary ciliary dyskinesia syndrome." Pediatr Pulmonol **16**(1): 9-12.

Ernst, M., C. Schmid and E. R. Froesch (1988). "Enhanced osteoblast proliferation and collagen gene expression by estradiol." Proc Natl Acad Sci U S A **85**(7): 2307-2310.

Esposito, T., R. Uccello, R. Caliendo, G. F. Di Martino, U. A. Gironi Carnevale, S. Cuomo, D. Ronca and B. Varriale (2009). "Estrogen receptor polymorphism, estrogen content and idiopathic scoliosis in human: a possible genetic linkage." J Steroid Biochem Mol Biol **116**(1-2): 56-60.

Everaerts, W., B. Nilius and G. Owsianik (2010). "The vanilloid transient receptor potential channel TRPV4: from structure to disease." Prog Biophys Mol Biol **103**(1): 2-17.

Fan, J., J. Liu, M. Culty and V. Papadopoulos (2010). "Acyl-coenzyme A binding domain containing 3 (ACBD3; PAP7; GCP60): an emerging signaling molecule." Prog Lipid Res **49**(3): 218-234.

Fan, Y. H., Y. Q. Song, D. Chan, Y. Takahashi, S. Ikegawa, M. Matsumoto, I. Kou, K. S. Cheah, P. Sham, K. M. Cheung and K. D. Luk (2012). "SNP rs11190870 near LBX1 is associated with adolescent idiopathic scoliosis in southern Chinese." J Hum Genet **57**(4): 244-246.

Farin, H. F., A. Mansouri, M. Petry and A. Kispert (2008). "T-box protein Tbx18 interacts with the paired box protein Pax3 in the development of the paraxial mesoderm." J Biol Chem **283**(37): 25372-25380.

Fendri, K., S. A. Patten, G. N. Kaufman, C. Zaouter, S. Parent, G. Grimard, P. Edery and F. Moldovan (2013). "Microarray expression profiling identifies genes with altered expression in Adolescent Idiopathic Scoliosis." Eur Spine J **22**(6): 1300-1311.

Foord, S. M., S. Jupe and J. Holbrook (2002). "Bioinformatics and type II G-protein-coupled receptors." Biochem Soc Trans **30**(4): 473-479.

Ford, D. M., K. M. Bagnall, K. D. McFadden, B. J. Greenhill and V. J. Raso (1984). "Paraspinal muscle imbalance in adolescent idiopathic scoliosis." Spine (Phila Pa 1976) **9**(4): 373-376.

Fournier, B., S. Gutzwiller, T. Dittmar, G. Matthias, P. Steenbergh and P. Matthias (2001). "Estrogen receptor (ER)-alpha, but not ER-beta, mediates regulation of the insulin-like growth factor I gene by antiestrogens." J Biol Chem **276**(38): 35444-35449.

Fredriksson, R., D. E. Gloriam, P. J. Hoglund, M. C. Lagerstrom and H. B. Schioth (2003). "There exist at least 30 human G-protein-coupled receptors with long Ser/Thr-rich N-termini." Biochem Biophys Res Commun **301**(3): 725-734.

Fredriksson, R., M. C. Lagerstrom, P. J. Hoglund and H. B. Schioth (2002). "Novel human G protein-coupled receptors with long N-terminals containing GPS domains and Ser/Thr-rich regions." FEBS Lett **531**(3): 407-414.

Frisen, J. and M. Barbacid (1997). "Genetic analysis of the role of Eph receptors in the development of the mammalian nervous system." Cell Tissue Res **290**(2): 209-215.

Fu, Y., A. Subramanya, D. Rozansky and D. M. Cohen (2006). "WNK kinases influence TRPV4 channel function and localization." Am J Physiol Renal Physiol **290**(6): F1305-1314.

Galligan, J. J. and D. R. Petersen (2012). "The human protein disulfide isomerase gene family." Hum Genomics **6**: 6.

Gao, W., C. Chen, T. Zhou, S. Yang, B. Gao, H. Zhou, C. Lian, Z. Wu, X. Qiu, X. Yang, E. Alattar, W. Liu, D. Su, S. Sun, Y. Chen, K. M. C. Cheung, Y. Song, K. K. D. Luk, D. Chan, P.

C. Sham, C. Xing, C. C. Khor, G. Liu, J. Yang, Y. Deng, D. Hao, D. Huang, Q. Z. Li, C. Xu and P. Su (2017). "Rare coding variants in MAPK7 predispose to adolescent idiopathic scoliosis." Hum Mutat **38**(11): 1500-1510.

Gao, W., Y. Peng, G. Liang, A. Liang, W. Ye, L. Zhang, S. Sharma, P. Su and D. Huang (2013). "Association between common variants near LBX1 and adolescent idiopathic scoliosis replicated in the Chinese Han population." PLoS One **8**(1): e53234.

Garland, H. G. (1934). "Hereditary Scoliosis." Br Med J **1**(3816): 328.

Geissele, A. E., M. J. Kransdorf, C. A. Geyer, J. S. Jelinek and B. E. Van Dam (1991). "Magnetic resonance imaging of the brain stem in adolescent idiopathic scoliosis." Spine (Phila Pa 1976) **16**(7): 761-763.

Gestri, G., B. A. Link and S. C. Neuhauss (2012). "The visual system of zebrafish and its use to model human ocular diseases." Dev Neurobiol **72**(3): 302-327.

Ghossoub, R., Q. Hu, M. Failler, M. C. Rouyez, B. Spitzbarth, S. Mostowy, U. Wolfrum, S. Saunier, P. Cossart, W. Jamesnelson and A. Benmerah (2013). "Septins 2, 7 and 9 and MAP4 colocalize along the axoneme in the primary cilium and control ciliary length." J Cell Sci **126**(Pt 12): 2583-2594.

Gibson, J. N., M. J. McMaster, C. M. Scrimgeour, P. J. Stoward and M. J. Rennie (1988). "Rates of muscle protein synthesis in paraspinal muscles: lateral disparity in children with idiopathic scoliosis." Clin Sci (Lond) **75**(1): 79-83.

Gorman, K. F. and F. Breden (2007). "Teleosts as models for human vertebral stability and deformity." Comp Biochem Physiol C Toxicol Pharmacol **145**(1): 28-38.

Gorman, K. F. and F. Breden (2009). "Idiopathic-type scoliosis is not exclusive to bipedalism." Med Hypotheses **72**(3): 348-352.

Gramage, E., J. Li and P. Hitchcock (2014). "The expression and function of midkine in the vertebrate retina." Br J Pharmacol **171**(4): 913-923.

Granet, C., N. Boutahar, L. Vico, C. Alexandre and M. H. Lafage-Proust (2001). "MAPK and SRC-kinases control EGR-1 and NF-kappa B inductions by changes in mechanical environment in osteoblasts." Biochem Biophys Res Commun **284**(3): 622-631.

Grant, S. F., D. M. Reid, G. Blake, R. Herd, I. Fogelman and S. H. Ralston (1996). "Reduced bone density and osteoporosis associated with a polymorphic Sp1 binding site in the collagen type I alpha 1 gene." Nat Genet **14**(2): 203-205.

Grauers, A., J. Wang, E. Einarsdottir, A. Simony, A. Danielsson, K. Akesson, A. Ohlin, K. Halldin, P. Grabowski, M. Tenne, H. Laivuori, I. Dahlman, M. Andersen, S. B. Christensen, M. K. Karlsson, H. Jiao, J. Kere and P. Gerdhem (2015). "Candidate gene analysis and exome

sequencing confirm LBX1 as a susceptibility gene for idiopathic scoliosis." Spine J **15**(10): 2239-2246.

Grimes, D. T., C. W. Boswell, N. F. Morante, R. M. Henkelman, R. D. Burdine and B. Ciruna (2016). "Zebrafish models of idiopathic scoliosis link cerebrospinal fluid flow defects to spine curvature." Science **352**(6291): 1341-1344.

Grivas, T. B., O. D. Savvidou, E. Vasiliadis, S. Psarakis and G. Koufopoulos (2006). "Prevalence of scoliosis in women with visual deficiency." Stud Health Technol Inform **123**: 52-56.

Grivas, T. B., E. Vasiliadis, V. Mouzakis, C. Mihas and G. Koufopoulos (2006). "Association between adolescent idiopathic scoliosis prevalence and age at menarche in different geographic latitudes." Scoliosis **1**: 9.

Grivas, T. B., E. S. Vasiliadis, G. Koufopoulos, D. Segos, G. Triantafyllopoulos and V. Mouzakis (2006). "Study of trunk asymmetry in normal children and adolescents." Scoliosis **1**: 19.

Gross, M. K., M. Dottori and M. Goulding (2002). "Lbx1 specifies somatosensory association interneurons in the dorsal spinal cord." Neuron **34**(4): 535-549.

Guo, L., H. Yamashita, I. Kou, A. Takimoto, M. Meguro-Horike, S. Horike, T. Sakuma, S. Miura, T. Adachi, T. Yamamoto, S. Ikegawa, Y. Hiraki and C. Shukunami (2016). "Functional Investigation of a Non-coding Variant Associated with Adolescent Idiopathic Scoliosis in Zebrafish: Elevated Expression of the Ladybird Homeobox Gene Causes Body Axis Deformation." PLoS Genet **12**(1): e1005802.

Guo, X., W. W. Chau, C. W. Hui-Chan, C. S. Cheung, W. W. Tsang and J. C. Cheng (2006). "Balance control in adolescents with idiopathic scoliosis and disturbed somatosensory function." Spine (Phila Pa 1976) **31**(14): E437-440.

Hadley-Miller, N., B. Mims and D. M. Milewicz (1994). "The potential role of the elastic fiber system in adolescent idiopathic scoliosis." J Bone Joint Surg Am **76**(8): 1193-1206.

Haller, G., D. Alvarado, K. McCall, P. Yang, C. Cruchaga, M. Harms, A. Goate, M. Willing, J. A. Morcuende, E. Baschal, N. H. Miller, C. Wise, M. B. Dobbs and C. A. Gurnett (2016). "A polygenic burden of rare variants across extracellular matrix genes among individuals with adolescent idiopathic scoliosis." Hum Mol Genet **25**(1): 202-209.

Hamann, J., G. Aust, D. Arac, F. B. Engel, C. Formstone, R. Fredriksson, R. A. Hall, B. L. Harty, C. Kirchhoff, B. Knapp, A. Krishnan, I. Liebscher, H. H. Lin, D. C. Martinelli, K. R. Monk, M. C. Peeters, X. Piao, S. Promel, T. Schoneberg, T. W. Schwartz, K. Singer, M. Stacey, Y. A. Ushkaryov, M. Vallon, U. Wolfrum, M. W. Wright, L. Xu, T. Langenhan and H. B. Schioth (2015). "International Union of Basic and Clinical Pharmacology. XCIV. Adhesion G protein-coupled receptors." Pharmacol Rev **67**(2): 338-367.

Hawasli, A. H., T. E. Hullar and I. G. Dorward (2015). "Idiopathic scoliosis and the vestibular system." Eur Spine J **24**(2): 227-233.

Hayes, M., X. Gao, L. X. Yu, N. Paria, R. M. Henkelman, C. A. Wise and B. Ciruna (2014). "ptk7 mutant zebrafish models of congenital and idiopathic scoliosis implicate dysregulated Wnt signalling in disease." Nat Commun **5**: 4777.

Hayes, M., M. Naito, A. Daulat, S. Angers and B. Ciruna (2013). "Ptk7 promotes non-canonical Wnt/PCP-mediated morphogenesis and inhibits Wnt/beta-catenin-dependent cell fate decisions during vertebrate development." Development **140**(8): 1807-1818.

Hitier, M., M. Hamon, P. Denise, J. Lacoudre, M. A. Thenint, J. F. Mallet, S. Moreau and G. Quarck (2015). "Lateral Semicircular Canal Asymmetry in Idiopathic Scoliosis: An Early Link between Biomechanical, Hormonal and Neurosensory Theories?" PLoS One **10**(7): e0131120.

Huang, B. K. and M. A. Choma (2015). "Microscale imaging of cilia-driven fluid flow." Cell Mol Life Sci **72**(6): 1095-1113.

Huang, T., J. Cui, L. Li, P. F. Hitchcock and Y. Li (2012). "The role of microglia in the neurogenesis of zebrafish retina." Biochem Biophys Res Commun **421**(2): 214-220.

Huang, Y. S., N. Y. Chiang, C. H. Hu, C. C. Hsiao, K. F. Cheng, W. P. Tsai, S. Yona, M. Stacey, S. Gordon, G. W. Chang and H. H. Lin (2012). "Activation of myeloid cell-specific adhesion class G protein-coupled receptor EMR2 via ligation-induced translocation and interaction of receptor subunits in lipid raft microdomains." Mol Cell Biol **32**(8): 1408-1420.

Ikegawa, S. (2016). "Genomic study of adolescent idiopathic scoliosis in Japan." Scoliosis Spinal Disord **11**: 5.

Inaba, H., H. Goto, K. Kasahara, K. Kumamoto, S. Yonemura, A. Inoko, S. Yamano, H. Wanibuchi, D. He, N. Goshima, T. Kiyono, S. Hirotsune and M. Inagaki (2016). "Ndel1 suppresses ciliogenesis in proliferating cells by regulating the trichoplein-Aurora A pathway." J Cell Biol **212**(4): 409-423.

Inoue, M., S. Minami, Y. Nakata, H. Kitahara, Y. Otsuka, K. Isobe, M. Takaso, M. Tokunaga, S. Nishikawa, T. Maruta and H. Moriya (2002). "Association between estrogen receptor gene polymorphisms and curve severity of idiopathic scoliosis." Spine (Phila Pa 1976) **27**(21): 2357-2362.

Inoue, M., Y. Nakata, S. Minami, H. Kitahara, Y. Otsuka, K. Isobe, M. Takaso, M. Tokunaga, T. Itabashi, S. Nishikawa and H. Moriya (2003). "Idiopathic scoliosis as a presenting sign of familial neurologic abnormalities." Spine (Phila Pa 1976) **28**(1): 40-45.

Ireland, D. C., S. Bord, S. R. Beavan and J. E. Compston (2002). "Effects of estrogen on collagen synthesis by cultured human osteoblasts depend on the rate of cellular differentiation." J Cell Biochem **86**(2): 251-257.

Ishida, K., Y. Aota, N. Mitsugi, M. Kono, T. Higashi, T. Kawai, K. Yamada, T. Niimura, K. Kaneko, H. Tanabe, Y. Ito, T. Katsuhata and T. Saito (2015). "Relationship between bone density and bone metabolism in adolescent idiopathic scoliosis." Scoliosis **10**: 19.

Jacquet, B. V., R. Salinas-Mondragon, H. Liang, B. Therit, J. D. Buie, M. Dykstra, K. Campbell, L. E. Ostrowski, S. L. Brody and H. T. Ghashghaei (2009). "FoxJ1-dependent gene expression is required for differentiation of radial glia into ependymal cells and a subset of astrocytes in the postnatal brain." Development **136**(23): 4021-4031.

Janssen, M. M., R. F. de Wilde, J. W. Kouwenhoven and R. M. Castelein (2011). "Experimental animal models in scoliosis research: a review of the literature." Spine J **11**(4): 347-358.

Janssen, M. M., J. W. Kouwenhoven, T. P. Schlosser, M. A. Viergever, L. W. Bartels, R. M. Castelein and K. L. Vincken (2011). "Analysis of preexistent vertebral rotation in the normal infantile, juvenile, and adolescent spine." Spine (Phila Pa 1976) **36**(7): E486-491.

Janusz, P., M. Kotwicka, M. Andrusiewicz, D. Czaprowski, J. Czubak and T. Kotwicki (2014). "Estrogen receptors genes polymorphisms and age at menarche in idiopathic scoliosis." BMC Musculoskelet Disord **15**: 383.

Jen, J. C., W. M. Chan, T. M. Bosley, J. Wan, J. R. Carr, U. Rub, D. Shattuck, G. Salamon, L. C. Kudo, J. Ou, D. D. Lin, M. A. Salih, T. Kansu, H. Al Dhalaan, Z. Al Zayed, D. B. MacDonald, B. Stigsby, A. Plaitakis, E. K. Dretakis, I. Gottlob, C. Pieh, E. I. Traboulsi, Q. Wang, L. Wang, C. Andrews, K. Yamada, J. L. Demer, S. Karim, J. R. Alger, D. H. Geschwind, T. Deller, N. L. Sicotte, S. F. Nelson, R. W. Baloh and E. C. Engle (2004). "Mutations in a human ROBO gene disrupt hindbrain axon pathway crossing and morphogenesis." Science **304**(5676): 1509-1513.

Jiang, H., X. Qiu, J. Dai, H. Yan, Z. Zhu, B. Qian and Y. Qiu (2013). "Association of rs11190870 near LBX1 with adolescent idiopathic scoliosis susceptibility in a Han Chinese population." Eur Spine J **22**(2): 282-286.

Jiang, J., B. Qian, S. Mao, Q. Zhao, X. Qiu, Z. Liu and Y. Qiu (2012). "A promoter polymorphism of tissue inhibitor of metalloproteinase-2 gene is associated with severity of thoracic adolescent idiopathic scoliosis." Spine (Phila Pa 1976) **37**(1): 41-47.

Joldersma, M., J. Klein-Nulend, A. M. Oleksik, I. C. Heyligers and E. H. Burger (2001). "Estrogen enhances mechanical stress-induced prostaglandin production by bone cells from elderly women." Am J Physiol Endocrinol Metab **280**(3): E436-442.

Justice, C. M., N. H. Miller, B. Marosy, J. Zhang and A. F. Wilson (2003). "Familial idiopathic scoliosis: evidence of an X-linked susceptibility locus." Spine (Phila Pa 1976) **28**(6): 589-594.

Juul, A. (2001). "The effects of oestrogens on linear bone growth." Hum Reprod Update **7**(3): 303-313.

Kamiya, N., J. Shen, K. Noda, M. Kitami, G. S. Feng, D. Chen and Y. Komatsu (2015). "SHP2-Deficiency in Chondrocytes Deforms Orofacial Cartilage and Ciliogenesis in Mice." J Bone Miner Res **30**(11): 2028-2032.

Kaplan, A., M. M. Gaschler, D. E. Dunn, R. Colligan, L. M. Brown, A. G. Palmer, 3rd, D. C. Lo and B. R. Stockwell (2015). "Small molecule-induced oxidation of protein disulfide isomerase is neuroprotective." Proc Natl Acad Sci U S A **112**(17): E2245-2252.

Karner, C. M., F. Long, L. Solnica-Krezel, K. R. Monk and R. S. Gray (2015). "Gpr126/Adgrg6 deletion in cartilage models idiopathic scoliosis and pectus excavatum in mice." Hum Mol Genet **24**(15): 4365-4373.

Kaufman, P. L. and C. A. Rasmussen (2012). "Advances in glaucoma treatment and management: outflow drugs." Invest Ophthalmol Vis Sci **53**(5): 2495-2500.

Kaviani, R., I. Londono, S. Parent, F. Moldovan and I. Villemure (2018). "Changes in growth plate extracellular matrix composition and biomechanics following in vitro static versus dynamic mechanical modulation." J Musculoskelet Neuronal Interact **18**(1): 81-91.

Keay, J. and J. W. Thornton (2009). "Hormone-activated estrogen receptors in annelid invertebrates: implications for evolution and endocrine disruption." Endocrinology **150**(4): 1731-1738.

Kesling, K. L. and K. A. Reinker (1997). "Scoliosis in twins. A meta-analysis of the literature and report of six cases." Spine (Phila Pa 1976) **22**(17): 2009-2014; discussion 2015.

Khan, S., M. Abdelrahim, I. Samudio and S. Safe (2003). "Estrogen receptor/Sp1 complexes are required for induction of cad gene expression by 17beta-estradiol in breast cancer cells." Endocrinology **144**(6): 2325-2335.

Kim, S., N. A. Zaghloul, E. Bubenshchikova, E. C. Oh, S. Rankin, N. Katsanis, T. Obara and L. Tsiokas (2011). "Nde1-mediated inhibition of ciliogenesis affects cell cycle re-entry." Nat Cell Biol **13**(4): 351-360.

Kim, S. C., J. E. Lee, S. S. Kang, H. S. Yang, S. S. Kim and B. S. An (2017). "The regulation of oxytocin and oxytocin receptor in human placenta according to gestational age." J Mol Endocrinol **59**(3): 235-243.

Kindsfater, K., T. Lowe, D. Lawellin, D. Weinstein and J. Akmakjian (1994). "Levels of platelet calmodulin for the prediction of progression and severity of adolescent idiopathic scoliosis." J Bone Joint Surg Am **76**(8): 1186-1192.

Klein-Nulend, J., R. G. Bacabac and A. D. Bakker (2012). "Mechanical loading and how it affects bone cells: the role of the osteocyte cytoskeleton in maintaining our skeleton." Eur Cell Mater **24**: 278-291.

Knodler, A., S. Feng, J. Zhang, X. Zhang, A. Das, J. Peranen and W. Guo (2010). "Coordination of Rab8 and Rab11 in primary ciliogenesis." Proc Natl Acad Sci U S A **107**(14): 6346-6351.

Kobayashi, D., A. Asano-Hoshino, T. Nakakura, T. Nishimaki, S. Ansai, M. Kinoshita, M. Ogawa, H. Hagiwara and T. Yokoyama (2017). "Loss of zinc finger MYND-type containing 10 (zmynd10) affects cilia integrity and axonemal localization of dynein arms, resulting in ciliary dysmotility, polycystic kidney and scoliosis in medaka (Oryzias latipes)." Dev Biol **430**(1): 69-79.

Kobayashi, D., N. Iijima, H. Hagiwara, K. Kamura, H. Takeda and T. Yokoyama (2010). "Characterization of the medaka (Oryzias latipes) primary ciliary dyskinesia mutant, jaodori: Redundant and distinct roles of dynein axonemal intermediate chain 2 (dnai2) in motile cilia." Dev Biol **347**(1): 62-70.

Kobayashi, T., S. Kim, Y. C. Lin, T. Inoue and B. D. Dynlacht (2014). "The CP110-interacting proteins Talpid3 and Cep290 play overlapping and distinct roles in cilia assembly." J Cell Biol **204**(2): 215-229.

Konieczny, M. R., H. Senyurt and R. Krauspe (2013). "Epidemiology of adolescent idiopathic scoliosis." J Child Orthop **7**(1): 3-9.

Kott, E., P. Duquesnoy, B. Copin, M. Legendre, F. Dastot-Le Moal, G. Montantin, L. Jeanson, A. Tamalet, J. F. Papon, J. P. Siffroi, N. Rives, V. Mitchell, J. de Blic, A. Coste, A. Clement, D. Escalier, A. Toure, E. Escudier and S. Amselem (2012). "Loss-of-function mutations in LRRC6, a gene essential for proper axonemal assembly of inner and outer dynein arms, cause primary ciliary dyskinesia." Am J Hum Genet **91**(5): 958-964.

Kou, I., Y. Takahashi, T. A. Johnson, A. Takahashi, L. Guo, J. Dai, X. Qiu, S. Sharma, A. Takimoto, Y. Ogura, H. Jiang, H. Yan, K. Kono, N. Kawakami, K. Uno, M. Ito, S. Minami, H. Yanagida, H. Taneichi, N. Hosono, T. Tsuji, T. Suzuki, H. Sudo, T. Kotani, I. Yonezawa, D. Londono, D. Gordon, J. A. Herring, K. Watanabe, K. Chiba, N. Kamatani, Q. Jiang, Y. Hiraki, M. Kubo, Y. Toyama, T. Tsunoda, C. A. Wise, Y. Qiu, C. Shukunami, M. Matsumoto and S. Ikegawa (2013). "Genetic variants in GPR126 are associated with adolescent idiopathic scoliosis." Nat Genet **45**(6): 676-679.

Kouwenhoven, J. W. and R. M. Castelein (2008). "The pathogenesis of adolescent idiopathic scoliosis: review of the literature." Spine (Phila Pa 1976) **33**(26): 2898-2908.

Krishnan, V., W. Porter, M. Santostefano, X. Wang and S. Safe (1995). "Molecular mechanism of inhibition of estrogen-induced cathepsin D gene expression by 2,3,7,8-tetrachlorodibenzo-p-dioxin (TCDD) in MCF-7 cells." Mol Cell Biol **15**(12): 6710-6719.

Krishnan, V., X. Wang and S. Safe (1994). "Estrogen receptor-Sp1 complexes mediate estrogen-induced cathepsin D gene expression in MCF-7 human breast cancer cells." J Biol Chem **269**(22): 15912-15917.

Kulis, A., A. Gozdzialska, J. Drag, J. Jaskiewicz, M. Knapik-Czajka, E. Lipik and D. Zarzycki (2015). "Participation of sex hormones in multifactorial pathogenesis of adolescent idiopathic scoliosis." Int Orthop **39**(6): 1227-1236.

Kwon, Y. H., J. H. Fingert, M. H. Kuehn and W. L. Alward (2009). "Primary open-angle glaucoma." N Engl J Med **360**(11): 1113-1124.

Lafortune, P., C. E. Aubin, H. Boulanger, I. Villemure, K. M. Bagnall and A. Moreau (2007). "Biomechanical simulations of the scoliotic deformation process in the pinealectomized chicken: a preliminary study." Scoliosis **2**: 16.

Lam, T. P., V. W. Hung, H. Y. Yeung, Y. K. Tse, W. C. Chu, B. K. Ng, K. M. Lee, L. Qin and J. C. Cheng (2011). "Abnormal bone quality in adolescent idiopathic scoliosis: a case-control study on 635 subjects and 269 normal controls with bone densitometry and quantitative ultrasound." Spine (Phila Pa 1976) **36**(15): 1211-1217.

Lambert, F. M., D. Malinvaud, J. Glaunes, C. Bergot, H. Straka and P. P. Vidal (2009). "Vestibular asymmetry as the cause of idiopathic scoliosis: a possible answer from Xenopus." J Neurosci **29**(40): 12477-12483.

Lamond, A. I. and D. L. Spector (2003). "Nuclear speckles: a model for nuclear organelles." Nat Rev Mol Cell Biol **4**(8): 605-612.

Lao, M. L., D. H. Chow, X. Guo, J. C. Cheng and A. D. Holmes (2008). "Impaired dynamic balance control in adolescents with idiopathic scoliosis and abnormal somatosensory evoked potentials." J Pediatr Orthop **28**(8): 846-849.

Leboeuf, D., K. Letellier, N. Alos, P. Edery and F. Moldovan (2009). "Do estrogens impact adolescent idiopathic scoliosis?" Trends Endocrinol Metab **20**(4): 147-152.

Lee, K. L., M. D. Guevarra, A. M. Nguyen, M. C. Chua, Y. Wang and C. R. Jacobs (2015). "The primary cilium functions as a mechanical and calcium signaling nexus." Cilia **4**: 7.

Lenke, L. G. (2005). "Lenke classification system of adolescent idiopathic scoliosis: treatment recommendations." Instr Course Lect **54**: 537-542.

Lepanto, P., C. Davison, G. Casanova, J. L. Badano and F. R. Zolessi (2016). "Characterization of primary cilia during the differentiation of retinal ganglion cells in the zebrafish." Neural Dev **11**: 10.

Letellier, K., B. Azeddine, S. Parent, H. Labelle, P. H. Rompre, A. Moreau and F. Moldovan (2008). "Estrogen cross-talk with the melatonin signaling pathway in human osteoblasts derived from adolescent idiopathic scoliosis patients." J Pineal Res **45**(4): 383-393.

Li, D., D. Mitchell, J. Luo, Z. Yi, S. G. Cho, J. Guo, X. Li, G. Ning, X. Wu and M. Liu (2007). "Estrogen regulates KiSS1 gene expression through estrogen receptor alpha and SP protein complexes." Endocrinology **148**(10): 4821-4828.

Li, H., B. Handsaker, A. Wysoker, T. Fennell, J. Ruan, N. Homer, G. Marth, G. Abecasis, R. Durbin and S. Genome Project Data Processing (2009). "The Sequence Alignment/Map format and SAMtools." Bioinformatics **25**(16): 2078-2079.

Li, W., Y. Li, L. Zhang, H. Guo, D. Tian, Y. Li, Y. Peng, Y. Zheng, Y. Dai, K. Xia, X. Lan, B. Wang and Z. Hu (2016). "AKAP2 identified as a novel gene mutated in a Chinese family with adolescent idiopathic scoliosis." J Med Genet **53**(7): 488-493.

Li, X. F., H. Li, Z. D. Liu and L. Y. Dai (2008). "Low bone mineral status in adolescent idiopathic scoliosis." Eur Spine J **17**(11): 1431-1440.

Li, Y. L., S. J. Gao, H. Xu, Y. Liu, H. L. Li, X. Y. Chen, G. Z. Ning and S. Q. Feng (2018). "The association of rs11190870 near LBX1 with the susceptibility and severity of AIS, a meta-analysis." Int J Surg.

Liang, G., W. Gao, A. Liang, W. Ye, Y. Peng, L. Zhang, S. Sharma, P. Su and D. Huang (2012). "Normal leptin expression, lower adipogenic ability, decreased leptin receptor and hyposensitivity to Leptin in Adolescent Idiopathic Scoliosis." PLoS One **7**(5): e36648.

Liang, J. and Y. Shang (2013). "Estrogen and cancer." Annu Rev Physiol **75**: 225-240.

Liang, J., D. Xing, Z. Li, S. Chua and S. Li (2014). "Association Between rs11190870 Polymorphism Near LBX1 and Susceptibility to Adolescent Idiopathic Scoliosis in East Asian Population: A Genetic Meta-Analysis." Spine (Phila Pa 1976).

Liedtke, W. B. (2007). TRPV Channels' Function in Osmo- and Mechanotransduction. TRP Ion Channel Function in Sensory Transduction and Cellular Signaling Cascades. W. B. Liedtke and S. Heller. Boca Raton (FL).

Liu, G., S. Liu, M. Lin, X. Li, W. Chen, Y. Zuo, J. Liu, Y. Niu, S. Zhao, B. Long, Z. Wu, N. Wu and G. Qiu (2018). "Genetic polymorphisms of GPR126 are functionally associated with PUMC classifications of adolescent idiopathic scoliosis in a Northern Han population." J Cell Mol Med **22**(3): 1964-1971.

Liu, S., N. Wu, Y. Zuo, Y. Zhou, J. Liu, Z. Liu, W. Chen, G. Liu, Y. Chen, J. Chen, M. Lin, Y. Zhao, Y. Ming, T. Yuan, X. Li, Z. Xia, X. Yang, Y. Ma, J. Zhang, J. Shen, S. Li, Y. Wang, H. Zhao, K. Yu, Y. Zhao, X. Weng, G. Qiu and Z. Wu (2017). "Genetic Polymorphism of LBX1 Is Associated With Adolescent Idiopathic Scoliosis in Northern Chinese Han Population." Spine (Phila Pa 1976) **42**(15): 1125-1129.

Liu, Z., F. Wang, L. L. Xu, S. F. Sha, W. Zhang, J. Qiao, H. D. Bao, Y. Qiu, Q. Jiang and Z. Z. Zhu (2015). "Polymorphism of rs2767485 in Leptin Receptor Gene is Associated With the Occurrence of Adolescent Idiopathic Scoliosis." Spine (Phila Pa 1976) **40**(20): 1593-1598.

Londono, D., I. Kou, T. A. Johnson, S. Sharma, Y. Ogura, T. Tsunoda, A. Takahashi, M. Matsumoto, J. A. Herring, T. P. Lam, X. Wang, E. M. Tam, Y. Q. Song, Y. H. Fan, D. Chan, K. S. Cheah, X. Qiu, H. Jiang, D. Huang, G. Japanese Scoliosis Clinical Research, T. I. C.

Group, G. International Consortium for Scoliosis, P. Su, P. Sham, K. M. Cheung, K. D. Luk, D. Gordon, Y. Qiu, J. Cheng, N. Tang, S. Ikegawa and C. A. Wise (2014). "A meta-analysis identifies adolescent idiopathic scoliosis association with LBX1 locus in multiple ethnic groups." J Med Genet **51**(6): 401-406.

Loot, A. E., R. Popp, B. Fisslthaler, J. Vriens, B. Nilius and I. Fleming (2008). "Role of cytochrome P450-dependent transient receptor potential V4 activation in flow-induced vasodilatation." Cardiovasc Res **80**(3): 445-452.

Lowe, T., D. Lawellin, D. Smith, C. Price, T. Haher, A. Merola and M. O'Brien (2002). "Platelet calmodulin levels in adolescent idiopathic scoliosis: do the levels correlate with curve progression and severity?" Spine (Phila Pa 1976) **27**(7): 768-775.

Lowe, T. G., R. G. Burwell and P. H. Dangerfield (2004). "Platelet calmodulin levels in adolescent idiopathic scoliosis (AIS): can they predict curve progression and severity? Summary of an electronic focus group debate of the IBSE." Eur Spine J **13**(3): 257-265.

Luo, N., M. D. Conwell, X. Chen, C. I. Kettenhofen, C. J. Westlake, L. B. Cantor, C. D. Wells, R. N. Weinreb, T. W. Corson, D. F. Spandau, K. M. Joos, C. Iomini, A. G. Obukhov and Y. Sun (2014). "Primary cilia signaling mediates intraocular pressure sensation." Proc Natl Acad Sci U S A **111**(35): 12871-12876.

Machida, M., J. Dubousset, Y. Imamura, T. Iwaya, T. Yamada, J. Kimura and S. Toriyama (1994). "Pathogenesis of idiopathic scoliosis: SEPs in chicken with experimentally induced scoliosis and in patients with idiopathic scoliosis." J Pediatr Orthop **14**(3): 329-335.

Machida, M., J. Dubousset, T. Satoh, I. Murai, K. B. Wood, T. Yamada and J. Ryu (2001). "Pathologic mechanism of experimental scoliosis in pinealectomized chickens." Spine (Phila Pa 1976) **26**(17): E385-391.

Machida, M., J. Dubousset, T. Yamada and J. Kimura (2009). "Serum melatonin levels in adolescent idiopathic scoliosis prediction and prevention for curve progression--a prospective study." J Pineal Res **46**(3): 344-348.

Machida, M., I. Murai, Y. Miyashita, J. Dubousset, T. Yamada and J. Kimura (1999). "Pathogenesis of idiopathic scoliosis. Experimental study in rats." Spine (Phila Pa 1976) **24**(19): 1985-1989.

Machida, M., M. Saito, J. Dubousset, T. Yamada, J. Kimura and K. Shibasaki (2005). "Pathological mechanism of idiopathic scoliosis: experimental scoliosis in pinealectomized rats." Eur Spine J **14**(9): 843-848.

Maggi, A., P. Ciana, S. Belcredito and E. Vegeto (2004). "Estrogens in the nervous system: mechanisms and nonreproductive functions." Annu Rev Physiol **66**: 291-313.

Maiocco, B., V. F. Deeney, R. Coulon and P. F. Parks, Jr. (1997). "Adolescent idiopathic scoliosis and the presence of spinal cord abnormalities. Preoperative magnetic resonance imaging analysis." Spine (Phila Pa 1976) **22**(21): 2537-2541.

McEwen, D. P., R. K. Koenekoop, H. Khanna, P. M. Jenkins, I. Lopez, A. Swaroop and J. R. Martens (2007). "Hypomorphic CEP290/NPHP6 mutations result in anosmia caused by the selective loss of G proteins in cilia of olfactory sensory neurons." Proc Natl Acad Sci U S A **104**(40): 15917-15922.

McNulty, A. L., H. A. Leddy, W. Liedtke and F. Guilak (2015). "TRPV4 as a therapeutic target for joint diseases." Naunyn Schmiedebergs Arch Pharmacol **388**(4): 437-450.

Miki, H., Y. Okada and N. Hirokawa (2005). "Analysis of the kinesin superfamily: insights into structure and function." Trends Cell Biol **15**(9): 467-476.

Miki, H., M. Setou, N. Hirokawa, R. G. Group and G. S. L. Members (2003). "Kinesin superfamily proteins (KIFs) in the mouse transcriptome." Genome Res **13**(6B): 1455-1465.

Miki, H., M. Setou, K. Kaneshiro and N. Hirokawa (2001). "All kinesin superfamily protein, KIF, genes in mouse and human." Proc Natl Acad Sci U S A **98**(13): 7004-7011.

Miller, N. H., B. Mims, A. Child, D. M. Milewicz, P. Sponseller and S. H. Blanton (1996). "Genetic analysis of structural elastic fiber and collagen genes in familial adolescent idiopathic scoliosis." J Orthop Res **14**(6): 994-999.

Miyake, A., I. Kou, Y. Takahashi, T. A. Johnson, Y. Ogura, J. Dai, X. Qiu, A. Takahashi, H. Jiang, H. Yan, K. Kono, N. Kawakami, K. Uno, M. Ito, S. Minami, H. Yanagida, H. Taneichi, N. Hosono, T. Tsuji, T. Suzuki, H. Sudo, T. Kotani, I. Yonezawa, M. Kubo, T. Tsunoda, K. Watanabe, K. Chiba, Y. Toyama, Y. Qiu, M. Matsumoto and S. Ikegawa (2013). "Identification of a susceptibility locus for severe adolescent idiopathic scoliosis on chromosome 17q24.3." PLoS One **8**(9): e72802.

Monk, K. R., J. Hamann, T. Langenhan, S. Nijmeijer, T. Schoneberg and I. Liebscher (2015). "Adhesion G Protein-Coupled Receptors: From In Vitro Pharmacology to In Vivo Mechanisms." Mol Pharmacol **88**(3): 617-623.

Monticelli, G., E. Ascani, V. Salsano and A. Salsano (1975). "Experimental scoliosis induced by prolonged minimal electrical stimulation of the paravertebral muscles." Ital J Orthop Traumatol **1**(1): 39-54.

Moore, C., F. Cevikbas, H. A. Pasolli, Y. Chen, W. Kong, C. Kempkes, P. Parekh, S. H. Lee, N. A. Kontchou, I. Yeh, N. M. Jokerst, E. Fuchs, M. Steinhoff and W. B. Liedtke (2013). "UVB radiation generates sunburn pain and affects skin by activating epidermal TRPV4 ion channels and triggering endothelin-1 signaling." Proc Natl Acad Sci U S A **110**(34): E3225-3234.

Moore, D. J., A. Onoufriadis, A. Shoemark, M. A. Simpson, P. I. zur Lage, S. C. de Castro, L. Bartoloni, G. Gallone, S. Petridi, W. J. Woollard, D. Antony, M. Schmidts, T. Didonna, P. Makrythanasis, J. Bevillard, N. P. Mongan, J. Djakow, G. Pals, J. S. Lucas, J. K. Marthin, K. G. Nielsen, F. Santoni, M. Guipponi, C. Hogg, S. E. Antonarakis, R. D. Emes, E. M. Chung, N. D. Greene, J. L. Blouin, A. P. Jarman and H. M. Mitchison (2013). "Mutations in ZMYND10, a gene essential for proper axonemal assembly of inner and outer dynein arms in humans and flies, cause primary ciliary dyskinesia." Am J Hum Genet **93**(2): 346-356.

Moreau, A., D. S. Wang, S. Forget, B. Azeddine, D. Angeloni, F. Fraschini, H. Labelle, B. Poitras, C. H. Rivard and G. Grimard (2004). "Melatonin signaling dysfunction in adolescent idiopathic scoliosis." Spine (Phila Pa 1976) **29**(16): 1772-1781.

Morocz, M., A. Czibula, Z. B. Grozer, A. Szecsenyi, P. Z. Almos, I. Rasko and T. Illes (2011). "Association study of BMP4, IL6, Leptin, MMP3, and MTNR1B gene promoter polymorphisms and adolescent idiopathic scoliosis." Spine (Phila Pa 1976) **36**(2): E123-130.

Nada, D., C. Julien, M. E. Samuels and A. Moreau (2018). "A Replication Study for Association of LBX1 Locus With Adolescent Idiopathic Scoliosis in French-Canadian Population." Spine (Phila Pa 1976) **43**(3): 172-178.

Naique, S. B., R. Porter, A. A. Cunningham, S. P. Hughes, B. Sanghera and A. A. Amis (2003). "Scoliosis in an Orangutan." Spine (Phila Pa 1976) **28**(7): E143-145.

Nakamura, T. (1980). "[Histopathological study on the intervertebral discs of idiopathic scoliosis (author's transl)]." Nihon Seikeigeka Gakkai Zasshi **54**(6): 523-538.

Nam, H. S., M. H. Shin, S. S. Kweon, K. S. Park, S. J. Sohn, J. A. Rhee, J. S. Choi and M. H. Son (2005). "Association of estrogen receptor-alpha gene polymorphisms with bone mineral density in postmenopausal Korean women." J Bone Miner Metab **23**(1): 84-89.

Narayan, D. S., J. P. Wood, G. Chidlow and R. J. Casson (2016). "A review of the mechanisms of cone degeneration in retinitis pigmentosa." Acta Ophthalmol **94**(8): 748-754.

Nault, M. L., P. Allard, S. Hinse, R. Le Blanc, O. Caron, H. Labelle and H. Sadeghi (2002). "Relations between standing stability and body posture parameters in adolescent idiopathic scoliosis." Spine (Phila Pa 1976) **27**(17): 1911-1917.

Nevzati, E., M. Shafighi, K. D. Bakhtian, H. Treiber, J. Fandino and A. R. Fathi (2015). "Estrogen induces nitric oxide production via nitric oxide synthase activation in endothelial cells." Acta Neurochir Suppl **120**: 141-145.

Newton Ede, M. M. and S. W. Jones (2016). "Adolescent idiopathic scoliosis: evidence for intrinsic factors driving aetiology and progression." Int Orthop.

Ni, Y. Y., Y. Chen, S. Y. Lu, B. Y. Sun, F. Wang, X. L. Wu, S. Y. Dang, G. H. Zhang, H. X. Zhang, Y. Kuang, J. Fei, M. M. Gu, W. F. Rong and Z. G. Wang (2014). "Deletion of Gpr128

results in weight loss and increased intestinal contraction frequency." World J Gastroenterol **20**(2): 498-508.

Nickells, R. W., S. J. Semaan and C. L. Schlamp (2008). "Involvement of the Bcl2 gene family in the signaling and control of retinal ganglion cell death." Prog Brain Res **173**: 423-435.

Nigg, E. A. and A. J. Holland (2018). "Once and only once: mechanisms of centriole duplication and their deregulation in disease." Nat Rev Mol Cell Biol **19**(5): 297-312.

Nikolova, S., V. Yablanski, E. Vlaev, L. Stokov, A. Savov and I. Kremensky (2015). "Association between Estrogen Receptor Alpha Gene Polymorphisms and Susceptibility to Idiopathic Scoliosis in Bulgarian Patients: A Case-Control Study." Open Access Maced J Med Sci **3**(2): 278-282.

Nilius, B. and T. Voets (2013). "The puzzle of TRPV4 channelopathies." EMBO Rep **14**(2): 152-163.

Nilsson, S., S. Makela, E. Treuter, M. Tujague, J. Thomsen, G. Andersson, E. Enmark, K. Pettersson, M. Warner and J. A. Gustafsson (2001). "Mechanisms of estrogen action." Physiol Rev **81**(4): 1535-1565.

Nishi, H., K. Hashimoto and A. R. Panchenko (2011). "Phosphorylation in protein-protein binding: effect on stability and function." Structure **19**(12): 1807-1815.

Ogura, Y., I. Kou, G. Japan Scoliosis Clinical Research, J. Scoliosis, M. Matsumoto, K. Watanabe and S. Ikegawa (2016). "[Genome-wide association study for adolescent idiopathic scoliosis]." Clin Calcium **26**(4): 553-560.

Ogura, Y., I. Kou, S. Miura, A. Takahashi, L. Xu, K. Takeda, Y. Takahashi, K. Kono, N. Kawakami, K. Uno, M. Ito, S. Minami, I. Yonezawa, H. Yanagida, H. Taneichi, Z. Zhu, T. Tsuji, T. Suzuki, H. Sudo, T. Kotani, K. Watanabe, N. Hosogane, E. Okada, A. Iida, M. Nakajima, A. Sudo, K. Chiba, Y. Hiraki, Y. Toyama, Y. Qiu, C. Shukunami, Y. Kamatani, M. Kubo, M. Matsumoto and S. Ikegawa (2015). "A Functional SNP in BNC2 Is Associated with Adolescent Idiopathic Scoliosis." Am J Hum Genet **97**(2): 337-342.

Ogura, Y., I. Kou, Y. Takahashi, K. Takeda, S. Minami, N. Kawakami, K. Uno, M. Ito, I. Yonezawa, T. Kaito, H. Yanagida, K. Watanabe, H. Taneichi, K. Harimaya, Y. Taniguchi, T. Kotani, T. Tsuji, T. Suzuki, H. Sudo, N. Fujita, M. Yagi, K. Chiba, M. Kubo, Y. Kamatani, M. Nakamura, M. Matsumoto, G. Japan Scoliosis Clinical Research, K. Watanabe, S. Ikegawa and G. Japan Scoliosis Clinical Research (2017). "A functional variant in MIR4300HG, the host gene of microRNA MIR4300 is associated with progression of adolescent idiopathic scoliosis." Hum Mol Genet **26**(20): 4086-4092.

Ogura, Y., K. Takeda, I. Kou, A. Khanshour, A. Grauers, H. Zhou, G. Liu, Y. H. Fan, T. Zhou, Z. Wu, Y. Takahashi, M. Matsumoto, G. Japan Scoliosis Clinical Research, G. Texas Scottish Rite Hospital for Children Clinical, E. Einarsdottir, J. Kere, D. Huang, G. Qiu, L. Xu,

Y. Qiu, C. A. Wise, Y. Q. Song, N. Wu, P. Su, P. Gerdhem, K. Watanabe and S. Ikegawa (2018). "An international meta-analysis confirms the association of BNC2 with adolescent idiopathic scoliosis." Sci Rep **8**(1): 4730.

Oliazadeh, N., K. F. Gorman, R. Eveleigh, G. Bourque and A. Moreau (2017). "Identification of Elongated Primary Cilia with Impaired Mechanotransduction in Idiopathic Scoliosis Patients." Sci Rep **7**: 44260.

Ouellet, J. and T. Odent (2013). "Animal models for scoliosis research: state of the art, current concepts and future perspective applications." Eur Spine J **22 Suppl 2**: S81-95.

Paavola, K. J. and R. A. Hall (2012). "Adhesion G protein-coupled receptors: signaling, pharmacology, and mechanisms of activation." Mol Pharmacol **82**(5): 777-783.

Papon, J. F., I. Perrault, A. Coste, B. Louis, X. Gerard, S. Hanein, L. Fares-Taie, S. Gerber, S. Defoort-Dhellemmes, A. M. Vojtek, J. Kaplan, J. M. Rozet and E. Escudier (2010). "Abnormal respiratory cilia in non-syndromic Leber congenital amaurosis with CEP290 mutations." J Med Genet **47**(12): 829-834.

Park, T. J., B. J. Mitchell, P. B. Abitua, C. Kintner and J. B. Wallingford (2008). "Dishevelled controls apical docking and planar polarization of basal bodies in ciliated epithelial cells." Nat Genet **40**(7): 871-879.

Patra, C., K. R. Monk and F. B. Engel (2014). "The multiple signaling modalities of adhesion G protein-coupled receptor GPR126 in development." Receptors Clin Investig **1**(3): 79.

Patra, C., M. J. van Amerongen, S. Ghosh, F. Ricciardi, A. Sajjad, T. Novoyatleva, A. Mogha, K. R. Monk, C. Muhlfeld and F. B. Engel (2013). "Organ-specific function of adhesion G protein-coupled receptor GPR126 is domain-dependent." Proc Natl Acad Sci U S A **110**(42): 16898-16903.

Patten, S. A., P. Margaritte-Jeannin, J. C. Bernard, E. Alix, A. Labalme, A. Besson, S. L. Girard, K. Fendri, N. Fraisse, B. Biot, C. Poizat, A. Campan-Fournier, K. Abelin-Genevois, V. Cunin, C. Zaouter, M. Liao, R. Lamy, G. Lesca, R. Menassa, C. Marcaillou, M. Letexier, D. Sanlaville, J. Berard, G. A. Rouleau, F. Clerget-Darpoux, P. Drapeau, F. Moldovan and P. Edery (2015). "Functional variants of POC5 identified in patients with idiopathic scoliosis." J Clin Invest **125**(3): 1124-1128.

Patten, S. A. and F. Moldovan (2011). "Could genetic determinants of inner ear anomalies be a factor for the development of idiopathic scoliosis?" Med Hypotheses **76**(3): 438-440.

Pazour, G. J. and G. B. Witman (2003). "The vertebrate primary cilium is a sensory organelle." Curr Opin Cell Biol **15**(1): 105-110.

Peng, Y., G. Liang, Y. Pei, W. Ye, A. Liang and P. Su (2012). "Genomic polymorphisms of G-protein estrogen receptor 1 are associated with severity of adolescent idiopathic scoliosis." Int Orthop **36**(3): 671-677.

Peradziryi, H., N. A. Kaplan, M. Podleschny, X. Liu, P. Wehner, A. Borchers and N. S. Tolwinski (2011). "PTK7/Otk interacts with Wnts and inhibits canonical Wnt signalling." EMBO J **30**(18): 3729-3740.

Perry, M. J., K. E. McDougall, S. C. Hou and J. H. Tobias (2008). "Impaired growth plate function in bmp-6 null mice." Bone **42**(1): 216-225.

Perry, R. J., C. Farquharson and S. F. Ahmed (2008). "The role of sex steroids in controlling pubertal growth." Clin Endocrinol (Oxf) **68**(1): 4-15.

Petz, L. N. and A. M. Nardulli (2000). "Sp1 binding sites and an estrogen response element half-site are involved in regulation of the human progesterone receptor A promoter." Mol Endocrinol **14**(7): 972-985.

Pignatelli, V., C. Champ, J. Marshall and M. Vorobyev (2010). "Double cones are used for colour discrimination in the reef fish, Rhinecanthus aculeatus." Biol Lett **6**(4): 537-539.

Porter, W., F. Wang, W. Wang, R. Duan and S. Safe (1996). "Role of estrogen receptor/Sp1 complexes in estrogen-induced heat shock protein 27 gene expression." Mol Endocrinol **10**(11): 1371-1378.

Pourquie, O. (2007). "Building the spine: the vertebrate segmentation clock." Cold Spring Harb Symp Quant Biol **72**: 445-449.

Prossnitz, E. R., J. B. Arterburn, H. O. Smith, T. I. Oprea, L. A. Sklar and H. J. Hathaway (2008). "Estrogen signaling through the transmembrane G protein-coupled receptor GPR30." Annu Rev Physiol **70**: 165-190.

Qin, X., L. Xu, C. Xia, W. Zhu, W. Sun, Z. Liu, Y. Qiu and Z. Zhu (2017). "Genetic Variant of GPR126 Gene is Functionally Associated with Adolescent Idiopathic Scoliosis in Chinese Population." Spine (Phila Pa 1976).

Qiu, X. S., N. L. Tang, H. Y. Yeung, K. M. Lee, V. W. Hung, B. K. Ng, S. L. Ma, R. H. Kwok, L. Qin, Y. Qiu and J. C. Cheng (2007). "Melatonin receptor 1B (MTNR1B) gene polymorphism is associated with the occurrence of adolescent idiopathic scoliosis." Spine (Phila Pa 1976) **32**(16): 1748-1753.

Qiu, Y., X. Sun, X. Qiu, W. Li, Z. Zhu, F. Zhu, B. Wang, Y. Yu and B. Qian (2007). "Decreased circulating leptin level and its association with body and bone mass in girls with adolescent idiopathic scoliosis." Spine (Phila Pa 1976) **32**(24): 2703-2710.

Quaynor, S. D., E. W. Stradtman, Jr., H. G. Kim, Y. Shen, L. P. Chorich, D. A. Schreihofer and L. C. Layman (2013). "Delayed puberty and estrogen resistance in a woman with estrogen receptor alpha variant." N Engl J Med **369**(2): 164-171.

Quigley, H. A. (2011). "Glaucoma." Lancet **377**(9774): 1367-1377.

Rachel, R. A., T. Li and A. Swaroop (2012). "Photoreceptor sensory cilia and ciliopathies: focus on CEP290, RPGR and their interacting proteins." Cilia **1**(1): 22.

Rachel, R. A., E. A. Yamamoto, M. K. Dewanjee, H. L. May-Simera, Y. V. Sergeev, A. N. Hackett, K. Pohida, J. Munasinghe, N. Gotoh, B. Wickstead, R. N. Fariss, L. Dong, T. Li and A. Swaroop (2015). "CEP290 alleles in mice disrupt tissue-specific cilia biogenesis and recapitulate features of syndromic ciliopathies." Hum Mol Genet **24**(13): 3775-3791.

Raczkowski, J. W. (2007). "The concentrations of testosterone and estradiol in girls with adolescent idiopathic scoliosis." Neuro Endocrinol Lett **28**(3): 302-304.

Ravenscroft, G., F. Nolent, S. Rajagopalan, A. M. Meireles, K. J. Paavola, D. Gaillard, E. Alanio, M. Buckland, S. Arbuckle, M. Krivanek, J. Maluenda, S. Pannell, R. Gooding, R. W. Ong, R. J. Allcock, E. D. Carvalho, M. D. Carvalho, F. Kok, W. S. Talbot, J. Melki and N. G. Laing (2015). "Mutations of GPR126 are responsible for severe arthrogryposis multiplex congenita." Am J Hum Genet **96**(6): 955-961.

Rieder, C. L., S. Faruki and A. Khodjakov (2001). "The centrosome in vertebrates: more than a microtubule-organizing center." Trends Cell Biol **11**(10): 413-419.

Riseborough, E. J. and R. Wynne-Davies (1973). "A genetic survey of idiopathic scoliosis in Boston, Massachusetts." J Bone Joint Surg Am **55**(5): 974-982.

Roberts, S., J. Menage and S. M. Eisenstein (1993). "The cartilage end-plate and intervertebral disc in scoliosis: calcification and other sequelae." J Orthop Res **11**(5): 747-757.

Roberts, S. B. and A. I. Tsirikos (2016). "Thoracolumbar kyphoscoliosis with unilateral subluxation of the spine and postoperative lumbar spondylolisthesis in Hunter syndrome." J Neurosurg Spine **24**(3): 402-406.

Rodan, G. A. (1991). "Mechanical loading, estrogen deficiency, and the coupling of bone formation to bone resorption." J Bone Miner Res **6**(6): 527-530.

Rondanino, C., P. A. Poland, C. L. Kinlough, H. Li, Y. Rbaibi, M. M. Myerburg, M. M. Al-bataineh, O. B. Kashlan, N. M. Pastor-Soler, K. R. Hallows, O. A. Weisz, G. Apodaca and R. P. Hughey (2011). "Galectin-7 modulates the length of the primary cilia and wound repair in polarized kidney epithelial cells." Am J Physiol Renal Physiol **301**(3): F622-633.

Rusova, T. V., V. I. Rykova, A. V. Korel, A. M. Zaidman and D. S. Tkachev (2005). "Glycosaminoglycans of the vertebral body growth plate in patients with idiopathic scoliosis." Bull Exp Biol Med **139**(6): 738-740.

Ryskamp, D. A., P. Witkovsky, P. Barabas, W. Huang, C. Koehler, N. P. Akimov, S. H. Lee, S. Chauhan, W. Xing, R. C. Renteria, W. Liedtke and D. Krizaj (2011). "The polymodal ion channel transient receptor potential vanilloid 4 modulates calcium flux, spiking rate, and apoptosis of mouse retinal ganglion cells." J Neurosci **31**(19): 7089-7101.

Ryzhkov, II, E. E. Borzilov, M. I. Churnosov, A. V. Ataman, A. A. Dedkov and A. V. Polonikov (2013). "Transforming growth factor beta 1 is a novel susceptibility gene for adolescent idiopathic scoliosis." Spine (Phila Pa 1976) **38**(12): E699-704.

Sadat-Ali, M., I. al-Habdan and A. al-Othman (2000). "Adolescent idiopathic scoliosis. Is low melatonin a cause?" Joint Bone Spine **67**(1): 62-64.

Safe, S. (2001). "Transcriptional activation of genes by 17 beta-estradiol through estrogen receptor-Sp1 interactions." Vitam Horm **62**: 231-252.

Sahlstrand, T., R. Ortengren and A. Nachemson (1978). "Postural equilibrium in adolescent idiopathic scoliosis." Acta Orthop Scand **49**(4): 354-365.

Sanders, J. O., R. H. Browne, S. J. McConnell, S. A. Margraf, T. E. Cooney and D. N. Finegold (2007). "Maturity assessment and curve progression in girls with idiopathic scoliosis." J Bone Joint Surg Am **89**(1): 64-73.

Satir, P. (1995). "Landmarks in cilia research from Leeuwenhoek to us." Cell Motil Cytoskeleton **32**(2): 90-94.

Schaab, M. and J. Kratzsch (2015). "The soluble leptin receptor." Best Pract Res Clin Endocrinol Metab **29**(5): 661-670.

Schlosser, T. P., G. J. van der Heijden, A. L. Versteeg and R. M. Castelein (2014). "How 'idiopathic' is adolescent idiopathic scoliosis? A systematic review on associated abnormalities." PLoS One **9**(5): e97461.

Schubert, F. R., P. Tremblay, A. Mansouri, A. M. Faisst, B. Kammandel, A. Lumsden, P. Gruss and S. Dietrich (2001). "Early mesodermal phenotypes in splotch suggest a role for Pax3 in the formation of epithelial somites." Dev Dyn **222**(3): 506-521.

Schultz, J. R., L. N. Petz and A. M. Nardulli (2005). "Cell- and ligand-specific regulation of promoters containing activator protein-1 and Sp1 sites by estrogen receptors alpha and beta." J Biol Chem **280**(1): 347-354.

Searle, B. C. (2010). "Scaffold: a bioinformatic tool for validating MS/MS-based proteomic studies." Proteomics **10**(6): 1265-1269.

Shapiro, I. M., W. J. Landis and M. V. Risbud (2015). "Matrix vesicles: Are they anchored exosomes?" Bone **79**: 29-36.

Sharma, S., X. Gao, D. Londono, S. E. Devroy, K. N. Mauldin, J. T. Frankel, J. M. Brandon, D. Zhang, Q. Z. Li, M. B. Dobbs, C. A. Gurnett, S. F. Grant, H. Hakonarson, J. P. Dormans, J. A. Herring, D. Gordon and C. A. Wise (2011). "Genome-wide association studies of adolescent idiopathic scoliosis suggest candidate susceptibility genes." Hum Mol Genet **20**(7): 1456-1466.

Shi, L., D. Wang, W. C. Chu, G. R. Burwell, T. T. Wong, P. A. Heng and J. C. Cheng (2011). "Automatic MRI segmentation and morphoanatomy analysis of the vestibular system in adolescent idiopathic scoliosis." Neuroimage **54 Suppl 1**: S180-188.

Shi, L., D. Wang, W. C. Chu, R. G. Burwell, B. J. Freeman, P. A. Heng and J. C. Cheng (2009). "Volume-based morphometry of brain MR images in adolescent idiopathic scoliosis and healthy control subjects." AJNR Am J Neuroradiol **30**(7): 1302-1307.

Shi, L., D. Wang, S. C. Hui, M. C. Tong, J. C. Cheng and W. C. Chu (2013). "Volumetric changes in cerebellar regions in adolescent idiopathic scoliosis compared with healthy controls." Spine J **13**(12): 1904-1911.

Shin, G., T. W. Kang, S. Yang, S. J. Baek, Y. S. Jeong and S. Y. Kim (2011). "GENT: gene expression database of normal and tumor tissues." Cancer Inform **10**: 149-157.

Shinohara, K. and H. Hamada (2017). "Cilia in Left-Right Symmetry Breaking." Cold Spring Harb Perspect Biol **9**(10).

Shnitsar, I. and A. Borchers (2008). "PTK7 recruits dsh to regulate neural crest migration." Development **135**(24): 4015-4024.

Sieber, M. A., R. Storm, M. Martinez-de-la-Torre, T. Muller, H. Wende, K. Reuter, E. Vasyutina and C. Birchmeier (2007). "Lbx1 acts as a selector gene in the fate determination of somatosensory and viscerosensory relay neurons in the hindbrain." J Neurosci **27**(18): 4902-4909.

Singleman, C. and N. G. Holtzman (2014). "Growth and maturation in the zebrafish, Danio rerio: a staging tool for teaching and research." Zebrafish **11**(4): 396-406.

Sipila, S., T. Finni and V. Kovanen (2015). "Estrogen influences on neuromuscular function in postmenopausal women." Calcif Tissue Int **96**(3): 222-233.

Skibinska, I., M. Tomaszewski, M. Andrusiewicz, P. Urbaniak, R. Czarnecka-Klos, M. Shadi, T. Kotwicki and M. Kotwicka (2016). "Expression of Estrogen Receptor Coactivator Proline-, Glutamic Acid- and Leucine-Rich Protein 1 within Paraspinal Muscles in Adolescents with Idiopathic Scoliosis." PLoS One **11**(4): e0152286.

Smith, E. P., J. Boyd, G. R. Frank, H. Takahashi, R. M. Cohen, B. Specker, T. C. Williams, D. B. Lubahn and K. S. Korach (1994). "Estrogen resistance caused by a mutation in the estrogen-receptor gene in a man." N Engl J Med **331**(16): 1056-1061.

Snyder, E. M., C. L. Small, Y. Li and M. D. Griswold (2009). "Regulation of gene expression by estrogen and testosterone in the proximal mouse reproductive tract." Biol Reprod **81**(4): 707-716.

Soderling, E., M. Knuttila and K. K. Makinen (1977). "Aminopeptidase B-like enzymes in leukocytes." FEBS Lett **76**(2): 219-225.

Song, F., Y. Wang, D. Jiang, T. Wang, Y. Zhang, H. Ma and Y. Kang (2016). "Cyclic Compressive Stress Regulates Apoptosis in Rat Osteoblasts: Involvement of PI3K/Akt and JNK MAPK Signaling Pathways." PLoS One **11**(11): e0165845.

Sponseller, P. D., G. H. Thompson, B. A. Akbarnia, S. A. Glait, M. A. Asher, J. B. Emans and H. C. Dietz, 3rd (2009). "Growing rods for infantile scoliosis in Marfan syndrome." Spine (Phila Pa 1976) **34**(16): 1711-1715.

Stavrou, I., C. Zois, J. P. Ioannidis and A. Tsatsoulis (2002). "Association of polymorphisms of the oestrogen receptor alpha gene with the age of menarche." Hum Reprod **17**(4): 1101-1105.

Stokes, I. A. (2007). "Analysis and simulation of progressive adolescent scoliosis by biomechanical growth modulation." Eur Spine J **16**(10): 1621-1628.

Stokes, I. A. (2008). "Mechanical modulation of spinal growth and progression of adolescent scoliosis." Stud Health Technol Inform **135**: 75-83.

Stokes, I. A., R. G. Burwell, P. H. Dangerfield and Ibse (2006). "Biomechanical spinal growth modulation and progressive adolescent scoliosis--a test of the 'vicious cycle' pathogenetic hypothesis: summary of an electronic focus group debate of the IBSE." Scoliosis **1**: 16.

Stokes, I. A., C. McBride, D. D. Aronsson and P. J. Roughley (2011). "Intervertebral disc changes with angulation, compression and reduced mobility simulating altered mechanical environment in scoliosis." Eur Spine J **20**(10): 1735-1744.

Stokes, I. A., C. McBride, D. D. Aronsson and P. J. Roughley (2013). "Metabolic Effects of Angulation, Compression and Reduced Mobility on Annulus Fibrosis in a Model of Altered Mechanical Environment in Scoliosis." Spine Deform **1**(3): 161-170.

Sun, C., Y. Qiu, G. Yin, H. Shu, Z. Liu, X. H. Wang, W. J. Liu and H. B. Li (2009). "[Abnormal expression and significance of Runx2 in osteoblasts of adolescent idiopathic scoliosis patients.]." Zhonghua Wai Ke Za Zhi **47**(19): 1495-1498.

Sun, X., Y. Qiu, Z. Zhu, F. Zhu, B. Wang, Y. Yu and B. Qian (2007). "Variations of the position of the cerebellar tonsil in idiopathic scoliotic adolescents with a cobb angle >40 degrees: a magnetic resonance imaging study." Spine (Phila Pa 1976) **32**(15): 1680-1686.

Sun, X., T. Wu, Z. Liu, Z. Zhu, B. Qian, F. Zhu, W. Ma, Y. Yu, B. Wang and Y. Qiu (2013). "Osteopenia predicts curve progression of adolescent idiopathic scoliosis in girls treated with brace treatment." J Pediatr Orthop **33**(4): 366-371.

Suzuki, M., A. Hirao and A. Mizuno (2003). "Microtubule-associated [corrected] protein 7 increases the membrane expression of transient receptor potential vanilloid 4 (TRPV4)." J Biol Chem **278**(51): 51448-51453.

Suzuki, T., T. Notomi, D. Miyajima, F. Mizoguchi, T. Hayata, T. Nakamoto, R. Hanyu, P. Kamolratanakul, A. Mizuno, M. Suzuki, Y. Ezura, Y. Izumi and M. Noda (2013). "Osteoblastic differentiation enhances expression of TRPV4 that is required for calcium oscillation induced by mechanical force." Bone **54**(1): 172-178.

Szklarczyk, D., J. H. Morris, H. Cook, M. Kuhn, S. Wyder, M. Simonovic, A. Santos, N. T. Doncheva, A. Roth, P. Bork, L. J. Jensen and C. von Mering (2017). "The STRING database in 2017: quality-controlled protein-protein association networks, made broadly accessible." Nucleic Acids Res **45**(D1): D362-D368.

Takahashi, Y., I. Kou, A. Takahashi, T. A. Johnson, K. Kono, N. Kawakami, K. Uno, M. Ito, S. Minami, H. Yanagida, H. Taneichi, T. Tsuji, T. Suzuki, H. Sudo, T. Kotani, K. Watanabe, K. Chiba, N. Hosono, N. Kamatani, T. Tsunoda, Y. Toyama, M. Kubo, M. Matsumoto and S. Ikegawa (2011). "A genome-wide association study identifies common variants near LBX1 associated with adolescent idiopathic scoliosis." Nat Genet **43**(12): 1237-1240.

Takahashi, Y., M. Matsumoto, T. Karasugi, K. Watanabe, K. Chiba, N. Kawakami, T. Tsuji, K. Uno, T. Suzuki, M. Ito, H. Sudo, S. Minami, T. Kotani, K. Kono, H. Yanagida, H. Taneichi, A. Takahashi, Y. Toyama and S. Ikegawa (2011). "Replication study of the association between adolescent idiopathic scoliosis and two estrogen receptor genes." J Orthop Res **29**(6): 834-837.

Takeuchi, K. (1966). "'Wavy-fused' mutants in the Medaka, Oryzias latipes." Nature **211**(5051): 866-867.

Tam, E. M., Z. Liu, T. P. Lam, T. Ting, G. Cheung, B. K. Ng, S. K. Lee, Y. Qiu and J. C. Cheng (2016). "Lower Muscle Mass and Body Fat in Adolescent Idiopathic Scoliosis Are Associated With Abnormal Leptin Bioavailability." Spine (Phila Pa 1976) **41**(11): 940-946.

Tam, E. M., F. W. Yu, V. W. Hung, Z. Liu, K. L. Liu, B. K. Ng, S. K. Lee, Y. Qiu, J. C. Cheng and T. P. Lam (2014). "Are volumetric bone mineral density and bone micro-architecture associated with leptin and soluble leptin receptor levels in adolescent idiopathic scoliosis?--A case-control study." PLoS One **9**(2): e87939.

Tanaka, K., A. Sutani, Y. Uchida, Y. Shimizu, M. Shimizu and M. Akita (2007). "Ciliary ultrastructure in two sisters with Kartagener's syndrome." Med Mol Morphol **40**(1): 34-39.

Tang, N. L., H. Y. Yeung, K. M. Lee, V. W. Hung, C. S. Cheung, B. K. Ng, R. Kwok, X. Guo, L. Qin and J. C. Cheng (2006). "A relook into the association of the estrogen receptor [alpha] gene (PvuII, XbaI) and adolescent idiopathic scoliosis: a study of 540 Chinese cases." Spine (Phila Pa 1976) **31**(21): 2463-2468.

Tang, X. L., Y. Wang, D. L. Li, J. Luo and M. Y. Liu (2012). "Orphan G protein-coupled receptors (GPCRs): biological functions and potential drug targets." Acta Pharmacol Sin **33**(3): 363-371.

Taylor, J. R. (1983). "Scoliosis and growth. Patterns of asymmetry in normal vertebral growth." Acta Orthop Scand **54**(4): 596-602.

Temiyasathit, S., W. J. Tang, P. Leucht, C. T. Anderson, S. D. Monica, A. B. Castillo, J. A. Helms, T. Stearns and C. R. Jacobs (2012). "Mechanosensing by the primary cilium: deletion of Kif3A reduces bone formation due to loading." PLoS One **7**(3): e33368.

Thillard, M. J. (1959). "[Vertebral column deformities following epiphysectomy in the chick]." C R Hebd Seances Acad Sci **248**(8): 1238-1240.

Trontelj, J. V. and J. M. Fernandez (1988). "Single fiber EMG in juvenile idiopathic scoliosis." Muscle Nerve **11**(4): 297-300.

Tsang, W. Y., C. Bossard, H. Khanna, J. Peranen, A. Swaroop, V. Malhotra and B. D. Dynlacht (2008). "CP110 suppresses primary cilia formation through its interaction with CEP290, a protein deficient in human ciliary disease." Dev Cell **15**(2): 187-197.

Vadlamudi, R. K., R. A. Wang, A. Mazumdar, Y. Kim, J. Shin, A. Sahin and R. Kumar (2001). "Molecular cloning and characterization of PELP1, a novel human coregulator of estrogen receptor alpha." J Biol Chem **276**(41): 38272-38279.

Valteau, B., G. Grimard, I. Londono, F. Moldovan and I. Villemure (2011). "In vivo dynamic bone growth modulation is less detrimental but as effective as static growth modulation." Bone **49**(5): 996-1004.

van Rhijn, L. W., E. J. Jansen, C. M. Plasmans and B. E. Veraart (2001). "Curve characteristics in monozygotic twins with adolescent idiopathic scoliosis: 3 new twin pairs and a review of the literature." Acta Orthop Scand **72**(6): 621-625.

Veland, I. R., A. Awan, L. B. Pedersen, B. K. Yoder and S. T. Christensen (2009). "Primary cilia and signaling pathways in mammalian development, health and disease." Nephron Physiol **111**(3): p39-53.

Veldhuizen, A. G., D. J. Wever and P. J. Webb (2000). "The aetiology of idiopathic scoliosis: biomechanical and neuromuscular factors." Eur Spine J **9**(3): 178-184.

Villemure, I. and I. A. Stokes (2009). "Growth plate mechanics and mechanobiology. A survey of present understanding." J Biomech **42**(12): 1793-1803.

Vyhlidal, C., I. Samudio, M. P. Kladde and S. Safe (2000). "Transcriptional activation of transforming growth factor alpha by estradiol: requirement for both a GC-rich site and an estrogen response element half-site." J Mol Endocrinol **24**(3): 329-338.

Wajchenberg, M., D. E. Martins, P. Luciano Rde, E. B. Puertas, D. Del Curto, B. Schmidt, A. B. Oliveira and F. Faloppa (2015). "Histochemical analysis of paraspinal rotator muscles from patients with adolescent idiopathic scoliosis: a cross-sectional study." Medicine (Baltimore) **94**(8): e598.

Wang, D., L. Shi, W. C. Chu, R. G. Burwell, J. C. Cheng and A. T. Ahuja (2012). "Abnormal cerebral cortical thinning pattern in adolescent girls with idiopathic scoliosis." Neuroimage **59**(2): 935-942.

Wang, D., L. Shi, S. Liu, S. C. Hui, Y. Wang, J. C. Cheng and W. C. Chu (2013). "Altered topological organization of cortical network in adolescent girls with idiopathic scoliosis." PLoS One **8**(12): e83767.

Wang, H., Z. Wu, Q. Zhuang, Q. Fei, J. Zhang, Y. Liu, Y. Wang, Y. Ding and G. Qiu (2008). "Association study of tryptophan hydroxylase 1 and arylalkylamine N-acetyltransferase polymorphisms with adolescent idiopathic scoliosis in Han Chinese." Spine (Phila Pa 1976) **33**(20): 2199-2203.

Wang, W. J., C. Sun, Z. Liu, X. Sun, F. Zhu, Z. Z. Zhu and Y. Qiu (2014). "Transcription factor Runx2 in the low bone mineral density of girls with adolescent idiopathic scoliosis." Orthop Surg **6**(1): 8-14.

Wang, W. J., H. Y. Yeung, W. C. Chu, N. L. Tang, K. M. Lee, Y. Qiu, R. G. Burwell and J. C. Cheng (2011). "Top theories for the etiopathogenesis of adolescent idiopathic scoliosis." J Pediatr Orthop **31**(1 Suppl): S14-27.

Wang, Y. J., Z. Z. He, Y. W. Fang, Y. Xu, Y. N. Chen, G. Q. Wang, Y. Q. Yang, Z. Yang and Y. H. Li (2014). "Effect of titanium dioxide nanoparticles on zebrafish embryos and developing retina." Int J Ophthalmol **7**(6): 917-923.

Wann, A. K. and M. M. Knight (2012). "Primary cilia elongation in response to interleukin-1 mediates the inflammatory response." Cell Mol Life Sci **69**(17): 2967-2977.

Weinstein, S. L., L. A. Dolan, J. C. Cheng, A. Danielsson and J. A. Morcuende (2008). "Adolescent idiopathic scoliosis." Lancet **371**(9623): 1527-1537.

Weisz Hubshman, M., S. Broekman, E. van Wijk, F. Cremers, A. Abu-Diab, K. Samer, S. Tzur, I. Lagovsky, P. Smirin-Yosef, D. Sharon, L. Haer-Wigman, E. Banin, L. Basel-Vanagaite and E. de Vrieze (2017). "Whole-exome sequencing reveals POC5 as a novel gene associated with autosomal recessive retinitis pigmentosa." Hum Mol Genet.

Westlake, C. J., L. M. Baye, M. V. Nachury, K. J. Wright, K. E. Ervin, L. Phu, C. Chalouni, J. S. Beck, D. S. Kirkpatrick, D. C. Slusarski, V. C. Sheffield, R. H. Scheller and P. K. Jackson (2011). "Primary cilia membrane assembly is initiated by Rab11 and transport protein particle II (TRAPPII) complex-dependent trafficking of Rabin8 to the centrosome." Proc Natl Acad Sci U S A **108**(7): 2759-2764.

Wilson, P. J., C. P. Morris, D. S. Anson, T. Occhiodoro, J. Bielicki, P. R. Clements and J. J. Hopwood (1990). "Hunter syndrome: isolation of an iduronate-2-sulfatase cDNA clone and analysis of patient DNA." Proc Natl Acad Sci U S A **87**(21): 8531-8535.

Wu, J., Y. Qiu, L. Zhang, Q. Sun, X. Qiu and Y. He (2006). "Association of estrogen receptor gene polymorphisms with susceptibility to adolescent idiopathic scoliosis." Spine (Phila Pa 1976) **31**(10): 1131-1136.

Wu, T., X. Sun, Z. Zhu, H. Yan, J. Guo, J. C. Cheng and Y. Qiu (2015). "Role of Enhanced Central Leptin Activity in a Scoliosis Model Created in Bipedal Amputated Mice." Spine (Phila Pa 1976) **40**(19): E1041-1045.

Wynne-Davies, R. (1968). "Familial (idiopathic) scoliosis. A family survey." J Bone Joint Surg Br **50**(1): 24-30.

Xiao, Y., L. Zhang, K. He, X. Gao, L. Yang, L. He, G. Ma and X. Guo (2011). "Characterization of a novel missense mutation on murine Pax3 through ENU mutagenesis." J Genet Genomics **38**(8): 333-339.

Xu, J. F., G. H. Yang, X. H. Pan, S. J. Zhang, C. Zhao, B. S. Qiu, H. F. Gu, J. F. Hong, L. Cao, Y. Chen, B. Xia, Q. Bi and Y. P. Wang (2015). "Association of GPR126 gene polymorphism with adolescent idiopathic scoliosis in Chinese populations." Genomics **105**(2): 101-107.

Xu, L., X. Qiu, X. Sun, S. Mao, Z. Liu, J. Qiao and Y. Qiu (2011). "Potential genetic markers predicting the outcome of brace treatment in patients with adolescent idiopathic scoliosis." Eur Spine J **20**(10): 1757-1764.

Xu, L., F. Sheng, C. Xia, Y. Li, Z. Feng, Y. Qiu and Z. Zhu (2017). "Common variant of POC5 is associated with the susceptibility of adolescent idiopathic scoliosis." Spine (Phila Pa 1976).

Xu, L., C. Xia, X. Qin, W. Sun, N. L. Tang, Y. Qiu, J. C. Cheng and Z. Zhu (2017). "Genetic variant of BNC2 gene is functionally associated with adolescent idiopathic scoliosis in Chinese population." Mol Genet Genomics **292**(4): 789-794.

Yan, Y. X., Y. W. Gong, Y. Guo, Q. Lv, C. Guo, Y. Zhuang, Y. Zhang, R. Li and X. Z. Zhang (2012). "Mechanical strain regulates osteoblast proliferation through integrin-mediated ERK activation." PLoS One **7**(4): e35709.

Yang, M., C. Li and M. Li (2014). "The estrogen receptor alpha gene (XbaI, PvuII) polymorphisms and susceptibility to idiopathic scoliosis: a meta-analysis." J Orthop Sci **19**(5): 713-721.

Yarom, R. and G. C. Robin (1979). "Studies on spinal and peripheral muscles from patients with scoliosis." Spine (Phila Pa 1976) **4**(1): 12-21.

Yazicioglu, A., I. O. Alici, N. Karaoglanoglu and E. Yekeler (2016). "Pitfalls and Challenges of Lung Transplant in a Patient With Kartagener Syndrome and Scoliosis." Exp Clin Transplant.

Yee, A., Y. Q. Song, D. Chan and K. M. Cheung (2014). "Understanding the Basis of Genetic Studies: Adolescent Idiopathic Scoliosis as an Example." Spine Deform **2**(1): 1-9.

Yeh, C. R., J. J. Chiu, C. I. Lee, P. L. Lee, Y. T. Shih, J. S. Sun, S. Chien and C. K. Cheng (2010). "Estrogen augments shear stress-induced signaling and gene expression in osteoblast-like cells via estrogen receptor-mediated expression of beta1-integrin." J Bone Miner Res **25**(3): 627-639.

Yeung, H. Y., N. L. Tang, K. M. Lee, B. K. Ng, V. W. Hung, R. Kwok, X. Guo, L. Qin and J. C. Cheng (2006). "Genetic association study of insulin-like growth factor-I (IGF-I) gene with curve severity and osteopenia in adolescent idiopathic scoliosis." Stud Health Technol Inform **123**: 18-24.

Ylikoski, M. (2003). "Height of girls with adolescent idiopathic scoliosis." Eur Spine J **12**(3): 288-291.

Yona, S., H. H. Lin, W. O. Siu, S. Gordon and M. Stacey (2008). "Adhesion-GPCRs: emerging roles for novel receptors." Trends Biochem Sci **33**(10): 491-500.

Yona, S. and M. Stacey (2010). "Adhesion-GPCRs: structure to function. Preface." Adv Exp Med Biol **706**: v-vii.

Yoshiba, S. and H. Hamada (2014). "Roles of cilia, fluid flow, and Ca2+ signaling in breaking of left-right symmetry." Trends Genet **30**(1): 10-17.

Young, M. F., J. M. Kerr, K. Ibaraki, A. M. Heegaard and P. G. Robey (1992). "Structure, expression, and regulation of the major noncollagenous matrix proteins of bone." Clin Orthop Relat Res(281): 275-294.

Zariwala, M. A., H. Y. Gee, M. Kurkowiak, D. A. Al-Mutairi, M. W. Leigh, T. W. Hurd, R. Hjeij, S. D. Dell, M. Chaki, G. W. Dougherty, M. Adan, P. C. Spear, J. Esteve-Rudd, N. T. Loges, M. Rosenfeld, K. A. Diaz, H. Olbrich, W. E. Wolf, E. Sheridan, T. F. Batten, J. Halbritter, J. D. Porath, S. Kohl, S. Lovric, D. Y. Hwang, J. E. Pittman, K. A. Burns, T. W. Ferkol, S. D. Sagel, K. N. Olivier, L. C. Morgan, C. Werner, J. Raidt, P. Pennekamp, Z. Sun, W. Zhou, R. Airik, S. Natarajan, S. J. Allen, I. Amirav, D. Wieczorek, K. Landwehr, K. Nielsen, N. Schwerk, J. Sertic, G. Kohler, J. Washburn, S. Levy, S. Fan, C. Koerner-Rettberg, S. Amselem, D. S. Williams, B. J. Mitchell, I. A. Drummond, E. A. Otto, H. Omran, M. R. Knowles and F. Hildebrandt (2013). "ZMYND10 is mutated in primary ciliary dyskinesia and interacts with LRRC6." Am J Hum Genet **93**(2): 336-345.

Zhang, H., S. Zhao, Z. Zhao, L. Tang, Q. Guo, S. Liu and L. Chen (2014). "The association of rs1149048 polymorphism in matrilin-1(MATN1) gene with adolescent idiopathic scoliosis susceptibility: a meta-analysis." Mol Biol Rep **41**(4): 2543-2549.

Zhang, H. Q., S. J. Lu, M. X. Tang, L. Q. Chen, S. H. Liu, C. F. Guo, X. Y. Wang, J. Chen and L. Xie (2009). "Association of estrogen receptor beta gene polymorphisms with susceptibility to adolescent idiopathic scoliosis." Spine (Phila Pa 1976) **34**(8): 760-764.

Zhang, K., L. Zhang and R. N. Weinreb (2012). "Ophthalmic drug discovery: novel targets and mechanisms for retinal diseases and glaucoma." Nat Rev Drug Discov **11**(7): 541-559.

Zhang, X., H. Liu, B. Li, P. Huang, J. Shao and Z. He (2012). "Tumor suppressor BLU inhibits proliferation of nasopharyngeal carcinoma cells by regulation of cell cycle, c-Jun N-terminal kinase and the cyclin D1 promoter." BMC Cancer **12**: 267.

Zhao, D., G. X. Qiu, Y. P. Wang, J. G. Zhang, J. X. Shen and Z. H. Wu (2009). "Association between adolescent idiopathic scoliosis with double curve and polymorphisms of calmodulin1 gene/estrogen receptor-alpha gene." Orthop Surg **1**(3): 222-230.

Zhao, L., D. M. Roffey and S. Chen (2016). "Association between the Estrogen Receptor Beta (ESR2) Rs1256120 Single Nucleotide Polymorphism and Adolescent Idiopathic Scoliosis: A Systematic Review and Meta-Analysis." Spine (Phila Pa 1976).

Zhou, S., X. S. Qiu, Z. Z. Zhu, W. F. Wu, Z. Liu and Y. Qiu (2012). "A single-nucleotide polymorphism rs708567 in the IL-17RC gene is associated with a susceptibility to and the curve severity of adolescent idiopathic scoliosis in a Chinese Han population: a case-control study." BMC Musculoskelet Disord **13**: 181.

Zhu, Z., N. L. Tang, L. Xu, X. Qin, S. Mao, Y. Song, L. Liu, F. Li, P. Liu, L. Yi, J. Chang, L. Jiang, B. K. Ng, B. Shi, W. Zhang, J. Qiao, X. Sun, X. Qiu, Z. Wang, F. Wang, D. Xie, L. Chen, Z. Chen, M. Jin, X. Han, Z. Hu, Z. Zhang, Z. Liu, F. Zhu, B. P. Qian, Y. Yu, B. Wang, K. M. Lee, W. Y. Lee, T. P. Lam, Y. Qiu and J. C. Cheng (2015). "Genome-wide association study identifies new susceptibility loci for adolescent idiopathic scoliosis in Chinese girls." Nat Commun **6**: 8355.

Zhu, Z., L. Xu, N. Leung-Sang Tang, X. Qin, Z. Feng, W. Sun, W. Zhu, B. Shi, P. Liu, S. Mao, J. Qiao, Z. Liu, X. Sun, F. Li, J. Chun-Yiu Cheng and Y. Qiu (2017). "Genome-wide association study identifies novel susceptible loci and highlights Wnt/beta-catenin pathway in the development of adolescent idiopathic scoliosis." Hum Mol Genet.

Zhuang, Q., J. Li, Z. Wu, J. Zhang, W. Sun, T. Li, Y. Yan, Y. Jiang, R. C. Zhao and G. Qiu (2011). "Differential proteome analysis of bone marrow mesenchymal stem cells from adolescent idiopathic scoliosis patients." PLoS One **6**(4): e18834.